MTC/Dan Schaper

Sponsored By
George C. Marshall Space Flight Center
and
Society of Automotive Engineers

missing 82+3+4

PROCEEDINGS OF THE CONFERENCE ON THE DESIGN OF

LEAK-TIGHT FLUID CONNECTORS

(August 4 - 5, 1965)

GEORGE C. MARSHALL SPACE FLIGHT CENTER

HUNTSVILLE, ALABAMA

NATIONAL AERONAUTICS AND SPACE ADMINISTRATION

FOREWORD

These technical papers were prepared for presentation at the Conference on Design of Leak-tight Fluid Connectors sponsored by the Society of Automotive Engineers and NASA/George C. Marshall Space Flight Center. This conference was planned to promote the direct exchange of technical information concerning separable, semipermanent and permanent leak-tight fluid connectors for space vehicle use. A conference emphasizing design of separable connectors was previously held on March 24 and 25, 1964.

The papers represent a cross section of significant topics on design, testing and instrumentation. This exchange of technical information between government agencies and private industry is certain to benefit the nation's space effort and other fields of technology.

The sponsors of the conference extend their thanks to all companies and individuals who have contributed toward this meeting.

CHAIRMEN AND COMMITTEES

Conference Chairman, C. C. Wood, Chief, Fluid Mechanics and Thermodynamics Branch, NASA/MSFC

Welcome Address, Dr. Wernher von Braun, Director, George C. Marshall Space Flight Center

Session Chairmen

- Session I - Egon E. Kafka, Manager, Apollo Vehicle Test Planning, NASA Headquarters, and former Chairman of SAE Committee on Aerospace Fittings and Flex Hose Assemblies (G-3)
- Session II - Kenneth R. Bragg, Chief Engineer, Parker Aircraft Company
- Session III - L. G. Gitzendanner, Consulting Engineer, General Electric Company
- Session IV - James R. Lawrence, Air Force Rocket Propulsion Laboratory

Review Committee

- Chairman - C. C. Wood, Chief, Fluid Mechanics and Thermodynamics Branch, NASA/MSFC

C. M. Richards, General Dynamics/Astronautics, Chairman of SAE Committee on Aerospace Fittings and Flex Hose Assemblies (G-3)

Joseph DeMarchi, North American Aviation, Inc., Member of SAE G-3 Committee

Peter Haas, Aerospace Engineer - Propulsion and Power, NASA/MSFC, Member of SAE G-3 Committee

Planning Committee

- Chairman - Russell L. Chandler, Aerospace Engineer, NASA/MSFC

A. J. Favata, SAE Staff

Kent R. Eby, Brown Engineering Company, Inc.

CONTENTS...

CONTENTS (Concluded)...

ASPECTS OF ZERO LEAKAGE TECHNOLOGY

By

P. G. Hass
NASA-George C. Marshall Space Flight Center
Huntsville, Alabama

ABSTRACT

Future launch and space vehicles need fluid connectors with reduced leakage and improved reliability. For the next generation of vehicles a trend is indicated to utilize mostly semi-permanent and permanent connectors wherever feasible. Advanced "zero leakage" connectors are the development goal, and coordinated effort will contribute to achieve it in proper time.

ASPECTS OF ZERO LEAKAGE TECHNOLOGY

The development of our launch vehicle projects demands a considerable technological effort to facilitate the set goals of space travel and the exploration of the universe. The success of these programs depends on the accomplishment of a large variety of tasks that cover all aspects of science and technology. One of these problems is that of the leak tight tube and duct connections, subjected to temperature, pressure, vibration and shock extremes present in space vehicles. Presently, extensive effort is being devoted to optimize the available connector concepts, and much work has yet to be performed to eliminate leakage, reduce weight, and improve reliability, three basic requirements for space mission success.

Let us review the status of the tube connections in the Saturn V space vehicle: about one half of the connectors are the flanged type, whereas another 25% of the connections, for tubes of smaller sizes, are threaded, essentially controlled by the MC design standards. All of these joints, commonly referred to as separable connections, require high accuracy and skill in order to fulfill the stringent leakage and load requirements of our launch and space vehicles. The existing connectors have not yet proven adequate, as far as leakage is concerned, and consequently, it was necessary to reduce the requirements to an attainable level, which means adapting our demands to the state-of-the-art. But the goal of our efforts is no leakage.

Repeatedly the question is asked: why can't you stand those minute leaks we hardly can measure? It is not hard to furnish an answer, considering the liquid propellant Saturn space vehicles that use almost 10,000 fluid connectors from 1/8 inch to 20 inches duct diameter, with operating pressures up to 4,000 psi, temperatures from -423 F (liquid hydrogen temperature) to approximately 800 F, and subjected to severe temperature shock, mechanical shock, and vibration loads. All of these requirements are imposed on systems containing high energy propellants, liquid hydrogen and liquid oxygen, and it is obvious that small but numerous leaks, together with any prevailing ignition source, constitute a severe fire or explosion hazard. Furthermore, because of the complexity of these vehicles, the mission success is safeguarded only if each component has an extremely high factor of reliability, or in other words, if we can operate with fluid connectors as fully reliable tools. This reliability begins to count during checkout of the vehicle on the launch pad or in the assembly building, where schedule is an important factor. To rework leaking connectors at that step is certainly not a feasible operation.

At the present time, a guideline for allowable leakage of fluid connections in the order of 10^{-4} cc/s is established. This admittedly is not a high leakrate, but because the reproducibility of leak rates is very poor, we could anticipate actual leak-rates several orders of magnitude higher. For space vehicles and extraterrestrial stations with mission times in the order of years and under hard vacuum, we will have to set the limit to a more desirable value, like 10^{-6} cc/s, and would accept this value as "zero" leakage.

Learning from current technology it appears straight-forward to set up a "wishing list" for a connector concept that could be used throughout most systems of future vehicles and maybe even for later editions of the current generation of vehicles. This concept is not new, but its application to space travel, with its specific requirements, would be a challenge. Having in mind that most of these troublesome separable connections are not necessarily separable for an unlimited number of times, the idea of the semi-permanent connector was established. Semi-permanent connection designates a joint that essentially is not designed to be taken apart and reassembled more than 3 or 4 times; breaking the seal should neither require machining of the connection for reassembly nor increase the number of possible leak paths; separation and reassembly must be possible with field tools and on the spot.

In addition, beyound its basic definition,

the semi-permanent connection should be easy to assemble and control, the quality of the joint should not depend upon the skill of the operator, and there must be enough reliability in the design to warrant reproducible zero leakage operation. The weight of the connector assembly should be minimal, a requirement stated only for the sake completness. Finally, joint operation should not cause contamination of the system.

It is furthermore necessary to give some data concerning environmental requirements of this new generation of fluid connectors. The preliminary work done in this direction shows definite trends towards operating pressures to 6,000 psi, extension of the temperature range to 1,500 F, and duct diameters up to 18 inches. The designer of connector concepts for the vehicles to come will be faced with a lot of problems with these extreme conditions. The currently studied question of the seal interface in all its aspects is one of the basic problems. Another essential design criterion is the elimination of human error as source of malfunction, and the capability of field assembly. A specific problem which has come up and will continue to come up whenever welding or brazing as connection technique is applied, is the checkout difficulty, especially after field assembly.

This projected evolution in fluid connector technology will eliminate the flanged and threaded connection in most places, but there will always be the necessity for separable connections and of course the permanent connections.

A number of promising welding and brazing techniques are being investigated for permanent connections on space vehicles, but their development is not finished and much work still lies ahead. Summarizing, we will see a small number of separable connections and a large family of semipermanent and permanent joints on our future vehicles.

Specifying and standardizing of materials and designs has always been difficult, and the large variety of requirements and applications of tube and duct systems in space vehicles surely does not simplify the matter. Therefore, the tendency is to use only one design and only one set of sizes, and we appreciate the inherent high reliability, easy production, checking and testing. But weight and environmental demands make such a choice unrealistic. The other extreme, optimizing design for each specific application, looks even worse; the probability of error will reduce the reliability considerably.

The best choice is made when just a few optimized designs and sizes can be specified. As an example, it certainly is necessary to specify the MC separable connector standards for more than one pressure level, and consequently a second level will be specified and design standards developed, a task that will result in weight reduction. We do not expect problems during the establishment of this addition to the MC standards, because continuity of development and testing is guaranteed.

The information about different connector and seal concepts, tested in various places throughout the country, indicates a major concern, namely, the lack of coordination of test data. Comparison of data is not possible if test procedures are not clearly defined or are basically different, giving deceptive results, or necessitating expensive duplications of tests. We hope that cooperation among all pertinent organizations and companies will enhance the common technology effort. This will help to establish new ideas and concepts to improve the state-of-the-art of fluid connector technology, a task required to be conducted now to achieve the goals of tomorrow.

DEVELOPMENT OF SEPARABLE CONNECTORS FOR THE SATURN S-IV STAGE

By

E. C. Wilson
R. J. Coronado
D. D. Pierson
Douglas Aircraft Company, Inc.
Space Systems Center
Huntington Beach, California

ABSTRACT.

The success of the Saturn S-IV Stage in flight and ground operations, to this time, is an excellent demonstration of the effectiveness of the connectors employed in its propulsion systems.

There are relatively few people who ever give more than a passing thought to the fluid line connectors used in the stage installations. To these relative few, however, the significance of the proper performance of these connectors is not lost.

How effective were these connectors? What type of connectors were they and who made them? How were they evaluated and selected? What were the criteria for their performance? How were they assembled and tested?

These are only a few of the questions generated by this subject. This paper attempts to answer some of the more important ones in a, hopefully, interesting and informative way.

THE PURPOSE OF THIS PAPER is to present information in the area of separable connectors as they pertain to the Saturn S-IV Program. We propose to delve into the philosophies, constraints and ultimate decisions of design; and the problems, methods, and practices of manufacturing. We shall review the installation process and attempt to probe into all its aspects; and finally, we shall summarize and analyze the checkout of the systems of the separate stages. It is only within the matrix, we believe, that a total evaluation of the effectiveness of the connectors, as they were employed in the S-IV stage, can be made.

It is hoped that this paper will focus most of the variables of this ostensibly simple technical area into a comprehensive and well defined source of information for the fluid line connector field. We particularly wish to emphasize that the process necessary to bring the drawing board concept into a hardware reality is difficult, expensive, and at times, quite frustrating. To interject some serious humor, "There has never been a leak in any of the various connectors of a piping installation -- on the drawing board!"

Assumptions that hardware will or can be built exactly to the specifications and standards set forth in drawings and their associated documents sometimes are fallacious. The accuracy and appropriateness of some specifications and standards are also sometimes open to question. Criteria that must govern the imposition of specifications and standards are as follows:

1. Are the specifications and standards capable of being met?
2. What mechanisms will verify compliance?

Neglect of these criteria can result in a profusion of problems and may lull designers and engineers into a false sense of security.

Design conclusions and decisions based on laboratory test results and one-shot prototype studies must be tempered with good judgment or expensive penalties will result. It must constantly be kept in mind that human beings of various degrees of skill and knowledge are involved in the total process. Motivation, pride of workmanship, man/machine interfaces, and communication effectiveness must be considered in the achievement of acceptable end results.

The task facing the designers of the S-IV tankage and pneumatic installations seemed formidable at the outset. They had the dual problems of containing considerable quantities of the low density gases, helium and hydrogen, and the cryogenic liquids, hydrogen and oxygen, and doing so with minimum (hopefully zero) leakage. These, of course, are not generally insurmountable problems, but they had the added problems of high-vibration levels and extreme temperature environments to contend with. Topping off the problems was the restriction to accomplish the task with flight-weight hardware.

The easy solution to the elimination of leakage in a system such as the S-IV Propulsion System is to eliminate the separable connectors. This is theoretically simple but practically impossible at this stage of development. The first step in seeking theoretical simplicity for S-IV was to minimize the number of separable connectors to those absolutely necessary. The tradeoff limit was soon reached, however. Transportation and handling restrictions, installation factors, and the necessity for allowing some flexibility for changes and improvements

still demanded a significant number of separable connections.

In the S-IV Program a high rejection rate of welded pipe assemblies was encountered, particularly in the smaller diameter pipe sizes. This was one of the problems resulting from the effort to minimize separable connections by use of welded subassemblies. Where the quality of the welded pipe assemblies was acceptable, each welded joint was one less connection that had to be leak checked. However, each welded pipe assembly subsequently removed and replaced, for whatever the reason, was that much more expensive and involved the breaking of the multiple connections incorporated in the welded assembly.

Selection and evaluation of seals and connectors suitable for the intended service was based, as much as possible, on past performance and known test results. There was very little data on elements suitable for liquid hydrogen temperature service. To remedy this, testing of seals and connectors was initiated simultaneously at MSFC and Douglas. Testing of metallic seals was given high priority at Douglas. It was evident at the beginning, that no startling new development in the connector and seal area would be immediately forthcoming. There was no time! The field of choice in commercial connectors and seals was quite limited and it took no great amount of testing to narrow the field even more. Good prospects within this limited group were the metal "crush" washers, pressure actuated flange seals, various metal conical gaskets, MS flares, and NAS 1367 flared tube fittings (AN fittings with baked-on molybdenum disulfide lubricant). For AN boss type connections, a metallic boss seal was the only promising candidate.

The decisions were finally made under pressure of schedule commitments and the necessity of early procurement. For tubing one inch in diameter and under, MS flares and NAS 1367 fittings were selected. Tubing over an inch in diameter was selected to be connected with Aeroquip's Marman couplings. Low-pressure ducting would also be connected by Marman couplings. Certain large ducting and components would be joined by bolted flanges utilizing metal seals (pressure actuated flange seal) to conform to interface requirements. Voishan copper and aluminum seals were to be used on flared tube connectors. The Marman metal conoseal was to be used with the bolted flange and V-Band coupling and spring loaded metal seals (metal boss seals) would be utilized on all AND 10050 ports.

Some concern was evidenced regarding some of the decisions, and Douglas was advised against the use of metal crush washers throughout the systems. This philosophy was based on in-house testing results and the desire to develop connectors for 1-inch and smaller diameter tubing that would not be dependent on seals for achieving leak-tight joints. The designers, however, viewed the metal crush washers as particularly promising, especially the Voishan conical metal seal. The metal boss seal was not quite as promising, but for its application, there seemed to be no better choice.

Checkout engineering, frankly, viewed the conical metal seals with some apprehension for the following reasons:

1. The seal in effect created an additional possible leak path.
2. The possibility of shredding during torquing of the connection was considered to have a high probability in cases of careless positioning of the seal.

Initially the results tended to support the first reason, but gradually as the technicians became familiar with their use the leakage rates dropped or repairs were effected generally on the first try. It became apparent that most leaks were due to undertorquing at these particular connections.

As for the second reason, to one of the writer's knowledge, during production checkouts there was only one definite known incident of a shredded conical seal. This appeared on the cold helium fill line at the first flexible hose connection. Immediately upon start of pressurization a distinctly audible leak was discovered and pressurization halted. Disconnection of the joint revealed complete shredding of the seal. The lines up to the two in-line filters were all removed, including the filters, and sent out for inspection and cleaning. Loss of one checkout shift resulted, but there was no permanent damage sustained by system components. This incident was utilized as a highly effective example for all concerned of the necessity for exercising the utmost care in installation and assembly.

The metal boss seal was used throughout the propulsion system, but particularly in the ambient helium, cold helium, and fuel tank pressurization subsystems. During checkout with ambient helium or nitrogen pressurant, either a seal could not be effected or it was effected only after multiple, very careful, attempts. These seals were therefore eliminated from the ambient helium subsystems installations and replaced by MS 28778 packing ("O" rings) and MS 28778 packing with MS 28777 rings. In the cold gas subsystems there was no alternative except to use the seal for the remainder of the program. Teflon "O" ring seals were considered but not utilized. The torques used were felt to be excessive for the cold flow characteristics of Teflon. One critical aspect of the use of the metal boss seal is that when a connection is disassembled, for whatever reason, the seal has to be cut off for removal from the fitting. Consequently, great care must be exercised by the technician to preclude damaging the fitting.

There was some concern over the use of the packing and rings in the ambient helium subsystems because generally they were applied to the control elements of cryogenic components. However, connector leakage was very noticeably reduced and results to date indicate no deleterious effects on system performance. Some

minor contamination has been encountered, but not enough to be considered serious. The cure date factor has to be considered here, but the short life of the S-IV provides a safety, and freedom from maintenance, factor.

Marshall did not consider the Marman coupling with metal conoseal a particularly desirable application because of the lack of adequate test data. Douglas, based on limited test data, experience with other programs, and the fact that P&WA was using a similar type angle gasket in RL-10 bolted flange connections, had confidence in the connector and seal. It proved to be an effective connector for cryogenic lines of over 1-inch diameters. The major problem is that the making of a good connection requires considerable care and skill. Distortion of flanges during welding is also a prevalent problem.

Experience on Saturn S-IV production acceptance checkout revealed the following sources of connector leakage:

1. Poor Installation Practices - a) No seals installed, b) Poorly installed seals, c) Preloaded lines, d) Lack of specific instructions.
2. Wrong Seal Application - a) Metal boss seals, b) Pressure actuated flange seals,
3. Poor Torquing - a) Low torque, b) Lack of torque.
4. Damaged Connectors - a) Damaged flares, b) Damaged fittings, c) Warped flanges, d) Damaged bosses, e) Damaged seals.
5. Contamination -

Lack of trained and skilled personnel during the early part of the program accounted for the first source. The second source was due to unwise selection of seals for the following reasons:

1. The pressure actuated flange seal is a hard flat flange seal incorporating a number of annular ridges on the inner periphery. The ridges are teflon coated and a groove is cut into the inner diameter for spring effect and pressure-actuated sealing. It was found that the seals were easily scratched, nicked, and the teflon flaked off. The majority of this was probably caused during installation. Also, the mating flanges were too rough a finish to seal against the smooth surfaces of the seal.
2. The problems in the application of the metal boss seal appeared to be primarily a dimensional one and secondarily a torque problem. In too many cases it was discovered that no sealing action occurred because no pressure had been applied to the seal. This resulted from too much clearance in the assembly or improper seating of the jam nut on the bearing surface. In many instances, it was questioned whether proper torquing was being applied, i.e., indicated torque was due to friction and not tightening torque.

The subsystems and subassemblies making up the Saturn S-IV Propulsion System are shown in Table 1. The approximate number of each type of separable connector for each subsystem is also given. The system as it finally evolved contained approximately 1338 external separable connections, excluding those of the engines. The pneumatic control subsystems of the six engines alone contained an approximate total of 234 connections. The connections on the other engine subsystems were not counted.

Table 1 - Subsystem Separable Connectors (External)

Subsystem	Flared Tube	Bolted Flange	AND Boss	V-Band Coupling	Approx. Total
Pneumatic Control	266	-	68	-	334
Fuel Tank Pressurization	93	1	17	10	121
Oxidizer Tank Pressurization	100	-	35	-	135
Oxidizer Tank	32	11	5	15	63
Fuel Tank	30	9	5	15	59
Fuel Tank Make-up Pressurization	31	-	6	-	37
Engine Vent Purge	47	-	15	-	62
Cold Helium Bubbling	53	-	10	-	63
Engine Injector Purge	60	-	-	-	60
Common Bulkhead Vacuum Monitoring Sys.	21	-	9	-	30
Nonpropulsive Venting	66	2	12	-	80
Internal Engine Vent	26	3	13	18	60
External Engine Vent*	-	-	-	-	-
Engine (6)	150	-	84	-	234
	975	26	279	58	1338

* Not installed during factory checkout

Initially the system was conceived as a four-engine propulsive system, but was then redesigned as a six-engine system. As the system evolved through its development, four subsystems (two major and two minor) were added and two subsystems were expanded to include purge subassemblies. Over 300 connections were added by these changes.

Table 2 gives the fluid media contained in the various subsystems of the Propulsion System and also gives the approximate temperature and pressure environments.

The Saturn S-IV Checkout Program was set up as follows:

PRODUCTION ACCEPTANCE CHECKOUT

FACTORY - Leak and functional tests were performed at the completion of manufacturing. This was perhaps the most extensive and thorough of all the checkouts. In practice, it was many times conducted in parallel with manufacturing operations.

Table 2 - Subsystem Operating Environments

Subsystem	Medium	Temperature	Pressure
Pneumatic Control	Helium	420-625° R	3000/455
Fuel Tank Pressurization	He, H_2	100-280° R	200, 300
Oxidizer Tank Pressurization	Helium	38-100° R	3000/250
Oxidizer Tank	LOX, He	160-300° R	45-48 psia
		162-166° R	
Fuel Tank	LH_2, He	60-255° R	30-32 psia
	GH_2	38-42° R	
Fuel Tank Makeup Press.	Helium	420-625° R	3000
Engine Vent Purge	Helium	420-625° R	3000/620
Cold Helium Bubbling	Helium	100° R	3000/320
Engine Injector Purge	Helium	420-625° R	3000/620
Common Bulkhead Vacuum Monitoring	Vacuum	-	1/4 psia 1 psig
Nonpropulsive Venting	He, GH_2	160-300° R	30-50
	GOX	60-255° R	
Internal Engine Vent	He, GH_2	60-420° R	15
Engine	He, GOX	-	-
	LOX, LH_2		
	GH_2		

PRESTATIC FIRING CHECKOUT

STATIC TEST SITE - Generally a less extensive and thorough checkout than production acceptance checkout was performed to prepare the stage for static firing. Subsystems modified after Phase I checkout were given a very thorough and extensive check.

POSTSTATIC FIRING CHECKOUT

STATIC TEST SITE - A check of a generally higher level than Phase II checkout was performed to evaluate system performance and to isolate any real or incipient problem areas resulting from the firing.

PRELAUNCH CHECKOUT

LAUNCH SITE - A thorough checkout of the stage was performed to isolate transportation induced discrepancies and to prepare the system for launch operations. This checkout was concerned also with testing integrity of the system after retro-fitting of modifications.

While the systems checkouts were basically the same, emphasis was applied on different aspects of system functions and installations in these four major checkout phases. Thus the total resultant stage system checkout for each stage was the optimum checkout possible.

Table 3 shows a broad comparison of system connector leakage. Unfortunately, retrieval of this information in a more accurate form was not possible because of inconsistencies in reporting and recording leakages. An inordinate amount of analysis and evaluation would also be required to make the comparison data meaningful because of the continuing development of the stage propulsion systems during their lifetimes.

Formulating the leak detection criteria and methods for the S-IV Program was one of the most difficult and unpleasant tasks experienced by the checkout groups. At the beginning, it seemed a frustrating and hopeless task. The extent of helium and cryogenic fluid containing lines and pressure vessels was considerable. Our problems were compounded by the fact that the leak checks would be conducted at ambient conditions and, of course, with constraints on the types of fluid media. In general, test pressures were considerably below subsystem operating pressures because of safety considerations. Some correlation of test results with the operating pressures, fluids and cryogenic environments would be necessary. The launch and static-firing vibration level environments were also factors to be considered.

Table 3 - System Leakage at Factory Checkout

C/O	Stage Desig. DAC	NASA	Approx. No. of Leaks	Approx. No. of Connections
1	2	Facility	40	500
2	Test	ASV	80	800
3	1	S-IV-5	*	900
4	3	S-IV-6	110	900
5	4	S-IV-7	70	1000
6	5	S-IV-9	70	1100
7	6	S-IV-8	90	1200
8	7	S-IV-10	60	1300

* Information not available

A survey of all available leak detector devices, methods, and philosophies was initiated, but unfortunately little or no documentation of this extensive and important effort was made. This omission was the subject of considerable regret later on and as a consequence much of this effort had to be duplicated.

The mass spectrometer, helium leak detector, and the halogen leak detector appeared promising at first. Initial cost, mobility, portability, maintainability, operator training, and lack of confidence in test results were prominent factors in their final discard after detailed analysis and evaluation. A mass spectrometer was procured, however, for further testing and experimentation at the static-firing site.

A big factor in selection of liquid oxygen compatible bubble solution as a prime leak detection method was the extensive and successful use of the fluid on the Thor system. Also, there was a record of unsatisfactory results in some applications of the halogen leak detector at Douglas. Cognizant personnel felt the bubble solution was a known quantity that produced positive results while the other methods were too much of an unknown nature in practice, although excellent in theory. The cost and nature of the S-IV Program dictated some conservatism, particularly in view of the schedules.

The bubble solution and audible detection were finally selected as the prime leak detection methods to be used in conjunction with flow meters for valve seat leakage measurements. Sometime later in the program, Douglas was directed to utilize the halogen leak detector for bellows and flexible metal hose leakage checks.

Audible leak detection is overlooked by many people as a particularly effective and inexpensive method of detecting major and medium rate leakage. In conjunction with this, tactile checks are also useful and effective. The use of bubble solution to detect minor - but not insignificant - leakage was quite effective and was a major part of leak testing operations on the S-IV. There were some problems to be overcome and there are certain disadvantages to its use; but, the basic objection to bubble solution for leak testing seems to be its lack of sophistication.

The philosophy of the checkout group was that leakage rates undetectable by the bubble solution test were insignificant as far as the mission of the S-IV was concerned. It was felt that detection of such leakage was maximization without justification. There was little assurance that attempts to repair or correct such leakage would not be an impractical effort.

The criteria utilized in the S-IV propulsion system leak checks were that no leakage was allowable at any of the systems separable con-

nections. The term "No Leakage Allowable" was defined as the complete absence of any visual formation of bubbles at a pressurized connection upon the application of LOX compatible bubble solution -- to the complete satisfaction of a qualified inspector. Selective assembly of components was sometimes necessary to achieve this "zero leakage" condition.

The general procedure used in leak checks was as follows:

1. Pressurization of the subsystem or subassembly at a slow rate while audible monitoring was performed.
2. Termination of pressurization at prescribed steps to allow careful audible leak checks.
3. Pressurization to the maximum test pressure at which time bubble solution checks were made.
4. Tagging and recording of detected leaks followed by rinsing of the connector with distilled water and drying.
5. Depressurization, inspection and repair of leaking connections.
6. Repetition of the above process until all of the leakage was eliminated.

If audible leakage was detected at any time in the operation, a quick evaluation of the leak was made and pressurization either continued or discontinued according to the severity of the leak. Initial checks were made with nitrogen and final checks were performed with helium, except for the tank checks which were made with nitrogen as the pressurant.

The first checkouts of S-IV at the Santa Monica production acceptance facility were on the Facility/Dynamics Stage (#2) and the All-Systems Test vehicle. The Facility/Dynamics Stage was an installation incorporating only those subsystems essential for propellant loading and tank pressurization. The All-Systems Test vehicle was an abbreviated version of the then current flight system and incorporated dummy (simulated) engines which were later replaced with Battleship RL-10A3 engines. It was immediately obvious that less than acceptable workmanship had been performed in installation and assembly of pneumatic components. Lack of experience was a significant factor. While leakage was prevalent throughout the installations, the major problem areas were at the Marman conoseal connections, the metal boss sealed connections, and the pressure actuated flange sealed connections.

These problems persisted through subsequent stage checkouts until the following actions were taken:

1. The metal boss seal was eliminated altogether from the ambient helium subsystems and replaced with MS 28777 rings and/or MS 28778 packing.
2. A search for a replacement of the pressure actuated flange seal was initiated and culminated in the procurement of the Creavy Astro-Seal. The Creavy Astro-Seal is a bolted flange-type aluminum seal incorporating a close-wound Inconel spring, enclosed by a teflon sleeve. This is bonded to the inner periphery of the seal. The sealing qualities of this seal were excellent and eliminated all problems at bolted flange connections. An additional benefit of this seal is that it may be reused with no deleterious effect on its sealing qualities, assuming no damage to the element.
3. Careful monitoring of the Marman V-Band Coupling installation revealed malpractices in the installation of the seal. Wrong indexing and/or inadvertent slight deformation were occurring during positioning of the seal. These malpractices were corrected and resulted in faster repairs of leaking connections and, subsequently, better first installations.
4. Checkout personnel received proper training and instruction and were certified by process engineering in all aspects of pneumatic and cryogenic systems installations.

These corrective actions by no means eliminated all these problems, but they minimized them to an acceptable degree.

The major remaining problems were the use of the metal boss seal in the cold helium subsystems and the V-Band couplings on the 1-1/2" fuel tank pressurization tubing. Throughout the remainder of the program, leakage problems were concentrated in these two areas.

Two other problems experienced on the S-IV Program were:

1. Procurement of a poor quality lot of NAS 1367 fittings and their eventual use in a couple of stages before the problem was isolated. The molybdenum disulfide coating was of inferior quality and flaked off during normal assembly and disassembly of components. System contamination and malfunction of components resulted.
2. Procurement of a lot of sleeves and "B" nuts that had been heat treated per the wrong process. These elements later had to be replaced.

Leak checking of the initial system installations revealed an excessive amount of connector leakage. Much of this leakage was of a severe type. There seemed to be no consistency in the type of connector affected -- the consistency was in the prevalence of leakage. Repairs of the leaking connectors seemed to be a hopeless task at first. Torque checks, retorquing, disassembly of connections with replacement of seals seemed to have little effect in reducing leakage. An evaluation of corrective actions was immediately initiated. Process engineering was requested to review their torque standards for adequacy in this application. On-the-spot demonstrations and instruction on assembly of separable connectors, torquing of fasteners, and lubrication of fittings, and seals were presented by process engineering for the benefit of checkout technicians and assemblers. Close (magnified) visual inspection of tube flares, fittings, and seals was performed on specimens that had been assembled, repaired and disassembled. Component bosses were also inspected with fittings installed and removed. No particularly significant

discrepancies were discovered, except for a suspicion of the torquing and growing belief that the metallic boss seal used on port connections was a poor application.

A step-by-step analysis of the installation process was undertaken by checkout engineering in an attempt to isolate any possible discrepancies in methods, practices, or techniques. A possible discrepancy was noted in the normal installation process which consists of: (1) installing the individual components on the stage as they become available, (2) connecting mating parts as continuity is achieved by tightening fasteners to finger pressure, (3) afixing of an inspection seal to the connection, and (4) when the assembly or subassembly is completely installed, the installation is torqued to the proper values. Upon completion of torquing, the connections are torque striped, where authorized.

Standard practices call for initial torquing to the minimum allowable value; when leakage is present this allows retorquing to the nominal and if necessary, retorquing to the maximum value. The technician performing the component installation and assembly is not necessarily the one performing the torquing. Many instances of failure to install seals were recorded and there was much evidence to indicate that seals were poorly installed, substandard parts were installed, lines were assembled in a preloaded condition, and a significant number of cases in which fasteners were not torqued but torque stripes were applied.

Douglas technicians performing torquing operations on contract end items must be trained and certified by Process Engineering or else be supervised during the torquing operation by certified inspection personnel. This is an area where a high degree of skill and knowledge is required. These requirements are not always met, and this is why checkout becomes so necessary!

An item worth noting here is that in a majority of cases the personnel doing the installation and assembly of fluid systems are never cognizant of whether their work is poor, average, good, or excellent. Unless one performs a leak check of fluid line connectors, one can never be certain whether the connections are leak free. In the Saturn Program at Douglas, checkout technicians were normally not engaged in performing initial installation and assembly. At the end of the S-IV Program (factory checkout phase), the checkout technicians were, generally speaking, much superior to the average installer or assembler in the quality of their work. They had a higher incentive, were very aware of the problems involved in making good installations, and exhibited a high degree of pride in workmanship.

It should be pointed out that as the S-IV Program proceeded, the propulsion system grew in extent and complexity. The number of separable connectors was probably doubled from the first conception of the flight system to the final design as it evolved from the manufacturing process, checkouts, static firing, launches, and added mission requirements. Simultaneously, improvements in installation and over-all decrease of leakage occurred. In summary, the success of the S-IV stage in flight and ground operations to this time is an excellent demonstration of the effectiveness of the connectors employed in the propulsion system. There is, of course, always room for improvement and mission requirements must always dictate applicability and appropriateness of hardware.

THE PRACTICAL ASPECTS OF STATIC-JOINT LEAKAGE MONITORING

By

D. E. Stuck
G. L. Dusenberry
Rocketdyne
A Division of North American Aviation, Inc.
Canoga Park, California

LEAKAGE MONITORING of separable connectors is being used to ensure that components of space vehicles and liquid propellant rocket engines will not be jeopardized by leakage to the extent of their not being able to complete the requirements for the intended mission. Leakage monitoring of hardware from initial component development provides confidence of the ability of a joint to seal. When used early in a program, leakage monitoring may uncover an inadequate joint which can then be redesigned without substantial loss of time or the high cost which might occur if the failure were discovered later in the program. Continuation of leakage monitoring through subsequent engine and vehicle assembly verifies the compatibility of the mating components of the joint, such as flanges, seals, and fasteners.

Leak-free separable connectors are very difficult to obtain because of severe working environments (i.e., temperature, pressure, and vibration). Therefore, leakage monitoring establishes the magnitude of leakage which is inherent in the design. This information can then be evaluated with respect to the resulting effect of leakage and its influence on the vehicle's mission. The common working media with the resulting effect of leakage are shown in Table 1.

Table 1 - Media and Results

Working Media	Effect of Leakage
Hot Gas	Blow-torch damage; ignition source
Oxygen	Fire; explosion
Hydrogen	Fire; explosion
Hydrocarbon Fuel	Fire
Hydraulic Fluids	Loss of function; fire
Inert Gas	Loss of function

Both the J-2 and F-1 engine programs require monitoring leakage from separable connectors on pressurized systems. Table 2 shows the magnitude of this requirement, and lists the fluid systems and number of joints which can be monitored.

Table 2 - Monitorable Separable Connectors

	Number of Monitorable Separable Connectors	
Fluid Systems	F-1	J-2
Hot Gas	20	43
Liquid Oxygen	22	39
Liquid Hydrogen	--	51
Hydrocarbon Fuel	14	--
Inert Gas	3	42
Total	59	175

JOINT PROVISIONS FOR LEAKAGE MONITORING

Leakage monitoring requires that the joint be designed with both a primary and secondary seal together with a cavity for porting leakage to a monitoring device. Figure 1 shows a typical pressure-actuated plate seal (used in cryogenic and hot gas systems) and an in-place molded plate seal (used in hydrocarbon fuel systems). The cryogenic and hot-gas plate seals have a deflection-loaded, pressure-assisted primary seal, and a simple gasket secondary seal. This secondary seal is capable of sealing pressures up to 50 psi, and should not be considered to be a back-up

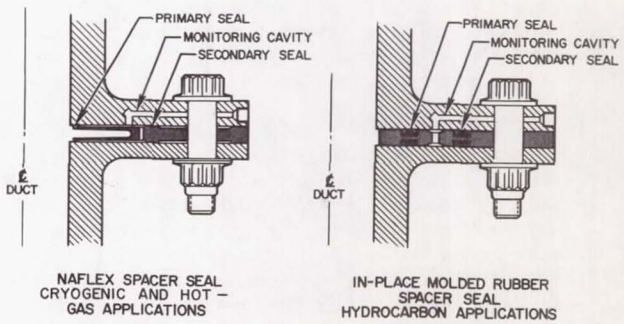

Fig. 1 - Provisions for leakage monitoring

primary seal, since it cannot prevent leakage in the event of a failure of the primary seal. The in-place seal is molded into both sides of the spacer plate with both the primary seal and secondary seal being identical.

The cavities between the primary and secondary seal on both types of seals are connected with crossover bleed holes for collecting the total joint leakage. This leakage is then ported through one of the flanges to a leakage detection or measuring device.

METHODS OF STATIC-LEAK DETECTION

While there are many methods for detecting leakage under controlled laboratory conditions, only those used by Rocketdyne to check engine components and systems will be discussed. No single method is used because none is completely universal. The most suitable method for a given situation depends on a number of criteria:

1. Fluid used for pressurization.
2. Magnitude of the anticipated leakage.
3. Configuration of the hardware to be checked.
4. Environment of the leak; i.e., temperatures and pressures involved.
5. Accuracy required.
6. Whether it must be quantitative or qualitative.
7. Time and facilities available for the effort.

SOAP SOLUTION - This method of leakage detection involves the brush application of a soap-like solution over the potential leakage source and observation for the formation of bubbles. This method is qualitative and practical for determining leakage in excess of approximately 10^{-1} scc/sec. It is advantageous for detecting leakage from tube fittings and welds on an assembly which is too cumbersome for other techniques. Leak-checking a large number of joints may be accomplished relatively fast and, in general, quite positively. It has the obvious disadvantage of being somewhat messy and unsuitable for detecting leakage from a joint which is either very hot or very cold.

PRESSURE LOCKUP - By pressurizing a closed system and maintaining the pressure for a period of time, an indication of the overall sealing capability may be observed by noting any pressure drop in the system. This is a convenient method for quickly checking a complex system having a great number of potential leakage sources. If the system is capable of maintaining the required pressure for the specified time period, there is no need for checking each leakage source at considerably greater expense of time and effort.

Pressure lockup is also useful for leak-checking a joint which is being tested at extreme temperature conditions, where other methods are not practical.

An advantage of this method is that quantitative measurements can be made without capturing the leakage. It has a wide range of measuring capability and is generally quite accurate. When leakage exceeds the desired level, this method must be followed by some joint-by-joint method for pinpointing the exact source of the leak.

Disadvantages of this method include:

1. Difficulty of determining complex internal volumes.
2. Necessity for closely controlling the gas temperature.
3. Necessity for precisely determining the sealing capabilities of the system closures (valves, cover plates, etc.).

The pressure lockup method is used in checking the sealing capability of the pneumatic (helium) control system on the J-2 engine. The pressure drop over a given period of time is related to an equivalent allowable mass loss.

LIQUID SUBMERSION - Submerging a pressurized component in a liquid (usually water) is a common method for detecting relatively small leaks ($>10^{-1}$ scc/sec). Usually the exact source of leakage is easily determined, and no further leak checking is required. This method, however, is only qualitative and is difficult for use with very large units.

ROTAMETER - The Rotameter, or differential-area flowmeter, consists of a small ball in a calibrated glass tube of varying area. As leakage gas is forced through the tube, the ball rises until a state of equilibrium is reached. The stabilized height of the ball in the tube is then read to determine the flow. Tubes of different sizes give a wide range of measuring capability.

Rotameters are used for all quantitative leakage measurements made during the static checkout of Rocketdyne engines. They are portable, quite accurate, simple to use, and easy to read and maintain. It is, of course, mandatory that the leakage be captured and plumbed to the flow tube. All monitorable separable connections on both the J-2 and F-1 engines are similar to those shown in Fig. 1.

The Rotameter must be read visually and must remain absolutely level (vertical) at all times. It is also seriously affected by vibrations and pressure changes, and is, therefore, unsuitable for monitoring leakage during a hot-fire test of a component or engine.

MASS SPECTROMETER - A mass spectrometer is an expensive, complex electromagnetic device which is capable of detecting extremely small quantities of a tracer gas (usually helium). It is capable of detecting leakage as small as 10^{-10} scc/sec, and is adaptable

to many applications. Mass spectrometer leak checks are performed on Rocketdyne engine components, such as heat exchangers, to determine the quality of welds. This method of leak detection is also used during laboratory static seal tests. It is limited to the detection of leaks less than 10^{-5} scc/sec.

METHODS OF LEAK DETECTION DURING ENGINE FIRING

Leak detection during an engine or component hot-fire test (i.e., a test in which the engine or component is fired under actual operating conditions of temperatures, pressures, vibrations, and loading) is more difficult than under laboratory, or static, conditions. None of the methods previously mentioned is readily adaptable to hot-fire conditions. Any method which is used must be able to be monitored remotely, either electrically or visually, with the aid of a movie camera. When only a qualitative indication is desired, a device, such as a burst diaphragm or a sight glass, can be used. The indication of a leak may be observed after the hot-fire test has been concluded.

The choice of a satisfactory method for accurately measuring joint leakage during a hot-fire test is largely determined by the following considerations:

1. Many joints are subject to great temperature changes. Consequently, the temperature of the leaking gas must be known so that the amount of standard leakage may be accurately determined.
2. Leakage from a joint must be captured and routed to a leakage monitoring device. Without a secondary seal, monitoring leakage during a hot-fire test is very difficult.
3. Components of the leakage monitoring system must be reasonably rugged and capable of withstanding temperature extremes and vibrations.
4. The method must have detection capability in the range of the anticipated leak rates. Obviously, a mass spectrometer-type system would be of little value if leaks greater than 10^{-5} scc/sec are expected.
5. The effects of cryo-pumping (reverse flows caused by the liquefaction of air in the flange leakage cavity) must not be interpreted as leakage by the flowmeter. This effect is of particular importance in a heated thermopile-type transducer (e.g., the Hastings-Raydist flowmeter) which is incapable of indicating the direction of flow.

The above considerations give rise to a brief discussion of the particular methods of hot-fire leakage detection which are, or have been, used at Rocketdyne.

BALLOONS - Rubber balloons have been attached to the leakage-monitoring ports for detecting gaseous leakage on F-1 engine joints. These balloons are observed during the test by motion picture cameras, but only a very rough indication of the actual leakage rate is obtained by this method. Hence, such balloons are unsuitable for detecting hot gas leaks, and, in general, are unsatisfactory for obtaining quantitative hot-fire leakage data.

SIGHT GLASS - A sight glass (Fig. 2) offers a convenient method for measuring the leakage of the fluid if it is a liquid at ambient temperatures. Sight glasses have been successfully used for detecting fuel leakage on the F-1 engine.

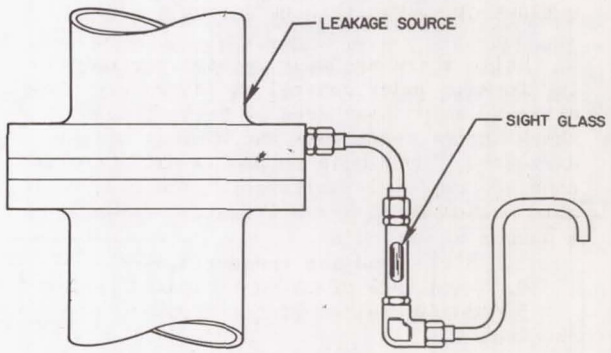

Fig. 2 - Sight-glass installation

The sight glass is inspected after the test, and the volume of the leakage measured. If the leakage is considered to have remained uniform throughout the test, the leak rate can be determined. The range of this type of device is obviously limited by the volume of the sight glass and the duration of the test.

WATER DISPLACEMENT - A widely used and well-known method for detecting leakage in the routing of the potential leakage to an inverted burette and the timing of the fall of an atmospheric-supported column of water (Fig. 3).

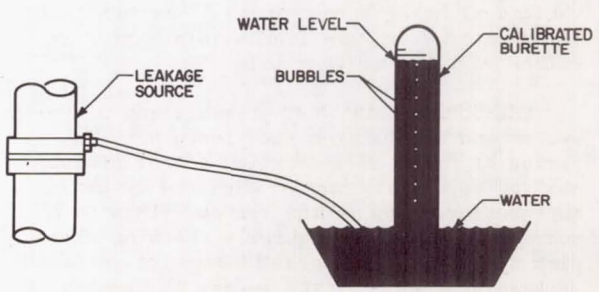

Fig. 3 - Water-displacement method for leakage measurements

Although it is not very suitable for a formal hot-fire leakage-monitoring program, the water displacement method is very convenient for a simple, quick setup to study a particular "problem joint." The burette is generally observed with a motion picture camera to obtain the most useful information relative to the performance of the joint during the test run.

BURST DIAPHRAGMS - A program of leakage monitoring has been in progress on the J-2 engine for over a year. To expedite the task of collecting as much leakage data as possible, a burst-diaphragm leak detector was developed. This detector was intended to serve as a method for screening out the "leakers" from the "non-leakers" (Fig. 4).

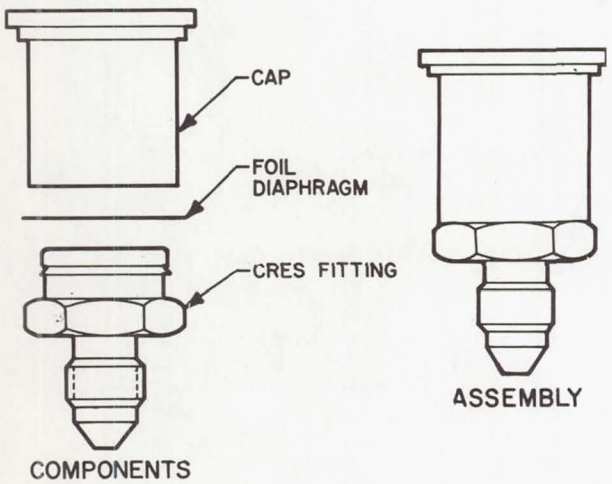

Fig. 4 - Typical burst diaphragm leak detector

Utilizing a thin (0.00015-inch) nickel diaphragm, the detector may be installed in nearly any temperature extreme. Pressure caused by the leakage will, if sufficient (10 psig at room temperature), cause the diaphragm to rupture, thus giving a positive indication of leakage.

Problems associated with this type detector (e.g., time dependency and reliability) led to the development of a vented burst-diaphragm leak detector. A minute hole in the diaphragm renders the device sensitive to a leakage rate (as opposed to a volume), and minimizes the problems inherent in the unvented type. Reliability, however, was only slightly improved; hence, burst diaphragms are no longer used.

HASTINGS-RAYDIST FLOWMETER - The majority of quantitative hot-fire leakage data at Rocketdyne has been obtained with Hastings-Raydist mass flowmeters. A major objective of the J-2 leakage-monitoring program is the development of an adequate technique for monitoring leakage during engine hot fire. This objective includes the evaluation of the leakmeters used by Rocketdyne.

The Hastings-Raydist flowmeter is convenient for measuring leakage rates, since any gas flow results in a proportional electrical output from the transducer. This electrical output is monitored remotely and transcribed onto permanent records. This flowmeter is more compatible with standard test stand instrumentation than any other previously discussed.

Principle of Operation - The Hastings-Raydist flowmeter (Fig. 5) consists of heated conduits which form the elements of a thermo-

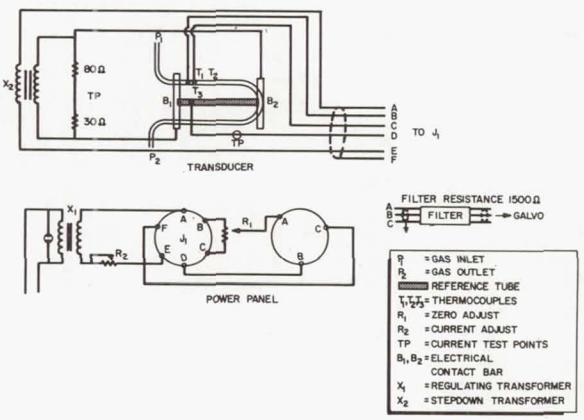

Fig. 5 - Hastings-Raydist gas flowmeter schematic

pile. Its output is derived from the cooling effect of a gas flowing through the conduits. The meter is rated at a full-scale output of 7 millivolts, which corresponds to 100 scim (approximately 25 scc/sec) of air flowing through the transducer. The meter is capable of measuring any dry gas whose temperature does not exceed 200 F. The transducer, however, must be calibrated at the proper temperature, although a relatively wide band of temperature deviation does not affect the calibration (e.g., the transducers are normally calibrated with gas at 70 F, and can then be used to measure gas whose temperature is 70 ±30 F). The manufacturer indicates that the meter has an accuracy of ±5 percent of full-scale output, but this accuracy is limited to calibrations performed under laboratory conditions.

Calibration - The calibration of the meters is performed in the laboratory. Rota-

meters have been used as the reference for determining the flowrates. Recently, however, the calibrations have been performed with a volumetric displacement device which is more accurate than the Rotameter, particularly in the low (0 to 2 scc/sec) flowrates. The output of the Hastings-Raydist flowmeter is dependent upon the density and specific heat of the gas measured. As shown in Fig. 6 , it is non-linear.

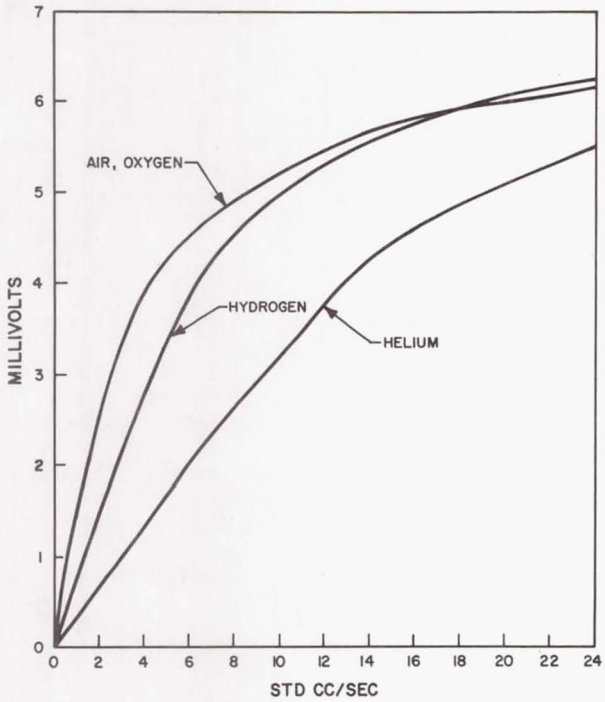

Fig. 6 - Typical calibration curves for Hastings-Raydist flowmeter

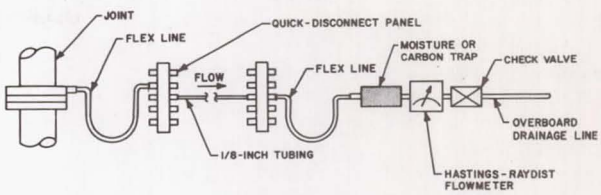

Fig. 7 - Typical leakage monitoring system schematic

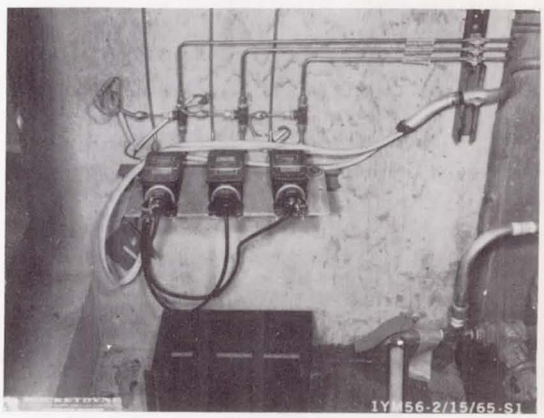

Fig. 8 - Installation of typical leakage monitoring system

Installation - A schematic of a typical leakage monitoring system using a Hastings-Raydist flowmeter and its installation are shown in Fig. 7 and 8 .

A check valve is required (1) to eliminate reverse flow resulting from cryo-pumping (the transducer is not capable of determining flow direction, and (2) to isolate the transducer's downstream vent from ambient changes due to engine firing.

The length of tubing from the leak source to the flowmeter must be sufficiently long to ensure that the gas flowing through the flowmeter has reached the calibration temperature range (40 to 100 F). However, the volume upstream from the flowmeter must be as small as practical to minimize the amount of leakage necessary to initially open the check valve. Twenty to 30 feet of 1/8-inch tubing is a compromise of these two considerations.

A trap upstream from the flowmeter is necessary to prevent moisture (in J-2 exhaust gas) or carbon (in F-1 exhaust gas) from entering the flowmeter. These traps are only necessary when exhaust gas leakage is being measured, and do not prohibit the modified flowmeter from measuring other gases.

To eliminate the potential hazard of hydrogen gas collecting in an enclosed or partially enclosed area, lines should be installed to drain the leakage overboard.

Quick-disconnect panels are used with flex lines to make the transfer and installation of leakmeter positions more convenient. The downstream panel is necessary when one set of leakmeters is intended for dual test-stand usage.

Evaluation - Extensive usage of the Hastings-Raydist flowmeter on the J-2 Leakage Monitoring Program on test engines has led to several conclusions regarding its limitations and performance characteristics under hot-fire conditions.

Perhaps the most serious drawback to the Hastings-Raydist flowmeter is its relative fragility. The internal wiring is quite delicate, and connections are frequently broken by test-stand vibrations. The meters require frequent calibration and checkout to ensure that they are functioning properly. A sometimes frustrating aspect of initially evaluating leakage data from this type of leakage monitoring system is that, when all the leakage traces show no deviation from zero, the question is raised as to whether or not the transducers and associated instrumentation are functioning properly. Conversely, when joints show signs of large leakage, it may be suspected that a part is malfunctioning. This is because of the parameter being measured, i.e., measurements are being made on a phenomenon which is not expected to occur. Leakage behavior is impossible to predict, and confidence in the data is gained only with experience.

Without modifications, the Hastings-Raydist flowmeter is unsuitable for measuring J-2 or F-1 engine exhaust gas leakage. As previously mentioned, however, the necessary modifications are relatively simple.

The meters have a range of 0 to 25 scc/sec, and a laboratory accuracy of ±5 percent of full scale. The required test-stand installation results in even less accuracy and, hence, the following qualifications (Table 3) apply.

Table 3 - Installation Qualifications

Indicated Leakage	Interpretation
0 to 1/4 scc/sec	"Zero leakage"; false reading because of system noise and ambient environmental changes during hot fire
1/4 to 1 scc/sec	Only a very rough indication of leakage
1 to 10 scc/sec	The most useful range; maximum accuracy
10 to 25 scc/sec	Accuracy drops because of shape of calibration curve

LEAKAGE MONITORING SYSTEM LIMITATIONS

It does not necessarily follow that a more sensitive flowmeter would increase the overall accuracy and sensitivity of the system. The following modifications would also be required:

1. Reduce the volume between the joint and the transducer by reducing the line size and the internal volume of the trap, if present. This reduces the amount of leakage necessary to initially open the check valve. However, a practical limit exists because of the sealing capability of the secondary seal. As the line size is diminished, the pressure gradient (a maximum at the joint) is rapidly increased. Thus, large leaks might go past the secondary seal and not be totally measured by the transducer.

2. Minimize the cracking pressure of the check valve. This reduced cracking pressure is limited, since there is evidence of a slight ambient pressure drop during a hot-fire test. If this pressure drop is sufficient to open the check valve, a false indication of leakage will occur.

3. Shorten the line length between the joint and the transducer. This reduction is limited to a length that will ensure that the leaking gas has warmed or cooled to the necessary temperatures for proper measurement by the transducer.

After the above improvements have been optimized, there is still the ever-present background "noise" inherent in the instrumentation system. This may be as high as 0.25 millivolt (equivalent to approximately 1/4 scc/sec).

Engine hot-fire leakage monitoring is obviously more difficult than leakage monitoring under laboratory conditions. The system in use at Rocketdyne is a satisfactory compromise of the aforementioned limitations.

RECOMMENDATIONS FOR IN-FLIGHT LEAKAGE MONITORING

Monitoring leakage during flight presents additional problems:

1. Present flight vehicles have an extremely large number of separable connections.

2. The reliability of the leakage monitoring system must necessarily be extremely high.

3. Components of the system would necessarily need to be lightweight and yet sturdy.

4. Changes in the transducer's environment (e.g., the temperature and pressure drop associated with increasing altitude) must not distort the leakage rate.

The large number of potential leak sources is perhaps the most important consideration of the overall program. A separate transducer and instrumentation channel for each of the separable connections (7200, for example, in the Saturn V propulsion systems) would be highly impractical. A more logical approach might be to monitor system leakages rather than individual joints. One transducer would then measure the accumulative leakage from a particular system. A great number of joints would thus be monitored with a minimum number of flowmeters and instrumentation channels. The leakage would then be plumbed overboard after passing through the flowmeters, thus reducing the potential hazard of leakage.

The most logical choice of leakage detection method would be one using the Hastings-

Raydist or similar flowmeter. This would permit remote monitoring of the leakage by normal instrumentation procedures. Modifications similar to those previously discussed would, of course, be necessary.

SUMMARY OF LEAK DETECTION METHODS

A summary of leak detection methods used at Rocketdyne is shown in Table 4. It should be noted that the indicated use of a Hastings-Raydist type flowmeter system to monitor in-flight leakage is a proposed, but not a proven, method.

Table 4 - Summary of Rocketdyne Leak Detection Methods

	Measurement Capabilities					Practical Applications					
Method	Liquid	Gas	Quantitative	Qualitative	Practical Lower Limit scc/sec	Joint Development	Component Checkout	Engine Checkout	Component Ground Test	Engine Ground Test	Flight Test
Soap Solution		X		X	10^{-1}			X			
Pressure Lockup		X	X	X	10^{-2}			X			
Liquid Submersion		X		X	10^{-1}		X				
Rotameter		X	X		10^{-1}	X	X	X			
Mass Spectrometer		X	X		10^{-10}	X	X				
Sight Glass	X		X		10^{-2}				X	X	
Balloon		X	X		10^{-1}				X	X	
Water Displacement		X	X		10^{-3}	X		X	X	X	
Burst Diaphragm		X		X	10^{-2}				X	X	
Hastings-Raydist Flowmeter		X	X		1	X			X	X	X

CONCLUSIONS

1. Adequate test-stand leakage monitoring techniques have been demonstrated. Based on this experience, the Hastings-Raydist flowmeter appears to be a feasible method for in-flight leakage monitoring.

2. Monitoring leakage during all stages of hardware development is necessary.

3. Techniques for monitoring leakage during engine hot-fire ground tests are more limited than under laboratory conditions.

4. The Hastings-Raydist flowmeter has been shown to be a feasible device for measuring leakage during a hot-fire test. It is moderately reliable for measuring leakage greater than 1 scc/sec.

5. The ability to consistently seal hydrocarbon fuels during F-1 engine operation has been demonstrated.

6. Tolerable levels of leakage must be established (i.e., "zero leakage" must be defined) to properly evaluate the sealing capability of a component.

7. Monitoring accumulative system leakage rather than individual joints offers a direct and more accurate method for determining overall sealing capability.

Page Intentionally Left Blank

A SEPARABLE CONNECTOR DESIGN HANDBOOK

By

F. O. Rathbun, Jr.
Advanced Technology Laboratories
General Electric Company
Schenectady, N. Y.

BEGINNING IN MARCH, 1962, the Advanced Technology Laboratories, under NASA Contract 8-4012, undertook a basic investigation of the fundamentals of separable fluid connector design. The problem was approached by dividing the investigation into two parts, that of the problem of the leakage existing across the interface in the sealing area and that of the design of the supporting structure which holds such interfaces together. After a year of efforts so directed, the National Aeronautics and Space Administration decided to reduce the information pertinent to sealing, and the procedures concerning substructure design to a form where it would be available to the connector designer. The General Electric Company was charged with the responsibility of writing a Design Handbook, suitable for use by designers having less than a college education in some cases. A goal also was to make the Handbook as self-contained as possible such that a designer would find essentially all the information he needed in order to reduce a concept of design to an actual configuration or design layout. The task of writing such a manual was undertaken by G. E. in March 1963 and was completed and placed into the NASA distribution system on April 21, 1965 (although the actual handbook is dated December 1, 1964). (1) *.

At this time, the Design Handbook has been in the hands of potential users for slightly over three months. Certainly, few flanges designed under its procedures are yet in the hardware stage. Those who have approached the separable connector design problem via the procedures of the Handbook will by this time have formed impressions as to the ease or difficulty of its use and its applicability to their particular problems. Certainly, insufficient use has been given of the Handbook to appraise the quality of the design which would result from its use. It is fitting, however, at this time and for this particular audience, to outline the contents of the Handbook, to explain in limited detail the procedures therein, and to discuss philosophically the goals of each of its sections. Also, at this point in time, members of the audience may have accumulated questions pertinent to one or more sections of the manual. It is only proper, then, that authors of the Handbook should be available to you for the possible answering of those questions. That is the case here today and it shall be an intended part of this presentation to receive questions about the handbook and its use.

ORGANIZATION OF HANDBOOK

Of the many aspects of separable connector design, it was decided to organize the handbook in terms of the particular configurations to be established, and to supplement those sections with information pertinent to the general design problem and common to any geometry. Basically, the procedures have been made available for the design of three different types of hardware, namely flanged connectors, threaded connectors, and pressure energized seals. While there are other configurations of wide applicability, such as Marman-type clamps, novel structural joining techniques, and a host of flexible seal configurations, it was felt that procedures general enough in scope only for those configurations acceptable for nearly all applications could be covered. Where particular geometries and flexible seals or structural joining techniques have evolved, companies supplying such configurations have, or should have, established design procedures. It is rather toward the designer who is faced with a typical flange, threaded connector, or pressure energized seal problem where only the inputs with regard to size, temperature, pressure, and environment vary that the Handbook is directed. In line with this, seven sections have been included and are listed in Table 1.

The goals and contents of each section will now be considered in detail.

* Numbers in parentheses designate References at the end of paper.

Table 1 - Contents of Separable Connector Design Handbook

Section	Title
1	Fundamental Considerations of Separable Connector Design
2	Flanged Connector Design
3	Threaded Connector Design
4	Pressure Energized Cantilever Seals and Hollow Metallic O-Rings
5	Leakage Measurement Techniques
6	Material Properties and Compatibility
7	Catalog of Seals

FUNDAMENTAL CONSIDERATIONS OF SEPARABLE CONNECTOR DESIGNS

A given separable connector can be evaluated by consideration of three factors: (1) the leakage rate through the connector under operational conditions, (2) the size and weight of the connector as compared to the duct section which the connector replaces, and (3) the reliability of the connector in maintaining its initial sealing characteristics throughout its operational life.

The problem of designing a given connector can be reduced to two separate problems which, although they can be considered separately, are coupled. Those problems are the interface sealing problem and the substructure design problem. This section deals with the modes of leakage possible in a separable connector, the surface deformation required of the interface surfaces, and some of the causes of development of leakage in a connector. The section is intended to be educational in nature and does not cite procedures for the design of any particular connector configuration. The intent here is that the connector designer, starting from scratch, can gain greater insight into the overall problem and put his tasks into perspective better if he has read the first section.

In particular, the problems of permeation flow and porosity (generally negligible in a separable connector) are discussed quantitatively; the most important leakage mode, that of flow through the sealing interface is discussed both qualitatively and quantitatively, with the equation for leakage flow under both viscous and molecular effects given as a function of the meaningful parameters.

The basic problem of attaining a seal in a separable connector is one of insuring that two surfaces, of some materials, some shapes, and some surface finishes, are held in close enough proximity that an adequate barrier to flow is effected. Based on experimental evidence, and reported upon in Reference 2 at this conference last year, the five regimes of material deformation that exist when two metal surfaces are brought together for the purposes of effecting a seal are cited. Also, for flat metal gaskets and flat metal-to-metal seals, the stresses required as the function of surface finish are listed, shown here in Table 2 and Table 3. The problems associated with the use of plastic seal materials and elastomeric seal materials are also briefly discussed. The positive attributes of incorporating shear deformation into seals wherein elastic-plastic materials are used is cited. Causes of the onset of leakage such as relaxation of seal and elastic components, the sensitivity of seals to load removal, and the shifting of mated surfaces are mentioned briefly.

After the designer has familiarized himself with the general problem and the pitfalls into which he may fall, he may then proceed to his

Table 2

METAL-TO-METAL SYSTEMS - REQUIRED SEALING STRESSES

Sealing Surface	Required Stress
Radially Ground ~ 40 μ -in, rms	$2.3\sigma_y$
Circumferentially Machined ~ 100 μ in, rms	$0.63\sigma_y$

Table 3

METAL GASKETS - REQUIRED SEALING STRESSES

Sealing Surface Finish	Required Stress
Diamond Burnished, ~ 4 μ -in, rms	$1.96\sigma_y$
Radially Ground ~ 40 μ -in, rms	$2.75\sigma_y$
Fine Circumferential Machining (100 μ -in rms)	$1.46\sigma_y$
Coarse Circumferential Machining (300 μ -in rms)	$1.96\sigma_y$

main design configuration at hand, either flange, threaded tube connector, or pressure-energized seal.

FLANGED CONNECTOR DESIGN

The section on flanged connector design presents a more rigorous way of analyzing flanged connectors than has been commonly used in the past. It gives a more complete picture of how the stresses and deformations are distributed and thus makes possible better optimization. Detailed design procedures are available for establishing flange configurations.

Four possible flanged connector configurations are possible under the procedures listed, those of two integral flanges with contact outside the bolt circle and without contact outside the bolt circle and those of one integral flange and one loose flange with the same possibilities of contact outside the bolt circle. Schematically, the four combinations are shown in Figures 1 and 2. Factors considered in the analysis include the effects of friction forces at the gasket, friction forces between loose and lap flanges, and eccentric loading on bolts. The basic approach to design in all four configurations is that of establishment of a preliminary design, sophisticated analysis of that design, and perturbation of that design based on a comparison of stresses with some predetermined criterion. Those parameters needed by the designer to begin his endeavor are the external loading, including pipe axial load and bending moment, pipe size and fluid identification, and fluid pressure-temperature-time history.

The actual design procedures are divided into four separate sections, those dealing with each of the principal configurations. Through the use of tables, simple equations, and design rules, an initial layout of the designed flange can be affected. Although the preliminary design layout is based on rational choice of parameters, the simplicity of the rules yield a design which is not guaranteed to be conservative nor in any case an optimized one. Hence, analysis of the stresses and deformations in such a flange under the applied loads and internal pressure must be accomplished.

To do this, cylindrical shell theory is called upon, along with flat plate theory. It is in this analysis that the rigorous evaluation of the pre-

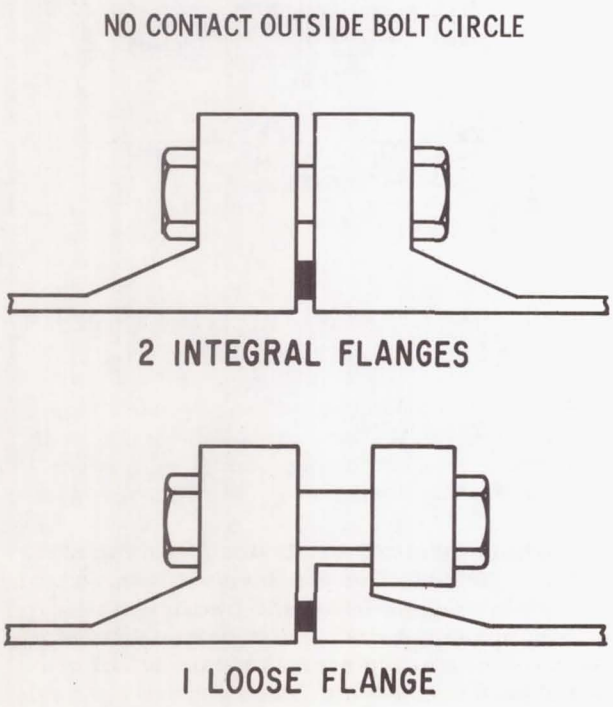

Fig. 1 - Types of Flanges Configurations

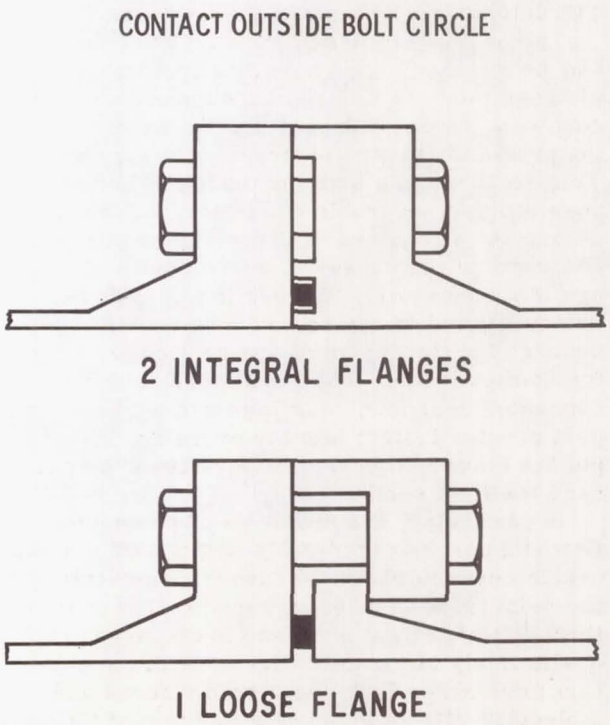

Fig. 2 - Types of Flanges Configurations

liminary design is done. The duct-hub-flange combination is broken into a minimum of five sections to be analyzed. The deformation of each piece is then determined using elastic stress analysis. The equations for such analysis are, when viewed "from afar", somewhat complicated; however, they are written such that the coefficients of the various terms can be calculated via the use of a table, and the use of the equations is accomplished proceeding from the duct toward the flange, thus never requiring the solution of a large number of simultaneous equations. The underlying theory on which the equations are based is found in an appendix to the chapter.

To aid the designer in the use of the initial design layout procedures and the analysis procedures, design examples have been cited. Each possible configuration has been laid out using each equation of the initial design procedures. An example of the simplicity of the calculations is shown in Figure 3. The equations for the

THE FLANGE THICKNESS (HFL) IS

$(HFL) = (COL.7)\sqrt{3(SB)/(SF)}$ $(HFL) = 0.340\sqrt{3\frac{100\,000}{100\,000}}$ $(HFL) = \boxed{0.589\ IN.}$

THE FLANGE OUTER RADIUS (RFLOT) IS GIVEN BY (RFLOT) = 2 (RBLT)-R ACCORDING TO PARAGRAPH (e) P. 2-34

RFLOT = 2 x 6.5 - 5 = $\boxed{8\ IN.}$

THE RADIAL WIDTH OF THE RAISED BEARING SURFACE AT THE OUTER EDGE IS

RFLOTB = 0.1 [COL.(I)] RFLOTB = 0.1 $\boxed{0.0748}$

THE HEIGHT OF THIS SURFACE IS

HBRG ≥ 0.002 COL.(I) HBRG ≥ $\boxed{0.001496}$

THE HUB THICKNESS IS

$(THBI) = \frac{2.5R\ P\ MAX\ OPER}{\sigma\ ALLOW}$

Fig. 3 - Sample Preliminary Flange Design Calculations

analysis of one of the combinations of design, that of integral flanges without contact outside the bolt circle are presented in detail as a design example. Matrix formulation of the equations has been used for clarity of presentation.

THREADED CONNECTOR DESIGN

The threaded connector design procedures can be used for two purposes, that of designing a connector for some intended application or that of checking the adequacy of a design already available. In that many separable connector designs are available commercially, it is the philosophy of the Handbook that, upon the determination of design requirements, available threaded connector designs should be sought prior to designing a new one. This varies from the philosophy of designing a flange connector based on each application.

In that a threaded connector can be viewed as a combination of elastic springs representative of the union, flange, and nut, a series of spring stiffness for each component is found for a given design. Again, because of the sophistication of analysis, the technique of design is the same as in Section 2, that of establishing an initial design, analyzing that design, and then making perturbations upon the design until an optimum configuration is found.

The generic threaded tube connector is a configuration such as shown in Figure 4 wherein a nut, union, flange, seal, tube-to-union junction, and tube-to-flange junction are shown. Any

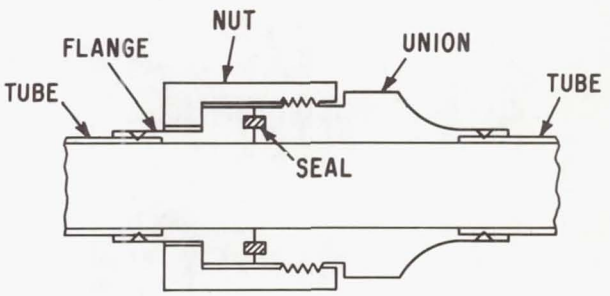

Fig. 4 - Typical Threaded Connector Configuration

threaded tube connector possessing such a combination wherein the seal can be described with regard to a necessary space envelope and sealing loads can be designed by the procedures listed.

Buttress threads are recommended suitable for union and nut. Elastic shell analysis is used in the analysis, with the coefficients in the equations being used determined by consideration of short cylinders where shear deformation becomes a factor.

To aid the designer in use of the procedures, a complete case history of the design is included as a design example. As a measure of the

sophistication of the procedures, the necessary inputs for use of the technique are shown in Figure 5. It can be stated that the difference between a successful threaded tube connector and an unsatisfactory threaded tube connector need not be an alteration of configuration or the use of an exotic design but merely a variation in the dimensions of standard configurations.

THE DETAILED DESIGN INPUT REQUIREMENTS ARE:

TUBING
- MATERIAL
- OUTSIDE DIAMETER
- INSIDE DIAMETER

FLUID CONTAINED IN THE TUBING
- NAME AND CHEMICAL COMPOSITION
- OPERATING PRESSURE
- CONSTANT PRESSURE
- CYCLICAL PRESSURE
- NUMBER OF CYCLES OF PRESSURE
- TEMPERATURE

ENVIRONMENTAL CONDITIONS
- SURROUNDING FLUID
- AMBIENT PRESSURE
- AMBIENT TEMPERATURE

EXTERNAL LOADS
- CONSTANT FORCE
- CYCLICAL FORCE
- NUMBER OF CYCLES OF FORCE
- CONSTANT TRANSVERSE MOMENT
- CYCLICAL TRANSVERSE MOMENT
- NUMBER OF CYCLES OF MOMENT

ALLOWABLE LEAKAGE LEVEL

Fig. 5 - Threaded Tube Connector Design Input Requirements

PRESSURE ENERGIZED CANTILEVER SEALS AND HOLLOW METALLIC O-RINGS

The problem of cantilever pressure energized seal design is an order of magnitudes simpler than that of designing a complete connector, whether it be flanged or threaded tube type. It has been determined by analysis that for the range of dimensions applicable to cantilever type seals beam analysis is adequate and circular plate analysis need not be utilized. In other words, the effect of tangential stresses does not present sufficient cause for sophistication of analysis. Because of the simplicity of the basic problem of cantilever seals design, rather than require that an initial design be effected and then analyzed and then altered, the problem has been reduced to one of merely following a set of design rules to synthesize the final design directly. Step by step procedures are listed for the design of straight legged cantilever seals, angled cantilever seals, and tapered cantilever seals. The three common possibilities of design are shown in Figure 6. Even with such simple geometries, the equations governing the design are extremely complicated. Hence, all equations have been

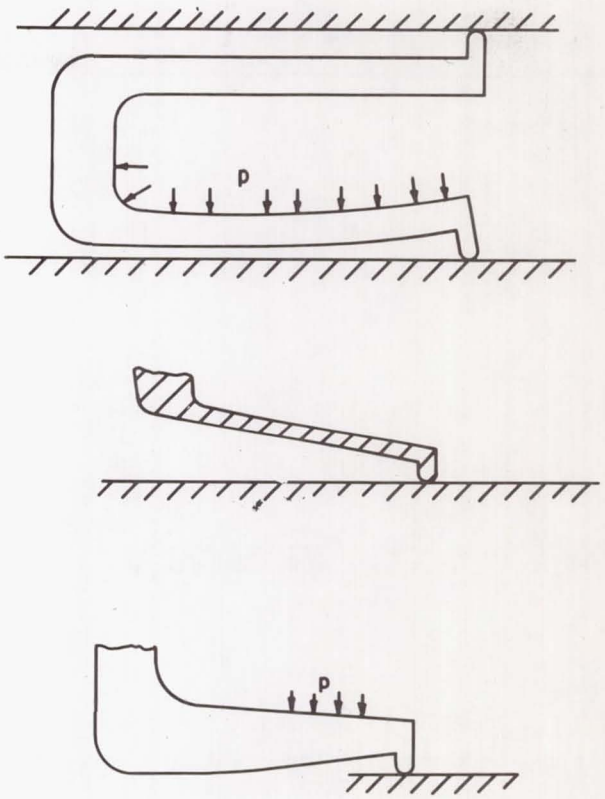

Fig. 6 - Schematic of Three Designs of Cantilever Seals.

reduced to nomograph form, resulting in a great burden being lifted from the designer. A typical nomograph and the equation from which it is derived is shown in Figure 7.

For the hollow metallic O-rings, the analysis is nowhere near as simple and only the spring stiffnesses for typical seals are cited.

LEAKAGE MEASUREMENT TECHNIQUES

The National Aeronautics and Space Administration, for separable connectors in its launch and deep space vehicles, requires leakage level far less than those acceptable to most other industries. Indeed, the term "zero leakage" has meaning. It is a design goal. Hence, liquid fluid leak tests where observation of liquid determines the presence of leakage, and the placing of a gas-filled connector under water while visually observing bubbles do not necessarily deter-

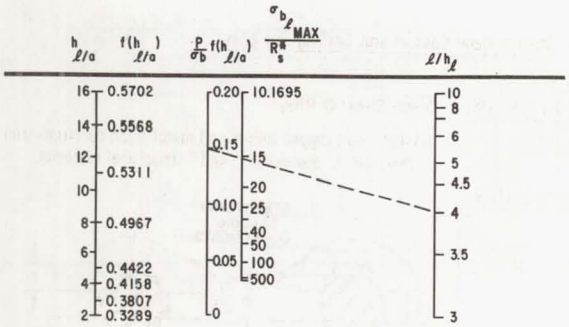

$$\frac{6R^*_s}{\sigma_{b\,MAX}} = \frac{3P}{\sigma_b} f(h_{\ell/a}) - (h_{\ell/a})^2 = \frac{3P}{\sigma_b}\left\{1 + \frac{\left[6(h_{\ell/a}-1) - 9(h_{\ell/a}-1)^2 - 6(h_{\ell/a})^2 \log h_{\ell/a} + 2(h_{\ell/a}-1)^3\right]}{(h_{\ell/a}-1)\left[(h_{\ell/a}-1)(3h_{\ell/a}-1) - 2(h_{\ell/a})^2 \log h_{\ell/a}\right]}\right\} - (h_{\ell/a})^2$$

Fig. 7 - Nomograph for Pressure Energized Seal Calculations

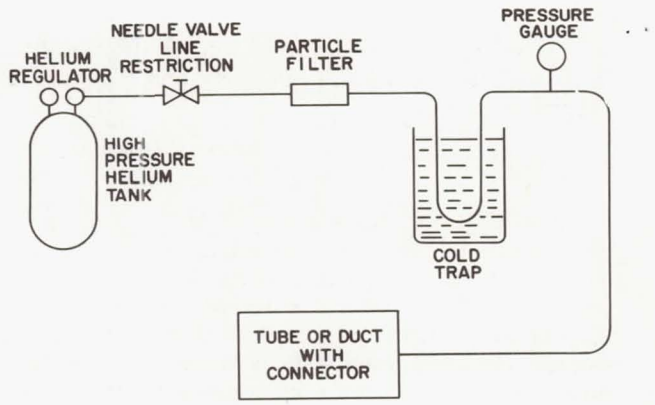

Fig. 8 - High-pressure System

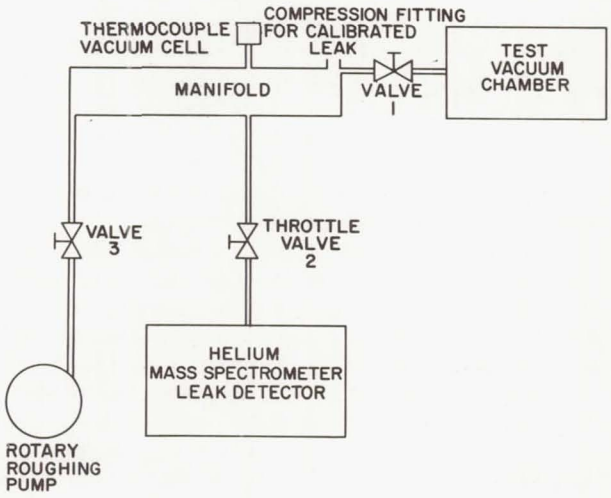

Fig. 9 - Leak Detector - Vacuum System

mine the adequacy of a connector design. Because of the smallness of the required leak levels, particular means for measuring leaks during a connector development program are necessary. In general, a helium spectrometer provides an adequate test, although other detection techniques such as the soap bubble test, immersion bubble test, sonic leak detection, halide torch leak detection, and constant volume pressure drop techniques offer some success in certain applications. This section of the handbook is devoted primarily to the description of an adequate helium mass spectrometer leak detection and measurement facility, to include a listing of mass spectrometers, calibrated helium leaks, detailed description of an adequate high pressure system (including particle filters and cold traps), leak detection vacuum systems, and detailed drawings and parts list for necessary components for testing tube connectors up through one-inch size. Figures 8 and 9 shown prescribed high pressure and vacuum system layouts.

MATERIALS PROPERTIES AND COMPATIBILITY

The awesome task of assembling a compendium of applicable properties for structural and sealing materials would be overpowering. Such would not be realistically possible in that new materials are made available continuously, and material properties vary within each material as a function of its manufacture and treatment. Because of these problems, a short chapter listing only widely used materials and their mechanical properties is present. The effect of temperature is considered with regard to strength, along with a measure of its compatibility with rocket propellants. A list of refer-

ences wherein more detailed information both with regard to material property and compatibility is included.

CATALOG OF SEALS

The most desirable solution to the sealing interface problem would be one wherein the problem could be solved in generic terms, and, for any seal configuration, material, and surface finish, an equation would be available for its design and evaluation. Such is not the case today, and based on the size, configuration, and materials, different seals respond in strikingly different manners. In that a wealth of data became available as a result of basic experimental studies on the sealing problem, a catalog of seals has been incorporated into the Handbook such that the information would be available to the designer. The catalog includes, at present, sixteen seals, categorized as metal-to-metal seals, flat metal gaskets, shear metal gaskets and sealing surfaces, plastic flat gaskets, elastomeric flat gaskets, and a few miscellaneous gaskets. Each entry in the catalog cites important characteristics such as material, temperature limitations, load deflection characteristics, sealing characteristics, advantages, and disadvantages. A sample of such an entry is shown in Figures 10, 11, and 12 for a metal shear O-ring configuration.

It is intended that, as more information concerning each of these entries becomes available and more and different seals become qualified by tests, new entries can be made. Those listed at present are those tested by the Advanced Technology Laboratories during the investigations on which the Handbook is based.

HANDBOOK IN PRESPECTIVE

When a component for any system is to be designed, a compromise must be made by the designer with regard to the degree of effort he may place toward optimizing the design as opposed to the gain in operational efficiency by attaining that design. In the case of separable fluid connectors, it is of note to compare the degree of sophistication in Appendix 2, Section 8, of the ASME Boiler and Pressure Vessel Code, Unfired Pressure Vessels. Therein, quite simplified rules for sealing loads, and flange design are given. The flanges thus designed and appraised are quite adequate for the use intend-

7.1.3 Shaped Metal Gaskets and Sealing Surfaces

7.1.3.1

CLASSIFICATION: Metal Shear O-Ring

MATERIAL: Gasket - soft copper (other soft metal such as aluminum nickel, etc.). Recesses "rigid" structural material.

CONFIGURATION:

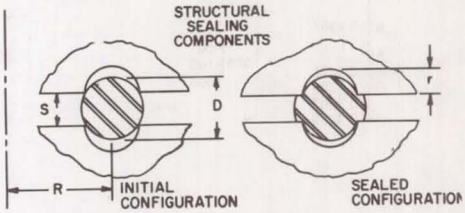

TEMPERATURE LIMITATIONS: Determined by creep properties of O-ring material.

LOAD DEFLECTION CHARACTERISTICS: (for copper at room temperature): See Figure 7.2

SEALING CHARACTERISTICS: (for copper at room temperature): See Figure 7.3

ADVANTAGES:
1. Utilizes principle of shear deformation.
2. Low sealing loads.
3. Insensitive to load removal if initially loaded well above initial sealing stress.

DISADVANTAGES:
1. Requires close tolerances to insure positioning of O-ring in recesses, particularly serious at large values of r.
2. Requires separate gasket.

COMMENTS:
1. Data based on tests where R = 0.5 inch, r = 0.02 incl D = 0.073 inch.
2. Structure recess material should have yield strengtl at least three times higher than O-ring material.

Fig.10- Sample Seal Configuration Data - Metal Shear O-ring

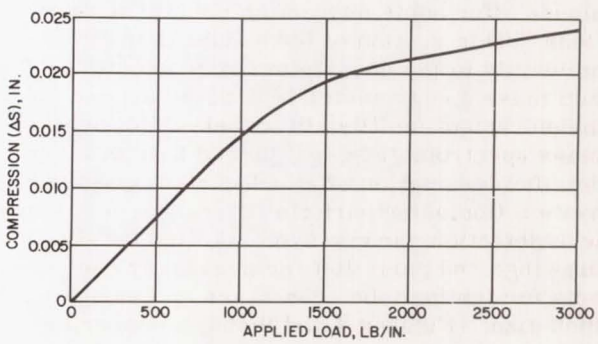

Fig. 11- Load Deflection Characteristics for Typical Metal Shear O-Ring Seal

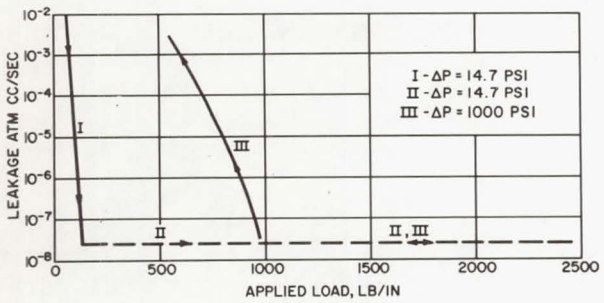

Fig. 12- Typical Leakage - Applied Load Response for Metal Shear O-Ring Seal

ed, namely chemical plants, steam power plants, and other earth-bound uses. In general, it does not pay to increase the sophistication of design techniques to any large extent in order to either reduce the weight of a connector or attempt to reduce the leakage. It would be extremely desirable to accomplish a design for an aerospace application with the same simplicity used in Appendix 2 of the Boiler Code. However, such is not possible in that optimization of design denotes sophistication of analysis. Hence, one is faced with having to spend more time in designing a separable connector for aerospace than he might initially desire. In the Separable Connector Design Handbook, the procedures, particularly for analysis (not those for initial design establishment) are more intricate than would be wholly desirable. Desk calculators must be used; digital computers simplify the work even more. However, it is felt that the resultant configurations will prove successful, where a design gained by other means will not be as light in many cases or, contrariwise, may not operate satisfactorily.

Recognizing, however, that some time must be spent in attaining design for both flanges and connectors under the handbook procedures, NASA has charged the Advanced Technology Laboratories with reducing those procedures to digital computer programming. Such is now being accomplished. It is felt that the procedures for cantilever pressure-energized seals have already been reduced to the state where a designer without a college technical degree can utilize them.

The extent to which the procedures in the Handbook have been evaluated are limited, at present, to a few configurations. Until such time as usage has shown the worth of connectors thus designed and used, the Handbook finds itself in the position of any new work, subject to minor modifications and the test of time.

The Handbook is available to users through the Defense Documentation Center or the NASA Representative, Code CRT, Scientific and Technical Information Facility, Post Office Box 5700, Bethesda, Maryland.

REFERENCES

1. F. O. Rathbun, Jr., Design Criteria for Zero Leakage Connectors for Launch Vehicles, "Separable Connector Design Handbook," NASA 8-4012, December 1, 1964.

2. F. O. Rathbun, Jr., "Five Regimes of Metal-to-Metal Sealing," Proceedings of the Conference on Design of Leak-Tight Separable Fluid Connectors, G. S. Marshall Space Flight Center, March 24-25, 1964.

APPLICATION OF LOW PROFILE FLANGE DESIGN FOR SPACE VEHICLES

By

W. P. Prasthofer
National Aeronautics and Space Administration
Marshall Space Flight Center
Huntsville, Alabama

ABSTRACT

There is evidence that the "low profile" flange configuration may be used advantageously in bolted flange connections.

Test data substantiate the concepts of the "low profile" design.

The application of this flange for short tubes, manhole, and manhole covers will increase the reliability, and reduce weight and space for the installation.

The low profile flange equalled or exceeded the performance of the Taylor forge-type flange. The tested specimens were up to 37 percent lighter and also less bulky.

No data are available yet on this flange design used on long tube connections. Additional testing is underway. Results will be published soon.

SUMMARY

There is evidence that a new approach to the design of bolted separable connectors may be used advantageously in missile and space vehicles as well as in other applications.

Test data substantiates concepts of the "low profile" design.

The application of this flange design for short tubes and manholes will increase the reliability of flange connections by reducing weight.

The "low profile" flange equalled or exceeded the performance of the Taylor Forge type flange. The tested low profile flanges were lighter (up to 37 percent) and were less bulky. Operating stresses in the "low profile" flanges are much more uniform and are lower than in conventional flanges.

No experience data are available yet on the behavior of this flange design as used on longer tube connections, but additional testing is underway. Test results will be published as time and accomplishment warrant.

BOLTED FLANGE JOINTS have been used extensively throughout the whole aerospace industry in missile and spacecraft design. These flange connections are exposed to all conceivable environments, such as high and low temperature, high and low pressure, exiting vibration, shock, pressure peaks, and differences of expansion and contraction of gasket and flange material as well as of the bolts themselves. These conditions made it more and more difficult for the designer to fulfill the requirements of leak tight connectors. We are all aware of the great risk to mission and of missile loss due to flange leakage which can cause an explosion, a pressure loss, or propellant or gas depletion, etc.

In man-rated vehicles, safety requirements do not permit leakage potentials which would jeopardize the astronaut's life. There has been a tremendous effort throughout the whole country to improve separable connectors. The results obtained are promising. We are not too far from reaching our final goal - absolutely no leaks.

This report introduces a concept of a flange design that is not yet very well known but test results are encouraging for the application of this configuration in the missile and spacecraft design as well as for other applications.

The basic principles of this design concept were developed and presented by Professor Ir. H. H. Boon and Mr. Ir. H. H. Lok in their article Investigation on Flanges and Gaskets (Untersuchungen an Flanschen and Dichtungen) published December 1958 in the Terman technical periodical VDI #100-34. This theory has been used as a basis for the development of equations for the design of "low profile" flanges. for practical applications.

BASIC THEORY OF THE "LOW PROFILE" FLANGE FROM THE REPORT INVESTIGATION ON FLANGES AND GASKETS BY PROF. E. F. BOON AND H. H. LOK DELFT, NETHERLANDS

From a comparison of the results of tests conducted on models and full size flanges, simple non-dimensional formulas were derived for the design of the low profile flange.

Because of the mathematical interrelation of loads and flange rolling (radial rotation), and since flange distortion can be measured quite reliabily, this interrelationship is used for determining the highest possible flange load. Flange Loads also have a great influence on the sealing characteristics of a joint. Model tests made it possible to determine the behavior of a flange under pressure and temperature fluctuation.

For the gaskets, it is known that the sealing characteristics depend on many factors which are often hard to define and standardize such as: the surface finish of the gasket and the flange, the influence of temperature, the applied pressure as a function of time, etc. It is also known that the method of leakage detection and the determination of the magnitude of a leak present still more problems, certainly at extremely high pressure and high and low temperature ranges.

In the last few years, major steps have been made in gasket design and in the development of new materials for gaskets.

The characteristics of the "low profile" flange configuration are as follows: (see Fig. 1 and 1a)

a. The distance "a_i" between the force acting along the tube and the one acting on the bolt is kept a minimum.

b. The axial tube pressure load F_T and gasket load F_D fall almost in the same line. This is done so that when F_T caused by pressurizing the tube is added to the resultant of the couple F_F and F_D, the relative movement of their lines of action is very slight and the resultant of tube load F_T and gasket load F_D do not shift relative positions. Thus, the flange will not deflect (rotate) additionally. For this assumption, the gasket is considered to be nonflexible (thin metal, for example). By placing the gasket close to the inner edge of the flange, it will oppose a flange rotation. In addition, the influence of the radial action force must be accounted for as it affects the flange distortion by tending to rotate it additionally, because the internal pressure, acting radially, stretches the tube wall more than the flange.

c. The neck is not thickened. This reduces the moment arm which simplifies the calculations since the position of the plastic joint is fixed at the transition from the tube to the flange.

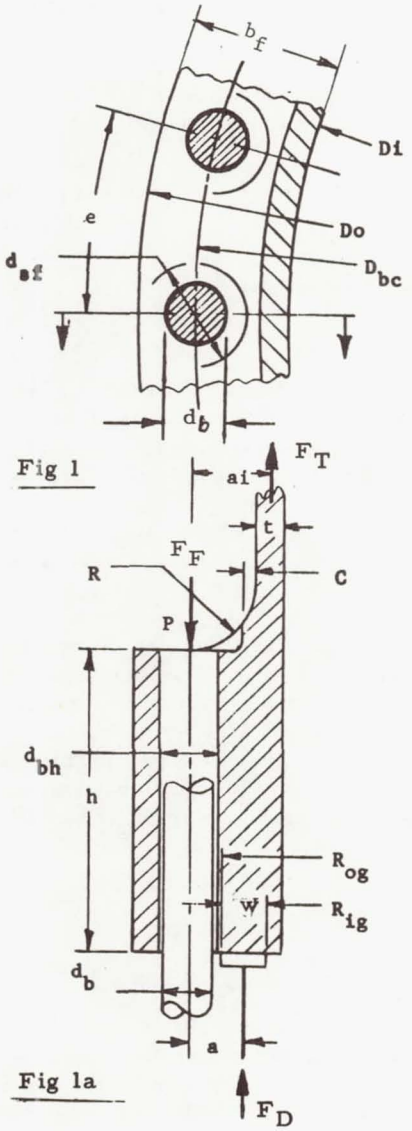

Fig. 1 - Cross-section of the low profile configuration

d. Size and type of gasket are chosen to suit the flange.

e. The bolts are under stress because of internal pressure which in turn acts on the area of the bolt circle diameter.

f. Creep of the material for bolts and flanges used can normally be neglected but if it is expected then insert the value for the pressure that will cause an elongation of 10^{-3}% after testing for 1,000 hrs.

Preliminary estimation of flange dimensions.

The wall thickness "t" of the tube has a value of

$$\frac{t}{R_i} = \frac{p_i \cdot N_f}{F_{yf}} \qquad (1)$$

where N_f assumes a value of 1.5.
The number of bolts "n" is expressed by

$$n = \frac{2\pi \cdot R_{bc}}{e}$$

according to assumption (e)

$$\pi \cdot R_{bc}^2 \cdot p_i = \frac{2\pi R_{bc}}{e} \cdot \frac{\pi \cdot d^2}{4} \cdot \frac{1}{N} \cdot F_{yb} \qquad (2)$$

Then from equation (1) and (2) we obtain

$$\frac{d}{t} = \frac{2}{\pi} \frac{R_{bc}}{R_i} \cdot \frac{F_{yf}}{F_{yb}} \cdot \frac{e}{d} \qquad (3)$$

The ratio R_{bc}/R_i is dependent on the internal pressure and the smallest possible bolt diameter and should fall between 1.05 and 1.5.

It is recommended that the bolts be as close as possible to the tube wall; therefore, many small diameter bolts should be used instead of fewer large diameter bolts.

Select bolt material having yield stress considerably higher than that of the flange or tube material.

According to this reasoning, one derives from equation (3)

$$\frac{R_{bc}}{R_i} = 1.2 \quad \text{and} \quad \frac{F_{yf}}{F_{yb}} = \frac{1}{3}$$

as well as $\frac{e}{d} = 4$

$t \approx d$

A flat cover base of the height "h" is regarded as a plate freely supported at the bolt circle. Then the following is considered valid through the elastic range.

$$\left(\frac{h}{R_{bc}}\right)^2 = 1.25 \frac{p_i N_f}{F_{yf}} \qquad (4)$$

For a rigid plastic material the plate begins to deform at:

$$\left(\frac{h}{R_{bc}}\right)^2 = \frac{2}{3} \frac{p_i}{F_{yf}} \qquad (5)$$

and it is advisable to choose:

$$\left(\frac{h}{R_{bc}}\right)^2 = 1.25 \frac{p_i}{F_{yf}} \qquad (6)$$

If in a compact flange with a cylindrical neck, the influence of the flange neck is neglected, then the internal tangential moment in the flange M_t resists the bolt moment in a flange sector of arc length 1 (one), i.e., $M_s/2\pi$. The forces acting on this flange sector are shown in Fig. 2 and 2a. If after deducting the

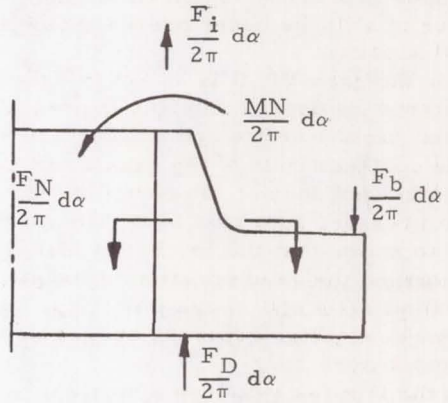

Fig. 2

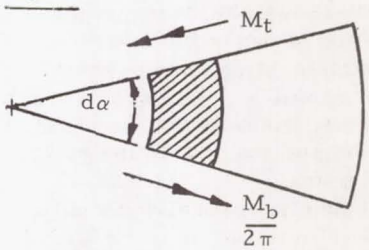

Fig. 2a

Axial loads: Axial internal pressure load F_{ii} gasket load F_D; external bolt load F_b.

Radial loads: Sheer load in flange neck F_N; radial internal pressure load; radial portion of the tangential pressure

Moments in the radial plans: Radial portion of the internal tangential moment M_t; internal moment in flange neck M_{Ni} moment of the sheer load in the flange neck; external boltload M_b. $d\alpha$; sector angle

Fig. 2 - Forces acting on flange sector

bolt hole the total stressed flange width is
2t + 1.3d
and the moment arm of the bolt is

$$a = 1.1d + 1.5t$$

then the value of $M_t = M_s/2\pi$

or with $d \approx t$

$$\left(\frac{h}{R_{bc}}\right)^2 \approx 1.6 \frac{p_i}{F_{yf}}$$

Using a safety factor factor of 1.5 we obtain

$$\left(\frac{h}{R_{bc}}\right)^2 \approx 2.4 \frac{p_i}{F_{yf}} \qquad (7)$$

The greatly simplified formulas recorded here show the relationship between the principal dimensions of a flange for a pressure vessel as follows:
Proportionality relationship of wall thickness "t" and tube radius "R_i" per equation (1).
Proportionality relationship of wall thickness "t" and bolt diameter "d" equation (3).
Proportionality relationship of flange height "h" and bolt circle radius R_{bc} per equation (7).
In these simplified equations of course the influence of the forces in the neck are not considered.
For the present, one can put in flanges with cylindrical necks

$$\left(\frac{h}{R_s}\right)^2 \approx 1.5 \frac{p_i}{F_{yf}} \qquad (8)$$

whereby the factor 1.5 is to be considered as a function of h/R_{bc} to be verified by the final test results.
Figures 3, 4 and 5 show how the shape of the flange ND 25NW1000 according to DIN (German Industrial Standards) changes when the preceeding equations or formulas are used.
The gasket dimensions are derived from the equilibrium of forces for the installed and operating condition. For the installed (unpressurized) condition the following equation applies:

$$\pi R_{bc} p_i = 2\pi . R_i . W_i . p'_G$$

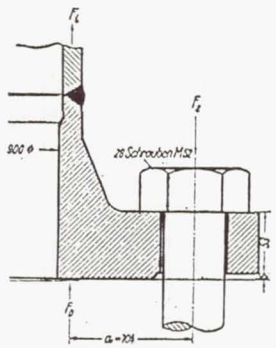

FIGURE 3

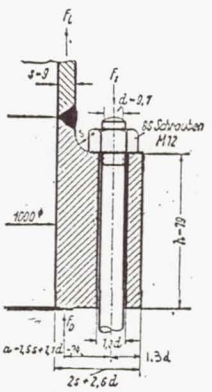

FIGURE 4

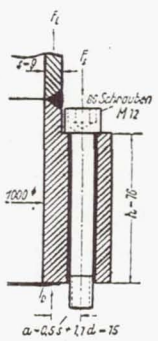

FIGURE 5

Fig. 3 - 4 - 5 - Changes in flange configuration resulting from application of different formulas

For the operating (pressurized) condition the equation is:

$$\pi R_i^2 p_i + 2\pi . R_i . W . p_G = \pi R_{bc}^2 p_i \; \pi . R_{bc}^2 . p_i$$

By again putting $R_{bc} = 1.2 R_i$ one obtains

$$\frac{2w}{1.2R_{bc} - R_i} \approx \frac{p_i}{p'_G}$$

and with $P_G > p_i$ we get the condition

$$\frac{2w}{1.2\,R_{bc} - R_i} < 1$$ which is always satisfied.

DERIVATION OF FORMULAS FOR THE DESIGN

Summarizing, it is established that the dimensions of the wall, flange and bolts, can first be approximated according to the following formulas:

1. $t = d$

2. $$\frac{t}{R_i} = e_1 \frac{p_i}{F_{yf}}$$

where $e_1 = 3/2$ for cylindrical tubes

$e_1 = 3/4$ for flanges on spheres

3. $$\frac{W}{R_i} = e_2 \frac{p_i}{p_G}$$

where e_2 is between .55 and 1.15

4. $$\left(\frac{h}{R_{bc}}\right)^2 = e_3 \frac{p_i}{F_{yf}}$$

where $e_3 = 1.25$ for circular plate

$e_3 = 1.5$ for a flange with cylindrical neck and

$e_3 = 2.4$ for a free flange

These formulas are dimensionless. They furnish the relations between the dimensions of the tube, the bolts, and the gaskets as a function of the proportion between internal pressure and stress; they are merely to enable a first estimate of the flange dimensions.

These formulas are not valid for conduit flanges unless external forces and moments are taken into consideration. The influence of corrosion and of impact forces in the system have likewise not been considered.

Using the above mentioned theory and combining it with existing theories on Taylor forge flanges, the following procedure to calculate dimensions of a low profile flange has been derived.

Flange design procedure

There are many variables and unknown parameters to consider in designing a flanged joint. The variables can be controlled by setting limits on design criteria, choice of materials, etc.; but for the unknowns, such as effects of temperature and other conditions, reasonable assumptions based on experience and judgment must be made until more data have been obtained.

Step one (Data Compilation)

Gather all known data (operating pressure, operating temperature, operating media, flange and gasket materials, size, external forces, available space, type of fastener, etc.). Establish criteria and factors for:

a. Performance and reliability required.
b. Weight restrictions.
c. Other items that could affect the design.

Step Two (Calculation of Wall Thickness)

Calculate the wall thickness (t) of the tube or vessel. Ordinarily, this will have been done already, but if not, the calculation can be performed with the usual formulas for pressure vessels:

$$t = \frac{p_i D_i N_f}{2F_{yf}} \quad \text{(cylinder)} \qquad \text{I}$$

Where:

P_i = Design internal pressure

D_i = Inside diameter of tube

N_f = Safety factor applied to flange material

F_{yf} = Yield stress of flange material

Step Three (Preliminary Determination of Bolt Size)

The bolt size will determine the flange width. It has been shown previously that a relatively high, narrow flange will be much more stable than a low, wide flange with approximately the same cross-sectional area. Therefore, the smaller the diameter of the bolt that is used, the narrower the flange may be. An assumption can be made at this stage--based on experience and judgment--for the smallest practical bolt diameter (d_b).

Step Four (Calculation of Bolt Circle Diameter)

With the bolt size tentatively established, the bolt circle diameter (D_{bc}) can then be determined by the following equation:

$$D_{bc} = D_i + 2t + 2C + d_{sf} \qquad \text{II}$$

Where:

d_{sf} = Spotface diameter

C = Minimum practical clearance between spotface and tube wall

The spotface is selected on the basis of wrench or washer requirements, whichever is applicable. The spotface diameter should be held to a minimum.

Step Five (Calculation of Flange Width)

Since the flange will be relatively high, there is no need for excessive edge-distance from the bolt circle to the outside diameter of the flange. Unless conditions dictate otherwise, an edge-distance of one nominal bolt diameter from the bolt circle to the outside diameter should be used. Now, we can find the outside diameter (D_o) and flange width (b_f) using the following equations:

$$D_o = D_{bc} + 2d_b \qquad \text{III}$$

$$b_f = \frac{D_o - D_i}{2} \qquad \text{IV}$$

Step Six (Calculation of Gasket Width)

For relatively low pressure (up to about 1,000 psi) a soft, flat gasket can be used to advantage. For higher pressures, a pressure-energized gasket of some type should be used. The problem of the gasket has been amply covered in other works; but, a useful formula for determining the width (w) of a soft, flat gasket is as follows:

$$w = \frac{p_i (R_{bc} - d_b + R_i) N_g}{2(F_{ug} - 2p_s)} \qquad \text{V}$$

Where:

F_{ug} = Ultimate or crushing strength of gasket material

N_g = Factor of safety for gasket

With the gasket width established, the inside and outside diameters may be determined. Whether the gasket will lie near the inside diameter of the flange, or near the bolts, will depend on the prevailing conditions and the judgment of the designer. However, the following items should be considered.

a. Placing the gasket close to the inside diameter of the flange will be advantageous because it minimizes the axial pressure load affecting the joint; also, any additional flange-rolling caused by pressurizing will be held to a minimum, because the moment arms between the tube wall and bolt and the gasket and bolt are more nearly the same. A disadvantage of this arrangement is that there is no locating ring or guide and the gasket could slip out of place causing trouble.

b. If the gasket is placed near the bolts, the bolts act as a guide to keep the gasket in position. This arrangement has the disadvantages of increasing the rolling phenomena when pressurizing, and of permitting the maximum axial pressure load to exist.

Step Seven (Calculation of Gasket Load)

After the gasket dimensions have been determined, calculate the total initial gasket load (P_g) with the following equation:

$$P_g = \pi p_i \left(\frac{R_{og} + R_{ig}}{2}\right)^2 + 2\, p_s\, w \left(\frac{R_{og} + R_{ig}}{2}\right) \qquad \text{VI}$$

Where:

R_{og} = Outside radius of gasket

R_{ig} = Inside radius of gasket

Step Eight (Calculation of Number of Bolts)

Calculate the number of bolts (n) required with the following equation:

$$n = \frac{P_g N_b}{P_{yb}} \qquad \text{VII}$$

Where:

N_b = Safety factor for bolt

P_{yb} = Yield load for bolt

Because bolt torques are subject to many variants, a high safety factor should be incorporated to ensure that the yield stress of the bolt is not exceeded. Other, more accurate methods allowing better employment of the bolt strength, have been used for determining bolt pre-load, but none of these methods have been found satisfactory for general use. A safety factor utilizing approximately 1/2 to 2/3 of the yield strength of the bolt is satisfactory, except in cases in which no lubricant is used (lubricant is mandatory in critical applications), and the

torque/tension ratio varies considerably.

Step Nine (First Design Check)

Bolt spacing (e) may be determined by dividing the circumference of the bolt circle (D_{bc}) by the number of bolts (n)

$$e = \frac{\pi D_{bc}}{n} \qquad \text{VIII}$$

At this point, the question of practicality should be introduced. If the bolt spacing is less than three times the nominal bolt diameter, a larger bolt should be used (or possibly a different bolt material). If it is decided that a larger bolt should be used, backtrack to Step Three and redesign the flange based on the larger bolt size. Step Five and Step Six may be used as originally calculated, because no significant change will result in these steps.

If the bolt spacing is greater than eight times the nominal bolt diameter, a smaller bolt may be used; however, this depends on the judgment of the designer or engineer. This does not preclude the use of bolts that are larger than necessary, but caution should be exercised, when using excessive bolt capacity, to specify a torque value that will not overstress the flanges or gasket.

Step Ten (Calculation of Flange Height)

The height of the flange depends primarily on the stresses introduced by the bolt-to-gasket and bolt-to-tube wall moments. Although these moments acting radially tend to roll the flange, the resisting moment is tangential (refer to section on Low Profile Flange Theory). The longitudinal dimension can be computed by the following equation:

$$h^2 = \frac{3(P_i a_i + P_s a_s)N_f}{\pi F_{yf}(b_f - d_{bh})} \qquad \text{IX}$$

(For rectangular flange section only)

Equation IX was derived by substitution into the basic equation for beam bending

$$F_b = \frac{M_a R_{cg} c}{I}$$

Where:

M_a (applied uniform radial moment per unit of circumference) is equal to the total applied moment (P . a) divided by the circumference of the locus of the cg of the radial section, or $\frac{P \cdot a}{2\ R}$ $c = \frac{h}{2}$, and $I = \frac{b_f h^3}{12}$

Then substituting:

$$f_b = \frac{\left(\frac{P.a}{2\pi R_{cg}}\right)\left(R_{cg}\right)\left(\frac{h}{2}\right)}{\frac{b_f h^3}{12}}$$

$$= \frac{3(P \cdot a)}{\pi b_f h^2}$$

Transposing for (h):

$$h^2 = \frac{3(P \cdot a)}{f_b b_f}$$

Now, applying a safety factor (N_f), substituting the effective width ($b_f - d_{fh}$) for total width (b_f) and the yield stress (F_{yf}) for the actual stress (f_b)

$$h^2 = \frac{3(P \cdot a)\ N_f}{\pi F_{yf}(b_f - d_{bh})}$$

Because there are two distinct moments involved--one from internal pressure load (P_i) with its moment arm (a_i) between the tube wall and bolt axis and one from the gasket seating load (P_s) with its moment arm (a_s) between the gasket center of pressure and bolt--that comprise the total moment (P . a), substituting these terms for (P . a) will result in equation IX for the longitudinal dimension.

If it can be seen that the internal pressure load moment will contribute a large portion of the total moment, then the following equation may be conservatively used to derive the height of the flange

$$h^2 = \frac{3(P_g a_i)(N_f)}{\pi F_{yf}(b_f - d_{bh})} \qquad \text{(X)}$$

Step Eleven (Second Design Check)

At this point, the flange height (h) should be checked against the bolt spacing (e) using the following formula:

$$\frac{3h}{e} > 1 \qquad \text{(XI)}$$

If this condition is not satisfied, more bolts should be used, or possibly smaller diameter bolts. If it is decided to use smaller-diameter

bolts, return to Step Three and redesign the flange based on the smaller bolt size. Again, Step Five and Step Six may be used as originally calculated. If it is decided to use larger bolts, caution should be exercised in specifying torque values to avoid overstressing the flange or gasket.

The eleven preceding steps, if followed, will produce a balanced flange design with relatively uniform stresses throughout. This, of course, is basic to any good design and will result in the "best" or "most efficient" use of the total material and a maximum strength-weight ratio. The flange face can be adapted to almost any seal configuration desired.

The effect of the tube wall on the flange has not been considered in this design procedure; because at initial tightening of the bolts it was conservative to ignore it,and when pressure is applied to the system, the influence of the tube wall diminishes. This happens because the tube wall resists the initial rolling of the flange, but when pressure is applied, the tube wall, being thinner than the flange, stretches more than the flange and relieves part--and possibly all--of the initial resistance to the rolling of the flange.

Actually, the most difficult part in the design of a flange is the selection of the gasket and the determination of how best to calculate its loads, allowables, etc. The equations in Step Five are for soft, flat gaskets only; equations for any other type of gasket or configuration must be formulated according to the peculiar requirements.

The preceding eleven steps are summarized below. There has been no attempt to present a detailed theoretical analysis of flange design,because it is felt that practical application of the simplest possible equations will produce a flange as close to the ideal as could be accomplished with a highly complicated theoretical approach. These equations are actually based on the theoretical form but have been modified to a semi-empirical form for practical applications.

SUMMARY OF DESIGN PROCEDURE

Step One: Collect all known data and factors.
Step Two: Calculate wall thickness (t)

$$t = \frac{p_i D_i N_f}{2F_{yf}}$$

Step Three: Assume a bolt size (d_b)
Step Four: Determine a bolt circle diameter (D_{bc})

$$D_{bc} = D_i + 2t + 2C + d_{sf}$$

Step Five: Using edge distance = d_b, determine outside diameter (D_o)

$$D_o = D_{bc} + d_b$$

and width of flange

$$b_f = \frac{D_o - D_i}{2}$$

Step Six: Establish the gasket dimensions. (For some gaskets this step may not be necessary; dimensions may have been established already for manufactured seals such as Naflex, Raco, etc.) For a soft, flat gasket, minimum width

$$w = \frac{p_i (R_{bc} - d_b + R_i) N_g}{2(F_{ug} - 2p_s)}$$

and choose outside diameter (D_{og}) and inside diameter (D_{ig}) to suit.
Step Seven: Calculate total initial gasket load. Again, for a soft, flat gasket, and no expected external loads

$$P_g = \pi p_i \left(\frac{R_{og} + R_{ig}}{2}\right)^2 + 2\pi p_s w \left(\frac{R_{og} + R_{ig}}{2}\right)$$

Step Eight: Calculate number of bolts required. If practical, round up to a number divisible by four.

$$n = \frac{P_g N_b}{P_{yb}}$$

and bolt spacing:

$$e = \frac{\pi D_{bc}}{n}$$

Step Nine: (First Design Check) At this point, the design should be reviewed from a practical standpoint. Optimum bolt spacing should fall within the range of

$$3 < \frac{e}{d_b} < 8$$

If this condition is not satisfied, start again at Step Three with another bolt size, bolt material, flanges, material, or both.
Step Ten: Determine flange height (h)

$$h^2 = \frac{3\ (P\ .\ a)\ N_f}{\pi F_{yf}\ (b_f - d_{bh})}$$

Step Eleven: (Second Design Check) Height to bolt spacing:

$$\frac{3h}{e} > 1$$

If this condition is not satisfied, use more bolts--or possibly, smaller diameter bolts.

Testing of the "low profile" flanges

These tests were performed to verify the integrity of the "low profile" flange design concept by direct comparison with the generally accepted standard flange design.

Test Fixtures

Two different test fixtures were used for the performance of this study.

Test fixture #1, which is the Saturn I center LOX tank manhole and manifold test setup, was modified by replacing three out of six conventional flanges with "low profile" flanges (Fig. 6, 7, and 8).

Test Fixture #2 (Fig. 9) was designed and manufactured to get comparison data on the Saturn I, 8-inch LOX suction line configuration.

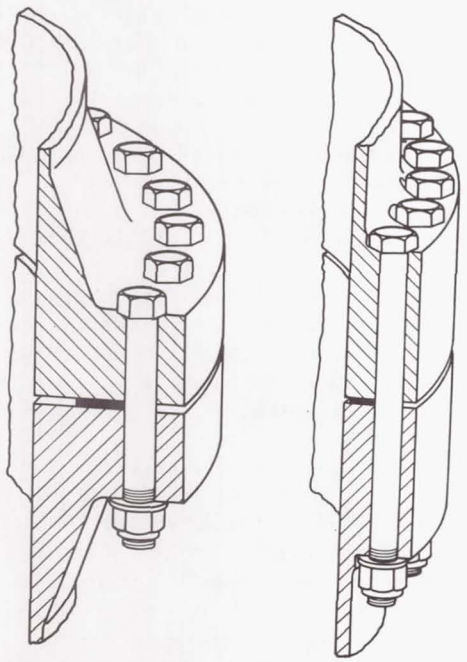

(a) SA-5 Configuration (b) Low Profile Configuration

Fig. 6 - LOX center tank aft manhole to cover joint

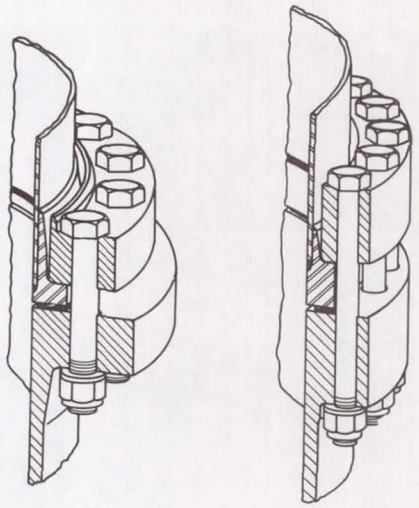

(a) SA-5 Configuration (b) Low Profile Configuration

Fig. 7 - LOX center tank aft manifold to interconnect joint

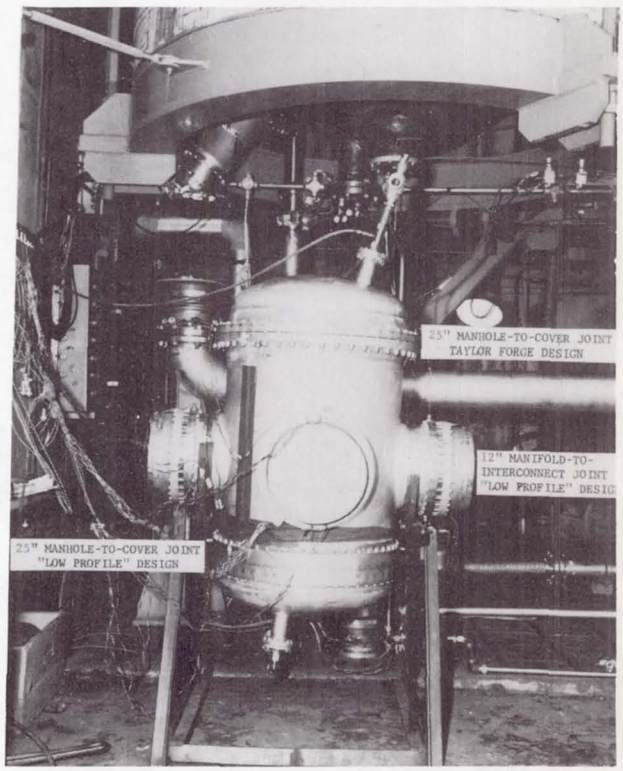

Fig. 8 - Test fixture used in comparison testing of flanged joints

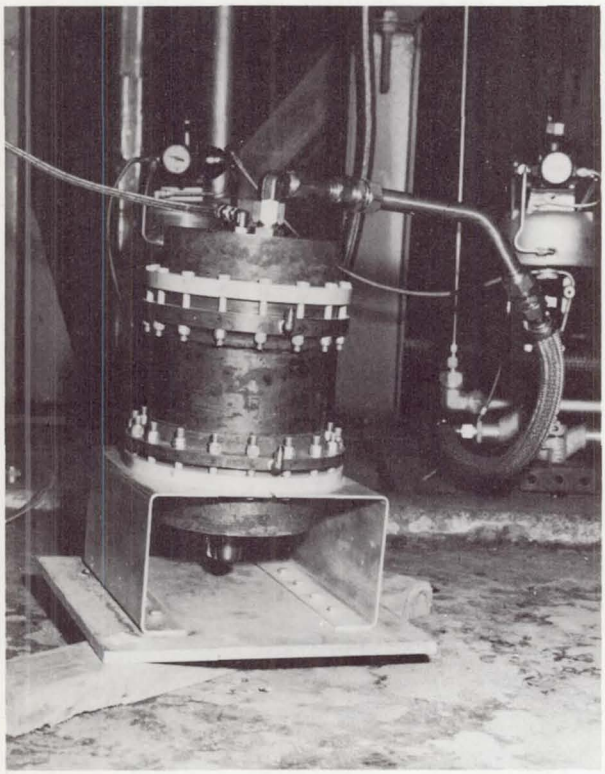

Fig. 9 - Test fixture No. 2

Table I. Torquing Sequence and Schedule

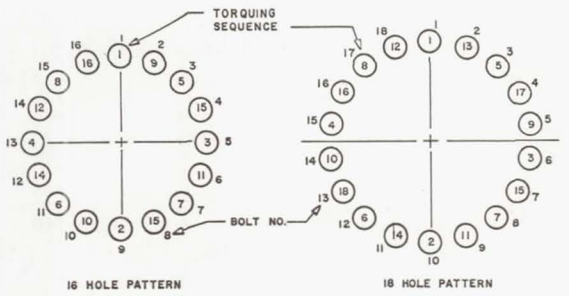

JOINT	TORQUE SCHEDULE						
	FIRST INCREMENT (IN. LBS)	TIME LAPSE (HRS)	SECOND INCREMENT (IN. LBS)	TIME LAPSE (HRS)	FINAL TORQUE	TIME LAPSE (HRS)	TORQUE CHECK
SAT I	40	8	70	16	100	48	100
LOW PROFILE	35	8	60	16	85	48	85

Gasket

Allpax 500 gasket material, Fluorolube treated per specification MS-750. 0B has been used throughout the testing except on the "low profile" interconnect joints on the last two tests where a new gasket material, Teflon FEP - a glass cloth laminated gasket developed by Narmco under the supervision of NASA - MSFC, was used.

Preparation of Test Fixtures

1. All flange surfaces were inspected for finish and flatness by quality control personnel.
2. Flange mating surfaces were cleaned with trichloroethylene.
3. All sliding surfaces between bolts, nuts, washers, and flanges were lubricated with Molylube spray dry film lubricant in accordance with procedure MSFC-PROC-226.
4. Before gasket installation, gasket thickness was measured at several locations. The gaskets were marked for orientation to the flange.
5. Strain gages were fitted to two bolts in each of the manifold flanges to determine the stress levels at which the bolts were being utilized. Unfortunately, readings from the strain gages under low temperature were erratic and therefore discounted.

Test Procedure

The flange connections were assembled using the established bolt torquing sequence shown in Table I which was developed at MSFC. Each test fixture was hydrostatically tested once for general reliability. After hydrostatic testing, each test fixture was carefully inspected for any signs of damage. A new gasket was installed and reassembled as before.

Liquid nitrogen was used as the test medium in all tests. Gaseous nitrogen was used to pressurize the test fixtures. While testing, periodic checks were made for evidence of leakage and abnormalities.

After the fixture was held the requested time under the maximum pressure, the test fixtures were depressurized and pressurized once more before final depressurization. After residual LN_2 draining and disassembling all parts, the flanges and gaskets were subjected to a thorough inspection.

Results

Table II lists the parameters of the two flange configurations of test fixture #1. A weight saving of 37% is shown for 25-inch diameter flange and 8% for the 12 inch.

The recorded test data for the flanges on test fixture #1 are given in Tables III and IV. The recorded test results show that the low profile flange is at least as effective as the conventional flange.

Table V lists the parameters of the flange configuration of the test fixture #2; a weight saving of 15% is shown for the 8-inch diameter flange.

TABLE II. TECHNICAL DATA ON TEST FIXTURE NO. 1.

		SATURN I BLOCK II DESIGN	LOW PROFILE DESIGN
	MAX. OPERATING PRESSURE (PSIG)	94	94
	TEST PRESSURE (PSIG)	113	113
	PROOF PRESSURE (PSIG)	125	125
MANHOLE JOINTS *	GASKET AREA — SQ IN.	52.769	29.965
	GASKET THICKNESS	.125	.125
	GASKET O.D.	27.500	25.810
	GASKET I.D.	25.000	25.060
	FLANGE THICKNESS	1.250	2.125
	FLANGE O.D.	29.250	27.000
	FLANGE I.D.	25.000	25.000
	BOLT (ALUMINUM)	AN7DD31A	AN6DD46A
	BOLT CIRCLE DIAMETER (B.C.)	28.000	26.250
	WASHER (ALUMINUM)	AN960PD716	AN960PD616
	NUT (SELF LOCKING)	MS20365-720A	MS20365-624A
	PITCH	1.955	1.586
	NO. OF BOLTS	45	52
	TOTAL WEIGHT OF JOINT (LBS)	64.58	40.55 (37% LESS)
INTERCONNECT JOINTS	GASKET AREA — SQ IN.	14.932	9.857
	GASKET THICKNESS	.062	.062
	GASKET O.D.	13.050	12.800
	GASKET I.D.	12.300	12.300
	FLANGE THICKNESS	.812	1.300
	FLANGE O.D.	15.000	13.812
	FLANGE I.D.	12.000	12.000
	BOLT (ALUMINUM)	MS35314-68	AN5DD33A
	BOLT CIRCLE DIAMETER (B.C.)	13.562	13.188
	WASHER (ALUMINUM)	AN960PD616	AN960PD516
	NUT (SELF LOCKING)	MS20365-624A	MS20365-524A
	PITCH	1.775	1.295
	NO. OF BOLTS	24	32
	TOTAL WEIGHT OF JOINT (LBS)	13.81	12.71 (8% LESS)

* UNLESS OTHERWISE SPECIFIED ALL DIMENSIONS IN INCHES

The recorded test data for the flanges on test fixture #2 are given in Table VI.

CONCLUSION

Test data shown on tables 1, 2, and 4 prove that the low profile flange design is superior to the Taylor Forge concept in the application of the test hardware in the following ways:

a. tighter seal
b. lighter weight, up to 37 percent lighter
c. more compact, up to 12 percent reduction in diameter

APPENDIX

SAMPLE CALCULATIONS

The following calculations are for the "low profile" versions of the 25-inch diameter aft LOX manhole-to-cover joint (Fig. 6), and an 8-inch diameter LOX suction line joint, being tested together with their Saturn counterparts, designed according to Taylor Force methods.

TABLE III. TEST DATA FOR 25-INCH CENTER LOX TANK MANHOLE COVER - TEST FIXTURE NO. 1.

TEST DATA
25 INCH I. D. MANHOLE JOINTS

TEST NO. & DATE	*FLANGE CONFIG	GASKET				NOM BOLT DIA	TORQUE (IN. LBS)	PRESSURE (PSIG)	RESULTS	REMARKS
		MATL	THICK	WIDTH	NEW					
1	B	ALLPAX	.125	.625	YES	7/16	270±10	113	NO LEAKS	
3/25/64	D	ALLPAX	.062	.375	YES	3/8	130± 5	113	NO LEAKS	
2	B	ALLPAX	.125	.625	NO	7/16	270±10	113	NO LEAKS	TORQUE RECHECKED
3/26/64	D	ALLPAX	.062	.375	NO	3/8	130±5	113	NO LEAKS	PRIOR TO TEST
3	B	ALLPAX	.125	.625	YES	7/16	270±10	113	NO LEAKS	
4/8/64	D	ALLPAX	.062	.375	YES	3/8	130±5	113	NO LEAKS	
4	B	ALLPAX	.125	.625	NO	7/16	270±10	113	NO LEAKS	NO TORQUE RECHECK
4/8/64	D	ALLPAX	.062	.375	NO	3/8	130±5	113	NO LEAKS	PRIOR TO TEST
5	B	ALLPAX	.125	.625	YES	7/16	270±10	113	NO LEAKS	
6/8/64	D	ALLPAX	.125	.375	YES	3/8	130±5	113	NO LEAKS	
6	B	ALLPAX	.125	.625	NO	7/16	270±10	120	NO LEAKS	
6/8/64	D	ALLPAX	.125	.375	NO	3/8	130±5	120	2 LN_2 LEAKS	AT 120 PSIG (IN AREA OF SLUGS)
7	B	ALLPAX	.125	.625	YES	7/16	270±10	113	2 LN_2 LEAKS	ICE BETWEEN FLANGES
6/24/64	D	ALLPAX	.125	.375	YES	3/8	145±5	113	NO LEAKS	WHERE LEAKS OCCURRED
8	B	ALLPAX	.125	.625	NO	7/16	270±10	145	NO LEAKS	TORQUE RECHECKED
6/25/64	D	ALLPAX	.125	.375	NO	3/8	145±5	145	NO LEAKS	PRIOR TO FILL

* FLANGE CONFIGURATION
B= SATURN I, BLOCK II, DESIGN
D= LOW PROFILE DESIGN

TABLE IV. TEST DATA FOR 12-INCH INTERCONNECT JOINTS ON TEST FIXTURE NO. 1.

TEST DATA
12 INCH I. D. INTERCONNECT JOINTS

TEST NO. & DATE	* FLANGE CONFIG	GASKET				NOM BOLT DIA	TORQUE (IN. LBS)	PRESSURE (PSIG)	RESULTS	REMARKS
		MATL	THICK	WIDTH	NEW					
1	A	ALLPAX	.062	.375	YES	3/8	135 ± 5	113	NO LEAKS	
3/25/64	C	ALLPAX	.062	.250	YES	5/16	90 ± 5	113	NO LEAKS	
2	A	ALLPAX	.062	.375	NO	3/8	135 ± 5	113	NO LEAKS	TORQUE RECHECKED
4/26/64	C	ALLPAX	.062	.250	NO	5/16	90 ± 5	113	NO LEAKS	PRIOR TO TEST
3	A	ALLPAX	.062	.375	YES	3/8	135 ± 5	113	NO LEAKS	
4/8/64	C	ALLPAX	.062	.250	YES	5/16	90 ± 5	113	NO LEAKS	
4	A	ALLPAX	.062	.375	NO	3/8	135 ± 5	113	NO LEAKS	NO TORQUE RECHECK
4/8/64	C	ALLPAX	.062	.250	NO	5/16	90 ± 5	113	NO LEAKS	PRIOR TO TEST
5	A	ALLPAX	.062	.375	YES	3/8	135 ± 5	113	NO LEAKS	
6/8/64	C	ALLPAX	.062	.250	YES	5/16	90 ± 5	113	NO LEAKS	
6	A	ALLPAX	.062	.375	NO	3/8	135 ± 5	120	NO LEAKS	NO TORQUE RECHECK
6/8/64	C	ALLPAX	.062	.250	NO	5/16	90 ± 5	120	NO LEAKS	PRIOR TO TEST
7	A	ALLPAX	.062	.375	YES	3/8	135 ± 5	113	NO LEAKS	
6/24/64	C	NARMCO	.062	.250	YES	5/16	90 ± 5	113	NO LEAKS	
8	A	ALLPAX	.062	.375	NO	3/8	135 ± 5	145	NO LEAKS	TORQUE RECHECKED
6/25/64	C	NARMCO	.062	.250	NO	5/16	90 ± 5	145	NO LEAKS	PRIOR TO FILL

* FLANGE CONFIGURATION
A= SATURN I, BLOCK II DESIGN
C= LOW PROFILE DESIGN

TABLE V. TECHNICAL DATA ON TEST FIXTURE NO. 2.

	SATURN I BLOCK II DESIGN	LOW PROFILE DESIGN
* FLANGES		
1. INTEGRAL		
MATERIAL	CRES	CRES
O. D.	10.250	9.520
I. D.	7.890	7.875
THICKNESS	.500	.766
2. FERRULE		
MATERIAL	CRES	CRES
O. D.	9.042	8.520
I. D.	7.875	7.875
THICKNESS	.300	.570
3. FLOATING RING		
MATERIAL	ALUMINUM 2024	ALUMINUM 2024
O. D.	10.252	9.520
I. D.	8.250	8.220
THICKNESS	.625	.700
GASKET		
O. D.	9.000	8.520
I. D.	8.125	7.915
THICKNESS	.062	.062
AREA (SQ IN.)	10.93	7.01
FASTENERS		
BOLT CIRCLE DIAMETER (B.C.)	9.410	8.890
NO. REQD & SPACING	18 AT 1.642	16 AT 1.746
BOLT (ALUMINUM)	MS35314-67	MS35314-42
NOMINAL DIAMETER	.3750	.3125
NUT (STEEL)	MS20365-624A	MS20365-524A
WASHER (ALUMINUM)	AN960PD616	AN960PD516
WEIGHT		
TOTAL WEIGHT OF JOINT (LBS)	10.864	9.237 (15% LESS)

* UNLESS OTHERWISE SPECIFIED ALL DIMENSIONS IN INCHES

MANHOLE-TO-COVER JOINT CALCULATIONS

Design Data:

Design pressure: 113 pounds per square inch gage (psig)

Design temperature: minus 297 degree Fahrenheit

Flange material: 5456-T651 Aluminum alloy F_{ty} = 30,000 psi

Gasket material: Allpax "500"

Assumed crushing stress - F_{ug} = 10,000 psi

Effective seating stress - p_s = 1,850 psi

Bolt material: 2024-T4 Aluminum alloy - F_{ty} = 40,000 psi (ANxxDDxxA)

Tube I. D. = 25 inch

d Tube wall = 0.188 inch

Design Calculations:

Tube wall (t) from design data = 0.188 inch

Bolt size: Assume approximately 1 1/2-inch spacing for bolts @ 25.00 inch diameter to estimate approximate number of bolts (n) required, then roughly estimate expected bolt load (P_b)

$$n = \frac{\pi (D_i)}{1.5} = \frac{\pi (25)}{1.5} = 52.36 \text{ Try } 52 \text{ bolts}$$

TABLE VI. TEST DATA FOR 8-INCH LOX SUCTION LINE JOINT - TEST FIXTURE NO. 2.

TEST DATA
8 INCH I. D. LOX SUCTION LINE JOINT

TEST NO. & DATE	*FLANGE CONFIG	GASKET				NOM BOLT DIA	TORQUE (IN. LBS)	PRESSURE (PSIG)	RESULTS	REMARKS
		MATL	THICK	WIDTH	NEW					
1 4/16/64	A B	ALLPAX ALLPAX	.062 .062	.375 .250	YES YES	3/8 5/16	100±5 85±5	200 200	NO LEAKS NO LEAKS	
2 4/16/64	A B	ALLPAX ALLPAX	.062 .062	.375 .250	NO NO	3/8 5/16	100±5 85±5	180 180	NO LEAKS NO LEAKS	
3 5/1/64	A B	ALLPAX ALLPAX	.062 .062	.375 .250	YES YES	3/8 5/16	100±5 85±5	200 200	NO LEAKS NO LEAKS	
4 5/1/64	A B	ALLPAX ALLPAX	.062 .062	.375 .250	NO NO	3/8 5/16	100±5 85±5	200 200	NO LEAKS NO LEAKS	
5 5/6/64	A B	ALLPAX ALLPAX	.062 .062	.375 .250	NO NO	3/8 5/16	100±5 85±5	200 200	NO LEAKS NO LEAKS	
6 5/22/64	A B	ALLPAX ALLPAX	.062 .062	.375 .250	YES YES	3/8 5/16	100±5 85±5	215 215	LN_2 LEAK NO LEAKS	
7 5/22/64	A B	ALLPAX ALLPAX	.062 .062	.375 .250	NO NO	3/8 5/16	100±5 85±5	260 260	LN_2 LEAK NO LEAKS	AT 180 PSIG

*FLANGE CONFIGURATION
A= SATURN I, BLOCK II, DESIGN
B= LOW PROFILE DESIGN

Approximate load per bolt, using 3/8-inch wide gaskets

$$P_b = \frac{P_i \cdot \pi \left(\frac{D_i}{2}\right)^2 + p_s (\pi) \left(D_i + 3/8\right) \left(\frac{3}{8}\right)}{52}$$

$$= \frac{113(\pi)\ (12.5)^2 + 1,850(\pi)\ (25.375)\ (0.375)}{52}$$

$$= \frac{55,470 + 55,300}{52}$$

$$= 2,130 \text{ pounds}$$

try 3/8 - 24 Aluminum bolt, AN6DDxxA, P_{yb} = 3,240 pounds

Aluminum bolts are necessary because the different thermal coefficient of expansion of steel bolts will cause the flanges to shrink away from the bolts and become loose at cryogenic temperatures.

Bolt circle diameter (D_{bc})

$$D_{bc} = D_i + 2t + 2C + d_{sf}$$

$$= 25 + 2(0.188) + 2(0.062) + 0.750$$

$$= 26,250 \text{ inches}$$

Flange O. D. (D_o)

Using edge distance = d_b

then:

$$D_o = D_{bc} + 2\, d_b$$

$$= 26.250 + 2(0.375)$$

$$= 27,000 \text{ inches}$$

and:

$$b_f = \frac{D_o - D_i}{2}$$

$$= \frac{27.00 - 25.00}{2}$$

$$= 1.00 \text{ inch}$$

Gasket dimensions

$$b_g = \frac{P_i (R_{bc} - d_b + R_i) Ng}{2 (F_{ug} - 2p_s}$$

$$= \frac{113(13.125 - 0.375 + 12.5)(1.5)}{2\ [10,000 - 2(1,850)]}$$

$= 0.340$ inch (Use 0.375 inch)

Setting gasket just inside the bolt circle

$D_{od} = D_{bc} - d_{bh}$

$= 26.25 - 0.406$

$= 25.844$ inches (Use 25.812 inches)

then:

$D_{ig} = D_{og} - 2b_g$

$= 25.812 - 2(0.375)$

$= 25.062$ inches

Loads

$$P_i = \pi p_i \left(\frac{D_{og} + D_{ig}}{4}\right)^2$$

$$= \pi(113)\left(\frac{25.812 + 25.062}{4}\right)^2$$

$= 57,425$ pounds

$$P_s = \pi p_s \left(\frac{D_{og} + D_{ig}}{2}\right)(b_g)$$

$$= (\pi)(1,850)\left(\frac{25.812 + 25.062}{2}\right)(.375)$$

$= 55,440$ pounds

$P_g = P_i + P_s$

$= 112\ 865$ pounds

Number of bolts (n)

$$n = \frac{P_g N_b}{P_{yb}}$$

$$= \frac{112,865(1.5)}{3,240}$$

$= 52.25$ (Use 52 bolts)

Bolt spacing (e)

$$e = \frac{\pi D_{bc}}{n}$$

$$= \frac{\pi(26.250)}{52}$$

$= 1.586$ inches

First design check

$$3 < \frac{e}{d_b} < 8$$

$$\frac{e}{d_b} = \frac{1.586}{0.375}$$

$= 4.23$ OK

Flange height (h)

$$h^2 = \frac{3(P_i a_i + P_s a_s)N_f}{\pi F_{yf}(b_f - d_{bh})}$$

$$= \frac{3\left[(57,425)(0.531) + (55,440)(0.406)\right]\ 1.25}{\pi(26,000)(1 - 0.406)}$$

$h = \sqrt{4.096445}$

$= 2.024$ inches (Use 2.125 inches)

Second design check (Height to bolt spacing)

$$\frac{3h}{e} > 1$$

$$\frac{3(2.125)}{1.586} > 1 \quad \text{OK}$$

SYMBOLS USED:

a: moment arm between bolts and gasket load

a_i: the moment arm between tube wall and bolt

b_f: Flange width

C: minimum practical clearance between spotface and tube wall

d: thread root diameter of bolts (inches)

d_b: bolt diameter

d_{bh}: bolt hole diameter

D_{bc}: bolt circle diameter

e: bolt spacing (inches)

F_{yf}: yield stress of flange material (psi)

F_{yb}: yield stress of bolt material (psi)

F_i: axial internal pressure load

F_{ug}: ultimate or crushing strength of gasket material

F_D: gasket load

F_b: external bolt load

F_N: shear load in flange neck

h: flange height (inches)

M_t: internal tangential moment in the flange

M_s: bolt moment

M_N: internal moment in flange neck

n: number of bolts

N_f: safety factor applied to flange material

N_b: safety factor for bolt material

N_g: safety factor for gasket material

p_G: pressure on the gasket (unpressurized)

P_{yb}: yield load for bolt

p_G: operating pressure on gasket

P_g: initial gasket load

P_s: effective seating stress

P_b: bolt load

P_i: internal pressure

R_{bc}: radius of the bolt circle (inches)

R_i: inside radius of the tube (inches)

R_{og}: outside radius of gasket

R_{ig}: inside radius of gasket

t: wall thickness of the tube (inches)

w: gasket width

REFERENCES

1. Prof. Ir. E. F. Boon and Ir. H. H. Lok, "Untersuchungen an Flanschen und Dichtungen," published inVDI-Z100 (1958) Nr. 34 1 December.

2. W. P. Prasthofer and G. A. Gauthier, "Low Profile Bolted Seperable Connectors," George C. Marshall Space Flight Center, Huntsville, Alabama, December 30, 1964.

3. J. C. Genter and R. B. White, "Interim Report on Low Profile Flange Tests," George C. Marshall Space Flight Center, Huntsville, Alabama, December 30, 1964.

4. J. E. Curry, "Status Report on Liquid Oxygen Seal Investigation," George C. Marshall Space Flight Center, Huntsville, Alabama, December 16, 1964.

Page Intentionally Left Blank

N66 31426

MATHEMATICAL APPROACH TO INTERFACE PHENOMENON

By

L. G. Gitzendanner
Advanced Technology Laboratories
General Electric Company
Schenectady, N. Y.

ABSTRACT

The need for increased understanding of the sealing phenomena in the design of reliable leak-tight fluid connectors is noted. Progress made in developing a mathematical model for estimating the probability of leakage exceeding a given level under stated conditions is reviewed, the steps yet to be developed before this estimate can be completed are also noted.

Work was performed as part of a NASA contract, NAS8-4012.

THE DESIGN OF CONNECTORS CAN, in a broad sense, be divided into 1) design of a seal system, and 2) design of the structure to support the seal. While the latter design problem is quite complex, the structure is usually designed to remain elastic and the solution is amenable to a mathematical analysis. The design of the seal, however, is at present still based largely on empirical data and is an art, not an engineering science. Yet the design of the seal is a critical element in achieving highly reliable connectors for rockets and spacecraft.

This paper discusses progress made in an attempt to develop mathematical models of seal systems so their statistical performance under various conditions may be estimated. The work has been sponsored by NASA under contract NAS8-4012, with technical management by the Propulsion and Vehicle Engineering Laboratory of the George C. Marshall Space Flight Center.

As an end goal, it is desired to be able to predict the probability that a leak greater than a given magnitude will exist in a connector given the specifications for the connector and its application. Further, the specifications for the connectors should be obtainable from the drawings used to produce them. It is important that predictions of this type be feasible for otherwise we have a poor basis for designing an optimum connector. If the designer makes the seal narrower, he will presumeably require less sealing force and produce a lighter weight design. There appears to be no inherent or theoretical limit to how far this can be carried, until reliability is considered. Thus, to achieve optimum designs we need an analysis relating seal parameters and the probability of leakage exceeding a given level.

We expect there may be pitfalls in developing an analysis, and it is conceivable that no meaningful total solution will be gained. Even then, we should still gain considerable useful insight into the importance of different parameters and be in a position to extrapolate empirical data, or to use it plus analysis, to make predictions in areas where currently we have no basis other than intuition.

The approach being followed is to first divide the sealing problem into a number of separate smaller ones. A brief description of the steps involved is as tabulated below; and the first step in particular will be discussed in detail in the remainder of this paper:

1. Develop sets of numbers which are mathematical descriptions of the surface contours of a hypothetical set of sample sealing surfaces selected at random from a large population of surfaces such as were specified.
2. For any two sets of numbers which describe a pair of surfaces in contact, and for a stated load, determine the deformation of asperities and the set of numbers describing the contour map of gap heights.
3. For a given contour map of gap heights and given fluid pressure, determine leakage flow.
4. Repeat the above steps a number of times and from the flow values obtained plot the probability integral of flow exceeding any given value.

The last step produces the answer we seek and it is a valid answer only if the samples used in obtaining the probability integral are selected at random from a population representative of the surfaces which will form the seal. Let us then focus our attention on developing mathematical representations of surfaces which meet

this criterian.

Before we can get anywhere we will need to know, via experimentally obtained information, something about surfaces in a quantitative sense. Fig. 1 shows a Talysurf trace of a lapped surface. Fig. 2 shows how we could represent this particular trace mathematically by first dividing the trace into small lengths and then assigning heights above or below some datum plane to each short length. Once we get the picture, there is no need to draw the stair step figure, the row of numbers will suffice.

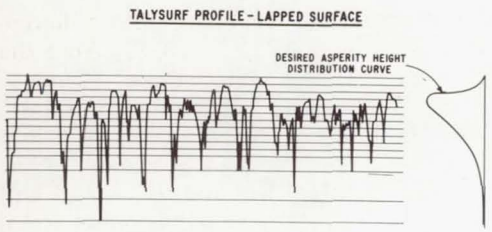

Fig. 1 - Typical Talysurf Trace of Lapped Surface, along with Experimental Continuous Probability Density Function of Asperity Heights

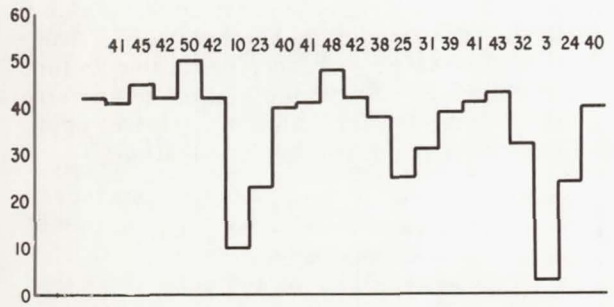

Fig. 2 - Digital Representation of Asperity Heights of Surface

Now, it is a simple extrapolation to realize that if we can represent a Talysurf trace with a row of numbers, we can represent an area with a series of rows of numbers, that is, with a matrix, such as is given in Fig. 3. Each number designates the height of a corresponding grid element on the real surface.

Questions immediately arise which must be answered before we can develop the matrix of numbers describing a surface. How small should the grid squares be? What inerements

8	9	9	10	8	10	10	9	
5	6	6	6	4	6	7	5	
6	6	5	5	4	6	8	5	
4	5	3	2	1	3	4		
9	10	8	6					
10	10	9	6					

Fig. 3 - Portion of a matrix of heights

of height should be used? What restraints are there on the assigning of heights to the grid elements?

None of the above questions can be answered in an absolute sense. A mathematical model is of necessity only a reasonable approximation to the truth, not the truth itself, and we must strike a realistic balance between the amount of labor and cost of obtaining a solution and the accuracy of that solution. The answers arrived at must then be viewed as merely our current judgment of the best compromise between two opposing desires.

On the matter of grid size, considerable insight can be gained from Talysurf traces, such as shown in Fig. 1. A low reading more likely represents a scratch or trough rather than a circular or square pit and thus is most significant in determining leakage. The grid size must be small enough so such troughs are identified and not "averaged in" with a larger area and lost in our model. The size grid which will have reasonable certainty to identify and not lose a trough has been estimated in several ways. For example, the fraction of time that the surface falls below a given level in a Profilometer trace, divided by the number of times per inch that it falls below the same level gives the average width of troughs having greater depth than the level selected. A second approach is to consider the actual geometry of surface undulations, and it is suggested that, temporarily, one forget about traces such as shown in Fig. 1 since for very sound reasons it has much greater

magnification on the vertical scale than on the horizontal scale and, unless this is clearly recognized, such traces will tend to be misleading. In truth, angles of inclination on surfaces are commonly within 10^{o} or possibly 20^{o} of the average plane of the surface. Consideration of such things as the shape of cutting tools, the angles possible on individual pieces of abrasive, the structure of metals, etc., leads to the conclusion that angles of greater than 45^{o} are extremely improbable. The summation of these two and other approaches to determining grid size is the conclusion, tentatively reached, that for lapped surfaces, grid size should not exceed approximately three times the CLA (center line average) roughness. Thus, for example, for a seal surface specified as 32 microinches, CLA, the grid size used in a model to represent the surface should not exceed 0.1 mil. Should we arbitrarily make it smaller to gain a safety factor on accuracy? A bit of reflection suggests we not do so. A typical seal having a specified roughness of 30 microinch CLA may be 1/16" wide and have a perimeter of several inches. Our grid system would thus be 625 by 20,000 and require a contour grid map of the same size. Clearly we are already at a point where techniques will be required to start with the solution to a portion of the grid map and extropolate to the full size. There is then no desire to arbitrarily select a grid size smaller than is necessary. Tentatively, for lapped surfaces it appears that a grid size of three times the specified CLA roughness will reasonably well pick up all important surface contour details, and should be used in a mathematical model.

What then about the third coordinate, grid height above or below a datum plane? What increments of height shall be used and how many steps will be needed? To answer at this, assume that we have a matrix of numbers representing the gaps between two sealing surfaces at various grid locations and consider how flow will vary as the surfaces are squeezed together. If we restrict ourselves to step changes in gaps, corresponding to the size of our increments in height, there will be a finite number of leakage flows we can calculate. True, we can probably arrive at a reasonable rule for interpolating between these points, but of particular concern is the last step, beyond which flow in our mathematical model would be zero. The last step in gap height, coupled with the other dimensions of the seal and the fluid pressure, must result in a calculated leakage that bears same relationship to the leakage rate specified as permissible. Such considerations applicable to a lapped surface, coupled with the desire again not to allow the solution to grow out of hand have led to the tentative selection of not over 20 increments of surface height and, for the most part, actual numerical work to date has used only 10 increments of surface height.

We have now a system for selecting a grid size and increments in surface height when a given roughness lapped surface is specified. While the specific criteria may be different for other types of surfaces, they can also be developed. The final concern is that of generating the numbers, representing height, which make up the contour grid.

For illustration purposes, let us designate these heights as 0, 1, 2, 3. . . . 8, 9. Note that the numbers are merely code names. Thus 0 does not necessarily mean "at the datum plane", and 2 is not, in general, twice as far as 1 from the datum plane. The frequency of each of the ten heights appearing in the matrix should be the same as the frequency of occurrance of the corresponding heights on a real surface we wish to represent. Hence, we need to know the distribution function for various surfaces. This information can be obtained from Talysurf traces.

For lapped surfaces, it has been determined that the distribution of surface heights is as shown on the left of Fig. 1. Since it is the intent that the data will be fed into a digital computer, there is no particular need to be able to describe the distribution algebraically. There is merit, however, in recognizing that in fact the distribution is extremely close to an extreme value distribution for which the relative probability density is given by the equation*

$$p = \frac{1}{\beta} e^{\left(\frac{x-u}{\beta}\right) - e^{\left(\frac{x-u}{\beta}\right)}}$$

and the probability integral is given by

$$P = 1 - e^{-e^{\left(\frac{x-u}{\beta}\right)}}$$

If we were to take samples at random from a given family of sealing surfaces, superimpose a grid system, and on each sample measure the heights of a particular grid element from the

*Usually the equation is written in a form which places the long tail on the right. As given here, the equation has been modified to place the long tail on the left, or negative coordinate side, since it is more logical to think of high areas having a + height and scratch marks and low areas a - height.

mean surface height, then we should expect these heights to have a frequency distribution equal to that determined from the Talysurf traces. It therefore follows that to assign a height to a grid element in the mathematical model we need simply select a height at random from a population of heights having the same distribution. In somewhat less mathematical terms, we could make a random selection from a box having many ping-pong balls, each with a height marked on it but otherwise identical, and the number of balls marked for any given height being proportional to the probability of that height. We can do the same job with a digital computer by giving the computer the information on distribution frequency and causing the computer to generate random numbers which are then used in selecting a height.

The process for selecting or "generating" the height of the next grid element is a bit more complicated and must take into account the height previously assigned to the first square. There is a correlation function between these two variables, or, since they are both part of the same surface, we call it the autocorrelation function of the surface. To illustrate, if the distribution frequency for the surface indicates a 10% chance of a grid being at height 3, and if the first square has previously been designated to beat height 3, then we would expect considerably more than a 10% chance that the adjacent square would also be a 3, a somewhat higher than "normal" chance of it being 2 or 4, and a less than "normal" chance of it being a 9 or 10. By "normal" chance is meant that determined by the distribution of heights for the surface as a whole. This is illustrated in Fig. 4 a and 4 b where two different assumptions are made concerning the selection for the first square and the distributions that apply to selecting heights for the second square are shown in the second square. The required distribution functions can be developed for any given degree of autocorrelation. It has been determined empirically that for a lapped surface the autocorrelation function ρ, is given by the exponential relationship

$$\rho = e^{-bx}$$

where x is the distance between points and b is a constant. For a 30 microinch lapped surface, b was found to be equal to 680 per inch, that is, if x is in inches, b = 680. Thus, for grid size of 0.1 mil, which is about three times the CLA roughness, the autocorrelation of adjacent grids is caluculated as 0.934.

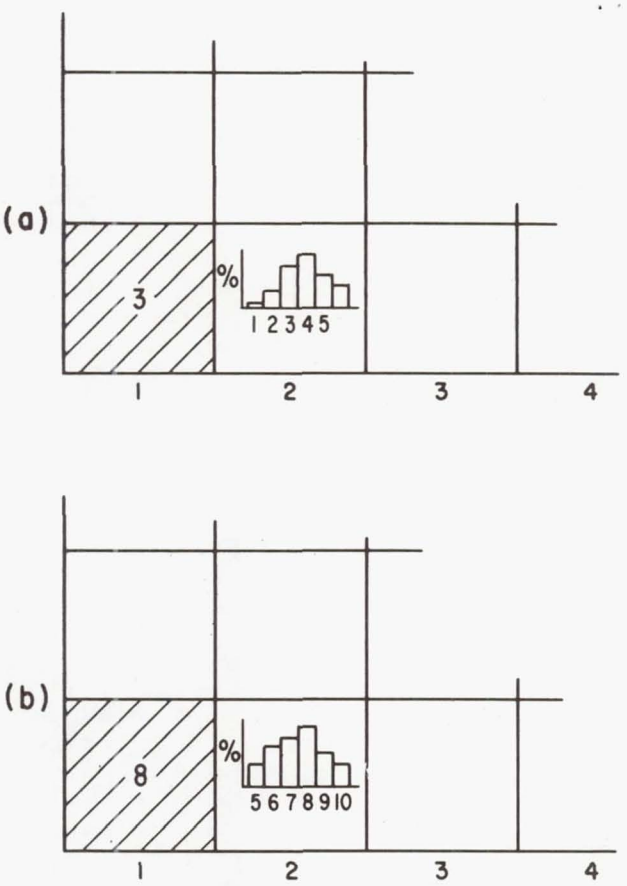

Fig. 4 - Dependence of Height in Location 2 on Height Registered in Location 1

To assign a height to the third square, the heights previously assigned to the first two must be taken into account and, in general, to assign a height to the nth square, the heights previously assigned to the (n-1) squares must be taken into account. A technique for handling multiple correlations has been worked on by various writers (see, for example, ref. 1 & 2), but unfortunately it is applicable only for Gaussian or Normal distributions and even then becomes extremely complex if more than just a few parameters are involved.

To select and assign a height to the third square the technique developed is to use a distribution function based on the height one would obtain using a linear extrapolation from the first two squares as shown in Fig. 5. The number in brackets in the third square is the linear extrapolated value. The distribution function is also shown. This distribution function of course peaks at or near the extrapolated value, but the height selected at random from the distribution

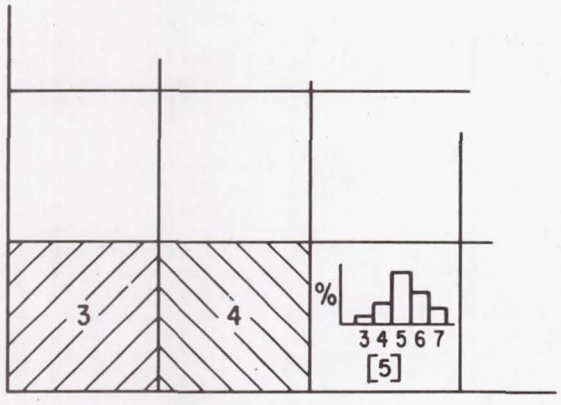

Fig. 5 - Selection of Height in Location 3

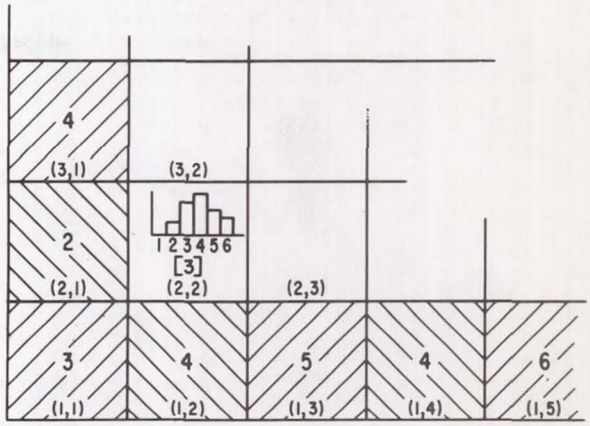

Fig. 6 - Selection of Height in Two Dimensional Array

can be higher or lower than the extrapolated value. To assign a height to the fourth square in a row, the same process is repeated using the preassigned heights for squares 2 and 3, neglecting square 1. From a rigorous viewpoint, neglecting square 1 introduces an inaccuracy. But from a practical viewpoint the error is relatively unimportant and we have a simple means for assigning heights to all elements in one row of the grid.

We can, of course, use the same process for assigning heights to squares in a column of the grid. It should be noted that the autocorrelation function in this direction could be different, and for many surfaces would be. For a lapped surface the autocorrelation function should be independent of direction. For this and other reasons it is the simplest produceable surface to investigate mathematically. It can be characterized as a surface having only random variations in height, with no periodic functions in either direction. (More complex surfaces can be developed by adding various periodic and random functions to be models for lathe turned, ground, and other types of machined surfaces.)

Assuming the process described above for a lapped surface has been carried out and heights have been assigned to all elements in the first row and first column of a grid, a technique is needed for filling in the remaining elements. A variation of the line extrapolation method used to develop heights along a row or column has been used and is illustrated in Fig. 6. An extrapolated height is calculated for the square (2, 2) based on the assigned heights of squares (1, 1), (1, 2) and (2, 1). The process for obtaining the extrapolated value is empirically arrived at to satisfy criteria for the surface. For symmetry reasons the values in squares (1, 2) and (2, 1) are given equal weight, but the value in square (1, 1) is not. A random requantizing operation is required to arrive at the extrapolated value. A random selection is then made from a distribution function associated with the extrapolated height and the value so selected is assigned. This process can be repeated to fill in the entire grid. Since the process of selecting heights for successive squares neglects most of the preassigned heights, we can expect some distortion of our mathematically generated surface compared to a real one. The critical question is whether the amount is significant, and this is discussed next.

Two criteria exist for the fidelity of a mathematically generated "surface", namely, 1) the distribution plot of heights and 2) the autocorrelation map. Early attempts to generate matrices representative of lapped surfaces were not successful for various reasons. However, with appropriate adjustments to the distribution curves and extrapolation means, surfaces can now be developed which reasonably well satisfy all criteria. Fig. 7 shows a 50 X 100 matrix of numbers representing such a surface. Included in the program for generating and printing this matrix are means for suppressing each number by a selected amount and reprinting the results with all zeros and negative numbers left blank as illustrated in Fig. 8 and 9. This has physical meaning if we assume 1) that the surface has been brought into contact with a smooth second surface and 2) that the Abbott bearing approach is valid. Under these assumptions the heights printed represent residual gap heights for various degrees of loading. There

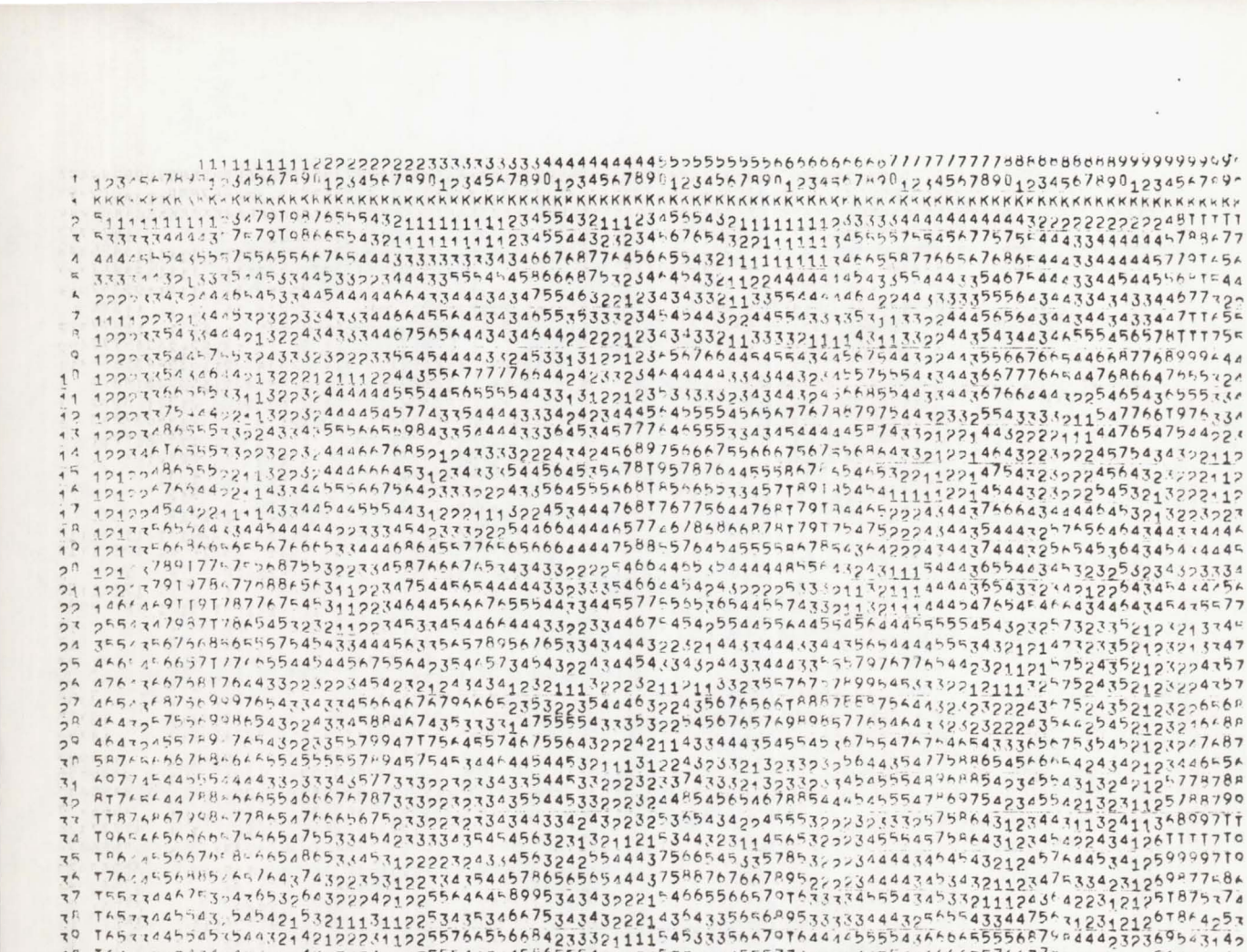

Fig. 7 - Uncompressed Mathematical Surface

is a gap of indicated height wherever a number appears; contact where no numbers appear. In Fig. 8 one can readily trace a flow path from the top row (numbered 2 in the column of numbers just to the left of the matrix proper)through to the bottom row (numbered 51). In Fig. 9 it will be found that no flow path exists. The computer has been programmed to search for flow paths and in the lower left of each print-out is the message indicating whether or not a path exists. At this stage of the computations the number suppression and flow path indication are premature, unless the two assumptions noted above are made. The features were included , however, in anticipation of future utilization of the program. At this stage, these two capabilities are most helpful, however, in examining surfaces to determine whether or not they are valid representations of real surfaces. Fig. 10, for example, was developed in an early run. It has an obvious diagonal pattern and is not a good representation of a lapped surface. This

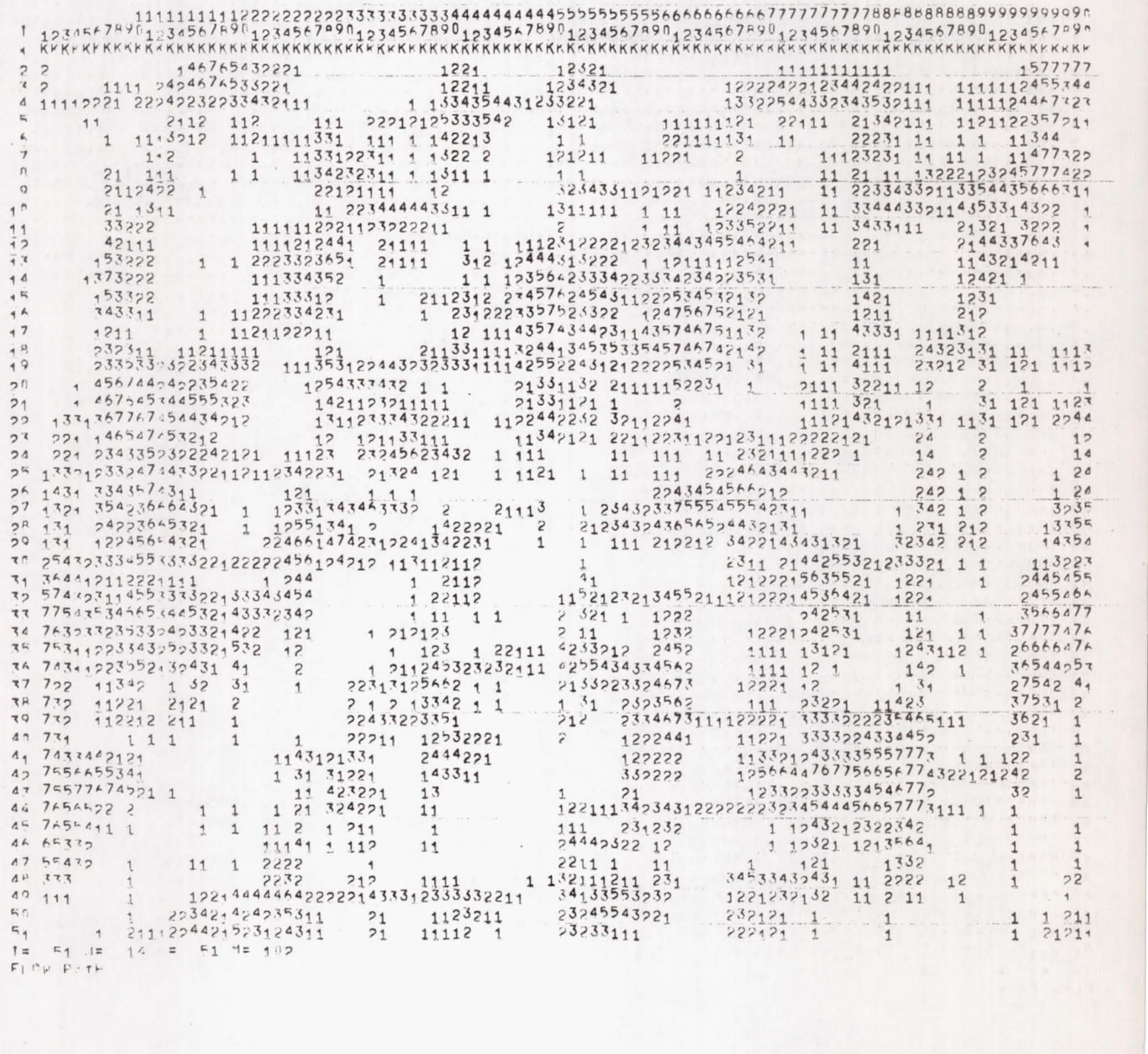

Fig. 8 - Gap Heights and Areas of Contact for Surface Shown in Fig. 7 after three increments of displacement. A Flow path still exists.

defect was corrected in later runs by adjusting the weighting factor given to the heights of squares used in obtaining an extrapolated value. An analysis of the data in Fig. 7 shows that for various separations between two points in any fixed direction, the autocorrelation function exponentially decays. Further, the constant, b, in the exponent, is very nearly the same along both major diagonals, and is the same along a vertical line as along a horizontal line. A complete polar plot of b versus bearing angle between points considered shows that the value of b is not quite constant but exhibits a four lobed shape. This is undoubtedly due to using height information from only a limited number (specifically, three) of the square to which height had

Fig. 9 - Gap Heights and Areas of Contact for Surface Shown in Fig. 7 after four increments of displacement. No Flow-path exists.

already been assigned. Or stated slightly differently, we have assigned a zero weighting factor to the heights of all but three squares and have thereby incorrectly implied a zero auto-correlation factor. Information on additional squares could be included, but it has been felt that the increase in complexity of program and of computer time would not justify such a change.

The results now obtained are believed to be sufficiently accurate, at least for present purposes, and require but little computer time.

To sum up, we believe we have developed a means of generating matrices which can be used to represent the surface heights on a lapped surface. Concepts exist, which have been pretty well thought through, for extending the analysis

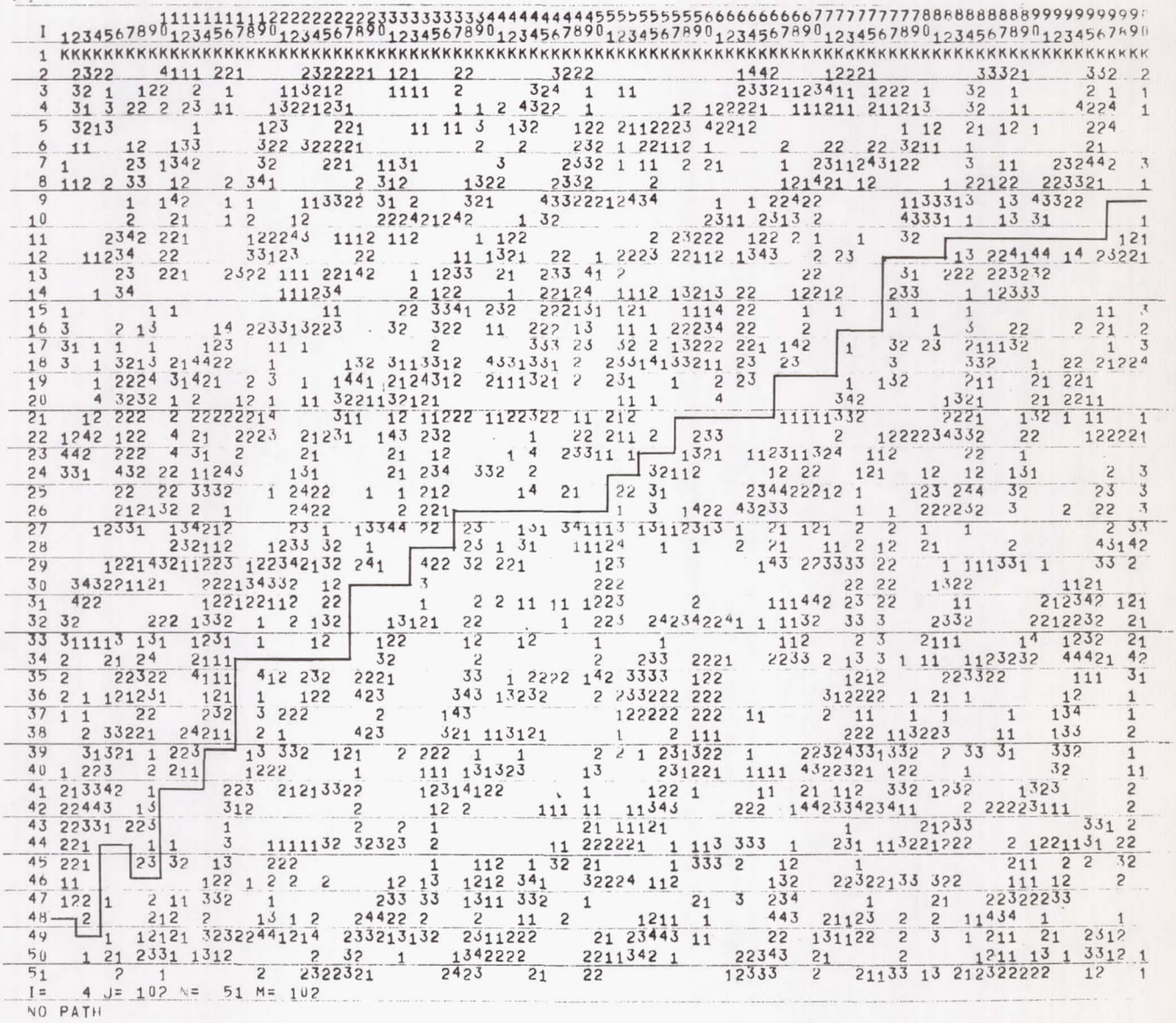

Fig. 10 - Earlier generated Surface Showing Barrier to Flow and Diagonal Pattern

to other types of surfaces, for relating load to gap height contour maps, and for calculating leakage for any given gap height map. It should not be inferred that these portions of the analysis will have no problems; they will, and some are already recognized. All that is inferred is that we have a general approach which we are confident will work and have successfully taken steps toward being able to predict what the probability will be that connectors of a given design will have less than a specified amount of leakage.

REFERENCES

1. M. G. Kendall, "Proof of Relations Connected with the Tetrachoric Series and its Generalization." Biometrika, Vol. 32 (1941), pp. 196-8.

2. M. G. Kendall and A. Stuart, "The Advanced Theory of Statistics." Vol. I, p. 155.

Page Intentionally Left Blank

PERFORMANCE OF AFRPL STAINLESS STEEL CONNECTORS

By

B. Goobich
R. L. Humphrey
Battelle Memorial Institute
505 King Avenue
Columbus, Ohio 43201

ABSTRACT

This paper describes the Type 347 CRES AFRPL connector developed at Battelle which is capable of sealing 4000-psi helium at -320 and at 600 F. Maximum leakage of 4×10^{-7} atm cc/sec was recorded in the testing of 28 specimens representing 1/2- and 3/4-inch unions, tees, and elbows. These were subjected to thermal shock at -320 and 600 F, stress reversal bending, vibration at resonant frequencies, and repeated assembly. Average maximum leakage was 2.6×10^{-8} atm cc/sec. The tests are described and results are detailed and evaluated. Design features which make the high performance level possible are discussed.

THE AFRPL SEPARABLE CONNECTOR WAS DEVELOPED to meet the Air Force need for a more reliable "zero" leakage separable connector for high-pressure missile systems subject to extreme temperatures and severe dynamic loads. The concepts that led to the AFRPL connector design and the evaluation results of a limited number of René 41 unions were discussed in a series of three papers presented in March 1964 (1, 2, 3)*. This paper describes the extensive laboratory evaluation of Type 347 CRES connectors, including elbows, tees, and unions.

SUMMARY OF RESULTS

A total of 20 unions, 4 tees, and 4 elbows were evaluated under conditions of thermal shock, stress reversal bending, and vibration at resonant frequency when pressurized with 4000-psi helium. Consistently, the leakage rates were less than 7×10^{-7} atm cc/sec, the maximum allowable leakage rate. A statistical summary was prepared on the basis of the maximum leakage recorded during each of the 28 tests. As shown in Figure 1, these data, when normalized on the basis of the logarithmic equivalent of the leakage rate, approximate a normal distribution, and the mean or average recorded maximum leakage was 2.6×10^{-8} atm cc/sec. This is equivalent to a leakage rate of less than 1 cc per year, as compared with the design limit of 2 cc per month.

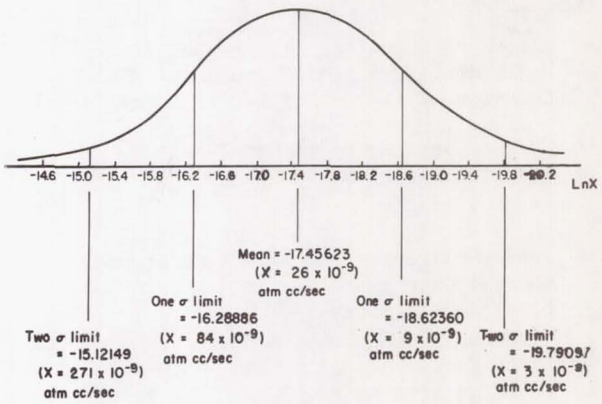

Fig. 1 - Normal distribution of maximum leakage rates

PERFORMANCE REQUIREMENTS

Design of the AFRPL stainless steel connectors was predicated on requirements determined by the Air Force. These included an operating pressure of 4000 psi, a proof pressure of 6000 psi, operating temperatures ranging from -423 to 600 F, dynamic loads approaching the fatigue limit of the tubing material, and a leakage rate for helium no greater than 7×10^{-7} atm cc/sec.

DESIGN FEATURES

In developing a connector that could satisfy these performance requirements, special features were incorporated into the design and certain unique analysis procedures were evolved. There are four separate components which make up the AFRPL connector, as shown in Figure 2--the Bobbin seal, the nut, and the two flanges. Several unique design features are embodied in the Bobbin seal and in the nut. These are:

*Numbers in parentheses designate References at end of paper.

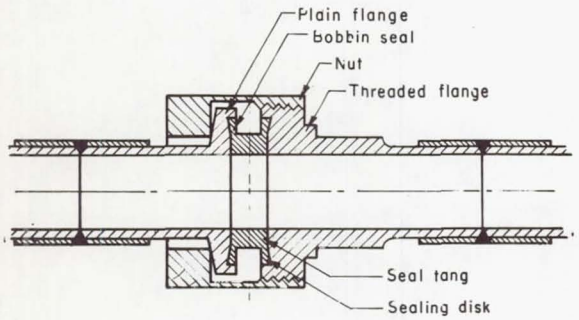

Fig. 2 - AFRPL connector assembly.

Bobbin Seal

- Plastic deformation at the seal interface
- Force amplification of the axial sealing load
- Location of the seal interface on a radial surface
- Radial yielding of the seal
- Parallel seal loading

Nut

- Predetermined spring rate to compensate for thermal expansions
- Prescribed preload.

The maximum effective height of the sealing interface required to seal 4000-psi helium at leakage rates no greater than 7×10^{-7} atm cc/sec is of the order of 1×10^{-7} inch or less. Many designers believe that this degree of contact can be established reliably only by means of plastic deformation. To accomplish this with lower contact forces and without damage to the flange seal cavity, the stainless steel Bobbin seal is plated with a soft nickel. A typical seal interface is shown in Figure 3.

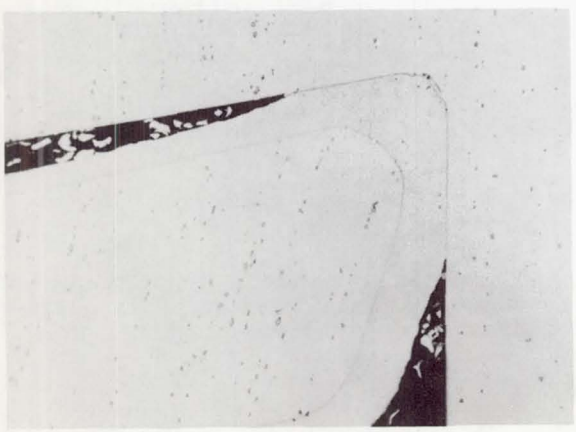

Fig. 3 - Enlarged view of Bobbin-seal interface

By utilizing the toggle action of the conical sealing disks, the axial sealing force is magnified by a factor of two, and lower assembly torques are required to create the seal. Furthermore, the radial seal created by the toggle action is relatively insensitive to axial load fluctuations caused by thermal and dynamic conditions. A unique feature of the Bobbin seal is the incorporation of the principle of radial yielding in its design. Radial yielding of the tang compensates for large dimensional variations and ovality of the sealing surfaces while maintaining a constant and controlled sealing force at the seal interface.

Preloading the connector is achieved by transmitting the axial load through the seal tang. This form of parallel loading enhances the connector's ability to sustain fluctuations in axial load without the load at the seal interface varying.

The nut of the AFRPL connector is designed with a specific spring rate based on the dynamic and thermal effects. In particular, the spring rate accommodates relative axial expansions and contractions which occur in the structural elements during operation.

By means of a preload analysis, a prescribed room-temperature preload is determined. Therefore, the design of the nut incorporates not only specific spring rates, but means for tightening the connector to a prescribed preload.

EVALUATION PROGRAM

Severity of the tests required in existing specifications (MIL-F-5509 and MIL-F-18280) were considered insufficient to measure the performance required for the AFRPL connector. For these specifications, leakage is not measured with a mass spectrometer, leakage rates of helium are not specified, and leakage is not measured during the thermal transient. The following four tests were formulated to evaluate the stainless steel AFRPL connectors:

Thermal Gradient

Leakage of helium at 4000-psi pressure was continuously measured at the temperature extremes of -320 and 600 F and during the transient phases when temperatures were varied from one extreme to the other.

Stress-Reversal Bending

Leakage of helium at 4000-psi pressure was continuously measured when a maximum reversed bending stress equal to 21,000 psi was applied at 600 F.

Vibration

Leakage of helium was measured during the vibration test at resonant frequency, the union and tubing assembly being mounted as an indeterminate beam. Elbows and tees were mounted as cantilever beams. The gas

pressure was 4000 psi, the temperature was 600 F, and the maximum bending stress at the connector was greater than 21,000 psi.

Repeated Assembly

Leakage of helium was measured after a connector had been assembled 20 times. The connector was pressurized to 6000 psi, the proof pressure.

THERMAL-GRADIENT EVALUATION - Experience indicates that the most severe thermal condition is imposed during the transient-temperature gradient rather than at the two extremes. This occurs because the contraction and/or expansion of the seal and the structural members is not uniform. Although the condition is only momentary, there is danger that once the mating of the sealing surfaces or the relationships of the forces which physically maintain the seal are disturbed, the leakage at steady-state conditions will increase.

In performance of this test, some connectors were assembled at minimum torque and some at maximum torque. Also, the connectors were fabricated so that the clearances between the seal and flange-seal cavity were at the minimum and maximum limits within the range of dimensional tolerances.

Thermal conditions from room temperature to 600 F were simulated with the arrangement shown in Figure 4. The connector was enclosed in an expandable chamber that was evacuated to a helium leak detector. An electric-sheath heater placed inside the connector assembly was used to raise the temperature to 600 F. The rate of heating was controlled by a voltage regulator. Generally, it required 5 minutes to bring the temperature to 600 F, and on each cycle the 600 F temperature was maintained for 5 to 10 minutes.

To simulate the thermal gradient in the cryogenic range, the entire connector and vacuum chamber assembly was immersed in a liquid-nitrogen bath, as shown in Figure 5. Cooling to -320 F required about 7 minutes and the assembly was subsequently maintained at -320 F for about 5 minutes on each cycle. The entire thermal-gradient test consisted of 9 cycles: 3 from room temperature to -320 F, 3 from room temperature to 600 F, and 3 from 600 to -320 F.

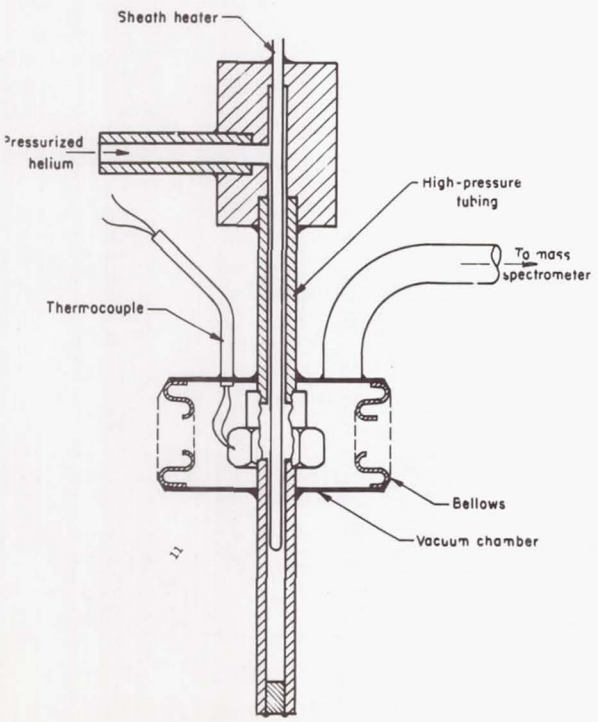

Fig. 4 - Experimental arrangement for hot-thermal-gradient test

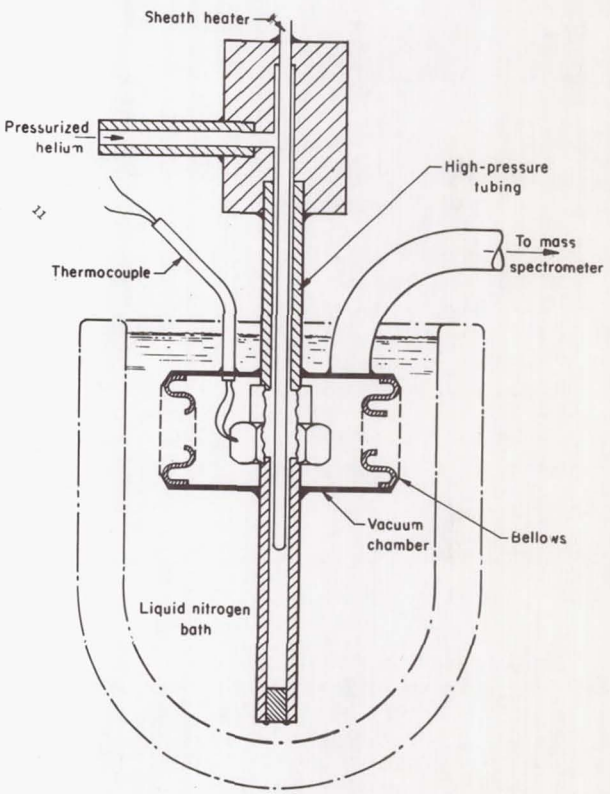

Fig. 5 - Experimental arrangement for cold-thermal-gradient test

The thermal-gradient test was performed with four 3/4-inch unions and four 3/8-inch unions. Although leakage rates were measured continuously, the results have been presented in Table 1 only on the basis of maximum leakage recorded during any one test condition. Maximum leakage recorded for the 8 specimens for the entire sequence of tests was of the order of 3.9×10^{-7} atm cc/sec. This is equivalent to 1.1 cc/month. The average value of the 172 leakage

. Table 1 - Leakage Results for Thermal Gradient Test of 347 Unions

Description	Approx Elapsed Time, min	Maximum Leakage, 10^{-7} atm cc/sec							
		12SU2	12SU1	12SU11	12SU12	6SU11	6SU12	6SU2	6SU1
Clearance[a]	--	N	N	X	X	N	N	X	X
Torque[b]	--	N	X	X	N	N	X	N	X
1000 psi, RT	2	--	.025	.024	.390	.240	.025	.175	.076
4000 psi, RT	2	--	.025	.024	.354	.250	.025	.160	.073
6000 psi, RT	5	.720	.025	.024	.341	.240	.025	.150	.073
6000 psi, 550 F	15	.720	.023	.590	.710	.320	1.100	.110	.780
4000 psi, RT	15	.094	.034	.030	--	.170	.220	.090	.034
Cool -320 F	15	.085	.021	.034	.097	.460	.150	.081	.061
Warm RT	15	.057	.016	.043	.097	1.300	.120	.087	.035
-320 F	15	.059	.360	.077	.097	.520	.160	.170	.051
RT	15	.043	.038	.058	.097	.580	.120	.130	.032
-320 F	15	.044	.670	.081	.130	3.900	.110	.190	.042
RT	15	.053	.064	.058	.091	.780	.088	.120	.029
Heat 550 F	15	.136	.080	.032	.164	.140	.590	.091	.630
RT	15	.028	.028	.037	.017	.088	.110	.015	.010
550 F	15	.108	.080	.260	.154	.094	.580	.780	.650
RT	15	.027	.028	.024	.007	.047	.110	.038	.025
550 F	20	.090	.075	.290	.119	.150	.530	.710	.620
-320 F	20	.036	.054	.032	.040	1.800	.098	.300	.042
550 F	20	.095	.080	.290	.128	.230	.510	.710	.600
-320 F	20	.038	.080	.043	.021	.280	.100	.081	.025
550 F	20	.095	.080	.066	.104	.120	.580	.660	.093
-320 F	20	.035	.098	.039	.033	.290	.140	.068	.025
6000 psi, 550 F	20	--	.044	.400	.120	.310	.490	.660	.710

(a) N clearance = 0.001 inch or less, X clearance = 0.003 or greater.
(b) N torque = 103 lb-ft for 3/4 in. and 27 lb-ft for 3/8 in.; X torque = 127 lb-ft for 3/4 in. and 34 lb-ft for 3/8 in.

measurements tabulated in Table 1 is only 2.26 x 10^{-8} atm cc/sec.

STRESS REVERSAL BENDING - Connectors are most vulnerable to fatigue failure at elevated temperatures. According to MIL-F-18280, the maximum stress in the tubing adjacent to the connector is limited to 20,000 psi. This includes the stress created by the fluid pressure. For a 3/4-inch annealed stainless steel tubing system at a fluid pressure of 4000 psi, the allowable bending stress would be of the order of 12,000 psi. The allowable bending moment for such a 3/4-inch tubing system would be 330 in-lb. In contrast, a moment of 353 in-lb was normally applied during evaluation of the AFRPL connector. The greater value was determined on the basis of the analysis described in Reference 4. For a 3/8-inch tubing system, the bending moment of 45 in-lb was computed. This value agrees with MIL-F-18280.

The arrangement used in testing the unions is illustrated in Figure 6. A connector was assembled and welded to a connecting rod at one end and to a rigidly mounted flange at the other end. A bellows that enclosed the connector was evacuated to a leak detector. The connector was heated to 600 F by the electric heater and maintained at that temperature throughout the test. The free end of the connecting rod was inserted into a spherical bearing assembled in the adjustable eccentric mounted on the motor shaft. Bending

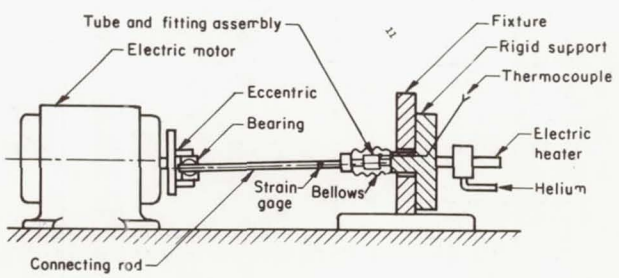

Fig. 6 - Experimental arrangement for stress-reversal-bending evaluation

moments were calibrated with strain gages mounted on the connecting rod. A similar arrangement was used in testing the elbows and tees.

A total of 8 unions, 2 tees, and 2 elbows were included in this evaluation. As indicated by the tabulation of results in Table 2, leakage did not exceed 2.7×10^{-8} atm cc/sec under dynamic conditions and at 4000 psi. Even at a proof pressure of 6000 psi and at a temperature of 600 F, leakage did not exceed 3.7×10^{-8} atm cc/sec. It should be noted that in testing Specimen 16, one million cycles were applied and the bending moment was increased threefold during the last 500,000 cycles.

Because of their geometries, it was not possible to enclose the tees and elbows in vacuum chambers during the test. A leak detector was subsequently used to measure leakage after the correct number of bending cycles had been applied. These leakage values are also tabulated in Table 2.

The stress-reversal-bending test was conducted at 600 F because of the reduced strength of the material at elevated temperatures. It is recommended that testing at maximum operating temperature become a standard practice for the evaluation of all connectors.

VIBRATION - Vibrational loads accelerate the relaxation of residual stresses, indirectly contributing to loosening of the nut, loss of preload, and possible movement of the seal. Evaluation of the relaxation effect was considered the major objective of this test.

Elbows and tees were tested by the cantilever-beam method with the test specimen mounted at the fixed end. Unions were tested by the indeterminate-beam method with the connector located midway between the rigid supports. These arrangements are illustrated in Figure 7a and b. Each specimen was vibrated at the lowest resonant frequency of the system with an amplitude sufficient to develop an applied bending moment equal to that applied during the stress-reversal-bending test. Each item was heated to 600 F and pressurized at 4000 psi.

Four unions, two tees, and two elbows were included in this evaluation. Most connectors were assembled at the minimum torque to simulate the condition most likely to develop leakage because of induced relaxation. Leakage was not measured by a leak detector during the test because of the technical problems of attaching a vacuum chamber that would not itself leak under these conditions. However, leakage was measured with a leak detector upon conclusion of the tests. These results are indicated in Table 3.

The maximum leakage recorded was 3.4×10^{-8} atm cc/sec, whereas the average was 1.7×10^{-8} atm cc/sec. Except for one case, when the tubing failed at one of the supports after 100,000 cycles, all specimens were subjected to at least

Table 2- Leakage Results for Stress-Reversal Test of 347 Unions, Elbows, and Tees

Description	Approx Elapsed Time, min	Maximum Leakage, 10^{-7} atm cc/sec											
		12U5	12U6	12U13	12U14	6U14	6U16	6U5	6U6	12L1	12L6	6T1	6T3
Clearance[a]	-	N	N	X	X	X	X	N	N	N	N	N	N
Torque[b], lb-ft	-	N	X	N	X	N	X	N	X	X	N	N	N
Bending moment, in-lb	-	353	353	353	353	45.4	45.4	45.4	45.4	353	353	45.4	45.4
4000 psi RT	5	.066	-	-	.029	.022	-	.180	-	-	-	-	-
6000 psi RT	5	.110	.034	.310	.130	.022	.120	.180	-	.084	-	-	-
6000 psi 550 F	15	.270	.370	-	.080	.008	.032	.270	-	-	-	-	-
4000 psi 550 F	5	.180	.340	.120	.080	.008	.032	.220	.032	-	-	-	-
Impose Bending Moment													
100,000 cycles	60	.230	.190	.087	.069	.035	.034	.110	.030	-	-	-	-
200,000 cycles	60	.230	.046	.061	.270	.024	.076	.081	.046	-	-	-	-
300,000 cycles	60	.190	-	.049	.110	.022	.068	.068	.016	-	-	-	-
400,000 cycles	-	-	-	-	-	-	-	-	.035				
500,000 cycles	-	-	-	-	-	-	-	-	.027[c]				
1,000,000 cycles	600	-	-	-	.058	-	-	-	-	-	-	-	-
6000 psi RT	-	.130	-	-	.069	.062	.089	-	-	.021[d]	.120[e]	.270[e]	.340[e]

(a) N clearance = 0.001 inch or less, X clearance = 0.003 or greater.
(b) N torque = 103 lb-ft for 3/4 in., and 27 lb-ft for 3/8 in.; X torque = 127 lb-ft for 3/4 in., 34 lb-ft for 3/8 in.
(c) The bending moment was doubled after 400,000 cycles, and tripled after 500,000 cycles before a weld broke.
(d) After 500,000 cycles, checked for leak after test.
(e) After 300,000 cycles, checked for leak after test.

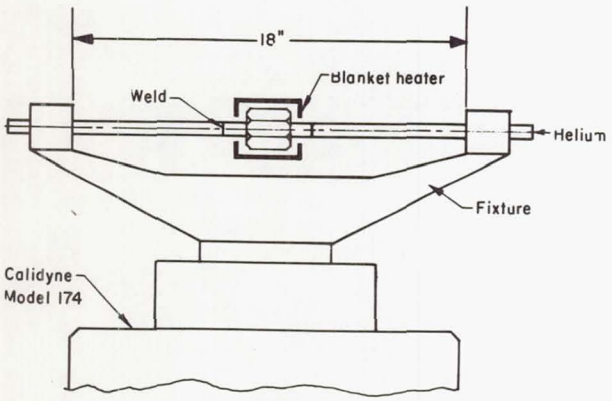

Fig. 7a - Experimental arrangement for vibration evaluation of unions

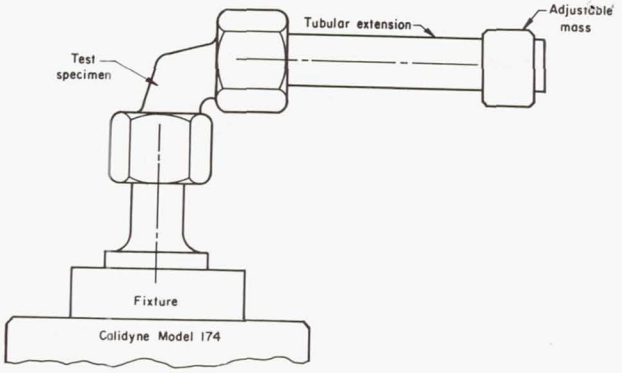

Fig. 7b - Experimental arrangement for vibration evaluation of elbows

300,000 cycles. In the case of Specimen 32, the test was extended for 1,250,000 cycles, equivalent to a period of 1 hour.

REPEATED ASSEMBLY - Leakage occurring after the first assembly has been of such concern that reassembly problems have received only secondary consideration in the development of improved connector designs. But separable connectors must be disassembled and reassembled repeatedly without structural damage resulting and without causing an increase in leakage. In performing this test, a 3/4-inch union was reassembled 20 times and a new Bobbin seal was inserted at each assembly. Leakage was measured with a leak detector after the first, ninth, fifteenth, and twentieth assemblies. Critical dimensions were measured after each assembly and sealing surfaces were examined for structural distortion or surface damage. The results are given in Table 4.

Because leakage measurements were taken at static conditions, the connector was pressurized to the proof pressure of 6000 psi. Leakages ranged from 1.3×10^{-8} to 8×10^{-8} atm cc/sec, with the lowest leakage rate recorded after the twentieth assembly when a torque of only 40 lb-ft was used to tighten the connector.

Although the connector was assembled at the maximum torque, there was no evidence of galling on threads or on bearing surfaces, and distortion or deformation of the seal cavity or the structural members was immeasurable. Lubricant was applied on only the first assembly.

Table 3 - Leakage Results for Vibration Test of 347 Unions, Elbows, and Tees

Description	Maximum Leakage 10^{-7} atm cc/sec							
	12SU15	12SU16	6ST2	6ST3	12SL5	12SL4	6SU13	6SU3
Clearance[a]	N	N	--	--	--	--	X	N
Torque[b]	N	X	N	N	X	N	N	N
Frequency of vibration, cps	353	353	120	120	120	127	160	160
After 300,000 at 550 F, 6000 psi RT	.175[c]	.073[d]	.257	.340[e]	.079	.190	.086	.160[f]

(a) N clearance = 0.001 inch or less, X clearance = 0.003 or greater.
(b) N torque = 103 lb-ft for 3/4 inch and 27 lb-ft for 3/8 inch; X torque = 127 lb-ft for 3/4 inch and 34 lb-ft for 3/8 inch.
(c) Surface temperature of nut dropped from 550 F to 275 F during test because one of the heaters burned out.
(d) Test for 1,250,000 cycles.
(e) After 300,000 cycles of vibration, tee was subjected to 300,000 cycles of full reverse bending moment of 45 lb-in, then leak checked.
(f) Tubing failed twice at vibration fixture support; therefore, testing was stopped at 100,000 cycles.

Table 4 - Results of Repeated Assembly Test of Type 347 CRES Union

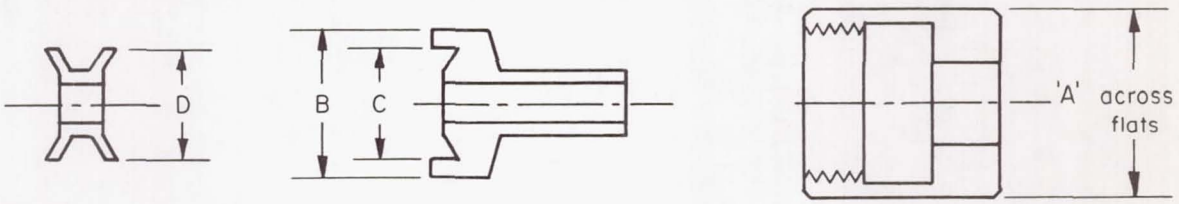

Assembly No.	A	B	C	D	Torque, lb-ft	Leakage, 10^{-7} atm cc/sec
0	1.190	0.9505	0.819	0.817	100	<0.8
1	1.195	0.9505	*	0.817	100	--
2	1.195	0.9506	*	0.816	95	--
3	*	*	*	0.817	95	--
4	*	*	*	0.816	95	--
5	1.1965	0.951	0.819	0.817	90	Leak in vacuum chamber
6	*	*	*	0.818	90	--
7	*	*	*	0.817	85	--
8	*	*	*	0.816	85	--
9	1.189	0.9505	0.8195	0.816	85	<0.345
10	*	*	*	0.816	95	--
11	1.194	*	*	0.816	80	--
12	*	*	*	0.816	75	--
13	1.1885	*	*	0.817	70	--
14	*	*	*	0.817	50	--
15	1.1885	*	*	0.816	100	<0.57 at 6000 psi
16	*	*	*	0.817	100	--
17	*	*	*	0.816	100	--
18	*	*	*	0.816	100	--
19	*	*	*	0.817	100	--
20	*	*	*	0.816	40	<0.126

* Not measured.

SUMMATION

The separable connector is, and will continue to be, a vital element in aerospace fluid systems and related support facilities. Where disassembly is periodically required for purposes of maintenance, repair, or replacement, a reliable, leakproof, separable connector will generally be more desirable than a permanent joint.

For these conditions, particularly where zero leakage is mandatory in systems operating at extreme temperatures, high pressures, and containing either corrosive fluids or low-density gases, the AFRPL connector would appear to represent a leading choice from among the available connectors.

REFERENCES

1. Everett C. Rodabaugh, "Significant Factors in the Design and Classification of Separable Tube Connectors", Paper presented at the Conference on Design of Leak-Tight Separable Fluid Connectors, George C. Marshall Space Flight Center, Huntsville, Alabama, March 24-25, 1964.
2. James W. Adam, "Elastic Displacements in the Design of Threaded Tube Connectors", Paper presented at the Conference on Design of Leak-Tight Separable Fluid Connectors, George C. Marshall Space Flight Center, Huntsville, Alabama, March 24-25, 1964.
3. Bernard Goobich, "Helium Leak-Tight Seal - Functional Analysis and Development", Paper presented at the Conference on Design of Leak-Tight Separable Fluid Connectors, George C. Marshall Space Flight Center, Huntsville, Alabama, March 24-25, 1964.

Page Intentionally Left Blank

A HIGH-TEMPERATURE THREADED CONNECTOR DESIGN

By

J. Wallach and J. P. Laniewski
Advanced Technology Laboratories
General Electric Company
Schenectady, N. Y.

ABSTRACT

A separable threaded tube connector for gases at temperatures to 1440°F and pressures to 4700 psi has been successfully designed and tested. Operating conditions for design consideration included vibration, shock, impulsive pressure, proof pressure and burst pressure. The connector consists of a triangular Nickel 200 gasket and a Rene' 41 flange, union, and nut. Recessed knife-edges on the union and flange cut into the gasket to effect a seal. The seal is isolated from load variations by an independent load path. A Buttress thread is used on the nut. The design proves out a previously prepared design manual.

THE HIGH-TEMPERATURE SEPARABLE CONNECTOR design and testing required a complete re-evaluation of present design and testing methods, and the development of new methods. The high-temperature connector is but one of the results of an extensive study of fluid connectors sponsored by the George C. Marshall Space Flight Center of the National Aeronautics and Space Administration under contracts NAS-4012 and NAS 8-11523. The contract work was done at the Advanced Technology Laboratories of the General Electric Company. The program was initiated to make possible the design of fluid connectors to meet the stringent requirements of the next generation of launch vehicles. Included in the program are research studies of the leakage mechanism, development of design procedures, and the development of connectors and connector components.

A major result of the study is a comprehensive Separable Connector Design Handbook (1)*. The manual includes the design of flanged and threaded connectors, the design of pressure-energized seals, a catalog of seals, a compilation of material properties, and a discussion of leakage measurement techniques. The threaded connector design procedure, formulated by Wallach, was used to design the connector described here. The procedure is for the design of separable tube connectors for tubing of about one inch diameter and smaller. The configuration of the generic connector is as shown in Fig. 1, except that the seal is unspecified.

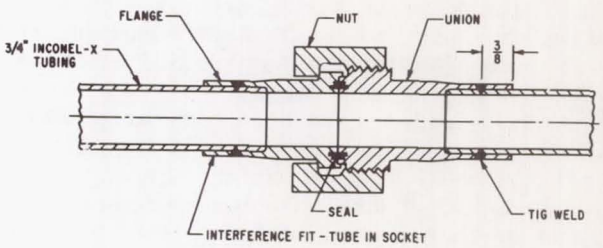

Fig. 1 - High-temperature connector configuration

Beginning with the general configuration, the procedure provides a step-by-step routine for calculating the connector dimensions. The design requirements are the input quantities. Once these are accurately determined, the manual provides a self-contained procedure for finalizing the design. The major steps of the procedure are outlined in subsequent sections. However, the details are too lengthy to include here and the interested reader will find them in the manual. In particular, the design example used in the threaded connector section is the high-temperature connector described here.

DESIGN PROBLEM

The design requirements call for a separable hot-gas connector for tubes of up to and including one inch diameter which will operate in a specified environment with "zero-leakage". The gas temperatures vary from ambient to 1440°F and the pressure to 4700 psi. The requirements also

*Numbers in parentheses designate References at end of paper.

include satisfactory operation during an externally induced vibration, an impulsive internal pressure, an externally applied shock, and an internal proof and burst pressure. The conditions are stated in Table 1.

Table 1 - Operating Conditions for High-Temperature Connector

Description	Temperature °F	Pressure psi	Leakage	Cyclic Loading
High-temperature	1440	4700	"zero"	none
Proof	70	9400	no req't	none
Burst	70	18800	no req't	none
Vibration	70	4700	"zero"	221 in.-lb. transverse moment -10^{6} cycles
Impulse	70	6000	"zero"	2000 pressure cycles
Shock	70	4700	"zero"	150 g shock

The "zero-leakage" requirement must be interpreted with regard to present standards and present leakage measuring methods. Based on these considerations the leakage requirement was interpreted as less than 1×10^{-6} atm cc/sec* of helium. Designing for this level of leakage and testing with a mass spectrometer capable of measuring to less than 1×10^{-7} atm cc/sec makes it possible to determine the accuracy of the design procedure. The high-temperature requirement has to be interpreted as "zero-leakage" at 4700 psi for approximately ten hours. This is to cover any problems which may arise in testing that would require keeping the connector at 1440°F for a few hours. The time at temperature is of course important in the stress relaxation considerations for the nut. The proof pressure is twice the operating pressure and is a structural rather than a leakage requirement. The proof pressure requirement is to prevent yielding in the connector so that the connector is again leak-tight at operating pressure. The burst pressure of four times operating pressure is a structural requirement to prevent a complete failure.

The impulse and vibration requirements are primarily leakage specifications. Most structural failures would first be detected as a leak. The impulse peak pressure of 6000 psi is maintained for only a small part of the cycle. During a major part of the impulse cycle the pressure is at approximately 4700 psi. Whereas the impulsive load is an internal pressure force, the vibration condition is due to forces transmitted from the supporting structure. The 221 in.-lb. transverse moment was chosen to give a maximum fiber stress of 10,000 psi at the connector-to-tube weld joint. The shock requirement, also primarily a leakage specification, was translated from a "g" loading to a fiber stress at the weld joint. Obviously the stress specification is more meaningful in design than a "g" loading which could result in any stress desired depending upon the location and type of tube supports relative to the connector.

The connector design is based upon these requirements and the further very important requirement of minimum weight and bulk. Of course, first and foremost, the connector could not leak, but neither could it be too conservative a design. Therefore, such other operating conditions as thermal transients were not considered in establishing the design. However, an allowable temperature difference between the nut and other parts of the connector was calculated after the design was completed. This is two to three hundred degrees Fahrenheit, which is adequate for moderate rates of heating. Actually, very little is known about the thermal transients experienced in applications.

DESIGN

DESIGN CONFIGURATION - The configuration is that recommended in the design manual (1), Fig. 1. The threaded connector, as compared to the bolted flanged connector, is better suited for small size tubing. A properly designed threaded connector will not require an excessive assembly torque, and avoids using small bolts or large flanges. The threaded connector consists of the seal, flange, union, and nut, Fig. 1. The seal consists of the removable gasket, Fig. 2, and its companion sealing surfaces on the flange, Fig. 3, and union, Fig. 4. The nut is detailed in Fig. 5.

The connector features a seal protected

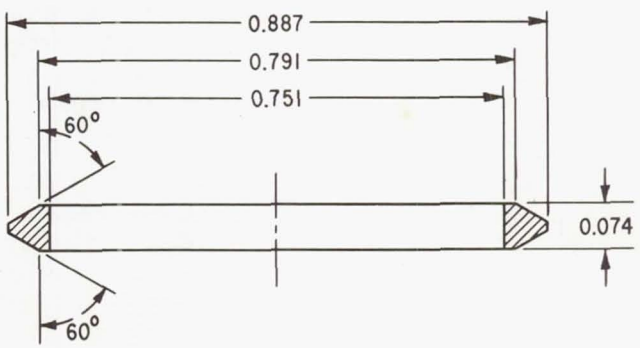

Fig. 2 - Triangle gasket (material Nickel 200)

*atm cc/sec - An atmospheric cubic centimeter is a cubic centimeter of gas at 14.7 psia and 68° F.

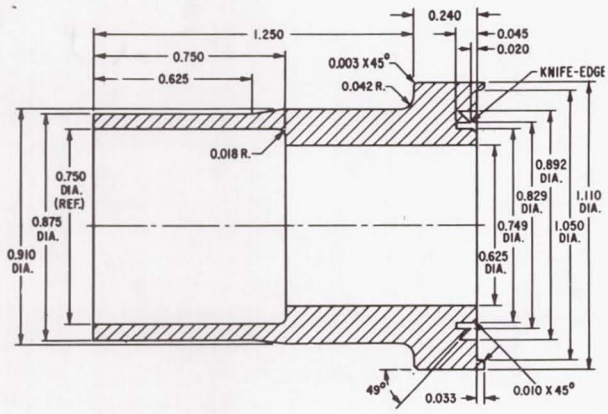

Fig. 3 - Flange (material Rene' 41)

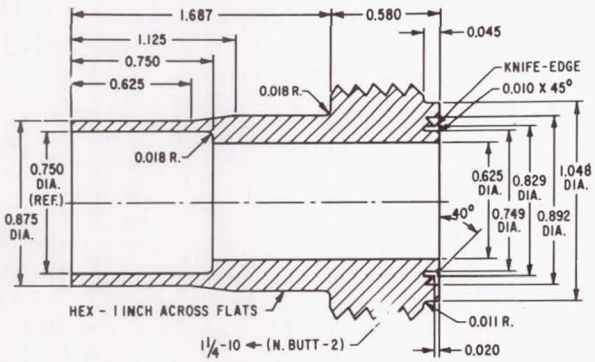

Fig. 4 - Union (material Rene' 41)

from relative movements and load variations. The lip on the flange locates the union during assembly and prevents relative radial motion of the flange and union. During assembly the knife edges cut into the gasket until the union seats on the flange. Seating occurs when approximately 1000 lbs. of the 4300 lbs. preload is applied and the additional 3000 lbs. is transmitted directly from the union to the flange. This independent load path protects the seal from load variations as there is always a compressive load between the flange and union during all operating conditions. Also, this compressive load resists relative radial movements because of the friction between the flange and union.

The preload is applied by torquing the nut on the union to a specified torque value. The use of a torque wrench is the most practical approach at present but not necessarily the most accurate.

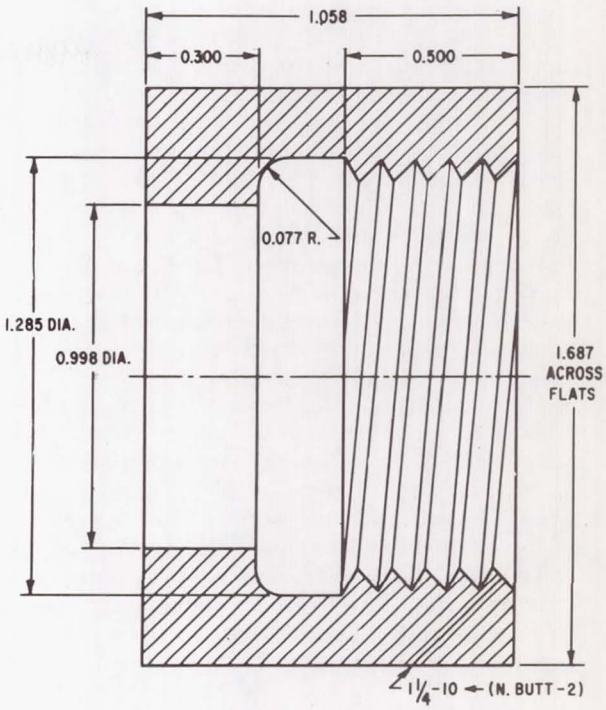

Fig. 5 - Nut (material Rene' 41)

In order to carry the high tensile load with a minimum of bending moments an American Standard Buttress Screw Thread is used on the nut and union. The seven degree angle on the load face of the thread nearly eliminates the induced radial load common in most thread forms. The result is the same tensile force with a smaller nut.

The connector-to-tube joint is a socket fusion weld. This provides a leak-tight high-temperature joint. The tube is lightly pressed into the socket so that the whole socket is utilized to transmit the load from the tube to the connector. Thus, additional static and fatigue strength is obtained. This type of connection was first developed as a permanent connection, (2) (3).

SEAL - The seal is based upon the principle that plastic deformation of one of the mating materials is required for a reliable leak-tight joint. Plastic deformation is most easily produced by a shearing action, (4). Therefore, use is made of knife-edges of a hard material cutting into a gasket of soft material. The gasket is permanently deformed and for maximum reliability should be disposed of every time the connector is opened. For this reason the gasket is a sim-

ple ring which is inexpensive. The knife-edges, with all the intricate details such as their being recessed for protection, are on the permanent parts of the connector.

The seal was chosen after a thorough study of the sealing mechanism and of various types of seals. The final selection was made by testing a number of seals from which the most suitable was chosen. It had a triangular cross-section, but the apices were cut off to facilitate manufacture of the mating parts. The included angle of the knife-edges is small in order to get the desired depth of cut with a minimum load. The center line of the cross-section of the knife-edge is at an angle with the center line of the connector to make the cutting action radial as well as axial and thus make the seal less sensitive to axial load variations. One side of the knife-edge is parallel to the connector center line, thus keeping the gasket from moving away from the knife-edge as it cuts into the gasket and providing a slight clamping action on the gasket.

MATERIALS AND PROCESSES - Materials are dictated by the high-temperature requirement. Rene' 41 was chosen for the connector because of its excellent static and creep strength at 1440°F and its availability in many sizes of bar stock. Rene' 41 tubing is available only on special order of large quantities. Therefore, Inconel X tubing was chosen. This material also has very good high-temperature properties and is compatible with Rene' 41 in the sense of welding and heat treatment.

These materials should be welded in the solution treated (annealed) condition and then heat treated. The welds are made by rotating the tube and union (or flange) past a tungsten electrode in an inert gas atmosphere. The electrode arc puddles the union and tube material to form the weld. No filler material is used. Prior to construction of the connector tested, sample welds were made, heat treated, and tested to determine the proper welding schedule and the strength characteristics.

The heat treatment chosen for the Rene' 41 optimizes the creep strength. However, as the flange and union are welded to Inconel X prior to heat treatment, the last step of the "three step" heat treatment for Inconel X was added. The heat treatment is:

1. 2150°F for 2 hours; air cool to room temperature
2. 1650°F for 4 hours; air cool to room temperature
3. 1300°F for 20 hours; air cool to room temperature.

STRESS ANALYSIS - Having chosen the configuration, seal, materials and heat treatment, the stress analysis follows and finalizes the dimensions. This part of the design is too lengthy to cover in detail here and is very well covered in Chapter 3 of (1). Using the procedure outlined in the manual the analysis began with a tabulation of the operating conditions. Any conditions which would obviously not influence the choice of preload or final dimensions were deleted.

As the preload determines the stresses and thereby, the final dimensions, and as the final dimensions determine the preload, this is an iterative procedure. The procedure began by calculating approximate dimensions using the formulas in the manual. Then, two axial spring constants were calculated, one for the nut and one for the flange-union combination. The external loads and internal pressure for each operating condition were converted to axial forces. Using the largest axial force acting on the two springs, which are in parallel, a preload was calculated so that the compressive force on the flange-union is never less than 1200 lbs. Before using the calculated preload of 4300 lbs., the corresponding assembly torque was calculated and found reasonable. As the nut acts like a spring in parallel with the flange-union, the more flexible the nut, the less axial tensile load it will carry and the nut can be made smaller. However, the preload increases linearly with the increase in axial tensile load carried by the flange-union and the corresponding assembly torque soon becomes too large. Thus a balance was struck between the size of nut and assembly torque.

Next the static and cyclic stresses were calculated for each operating condition. These stresses were calculated at a number of high stress locations and consideration was given to the tri-axiality of the stresses, stress concentration factors, localized flexibilities, and shear deformation. The static stresses were compared to yield and creep strengths, and the cyclic stresses to fatigue strengths. The dimensions were changed and the preload and stress calculations were repeated. Three complete calculations were made before finalizing the dimensions.

Four operating conditions were considered critical. The high temperature, vibration, and impulse conditions all require "zero leakage" and, therefore, were con-

sidered in the preload determination. The high temperature, vibration, and proof conditions were considered in the static strength determination. The vibration and impulse conditions were considered in the fatigue strength determination. A complete set of calculations were made for each operating condition. It turned out that the vibration condition determined the preload, the high temperature condition resulted in the most severe static stresses, and the impulse condition resulted in the most severe fatigue stresses.

MANUFACTURE

The connector was manufactured in the General Electric Company's Advanced Technology Laboratories' development machine shop. Nickel alloys, such as Rene' 41 and Inconel X, are difficult to machine and special methods were used (5).

TESTS

The connector was assembled with the prescribed preload and put through the sequence of tests in Table 2 without being taken apart. It was retorqued once as indicated in the table. The preload was accurately set by using a torque wrench and strain gages on the nut. Both the wrench and gages were calibrated by loading the nut in a standard testing machine.

The sequence of tests and results are given in Table 2. The connector performed satisfactorily in all tests, although a slight degradation of performance is noted after the connector was retorqued.

All leakage measurements were made by introducing high pressure helium to the inside of the connector, collecting the leakage in a vacuum chamber around the connector, and measuring the quantity using a mass spectrometer. Bottled helium at about 2000 psi was used in conjunction with a booster compressor with an output capacity of 30,000 psi, Fig. 6.

The vacuum chamber consists of two end plates welded to the tubing and a cylindrical can that slides over the connector and is attached to the end plates, Fig. 7. For room temperature testing, the bellows, shown in Fig. 7, was bolted to the end plates and rubber O-rings were used as gaskets. For the high temperature test, the pipe section, shown in Fig. 8, was welded to the end plates and heating units were placed around the pipe. A piece of tubing welded to one of the end plates was connected to the mass spectrometer and also used to lead-out thermocouple instrumentation used during the high temperature test.

For the vibration test, the connector and vacuum chamber were mounted on a special vibration fixture, Fig. 9. Leakage measurements were made during the vibration test. This fixture was also used for the shock test on a Vari-Pulse machine, Fig. 10.

Impulse testing of the connector was not accomplished since equipment for carrying out

Table 2 - Tests in Sequence as Run and Results

Description	Loading	Temperature °F	Pressure psi	Leakage atm cc/sec	Notes
Room temperature	(1)	70	4700	n. m.(4)	
Vibration	(1) & (2)	70	200	n. m.	
	(1)	70	1500	n. m.	
Room temperature	(1)	70	7500	n. m.	
			8000	3.8×10^{-5}	(5)
Shock	(3)	70	0	-	
Room temperature	(1)	70	4700	n. m.	
Proof	(1)	70	5500	n. m.	
			6000	5.5×10^{-5}	(6)
Room temperature	(1)	70	4700	n. m.	
Retorqued					
Proof	(1)	70	5000	n. m.	
			5400	3×10^{-6}	(7)
Room temperature	(1)	70	4000	n. m.	
			4700	1.2×10^{-6}	
High-temperature	(1)	1440	4700	n. m.	(8)
Burst	(1)	70	18800	-	(9)

Footnotes to Table 2

(1) Static internal pressure
(2) Transverse cyclic moment of 221 in lb applied for 200,000 cycles at 83.6 cps.
(3) 100 g's input to fixture holding connector which resulted in maximum stress at weld of 75,000 psi.
(4) n.m. - not measurable on mass spectrometer leak detector. Less than 1×10^{-7} atm cc/sec.
(5) Leak closed when pressure reduced to 5000 psi
(6) Pressure raised to 9400 psi; leak closed when pressure reduced to 2000 psi; no visible gross yielding
(7) Pressure raised to 9400 psi; no visible gross yielding
(8) At 1440°F with pressure at 2000 psi and above, momentary leaks of about 1×10^{-6} atm cc/sec were observed during sudden pressure increases. Connector at 1440°F for 3 hours.
(9) Hydraulic fluid used; no visible failure

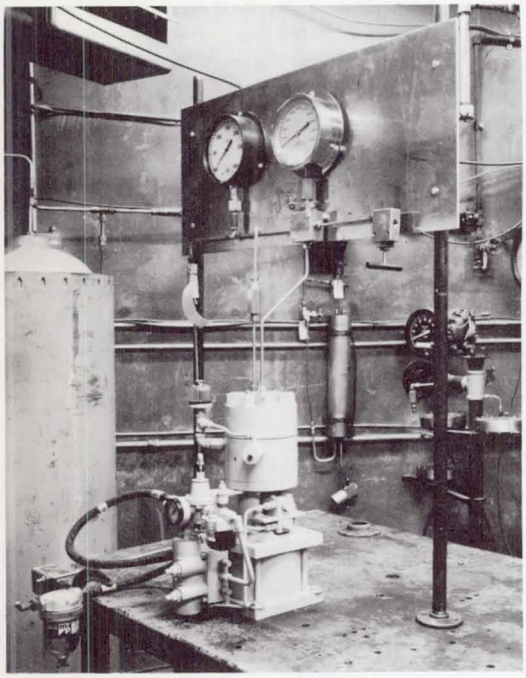

Fig. 6 - Booster helium compressor

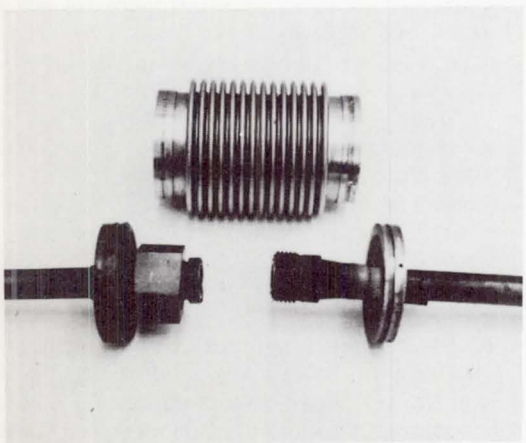

Fig. 7 - Vacuum chamber and connector

a test such as this would be costly and with the value of such results being questionable by comparison with the other tests, the fabrication of the equipment could not be justified.

In this vein, too, the original one million cycles of vibration cycles was not attained because it was felt that 200,000 cycles would be a satisfactory period of vibration. The first

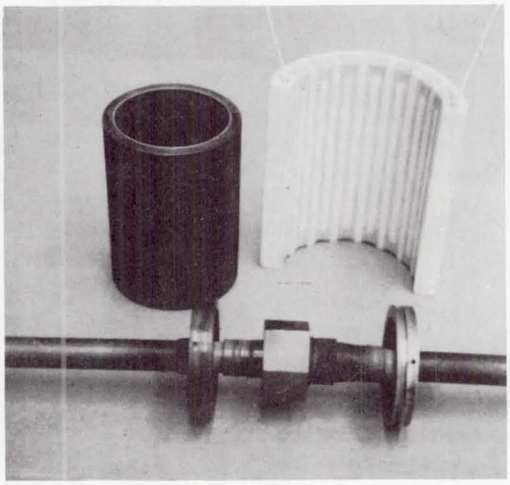

Fig. 8 - High temperature vacuum chamber cylindrical can and heater

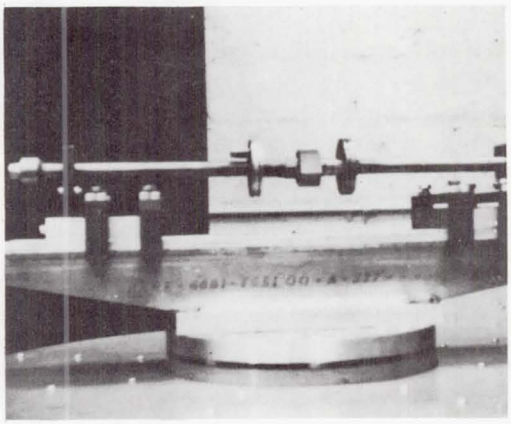

Fig. 9 - Vibration test fixture with connector (without bellows attached)

200,000 cycles were the critical period, and once the connector was beyond this, probability of failure was small.

CONCLUSIONS

The results of the tests show that the connector satisfactorily met all design requirements. However, further improvements are possible. Design requirements can be more precisely stated and can include transient conditions. The design procedure can be refined using the experience gained from testing. The result will be an optimized design for a particular set of operating conditions.

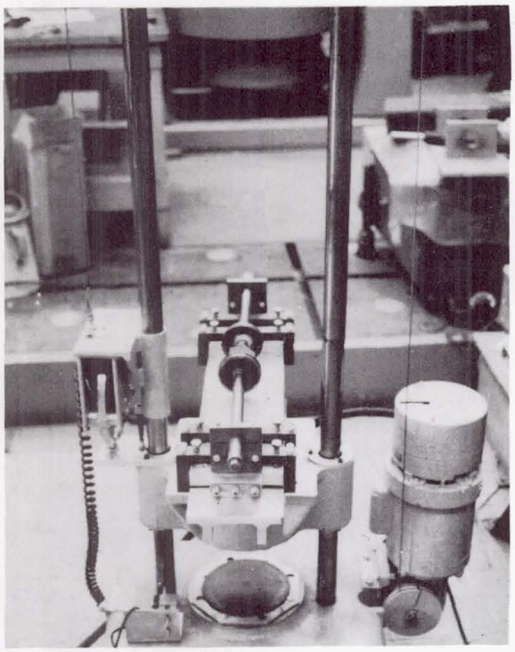

Fig. 10 - Shock test fixture with connector

It may also be possible to reduce the weight and size of the connector. However, considering the high temperature, high pressure, and "zero leakage" requirements and comparing this design to present connector designs for lower temperatures and less stringent leakage requirements, the connector does not seem too heavy or large. There is very little experience in designing connectors for this service, and until such experience is gained, a complete appraisal of this connector is not possible.

REFERENCES

1. F. O. Rathbun, Jr., Design Criteria for Zero Leakage Connectors for Launch Vehicles, "Separable Connector Design Handbook," NAS 8-4012, December 1, 1964.

2. G. R. Barton, "Tubular Joining by Induction Brazing and Fusion Welding Methods," Paper presented at the 25th SAE National Aeronautics and Space Engineering and Manufacturing Meeting, Los Angeles, October 1962.

3. M. H. Weisman, "Applied Research and Development Work on Families of Brazed and Welded Fittings for Rocket Propulsion Fluid Systems." Technical Document Report No. RTD-TDR-63-1027, November 1962.

4. F. O. Rathbun, Jr., Design Criteria for Zero Leakage Connectors for Launch Vehicles, Vol. 3, "Sealing Action at the Seal Interface," NAS 8-4012, March 15, 1963.

5. H. M. Schrier, "How to Machine Those HT Alloys," Aircraft and Missiles Manufacturing, May 1959.

Page Intentionally Left Blank

MINIATURIZED TUBE FITTINGS

By

John Nicol
The Weatherhead Company
300 East 131st Street
Cleveland, Ohio 44108

ABSTRACT

MINIATURIZED TUBE FITTINGS

Stress analysis of MIL-F-18280 tube fittings revealed that by taking advantage of the strength-to-weight ratio of titanium, weight reductions of 4 to 1 and volume reductions of 3 to 1 were possible.

Titanium miniaturized flareless fittings were made and their performance capabilities were verified by tests to MIL-F-18280 requirements with additional impulse-vibration at 600°F and thermal shock tests at -320°F. A flareless fitting sleeve with serrated cutting edge was found to have better gas sealing and retention characteristics than the standard MS21922 sleeve.

This is a review of some of the work that has been done to develop compact tube fittings for fluid systems in advanced flight vehicles to operate reliably thru broader temperature ranges; particularly for hydraulic fluids at higher temperatures and for low molecular weight gases in cryogenic environments.

These all-metal miniaturized fittings are for tube-to-tube connections such as straight connectors, elbows, tees and crosses; or for direct connection to component bosses.

MINIATURIZED FITTINGS - Rather than introduce a radically different concept for tube-to-tube connections, with the possibility that inherent shortcomings of the fittings would be discovered only after many engineering test and service hours, this program was one of miniaturizing the proven Military Standard "Ermeto" flareless fitting.

One approach to weight reduction of high-pressure tube fittings has been to make the Standard MS-flareless fitting from a titanium alloy without change in physical dimensions. Although the resulting product is much lighter in weight, as compared to steel, retaining the same size does not take full advantage of the higher strength/weight ratio of titanium.

The broader objective, therefore, was to design a new fitting from titanium alloy that would use the proven Ermeto flareless principle, take full advantage of the inherent high endurance strength of the metal, (to reduce the overall size and further reduce the weights) and at the same time, improve sealing qualities for gas as well as liquid systems.

The first step in this development was to make an extensive study of the basic properties of titanium alloys, including fatigue limits of the metal. The specific property of high endurance strength over a fairly wide temperature range, permits reduced section thickness. It was decided to maintain the basic MS33514/MS33515 seat dimensions and inside diameters.

Based on stress analysis, several fitting designs incorporating these features were made and tested before arriving at a suitable design that would meet the performance requirements. Close coordination was maintained in the manufacturing phase to develop machining and forging techniques for the titanium alloy. Also, acceptance criteria were developed for suitable titanium metallurgy, as related to the Alpha/Beta relationship and surface or "skin conditions"

The major design criterion for fitting working stress was that it should outperform the tubing to which it was attached and without damage to the fitting itself.

SLIDE 1 - This depicts the familiar relationship of hoop and longitudinal stresses resulting from internal fluid pressure and bending. As the sum of longitudinal stresses resulting from bending and pressure are usually higher than hoop stress due to pressure alone, the longitudinal stress becomes the principal stress in the calculations.

Tubing: MIL-T-6845 at Room Temperature

Dash Number	Tube Size in.	Wall Thickness inches	Hoop Stress (Transverse) psi	Long. Stress Due to press. psi	Allowable Bending Stress psi	Combined Long. Stress psi	Set-up Length - inches
12	3/4	.049	34,400	18,400	24,000	42,400	7.3

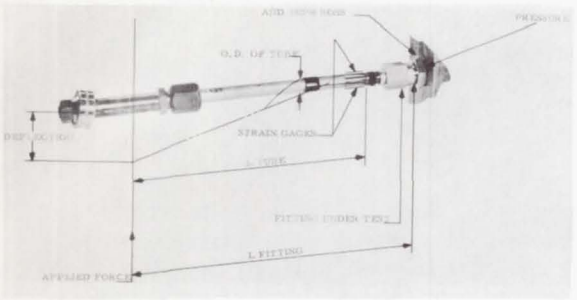

Stress Due to Pressure:

Hoop: $S = \frac{Pd}{2t}$

Longitudinal: $\approx \frac{Pd}{4t}$

BENDING STRESS

$S = \frac{MC}{I} = \frac{FLC}{I}$, $D = 1/3\ \frac{FL^3}{EI}$: Combining these; $L = \sqrt{\frac{3DEC}{S}}$ or $S = \frac{3DEC}{L^2}$

Slide 1 - Stress analysis of tube and fitting assembly

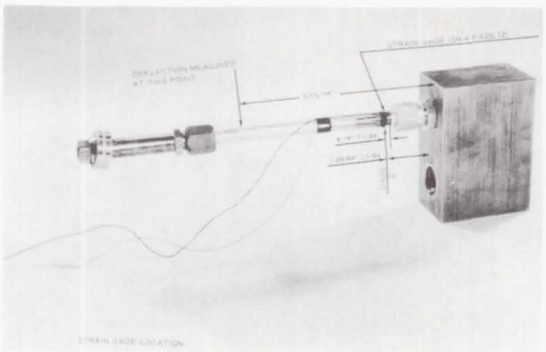

Slide 2 - Vibration test assembly

For test purposes, the bending stress is applied by repeatedly flexing the tubing as a cantilever beam with either planar or rotary motion.

SLIDE 2 - On the second slide, we see the method of applying strain gagesto the tubing of test samples to provide correlation between calculated and actual stress values. Proper alignment is very important in the test set-up to eliminate prestresses that produce premature failure.

SLIDE 3 - The next slide is a tabulation of the mechanical properties of 6AL4V titanium, shown in comparison with the properties of more conventional tube fitting materials.

As the slide shows, titanium maintains adequate strength at appreciably higher temperatures than aluminum. Also, the endurance limit for titanium is over 80, 000 psi as compared with 18, 000 psi for aluminum. This is a decided advantage where fittings are connected to long lengths of tubing, producing high cantilevered bending stresses. The material was used in the annealed condition, mainly because of its better low temperature properties and machinability.

Other materials having mechanical properties equivalent to titanium can also be used for miniaturized fittings of these same dimensions, where this is necessary

		Ultimate Tensile Strength	Yield Strength	Elongation	Endurance Limits	Tensile Strength/Density X1000
Aluminum						
2014-T6	R.T.	70,000	60,000	13%	18,000 psi	70,000/2.7 = 26.0
	300F	40,000	35,000	15%		40,000/2.7 = 14.8
	600F	6,500	5,000	65%		6,500/2.7 = 2.4
2024-T6	R.T.	69,000	57,000	10%	18,000 psi	69,000/2.7 = 25.
	300F	45,000	36,000	17%		45,000/2.7 = 16.7
	600F	8,000	6,000	75%		8,000/2.7 = 2.9
Steel						
C-1141 Cold drawn		110,300	99,000	14.8%	45,000 psi	110,300/7.8 = 14.2
C-1141 Hot Rolled		90,000	57,800	26.5%	40,000 psi	90,000/7.8 = 11.5
304 Stainless Annealed		85,000	35,000	60%	34,000 psi	85,000/7.75 = 11.0
304 Stainless Annealed & Cold drawn		100,000	60,000	45%	48,000 psi	10,000/7.75 = 12.9
Titanium						
6AL4V	R.T.	148,000	136,000	15%	87,000	148,000/4.42 = 33.5
	300F	125,000	105,000	16%		125,000/4.42 = 28.3
	600F	105,000	93,000	15%		105,000/4.42 = 23.8

Slide 3 - Titanium - mechanical properties of compared to aluminum and steel

for compatibility of the material with specific fluids, or where temperatures are too high for titanium. The same stress analysis procedure used here for titanium has been successfully applied in the selection of materials for higher temperature applications, where Inconel-X, AM-355 and Rene 41 were chosen. Production miniaturized fittings have been made mainly from 6AL4V titanium, and some were made of AM-355 stainless steel.

SLIDE 4 - This bar chart, comparing the strength of titanium, aluminum and stainless steel, is used only as a model to show the calculated wall thickness for a 1" O.D. section subjected to hoop stress to burst at 12, 000 psi internal pressure. It is obvious that a much smaller section is required for titanium, and that at higher temperatures aluminum is out of the picture.

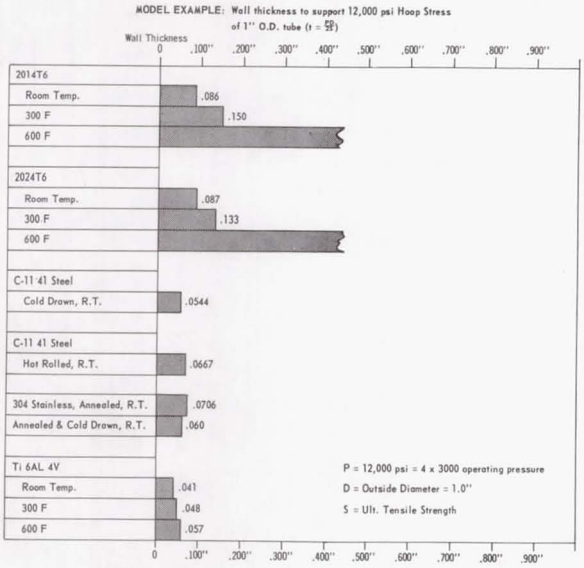

Slide 4 - Strength comparison of tube materials

SLIDE 5 - To assure proper metallurgy, close coordination was required between material supplier and manufacturing plant, particularly with respect to forgings.

This slide shows various conditions of the Alpha/Beta matrix and depicts acceptable and unacceptable conditions. This control was instituted to prevent field failures due to intergranular corrosion; although, in laboratory tests, fittings deliberately made with very extensive basket weave condition satisfactorily met the burst and impulse test requirements of MIL-F-18280B.

Acceptable microstructure is indicated by the familiar pattern of small islands of

ACCEPTABLE

7294-29

Magnification 100X, Kroll's etch
6-4 titanium bar - nuts or unions

Typical microstructure for acceptable bar stock.

The reduction in the α-B field is considerably larger than it is in shapes, however, in the above shown structure it was not large enough to sufficiently deform and break up the α-plates into an equiaxed α-B.

UNACCEPTABLE

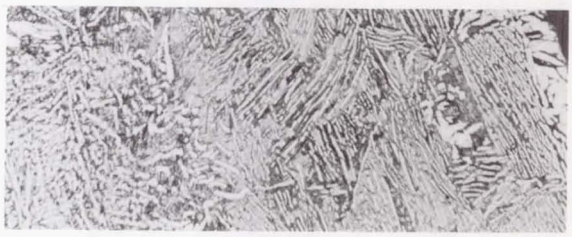

7294-30

Magnification 100X, Kroll's etch
6-4 titanium forging - Tee

Unacceptable quality because:

1) The hardness of the embrittled skin exceeded 414 KHN.

2) The microstructure shows close to the surface evidence of severe overheating with α-phase in grain boundaries. The remaining structure was basketweave type without primary α.

Slide 5 - Microstructure of 6AL4V titanium

Alpha which occur in the Beta stablized 6AL4V during cooling. Unacceptable microstructures are indicated by excessive acicular Beta in the body of the material, or brittle primary Alpha concentrations at the surface.

This brittle acicular Beta is depicted by a needle-like microstructure which, in the unacceptable condition has a basket weave appearance. This can occur from forging the material above the Beta transus temperature of about 1825°F. Correct preparation of metallurgical specimen cannot be overemphasized. Special care is required to achieve good contrast between the Alpha/Beta phases.

SLIDE 6 - Surface contamination occurs from the diffusion of oxygen in the air during high temperature fabrication of the bar or forging. In this case the surface will be formed of primary Alpha instead of Alpha/Beta because the oxygen stablizes the Alpha phase at the surface.

Photo 293 E-9-1 Magnification 250X, Kroll's etch 6-4 titanium forging - elbow

Unacceptable quality because:

1) The contaminated skin was not removed.

2) Large grains, basketweave structure and segregations indicate that the forging was fabricated above the B transus temperature.

Slide 6 - Surface contamination of 6AL4V titanium

During processing, the metal is protected from oxygen contamination by conversion coatings of silicone or other materials.

Slight surface contamination, generally referred to as "skin condition" is removed from fittings by sand blast followed by brief etching in a pickling solution of 16% nitric and 3% hydroflouric acid. Surface cracks which exceed .008" are not acceptable in the final product.

Also, hydrogen contamination, as determined by gas analysis, should not exceed 125 parts/per million.

In production, precision surface finishes were maintained, and threads were produced by the Cri-Dan single point method which closely controls thread contour. This method results in an even distribution of thread load to minimize creep, a characteristic very important in metal-to-metal seals.

SLIDE 7 - This slide shows the vibration-impulse test set-up conditions where the calculated bending stress averaged 24,000 psi with a combined longitudinal stress of 42,000 psi due to bending and fluid pressure. Note that the tubing was MIL-T-6845, which is Type 304 stainless steel, 1/8" to 1/4" hard.

TEST NO. 70385 F

1. Vibration-Impulse Test at Room Temperature -12 Size Miniature Fittings

A. Test Conditions

Fittings Used:

Nuts	ER00921-12T
Unions	ER00902-12T
Sleeves	MS-21922-12

Tubing Used:

3/4" x .049" wall, MIL-T-6845

Assembly Conditions:

Machine preset pressure	96 psi
Reset Torque	1400 in lbs.
Union to block torque	750 in lbs.

Test Set-Up Conditions:

Effective length	6.3
Cut length of tubing	8"
Length from fixed end	7 5/16"
Moment of inertia of tubing	(.00667")⁴
Rate of cycling - vibration	1750 C/M
Rate of cycling - impulse	35 ± 5 C/M
Pressure	3000 psi
Peaks	150% (4500 psi)
Deflection	.042"
Temperature	Room

Formula used to calculate stress:

$S = \frac{FLC}{I}$ where

S = Stress in psi
F = Load in pounds
L = Distance from point of last support in inches
C = 1/2 O.D. of tubing in inches
I = Moment of inertia of tubing in inches⁴

Slide 7 - Vibration-impulse test conditions (room temperature set-up)

SLIDE 8 - This table shows the flexure failure range. The test was stopped at just over 20 million vibration cycles. Note that the two tubing failures occurred at the ring cut. In this type of test, approximately 80% of the failures normally occur not at the ring cut but at the last point of support; that is, under the sleeve shoulder.

There were no fitting failures in this test, and the minimum and mean life of the tubing was in excess of that usually encountered in this flexure test.

SLIDE 9 - On combined vibration-impulse tests at 600°F, bending stress was reduced to 16,000 psi, based on the reduction in tubing material strength and endurance limits at 600°F. For this test the sleeves were coated with a vapor-deposited chromium alloy since cadmium plating would have vaporized at that temperature. The test fluid was GE-F50 Versilube, silicate ester. There was no

TEST NO: 70385 F

B. Test Results

Sample	Deflection Inches	Weight for Deflection lbs.	Stress per Weatherhead PSI	Vibration Cycles	Impulse Cycles	Burst Pressure PSI	Remarks
1	.042	71	25,100	9,030,000	180,600	-	Tubing cracked at ring cut on vibration impulse test.
2*	.042	65	22,980	20,313,500	406,140	17,500	End blew off (See Note #1) on burst test
3*	.042	84	29,700	20,313,500	406,140	16,200	End blew off on burst test
4*	.042	64.5	22,810	20,313,500	406,140	16,000	End blew off on burst test
5*	.042	65	22,980	20,313,500	406,14	15,500	End blew off on burst test
6	.042	61.5	21,750	4,987,500	99,750	-	Tubing cracked at ring cut on vibration impulse test

* - No failure during vibration-impulse test.

NOTE: #1 - On first attempt to burst sample, the end plug (not part of test sample) blew off at 17,500 psi. On second attempt (using new end plug) the sleeve and titanium fitting blew off at 14,000 psi.

Slide 8 - Vibration-impulse test results (room-temperature set-up)

TEST NO. 71138 F

B. Test Results (600 F Vibration-Impulse Test)

Sample	Total Vibration Cycles	Total Impulse Cycles	Remarks
1	11,917,500	200,191	No Failure
2	11,917,500	200,191	No Failure
3	11,917,500	200,191	No Failure
4	11,917,500	200,191	No Failure
5	11,917,500	200,191	No Failure
6	11,917,500	200,191	No Failure

After completion of testing all assemblies were disassembled and visually inspected for irregularities. Visual inspection showed all samples to be in excellent condition after completion of testing.

Slide 9 - Vibration-impulse test results (600°F set-up)

leakage on either the room temperature or 600°F vibration tests. The latter test was stopped at just under 12 million cycles, with no failures.

SLIDE 10 - Following the 600°F combined impulse-vibration test the same assemblies were impulse tested at -65F to verify their integrity. There were no failures or leakage on this test.

TEST NO. 72338 F

Impulse Test at -65°F, -12 Size Miniature Fittings

A. Test Conditions:

Fittings Used:

Same assemblies previously vibration-impulse tested at +600°F (Reference Test No. 71138 F)

Tubing Used:

See Above

Test Set-Up Conditions:

Pressure	3000 PSI
Peaks	150% (4500 PSI)
Rate of Cycling	35 ± 5 C/M
Fluid Used	MIL-O-5606
Temperature	-65°F

B. Test Results:

Sample	Reset Torque Inch lbs.	Total Cycles	Remarks
1	1565	70,100	No Failure
2	1565	70,100	No Failure
3	1565	70,100	No Failure
4	1565	70,100	No Failure
5	1565	70,100	No Failure

Slide 10 - Impulse test results (-65°F set-up)

The same six assemblies were then subjected to a 96 hour salt spray test per Federal Standard 151, Method 811. There was slight corrosion between the sleeve and tube on one assembly and minute pitting on the sleeve of another, with no corrosion on the other four assemblies. As a result of later investigation, improved coatings have been found which are suitable to 900°F, and these easily pass the salt spray test.

SLIDE 11 - In the repeated assembly test, the fittings were completely disassembled 15 times and reset each time with a torque wrench to 1600 in/lbs. torque. A 6000 psi hydrostatic proof test was conducted after every third reset and 12,000 psi (burst value) proof test after the 15th reset. There were no failures or leakage.

SLIDE 12 - On the thermal cycling/shock test, several 3/4" tube assemblies were pressurized with 3000 psi Helium (entrapped gas), and were alternately immersed in 200°F water and -300°F liquid nitrogen baths for 60 cycles. This test was also conducted on 1/4" fittings, because our experience has shown that sealing of gases is generally more diffi-

TEST NO. 71138 F

11. Repeated Assembly Tests -12 Size Miniature Fittings

A. Test Conditions:

Fittings Used:

Nuts	ER00921-12T
Unions	ER00902-12T
Sleeve	MS-21922-12

Tubing Used:

3/4" x .042" wall, MIL-T-6845

Test Set-Up Conditions:

Sleeves preset on Weatherhead Model 10062 Preset Machine
Kel-F lubricant on first reset only
Repeated Assembly Test per paragraph 4.3.3.1 MIL-F-18280A

B. Test Results:

No. of Reassemblies	Reset Torque In. lbs.	Proof Test* PSI	Remarks
1	1600		
2	1600		
3	1600	6000	No Leakage
4	1600		
5	1600		
6	1600	6000	No Leakage
7	1600		
8	1600		
9	1600	6000	No Leakage
10	1600		
11	1600		
12	1600	6000	No Leakage
13	1600		
14	1600		
15	1600	12,000	No Leakage

* Hydrostatic Pressure Test

Fittings were disassembled after the 15th reassembly and visually inspected. There were no indications of deleterious effects.

Slide 11 - Repeated assembly test results (MIL-F-18280A)

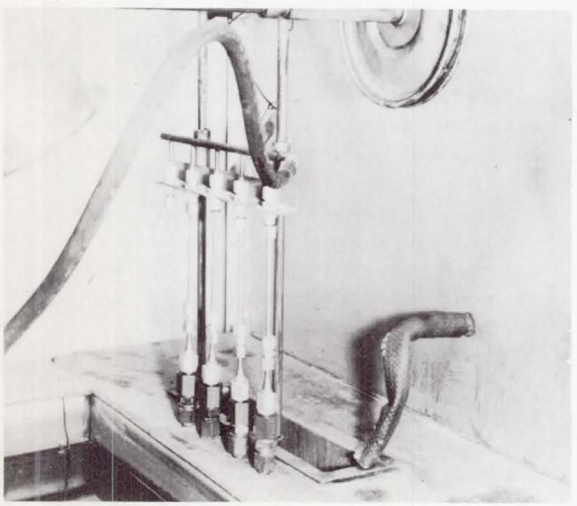

Slide 12 - Thermal shock test apparatus

cult in this size. MS-sleeves, precision machined per AS-1042, were used for this gas sealing test on both the 3/4" and 1/4" sizes.

Following the thermal cycle test the assemblies were pressure cycled under water with Helium from 0 to 3000 psi. The assemblies were then repeatedly disassembled and reassembled 10 times, and then pressurized with Helium at 3000 psi. There was no leakage as measured either by Halogen Snifter or bubbles-under-water equipment.

SLIDE 13 - In this photograph the size reduction is readily apparent. For example, the 3/4" titanium union has one-third the volume of the equivalent "MS" steel union.

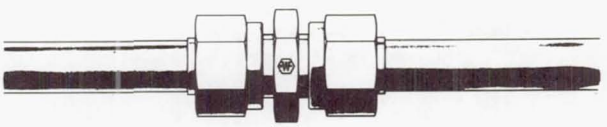

MS-21902 Steel Union
-12 Size

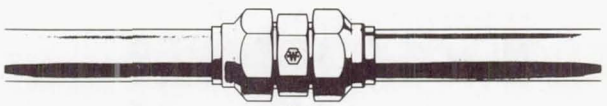

ER00902 Miniature Union
-12 Size

Slide 13 - MS and miniature fitting comparison

SLIDE 14 - Weight comparison, tabulated on Slide 14 shows that the titanium miniaturized fittings are, on the average, one-fourth the weight of standard MS-steel or stainless steel fittings with equal strength capability.

Although these titanium miniaturized fittings exceeded the minimum burst pressure values of MIL-F-18280, improvements were sought to eliminate blow-offs on the burst test after impulse, and to improve sealing characteristics with low molecular weight gases without resort to precision machined sleeves.

SIZE	ER-00902 VOLUME (IN.^{3})	ER-00902 WEIGHT (LBS.)	MS-21902 VOLUME (IN.^{3})	MS-21902 WEIGHT (LBS.)	*VOLUME SAVING MS vs MINIATURE	*WEIGHT SAVING MS vs MINIATURE
-2	.0917	.0031	.1163	.0328	83.0%	90.5%
-3	.0479	.0079	.1351	.0381	64.5%	79.3%
-4	.0721	.0118	.1270	.0358	43.2%	67.0%
-5	.0889	.0146	.1500	.0423	40.7%	65.5%
-6	.1185	.0195	.2227	.0628	46.8%	68.9%
-8	.1431	.0235	.3897	.1099	63.3%	78.6%
-10	.2431	.0399	.5720	.1613	57.5%	75.3%
-12	.3758	.0616	.9663	.2725	61.1%	77.4%
-16	.6844	.1122	1.2777	.3603	46.4%	68.9%
-20	1.0343	.1695	1.7851	.5034	42.1%	66.3%
-24	1.8400	.3018	2.0103	.5669	8.5%	46.8%
-32	2.7153	.4452	3.2131	.9061	15.5%	50.9%

* Weight and Volume Savings, expressed as percentages of standard MS steel fitting weights, were determined by the following relationship:

$$\% \text{ Saving} = \frac{\text{MS Fitting} - \text{Miniature Fitting}}{\text{MS Fitting}} \times 100$$

Slide 14 - Volume and weight comparison of MS (steel) and miniature titanium connectors (MS21902 vs ER00902)

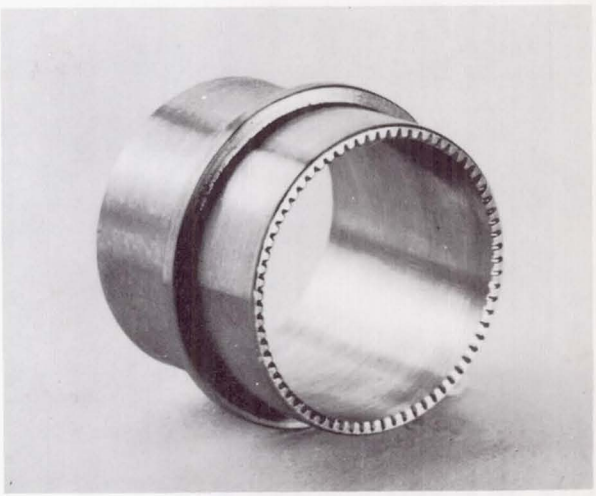

Slide 15 - Serrated sleeve for flareless tube fitting

This was accomplished by the development of an improved flareless sleeve. The serrated sleeve (Slide 15) in conjunction with standard MS-fittings, has demonstrated greatly improved retention, and produces a more reliable gas tight seal. Also, this sleeve will produce consistently good bites into hardened tubing, including tubing of AM-350 precipitation hardened stainless steel in the CRT-1000 condition with hardness to Rc-43.

For even higher pressure systems, particularly where larger sizes are used, a newer type serrated sleeve in the 1" size has achieved retention values of 30,000 to 40,000 psi, compared to approximately 16,000 psi maximum for MS-flareless sleeves.

IN CONCLUSION - Under Laboratory test and actual service conditions miniaturized titanium fittings with standard and precision machined MS-flareless sleeves have demonstrated reliable performance over a wide temperature range.

Additional reliability in sealing gases and in tube retention are possible by combining miniaturized fittings with serrated flareless sleeves.

Page Intentionally Left Blank

THE IMPORTANCE OF QUALITY CONTROL AND INTEGRITY CHECKING*

By

J. C. Bronson
Los Alamos Scientific Laboratory
University of California
Los Alamos, New Mexico

ABSTRACT

Methods used to obtain reliability in the use of seperable connectors in a cryogenic environment are discussed Bubble tight and vacuum vessel methods of leak checking are covered. Many illustrations of damaged and poorly machined fittings are included. Specific recommendations are given for enhancing the reliability of seperable connectors.

DURING THE PAST FIVE YEARS the major effort in developing the KIWI reactors has been directed toward improved core design, pressure vessels, and nozzles. As a consequence much of the service hardware has been given less attention. A history exists, during reactor runs, of small leaks resulting in superficial damage to some components although no runs have been cancelled because of these leaks.

With the assumption that future reactors will run at higher power levels and pressures, a survey of all cryogenic service piping adjacent to the reactor, for integrity, was instigated. Testing has not been limited solely to cryogenic hardware but instrumentation pass-throughs, gas service piping, hydraulic seals, actuators, etc. have also been checked. In addition to components that have been used or are now in use, cold seals and new hardware are evaluated before they are incorporated into new reactor designs.

Cryogenic pressure checking of these components is just the first phase of complete analysis. Environments including nuclear radiation, radiant heating, vibration, acceleration, and temperature gradients need thorough investigation.

Testing is conducted by the Cryogenic Engineering Section of CMF-9 at the Los Alamos Scientific Laboratory. Figures 1, 2 show a typical test setup where budget and personnel involvement are held to a minimum. For initial mechanical testing of seals, connectors, and other cryogenic components the facility is capable of producing 20,000 psi hydraulic pressure or 9,000 psi inert gas pressure.

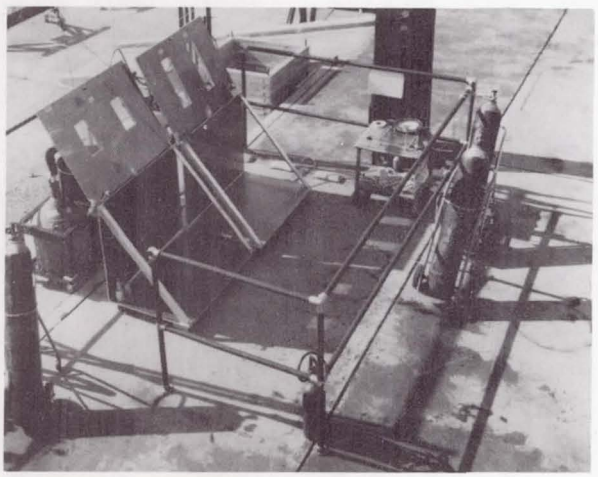

Fig. 1 - Test facility, operator side

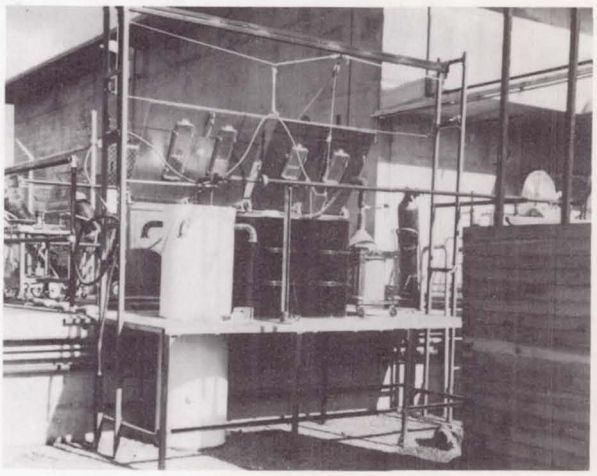

Fig. 2 - Test facility, test side

*Work done under the auspices of the U.S. Atomic Energy Commission.

Leak rates are determined by two different methods. First: Two different size vacuum jacketed test vessels that can accommodate flange pairs with a maximum diameter of 24 in. are used. With this method the actual leak rate of the piece being tested can be calculated from the pressure rise in the vacuum jacket. Theoretically a leak rate as small as 2.7×10^{-9} atm cc/sec can be determined by this method; actually from practical considerations the leak rates determined fall in the range of 1×10^{-7} atm cc/sec. Figure 3 shows a test vessel used with this method and Fig. 4 shows the internal vessel with a typical flanged test pair. Second: A gross type of leak checking called a bubble tight leak check is used. This is a go or no go type of check and seems to meet most requirements for checking the integrity of cryogenic seals. An estimate of the leak rate that can be determined by this method is

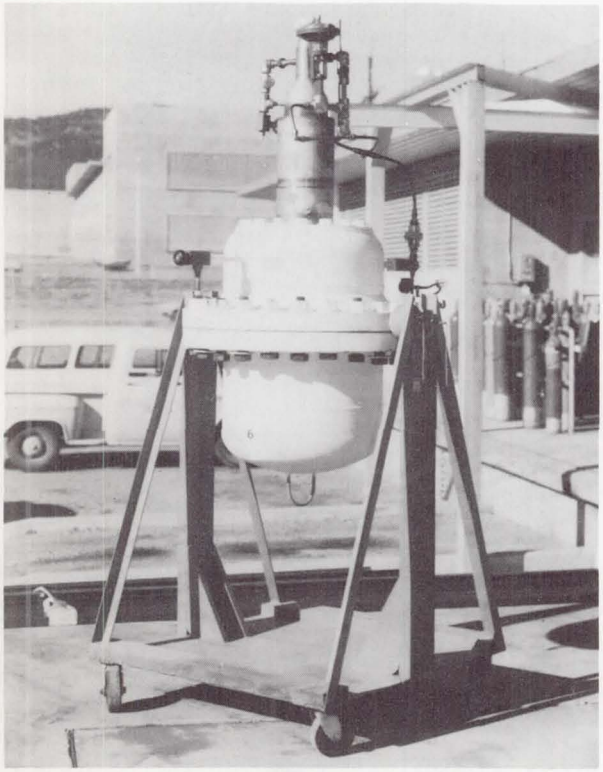

Fig. 3 - Test vessel, 24" I.D. vacuum jacket

2.7×10^{-4} atm cc/sec. This amounts to one 1/16 in. diameter bubble per minute. Figure 5 shows a typical manifolded setup for bubble checking cryogenic connectors. Figure 6 shows the samples after testing and what pitfalls you can run into following the manufacturers assembly specifications.

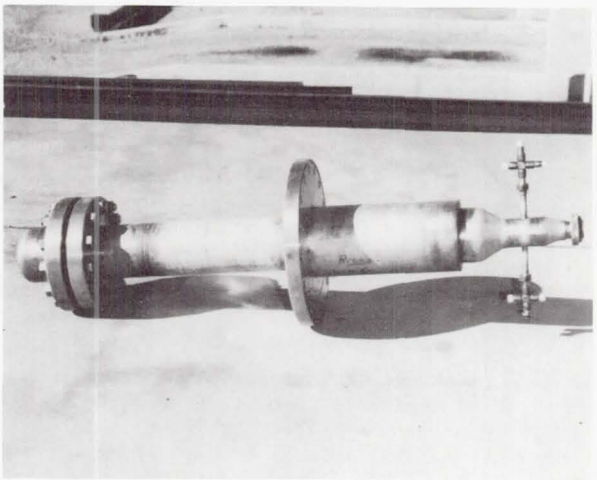

Fig. 4 - Test vessel, inside configuration

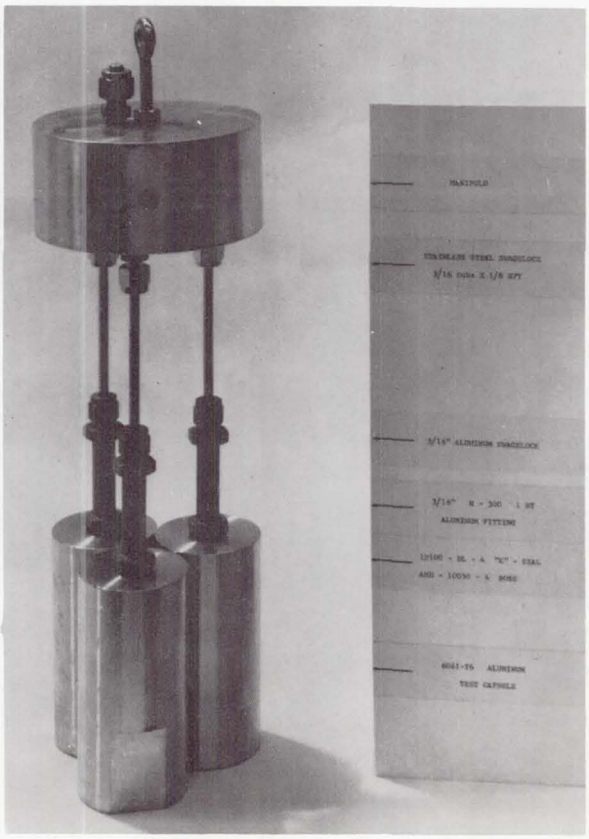

Fig. 5 - Typical setup for bubble leak check

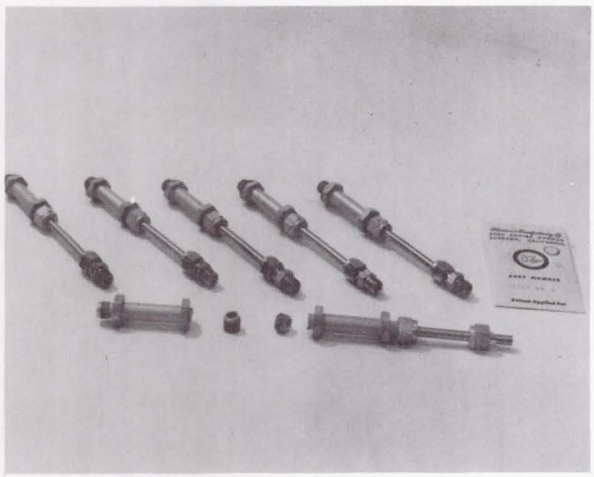

Fig. 6 - Connector samples after leak checking

Testing for bubble tightness is done in the following manner. After the unit under consideration has been tested to 1.25 to 1.5 times the maximum working pressure it is immersed in a warm water bath at 160-180°F and the internal pressure, usually helium gas, is raised to the required test pressure and the line valve closed. The water bath is watched for bubbles, indicating leaks, and the system pressure gauge is monitored for internal pressure drop. If no leaks are apparent the internal pressure is lowered to approximately 100 psi and the unit is moved to a liquid nitrogen bath for precooling. Here again the internal helium pressure is raised to the required test level and valved off and the pressure is monitored for evidence of leakage. When the unit has cooled to liquid nitrogen temperature the internal pressure is reduced to 100 psi and the unit is moved to the liquid hydrogen bath. There the internal pressure is again raised to the required test level and valved off. The internal pressure is monitored for leakage as in the two previous baths. Again the internal pressure is dropped to 100 psi and the cold unit is taken directly to the 180°F water bath where it is again pressurized to the test pressure. This gives the test unit a 600°R thermal shock in approximately 10 seconds. If no leaks develop this series of tests is repeated for a total of six complete cycles.

The following types of connections have been found leak tight by the bubble method if assembled using the following recommendations:

Female pipe threads 1/8 in. to 1 in. NPT lubricated with "Ledplate 250" or vacuum grease mixed with powdered molybdenum disulfide. Other effective pipe thread sealants where heat or radiation are not a consideration are "Loctite" and soft solder. Female pipe threads must be checked for depth by plug gauges and inspected for good thread form according to (ASA B2.1-1945). Good threads and proper depth are especially important where stainless steel fittings are assembled into aluminum units. No torque specifications exist, as far as is known, for making up pipe threads, especially those in aluminum. Male pipe threads must be inspected for proper form and number of threads and those items having torn or smeared threads must be rejected. Pipe threads are often not used, for the previously mentioned quality and assembly reasons, when they would make an effective joint.

Crawford "Swagelok" fittings in sizes 3/16 in. to 3/4 in. have been found leak tight by both the bubble check and vacuum check method and are used routinely for high pressure cryogenic work at LASL. There are three things that must be done to use "Swagelok" fittings. Routinely polish the end of the tubing in a radial direction where it enters the fitting. When the tubing is as much as 0.005 inches oversize it is necessary to deburr the conical ring in the fitting or the fitting will leak. Also all parts of the fitting must be clean and free from foreign matter. "Swagelok" fittings are used on copper, aluminum, and stainless tubing. An all aluminum "Swagelok" fitting has even been used successfully on stainless tubing at liquid hydrogen temperatures. "Swagelok" fittings have been found to be reliable and reusable.

Recently we have tested by the bubble method a "Parker Hannifin" tube fitting in the 1/2 in. tube size. This fitting is unique in that the ferrule is threaded onto the tube with a left hand thread. This fitting was easy to assemble and was found to be bubble tight at liquid hydrogen temperatures with an internal pressure of 1500 psi. Figure 7 shows the unit

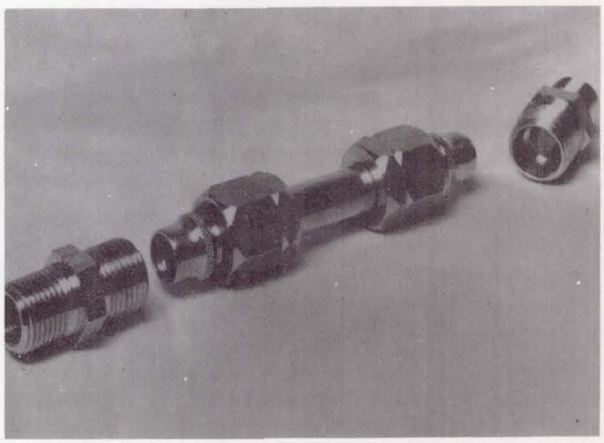

Fig. 7 - "Parker Hannifin" fitting before assembly

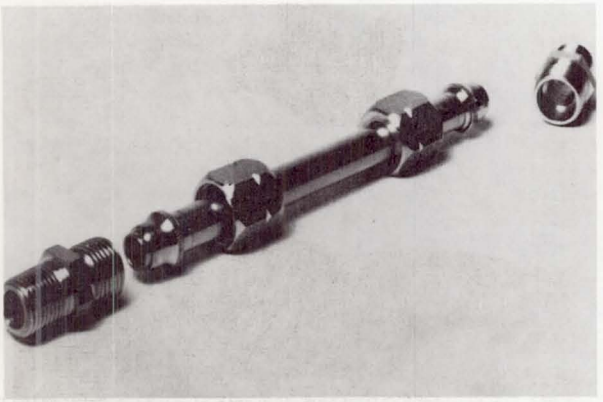

Fig. 8 - "Parker Hannifin" fitting after testing

prior to assembly and Fig. 8 shows the unit after assembly and test. Notice that the ferrule is swaged onto the tube at assembly. "Koncentric Unions" in 1/8 in. to 1 in. pipe and tube sizes are routinely used for high pressure gas and liquid hydrogen and nitrogen service where radiation is not a consideration. The only precaution necessary in using these connectors is that the "Teflon" gasket must be removed when the fittings are soldered or welded to the tubing. The gaskets are cheap and easily replaced if they are damaged or become impregnated with foreign matter. These unions are leak tight by both the bubble method and the vacuum test vessel method. Figure 9 shows a typical union for use on pipe and Fig. 10 shows the unions used in a typical leak test setup.

"Conoseal" manufactured by "Aeroquip" in the stainless steel screwed union type in

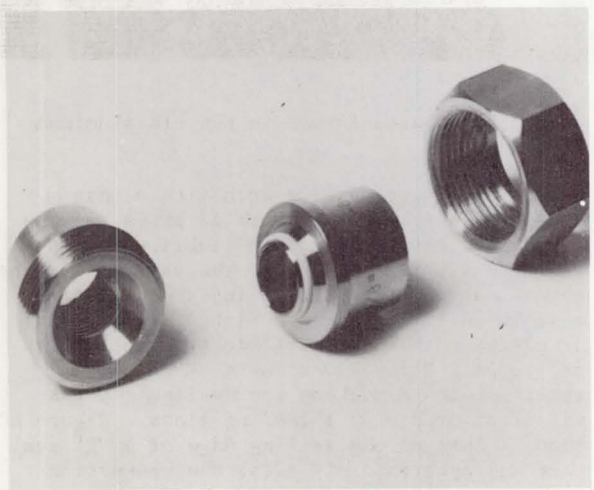

Fig. 9 - "Koncentric" union

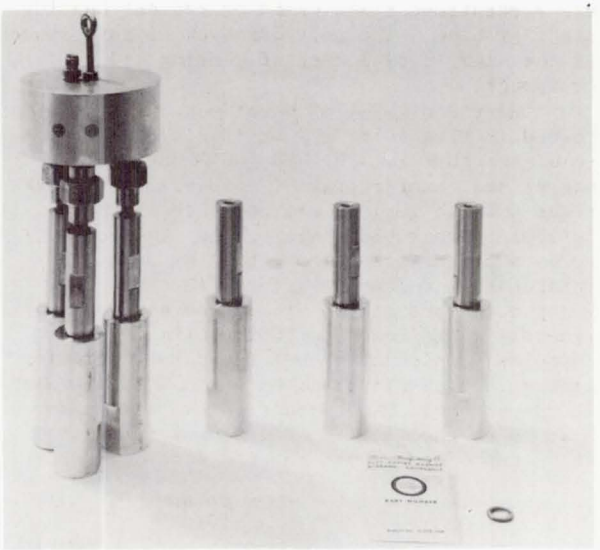

Fig. 10 - "Koncentric" unions used in typical test setup

sizes 1/8 in. to 2 in. NPT are easy to use and have been found leak tight by the bubble method and the vacuum vessel method. The union components must be absolutely clean when assembled. The union halves are reuseable but the conical gasket usually is not. Figure 11 shows a typical "Conoseal" union for tubing service.

Two samples of 1/2 in. tube size induction brazed gold alloy flight weight fittings produced by "Aeroquip" were tested and found to be bubble tight at 2200 psi internal pressure and at liquid hydrogen conditions. These joints should be particularly useful in applications where minimum weight and dimension

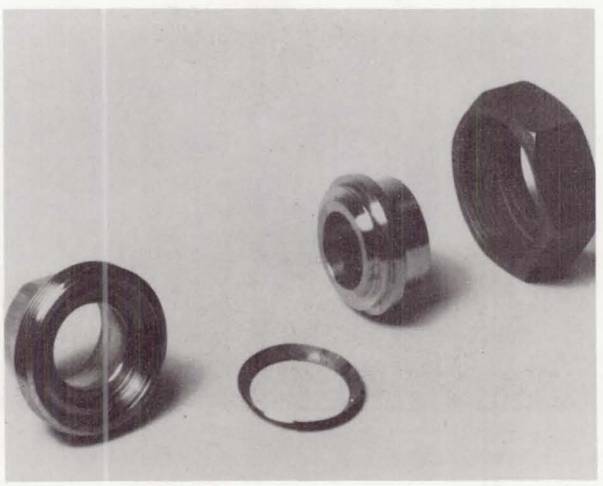

Fig. 11 - "Conoseal" union

are a requirement and gamma or radiant heating are a problem. The only drawback to this system is the high initial cost of tooling and equipment.

"Harrison K-Seals" have been bubble tested in size #4 to #32 or 1/4 in. to 2 in. tube size that fit the AND-10050 series of bosses and counterbores. These seals are leak tight and the gaskets are reusable if the following precautions are taken. The counterbores and chamfers must be free of nicks, scratches, and lumps. Figures 12 through 17 are photographs of the nicks, gouges and general damage found in 6061T6 aluminum test capsules. This damage was found on inspection with a reading glass and rejections run as high as 90 percent. The threads below the chamfer must be of good quality and gauged for proper depth and size. These threads must be lubricated to prevent galling both with aluminum and stainless steel. Figure 18 shows galling of threads caused by lack of lubrication on anodized aluminum threads. The sealing surface on the mating connector or instrumentation must be well finished and flat. The "K" seal or gasket must be free of nicks, scratches, and lumps. Figure 19 shows a "K" seal as received with a nick on the sealing lip that was discovered with a reading glass. Figure 20 shows a lump on the sealing edge of a "K" seal that was apparent only after the connection leaked and was torn down.

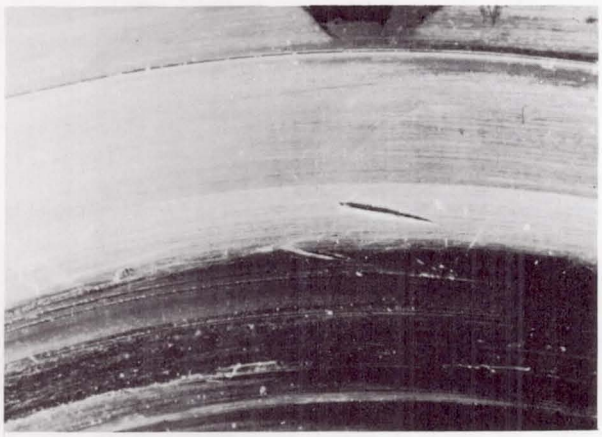

Fig. 12 - Nicks, scratches, and gouges found in AND-10050

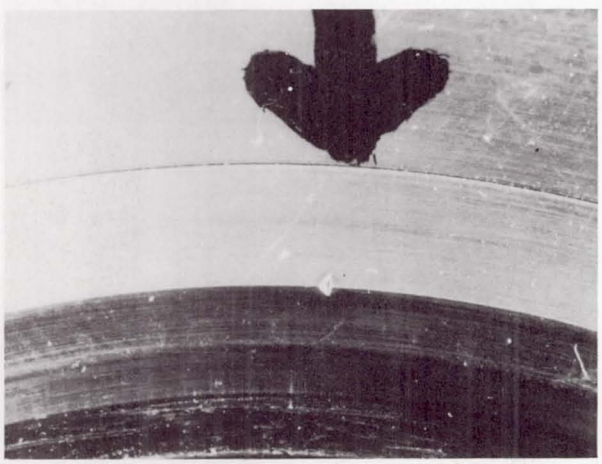

Fig. 13 - Bosses formed in 6061-T6 aluminum

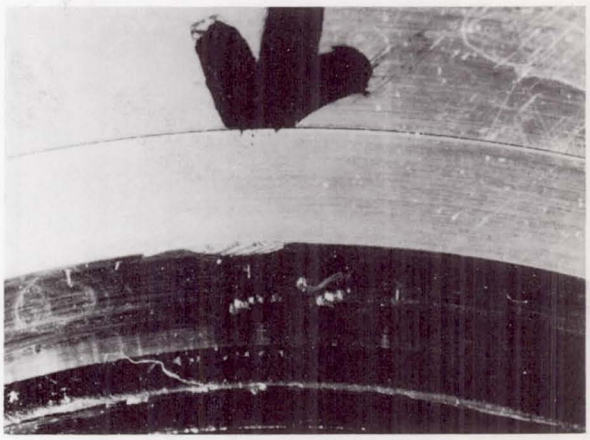

Fig. 14 - Bosses formed in 6061-T6 aluminum

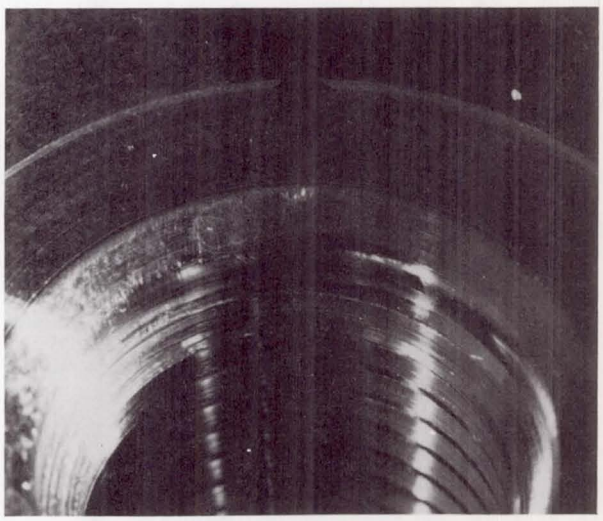

Fig. 15 - Bosses formed in 6061-T6 aluminum

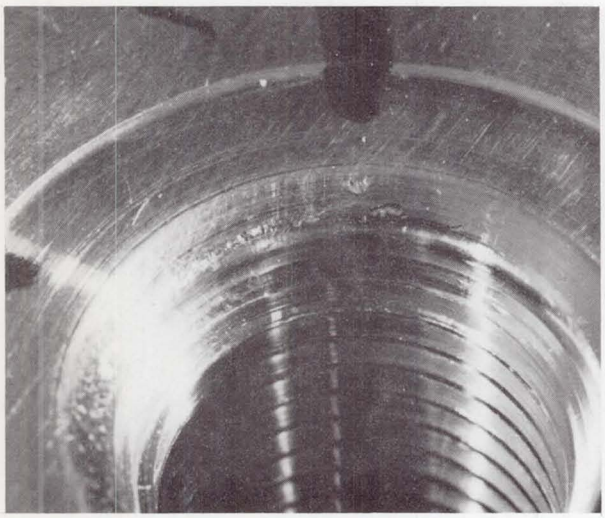

Fig. 16 - Bosses formed in 6061-T6 aluminum

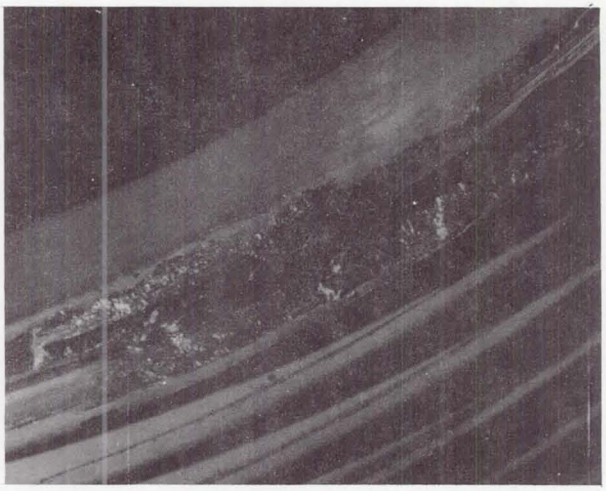

Fig. 18 - Galled aluminum threads

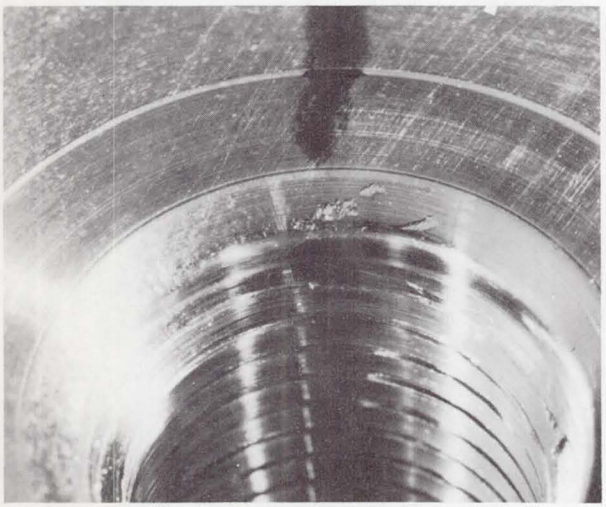

Fig. 17 - Bosses formed in 6061-T6 aluminum

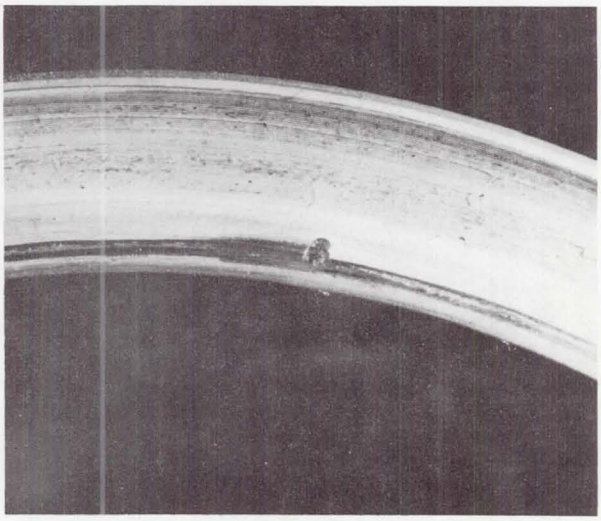

Fig. 19 - "K-seal" with damaged sealing lip

The "K" seal or gasket must be lubricated with a light coat of "Dow Corning #11" or its equivalent because of the twisting and sliding of the gasket during assembly. Figure 21 shows the scuffed sealing lip caused by a dry gasket. Figure 22 shows scuffing on the heel

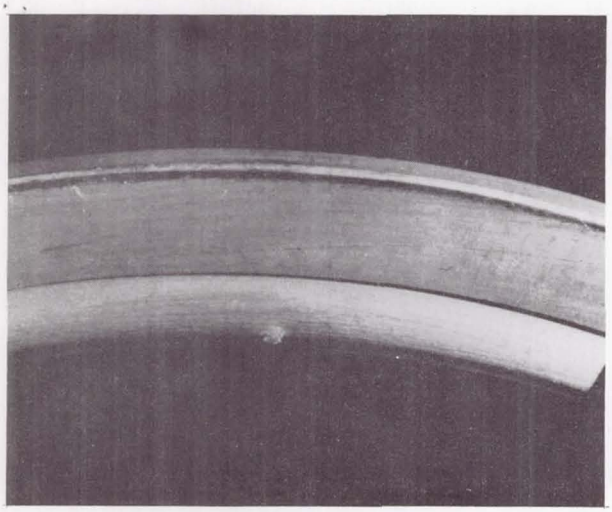

Fig. 20 - "K-seal" with plating lump on sealing lip

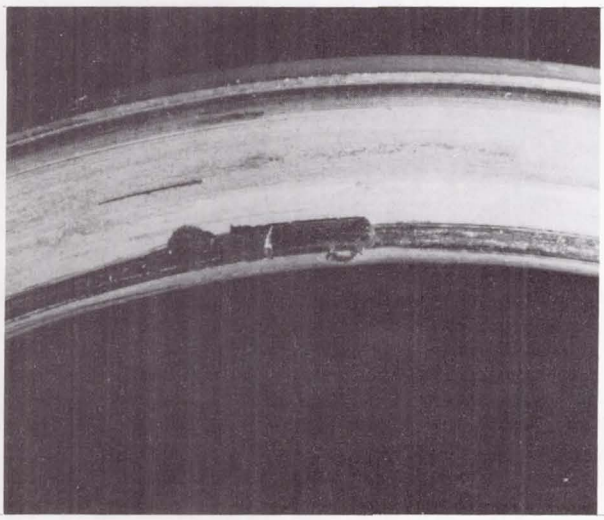

Fig. 21 - "K-seal" scuffed sealing lip caused by dry assembly

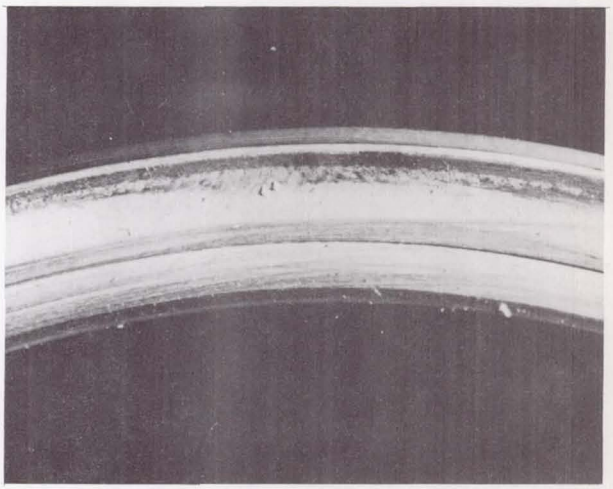

Fig. 22 - "K-seal" scuffed heel caused by dry assembly

or spine of the gasket caused by no lubricant. With this assembly all sealing surfaces and the seals themselves must be inspected for nicks, scratches, and surface finish before assembly.

In conclusion I would like to state that very few high pressure cryogenic connectors fail because of design deficiencies. To make most connectors leak tight the following steps are vital:

1. One hundred percent inspection of all connector components for dimension, flatness, surface finish, cleanliness, and damage.
2. Complete written instructions with check list for use in field assembly, including cleaning techniques, lubricants, handling of gaskets and parts, torque values, and proper use of tools.
3. An integrity or leak check of a representative number of assemblies, simulating actual use conditions, before incorporation into final designs.
4. A field inspection of connector assemblies before, during and after assembly by a competant and authoratative inspector.

Page Intentionally Left Blank

PRECISION TUBE FLARING BY CONTROLLED METAL DISPLACEMENT

By

Joseph E. Carlin
General Dynamics/Convair
1128 P. O. Box
San Diego, California

ABSTRACT

This paper presents a new concept in precision tube flaring for leak-proof separable connector joints.

This new approach to production of precision tube flares is called "The Dynaflare Process".

During the past year, Convair has developed a technique for producing precision tube flares. The device employs several new design concepts and mechanical applications compared with other types of tube flaring machines now used in the aerospace industry. It is a completely mechanical cycle machine, eliminating requirements for skilled operators. The power source is electro-hydraulic, controlling a unique clamping and ram-type flaring mechanism. The flare is formed in a closed, trapped-die arrangement using full mechanical control of material displacement, stroke, and pressure during the flaring cycle.

The text of this paper will cover technical accomplishments and state-of-the-art improvements of flaring capability related to leak-proof, separable connector joints.

DYNAFLARE ORIGIN

THE DYNAFLARE MACHINE, shown in Fig. 1, was conceived, designed, and fabricated by production engineers at Convair. The concept was a result of need. Its producibility was engineered to meet MC-146 specifications. Its birth, in November 1964, was many years overdue. The problems faced by manufacturers of missiles and space vehicles in the areas of leaks, rejections, and tube assembly replacements was adequate justification for fabricating, proofing, and testing the Dynaflare concept.

MACHINE DESCRIPTION

The Dynaflare machine is powered by an electro-hydraulic pumping unit. The pump is capable of delivering 10,000 psi to each of two hydraulic cylinders. Each cylinder has a maximum pressure delivery of 50 tons. To date, only 24 tons have been used. These cylinders supply the required force for closing the clamp die and flaring the tube end. The clamp die stroke is 2.375 in. The flaring stroke is 1.00 and retracts 5.0 in. when changing the male punch.

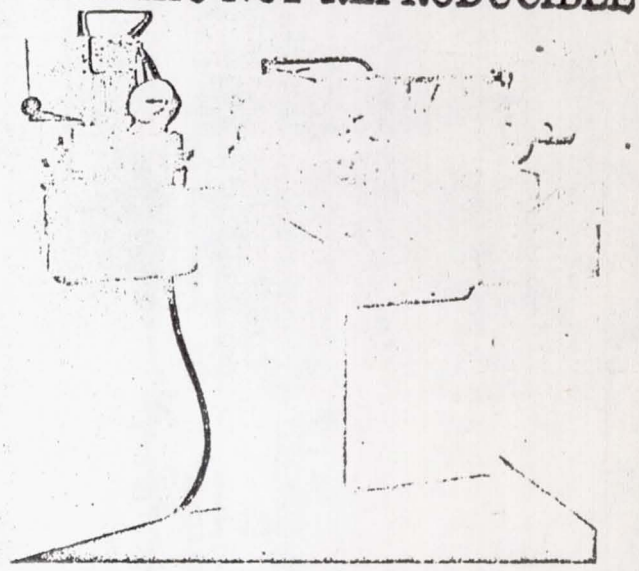

Fig. 1. Dynaflare prototype machine (Patent Pending)

A complete set of 10 flare dies and 32 punches provides a capability of flaring 0.125 O.D. x 0.020 wall through 1.250 O.D. x 0.049 wall tubing. The displacement, clamping, and ram pressure have been developed for each tube diameter and wall thickness to meet MC-146 specifications. It should be noted that flare geometry is basically controlled by the 33° flare die and the 37° flaring tool. With the Dynaflare process, however, configuration and tolerances are further achieved by varying displacement, stroke, and pressure. This is discussed in a later section of the paper.

DYNAFLARE COMPONENTS

Fig. 2 shows a cross section of the six basic components of Dynaflare. This arrangement is illustrated with the combination clamp-flare dies in the closed position. The tube stock, gage pin, and male flaring

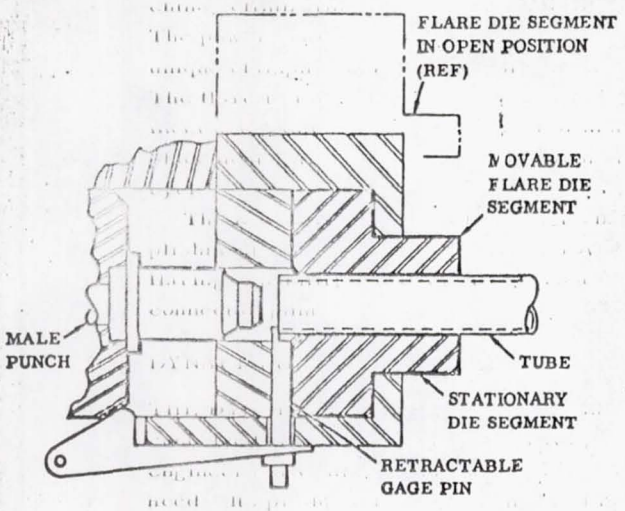

Fig. 2. Die segment in closed position prior to flaring cycle

punch are in the open position prior to flaring the tube. The arrangement of these components demonstrates the true concept of precision displacement control, i.e., true axial alignment of the male punch to the female flare dies; trapping and displacing the gaged tube stock to exacting configuration under controlled stroke and pressure.

DESCRIPTION OF FLARE CYCLE

The forming of a flare in the Dynaflare machine is simple and easy to accomplish. The operator places the tube end to be flared in the die housing against the gage stop with clamp die return valve closed. The power switch is turned on closing the clamp die. When the die is closed, the operator moves the hydraulic selector control lever to flare position. The flaring ram strokes to preset pressure and shuts off. The operator then returns the control lever to the open position and opens the clamp die return valve; both cylinders return to the open position, completing the flaring cycle. The cycle requires eight seconds for the prototype machine shown in Fig. 1. The flaring cycle on the production model is three seconds.

FLARE DIES

The flare dies are the two-segment type with special clamping capability added to prevent slippage during the flaring cycle. The die segments in the closed position form a precision ground circle from the lower tangent point of radius through the flare surface portion. The tube clamping area is taper-ground and vapor-honed to a length of three times tube diameter. Tube diameters of 0.25 in. require 0.75 in. clamping length; 0.50 in. requires 1.5 in., etc. No slippage has ever been noted on commercial-type tubes of nominal diameter and larger.

TRAP DIE SEGMENTS

The trap-die portions, like the flare dies, are made in two symmetrical segments. Each segment is coordinated, aligned, and attached to the flare die to complete the flare die set. The inner and outer diameters of the trap ring are coordinated to the flare-die diameters. The precision bore of the trap die is nominal MC-146 lip diameters. For example: a 0.25 in. die set has a 0.354 + 0.0002 - 0.0000 diameter or one-half the tolerance of 0.359 + 0.000 - 0.010. The trap die serves as the medium of true axial alignment of the male punch to the female flaring dies during the flaring cycle. Deflection forces on the male punch caused from tube variables in wall thickness are overcome, resulting in near perfect roundness and concentricity on the formed flare. The thickness of the trap die is precision ground and coordinated to the male punch to control flare stroke.

MALE PUNCH

This component is the flaring tool. It is of a unique configuration and provides all important functions relative to precision flaring. From the point of tube contact of the pilot portion to the stop shoulder that controls flare stroke, the punch dimensions, including radius, angle, lip, off set, shaft diameter and length, are critical. The pilot portion is ground to -0.002 below tube nominal inside diameter at the lower tangent point of the radius. The radius is ground to MC-146 specifications plus tube wall thickness. The flare angle is 37°, the lip offset is ground relative to the 33° and 37° angles, plus material displacement and tube wall thickness. The shaft portion is slip-fit to the trap-die diameter. The shaft length between lip offset and shoulder stop area is coordinated to the trap die for controlling and maintaining true axial alignment.

If the 33° dies are considered as the backup or flare-cycle stops, then the punch becomes the element of control for the entire flare geometry by virtue of displacement, stroke, and pressure.

GAGE PIN

The displacement control gage pin provides the exact location of the tube end prior to flaring. The pin is spring loaded to hold it in the tube-stop position, as shown in Fig. 2. During the flaring stroke and before tube and punch contact, it is retracted by a cam mechanism to clear the punch and trap-die housing. When

the flaring ram retracts, the pin returns automatically to the gage position. The displacement offset is ground to provide the correct amount of material for finish-flare configuration.

COMPARISON TESTS AND MEASURING RESULTS

As stated earlier, the Dynaflare machine was designed, engineered, and fabricated to meet all of the geometric measurements, finishes, and tolerances defined in MC-146. Five of the specifications listed below are of vital importance to effect a leak-proof separable joint.

1. Concentricity.
2. Roundness.
3. Micro finish of the seal surface.
4. 37° inner angle.
5. 33° outer angle.

The remaining specifications are of major importance to the quality and reliability of a leak-proof flare only after the first five have been achieved. They are:

6. Outer radius at the 33° angle.
7. Concavity and convexity of flare angles.
8. Lip diameter or "D" dimension.
9. Wall thickness variations of the flare.
10. 33° surface die marks and scratches.

The prototype Dynaflare machine was completed in September 1964. At this time, an extensive measuring and testing program was conducted by Quality Control and Fluid Systems Engineering personnel employing outside testing facilities. The first tests were conducted in October on 0.25 in. O.D. x 0.035 in. wall 6061-T-6 aluminum alloy tubing and 0.25 in. O.D. x 0.035 in. 304 1/8 Hard CRES tubing. All the tests were conducted on a comparison basis to flares produced on Convair's standard eccentric cam-action machines. The tests required that 9 samples of each type of material be flared by each process; a total of 36 flares. The comparison tube samples were cut to 18 in. lengths and the identity was added to each end of the 18 in. piece of tube stock. The tube was then cut in the center to 9 in. test-sample lengths, burred, and flared by each process. The results are shown in Figures 3, 4, 5, and 6.

These charts indicate that the Dynaflare process is superior to the standard flares and well within the tolerance limits of MC-146. Rockwell and photo-micrograph tests showed no significant differences in micro structure of the flares by either process.

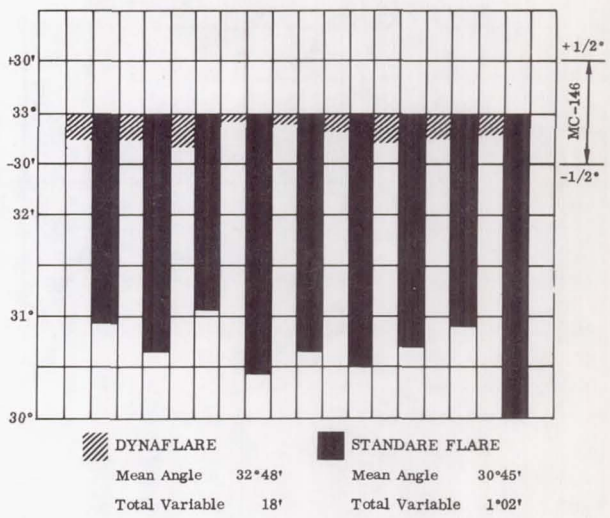

Fig. 3. 33° Flare-angle comparison, material 0.25 in. O.D. x 0.035 in. wall, 6061-T-6

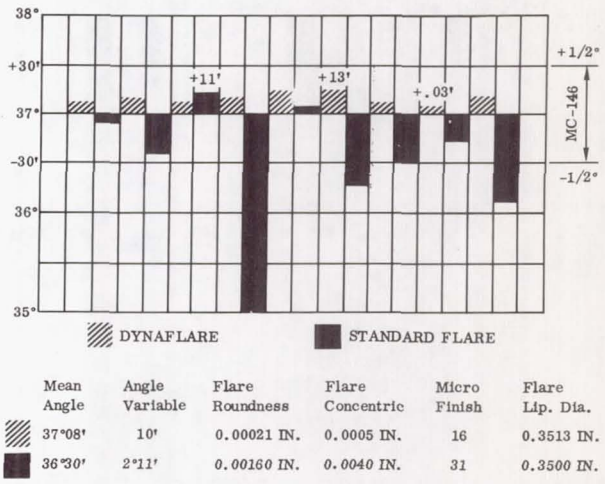

	Mean Angle	Angle Variable	Flare Roundness	Flare Concentric	Micro Finish	Flare Lip. Dia.
	37°08'	10'	0.00021 IN.	0.0005 IN.	16	0.3513 IN.
	36°30'	2°11'	0.00160 IN.	0.0040 IN.	31	0.3500 IN.

Fig. 4. 37° Flare-angle comparison, 0.25 in. O.D. x 0.035 in. wall, 6061-T-6

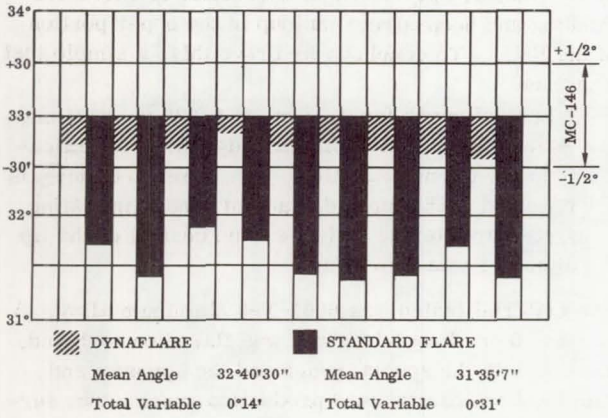

Fig. 5. 33° Flare-angle comparison, material, 0.25 in. O.D. x 0.035 in. wall, 304 1/8-hard CRES

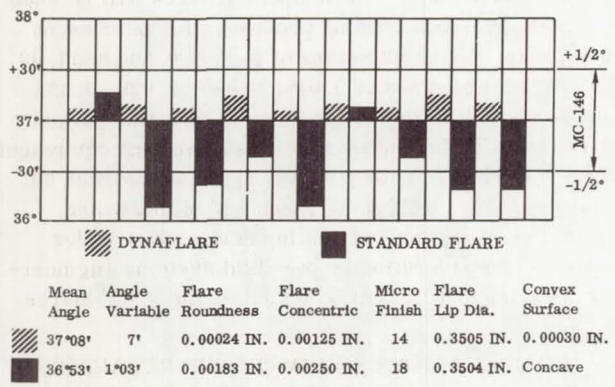

	Mean Angle	Angle Variable	Flare Roundness	Flare Concentric	Micro Finish	Flare Lip Dia.	Convex Surface
▨	37°08'	7'	0.00024 IN.	0.00125 IN.	14	0.3505 IN.	0.00030 IN.
■	36°53'	1°03'	0.00183 IN.	0.00250 IN.	18	0.3504 IN.	Concave

Fig. 6. 37° Flare-angle comparison, 0.25 in. O.D. x 0.035 in. wall, 1/8-hard CRES

HIGH PRESSURE - MINIMUM TORQUE

Once the capability of producing a precision flare on a repeatable basis had been established, Convair wanted to know if the ultimate goal had been achieved - the capability of sealing small molecule gas under high pressure, with minimum torque.

We are all familiar with the old adage "The proof of the pudding is in the eating". This being true, then we can assume that the proof of an effective seal is in the testing. Testing and proofing were accomplished by Dynaflaring eight test samples of 0.25 in. O.D. x 0.035 in. wall, 6061-T-6 aluminum alloy tubing. The eight test samples were flared on each end using standard steel sleeves and aluminum "B" nuts effecting a total of 16 test joints. The 16 joints were series-assembled under standard manufacturing controls and practices using run of the mill AN connectors. The torque on each joint was 80 in.-lb. The complete assembly was then submerged in water and Helium gas pressurized to 6,000 psi. No leaks were detected after 20 minutes of submersion. Convair standard torque is 125 in.-lb.

Today Convair uses 0.25 in. x 0.035 in. wall 304 1/8-Hard CRES tubing in its hydro-bulge forming facility. Operating pressures of 14,000 psi have been subjected to the joints with no leaks or failures.

A NEW DIMENSION IN CONTROLLED FLARING (FIG. 7A AND 7B)

The Dynaflare process with controlled stroke, pressure, axial alignment, and material displacement added a new dimension to controlled flaring. This dimension is the long-ignored but critical area at the heel of the 37° angle. Standard tube-flaring machines and processes do not control material movement in this highly stressed area. The straight cone on a conventional-type machine rolls and stretches the tube stock allowing the material to flow toward the heel and lip area. This results in excessive thinning of the flare wall and forces a metal buildup inside the tube diameter at the inside heel area. The Dynaflare male forming tool has a precision radius and taper ground pilot that controls inner tube diameter and radius during the flaring cycle.

CONVEXITY AND CONCAVITY CONTROL

Standard Process (Fig. 7A). Standard eccentric cam rolling machines do not control material movement at either the heel or lip area of the flare. The material is thinned to the 37° x 33° configuration by the rolling and stretching process to meet angular and lip diameter requirements. The upper portion of the flare is thinner, with high hoop tension. This results in material spring back, causing a concave condition on the 37° seal surface.

Dynaflare Process. In Fig. 7B, the flare is shown in the finished position at the end of the flaring cycle. The material is completely trapped and set to the punch and die configuration. The natural convex condition is the result of controlled stroke and pressure in relation to material displacement by volume; i.e., the material in the lip diameter area is trapped and set to punch and die configuration. Hoop tension and spring-back is eliminated. The amount of convexity desired for effective low torque sealing is controlled by pressure, material displacement, and male punch configuration.

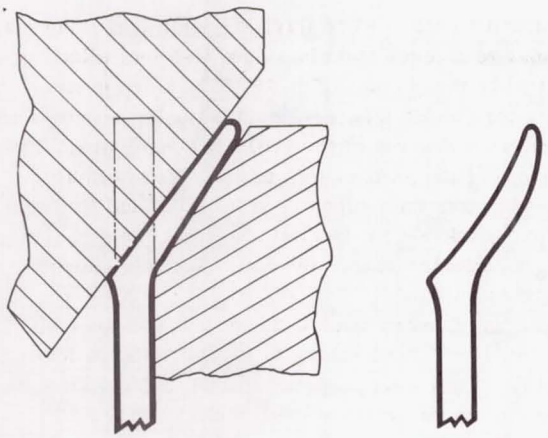

Fig. 7A. Standard process

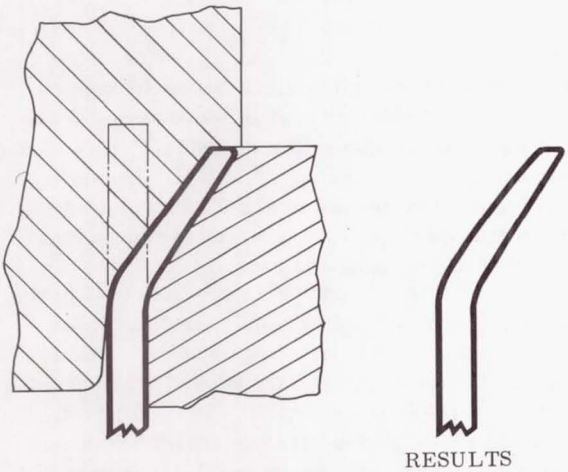

Fig. 7B. Dynaflare process

CONVEX AND CONCAVE PROOF TEST

The natural convex condition on the flare seal surface is a result of 100% trapped control of material displacement. The natural concave condition produced by the standard process was accredited to excessive thinning and hoop-stress buildup in the upper portion of the flare. To conclusively prove this, a simple test was made:

> A special punch for 0.25 in. x 0.035 in. wall material was ground to standard dynaflare specifications, with one exception. The flare lip offset was removed. This provided a bald punch simulating a standard flaring tool, i.e., no control of the lip diameter was provided.

The material tested was 6061-T-6 aluminum alloy. A piece of 6-in. long tube stock was flared on each end, one end with the special punch and the opposite end with the Convair standard production punch. The surface contour of each is shown in Fig. 8. The roundness is shown in Fig. 9. Roundness is also effected when the flare lip is not controlled.

DYNAFLARE FOR PERMANENT WELDED JOINTS

At the time of this writing, special punches and dies are being fabricated to provide precision 90° flat flares on tube ends. These special flares will be used for testing various welding processes for permanent tube joints. Tube diameters of 0.250, 0.500 and 1.00 with wall thicknesses of 0.016, 0.020, 0.028, 0.035 and 0.049 will be flared for these tests. Our primary objective is to determine specialized welding equipment needs, particularly for portable applications such as final assembly, field installation and maintenance. Special semi-permanent sealing devices now under study and consideration by our fluid systems engineering department will also be tested on these 90° flares.

RECOMMENDATIONS FOR IMPROVED SEPARABLE CONNECTOR JOINTS

Results and evaluation of extensive testing of flared connector joints, reflect that certain changes to Military Specification 33584 and MC-146 will improve the seal and fatigue life of the joint.

Recommended changes are as follows:

1. Increase the $33^{\circ} \pm 1/2^{\circ}$ to $33^{\circ} +1^{\circ}/-0^{\circ}$. This would ensure sleeve and flare contact in the desired seal area. This area is above the upper tangent points of the flare and sleeve radius. A minus condition on

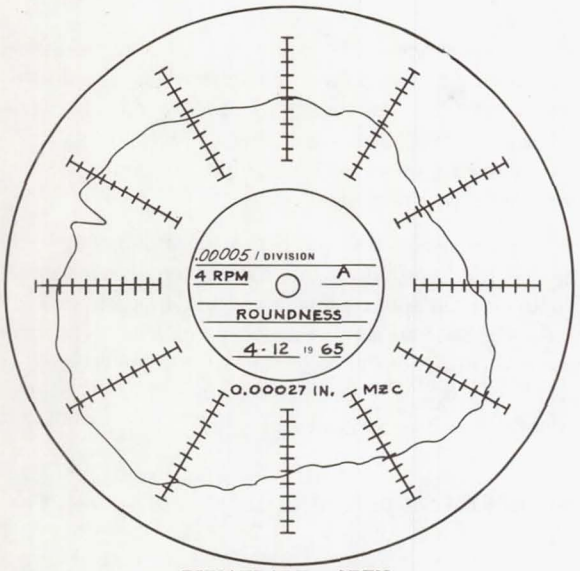

DYNAFLARE - OPEN
MZC — 0.00027 IN.

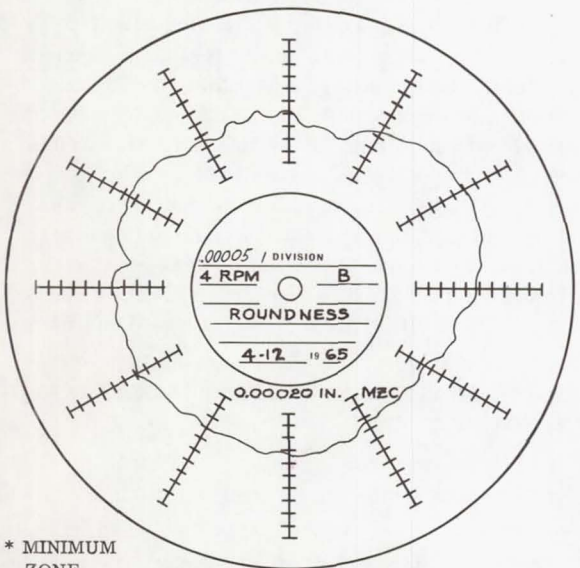

* MINIMUM ZONE CENTER

DYNAFLARE - TRAPPED
* MZC — 0.00020 IN

Fig. 8. Indi-ron roundness -0.00005 in. divisions

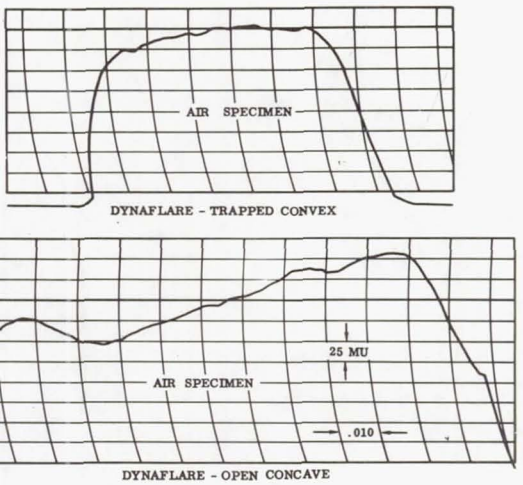

Fig. 9. Indi-ron waviness vertical 25 mu in., horizontal 0.010 in.

the 33° flare angle causes interference of the sleeve and flare radius. When this condition occurs, fatigue life is greatly reduced, resulting in leakage and failure of the joint.

2. Reduce the flare lip minimum diameters as related to maximum sleeve diameters to reduce hoop tension, surface checking and cracking.

Further testing on a comparison basis of all flares produced by existing machines and fabricating processes is required. The primary objective of these tests would be to determine flare geometry and the production process most effective. Particular emphasis should be placed on flare geometry and production method as related to seal effectiveness and fatigue life under known conditions.

The writer is of the opinion that from the conclusion of these recommended changes and comparison testing, there will emerge a reliable separable connector joint to meet MS and MC specifications. More important, to Aerospace and Space Vehicle Manufacturers, the problem of leaks and failures will be greatly reduced. They may even be eliminated.

LEAKAGE DETECTION AND MEASUREMENT

By

R. I. Cedar-Brown
General Electric Company
Apollo Support Department
Daytona Beach, Florida

ABSTRACT

In this missile age, the use of exotic fuels -- various types and combinations of liquid propellant fuels and oxidizers -- has become a common practice. Most of these propellants are highly reactive chemicals with certain hazardous properties which must be fully understood by all personnel who handle them. Two of the most hazardous properties which concern us are: (1) Explosibility, and (2) Toxicity. The problem, then, is to provide a means of detecting leakage of these gases to prevent the formation of an explosive mixture in the air.

The sensors discussed in this paper are divided into three groups for specific gas applications: (1) Hydrogen Sensors, (2) Oxygen Sensors, and (3) Non-Specific Sensing Methods. A recent survey conducted by the General Electric Company has determined the state of the art, as well as commercial availability, of these transducers.

The discussion of the sensors presents general characteristics of commercially available sensors and is followed by scope of work on recent research and developments in leak detection conducted by the Apollo Support Department (ASD) of the General Electric Company.

Conclusions and recommendations are presented as the distillation of the suggestions which have come to light in the course of these investigations. It is hoped that these may result in real progress in the direction of the ultimate leak detector.

COMMERCIALLY AVAILABLE SENSORS

IN THE ROCKET BOOSTERS using very large amounts of liquid hydrogen, liquid oxygen, and unsymmetrical dimethylhydrazine, considerable precautions have to be taken to prevent the formation of an explosive mixture in the air as a result of leaks.

The sensors discussed below are divided into three groups for specific gas applications: (1) Hydrogen Sensors, (2) Oxygen Sensors, and (3) Non-Specific Sensing Methods.

HYDROGEN SENSORS -

Catalytic Reaction Sensors - The most common commercially available hydrogen gas detection sensor is based on the measurement of one of the physical phenomena resulting from the catalytic reaction of hydrogen and oxygen. Typical operation may be briefly outlined as follows: gas permeates the area around the sensor and hydrogen, if present, flows through a filter onto a hot platinum filament (300°C). Here the oxygen and hydrogen combine with a result that heat and water are released in proportion to the rate of reaction. Therefore, a measure of either of these parameters, or a secondary effect such as the change in the resistance of the platinum element due to temperature change, will yield a quantitative measure of the hydrogen present. This method requires the presence of a sufficient amount of oxygen to support this reaction.

The advantages of this type of sensor are: (1) they offer a means of quantitatively measuring the hydrogen content of surrounding gases, (2) they are capable of sensitivities of a few parts per million of hydrogen under stable ambient conditions and a few parts per thousand under varying ambient conditions, and (3) they can be made selective to hydrogen by the use of suitable fittings.

The disadvantages of this sensor are: (1) these sensors are relatively large, (2) they require oxygen and are, therefore, inoperable in any other inert atmosphere, (3) they are also position sensitive and must be oriented correctly to operate efficiently, (4) they operate at an elevated temperature, (5) the sensors are subject to poisoning, which in turn makes them useless, and (6) they require removal of water which is generated during operation.

Thermalconductivity Sensors - Thermalconductivity sensors operate on the principle of the change in resistance of a bridge element due to the presence of hydrogen in the atmosphere around that element. This conductor forms one leg of a balanced bridge circuit which is thrown out of balance by the presence of hydrogen. The active element in the bridge is usually a hot wire or a thermistor.

Advantages are: (1) these sensors are not affected by the atmosphere in which they are used, except in the presence of helium, (2) they are rugged in construction and are not sensitive to shock, and (3) they can be set to operate over wide ranges.

Disadvantages are that this type of detector requires a hot wire and, therefore, is objectionable for use with a highly flammable (H_2) atmosphere unless it is installed in an explosion-proof housing.

Polarographic Hydrogen Sensors - The polarographic-type sensor is based on the principle of applying a polarizing voltage across two electrodes.

These electrodes are enclosed in a gel which is specifically permeable only to the gas being tested. Hydrogen diffuses through this gel and is oxidized at the gold, platinum-plated anode. The cathode is composed of zinc sulfate to form the coupling necessary to complete the circuit.

Advantages are that this type of sensor can be made specific and should work in the purged atmosphere found in the vehicle.

Disadvantages are that this sensor is only a one-shot type transducer, i.e., once the sensor has become saturated, it has to be replaced.

Mass Spectrometers - The mass spectrometer can give more answers in a wider variety of applications than any other single analytical instrument available today, from basic research on atomic and molecular species to complex mixture analysis; from geologic age dating to high-temperature chemistry; from quality control checks to continuous process monitoring. Mass spectrometry is providing answers faster and more accurately than any other technique. It is the role of the mass spectrometer analyzer to separate ions issuing from the source. There are three characteristics of a moving charged particle that can be measured: momentum, energy, and velocity. If one measures only two of these, then the mass of an ion is defined. A simplified explanation of mass spectrometer analyzer shows that positive ions accelerated in a vacuum will be deflected by a magnetic field according to their mass. Adjustment of potentials can focus the desired ion beam on the collector.

Consider, now, some of the advantages of the mass spectrometer.

- Selectivity must be considered of prime importance. Under normal operating conditions, instrument response is only a function of the partial pressure of each particular species. If, for example, oxygen is being studied, the instrument does not know or care if the O_2 is pure or contains one, two, or 50 other substances. The response or output for O_2 is only a function of the O_2 partial pressure.
- Sensitivity depends on the type of instrument and degree of similarity between compounds. Available instruments can detect concentrations as low as 10 ppb and partial pressure below 10-12 torr.
- Average sample size is on the order of 0.1 cc at standard conditions, but with special instrumentation, samples of 10^{-8} cc or less can be analyzed.
- Response time is extremely rapid, once the sample is injected into the analyzer, and is dictated only by the inlet and detector system used.
- Resolution is the ability of a mass spectrometer to separate ions of different masses reaching the collector. Instruments today are capable of resolving differences of from 1 part in 20 to 1 part in 30,000.

Three types of mass spectrometers are now commercially available. The most prevalent is the magnetic type which separates ions according to momentum and requires a source that provides a mono-energetic ion beam to fix the second measurable quantity.

The second one is an electrostatic analyzer that will separate ions according to energy, but by itself it is useless as a mass spectrometer since there is no way to distinguish one mass from another.

The third type, commonly known as a "time-of-flight" instrument, can observe all the ions created during a single ion pulse and is capable of very rapid scanning (several thousand scans per second). Time-of-flight spectrometers available today are limited to resolution to around 1 part in 200, due to their design, and normally do not have the analytical accuracy of the magnetic instruments. The outputs of the spectrometers are usually displayed or recorded in one of three ways: (1) a potentiometric pen-and-ink recorder or a multitrace oscillographic recorder, (2) a photographic plate recording, and (3) oscilloscope display.

The main disadvantages of the mass spectrometers are as follows:

1. A very high initial cost.
2. Complexity of operation; large vacuum systems, lengthy tubing for missile applications, etc.
3. Heavy power consumption.
4. Large and heavy configurations.

Fuel Cells - The fuel cell has been successfully used as a specific hydrogen or oxygen leak detector. Its principles and mode of operation are described in the following pages under (1) Oxygen Sensors, and (2) General Electric Experimental and Development Devices.

OXYGEN SENSORS -

Polarographic Oxygen Sensors - The polarographic oxygen sensor is identical to the hydrogen polarographic sensor except that (1) the polarizing voltage is opposite in polarity and is 0.8 volt, and (2) the materials used to construct the electrodes are different. The oxygen cathode is platinum and the anode is silver. The gel in which the electrodes are contained is composed of KC1. Any oxygen in the vicinity of the sensor diffuses through a Teflon membrane and is reduced at the cathode, which results in a current proportional to the oxygen partial pressure in the atmosphere around the sensor.

Advantages are: (1) the polarographic type oxygen sensor has the advantage of being small; (2) it is not position-sensitive; (3) output reading is not affected by changes in relative humidity, total pressures, or the temperature of the gas being monitored; and (4) it has a large output current so signal-conditioning equipment can be remote.

Disadvantages are: (1) the principal disadvantage is that the sensor can become poisoned by an atmosphere rich in oxygen; (2) it is a one-shot item in that when it becomes poisoned, total replacement is necessary; and (3) liquid oxygen vapor can freeze the electrolyte if it contacts the sensor, which would then be inoperable.

Paramagnetic Oxygen Sensors - The operation of a paramagnetic oxygen detector is based on the production of a convection current in a gas sample as a function of its oxygen content. The gas is drawn into the field of a magnet which applies a force to the oxygen by virtue of its paramagnetic

properties and at the same time reduces the thermal energy of the oxygen molecules. An element of a bridge downstream of the magnetic field is cooled by the absorption of thermal energy as the gas passes over it, when it is in the process of reverting to its normal state.

Detection systems based on the use of the paramagnetic properties of oxygen would be far too cumbersome to be practical at a launch complex. Their utility would be further reduced because tubing would have to be run to the sample area. If more than one sample tube were to be used, a means of discriminating gas samples would be required.

Fuel Cell Oxygen Sensors - The fuel cell sensor is a device which intercepts and channels current carriers of a catalytically forced chemical reaction through a load to produce electrical power. Fuel cells have largely been developed about the hydrogen-oxygen reaction.

A local supply of hydrogen is fed to the cell in a controlled stream. Oxygen from the air permeates through a filtering membrane to the cell. The result of transferral through an electrolyte, and catalytic action on an electrode, is an electrical current. The current is in direct ratio to the rates of reaction, which is in turn a function of the oxygen flow rate through the membrane. Since the flow rate through the membrane is a function of the partial pressure of the oxygen content of the ambient gas, the current amplitude is also a function of the quantity of oxygen in the ambient gas.

If the means of supplying hydrogen and oxygen to the cell were reversed, the current from the cell would then be a function of the partial pressure of hydrogen in the ambient gas.

One of the obvious advantages in the use of a fuel cell is that the device is its own power supply. Thus, the need for prime equipment is reduced. In fact, the sensor may be used to power its signal conditioner and amplifier.

NON-SPECIFIC METHODS - There are several methods other than using sensors individually responsive to the presence of hydrogen or oxygen which may be applicable in determining hydrogen and oxygen leakage on launch complexes.

TV Systems - Significant leakage of cryogenics into an atmosphere containing water vapor produces a visible plume. In many instances, a TV camera chain and monitor would be useful to display evidence of such leakage. A rigorous quantitative determination of the rate of leakage is impossible; however, an experienced observer can readily estimate the requirement for action based on the hazards created by a given situation. The long runs of the fill and drain lines, the tank farm, and the vent lines are particularly appropriate areas for application of this type system.

Vacuum Gage - Cryogenic supply lines to the vehicle are commonly vacuum jacketed lines. Therefore, loss of vacuum is indicative of leakage, but does not indicate whether the leak source is the cryogenic line or the ambient atmosphere. Regardless of the source of the leak, a vacuum gage would indicate that a leak existed, and could be used to control a vacuum pump which would maintain safe conditions unless the leak became severe. Observation of fracturing or lack of frosting near the leak would give some indication of the source of the leak.

Ultrasonic Detectors - Ultrasonic techniques may be useful in detecting and locating small leaks. One of the characteristics of the small leak of a gas under pressure is the emission of an ultrasonic output near 40 kc. There are devices on the market capable of detecting these ultrasonic frequencies from some distance. These devices are directional and peak when pointing directly at the leak, giving either an audio or electrical signal. These devices are generally portable and designed to aid in locating leaks.

GENERAL ELECTRIC EXPERIMENTAL AND DEVELOPMENT DEVICES - At present, leak detection techniques are being considered for the specific application in the following areas:

1. Component and subassembly quality control testing.
2. Tests during assembly of system.
3. Tests of the completely assembled systems.
4. Tests during the tanking and static firings.
5. All types of prelaunch checkout.

Encapsulation Type Leak Detectors - The General Electric Company has undertaken a laboratory program of research to develop new materials and techniques suitable for utilization as leak detectors. Certain plastomers and elastomers have been developed which show promise of improving detectability of leaks in missile systems.

The mechanism envisioned is the application of these materials at "susceptible-to-leak points" as films, whereupon deformation from leak pressure and visual indication indicate such leakage. Ultimately, we aspire toward a system that will automatically detect leaks using this basic mechanism in a sensing role. The current research program was tuned toward developing techniques required in the use of these materials to be applied as films over tubing connections, welds, etc., which will permanently deform under leakage pressure, thus providing readily visible detecting means. This type of system is especially adaptable to quality assurance and acceptance testing of components, subsystems, and complete systems of launch vehicles. The second stage of the research was concerned with the development of elastomers and the techniques necessary for applying these materials onto space hardware.

The basic operation of elastomers, in contrast to plastomers, is that the material, due to its elasticity, will expand under leak pressure and will form a "bubble." The size of this "bubble" can determine quantitative size of leakage in a given place. The use of these elastomers, combined with especially developed strain gage sensors or the resistive tape, will produce an electrical read-out proportional to the magnitude of the leak, thus forming the basis for an ultimate sensing system which can include audible or vis-

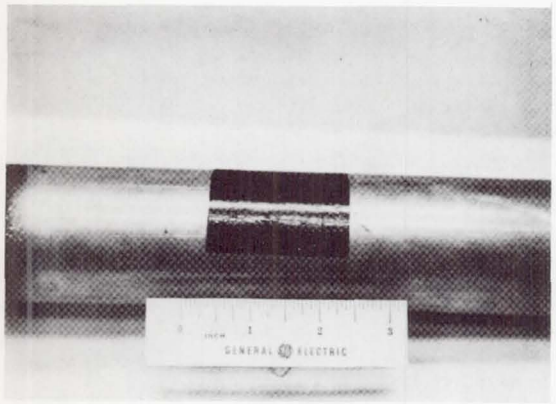

(a) Initial Appearance of Tape

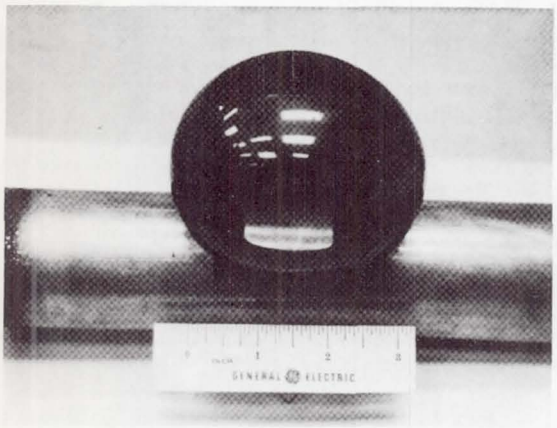

(b) Maximum Size of Blister

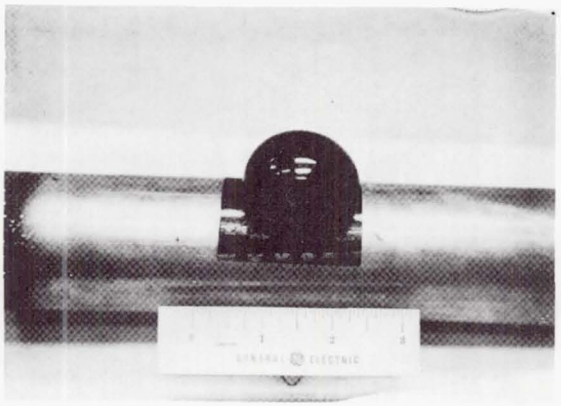

(c) Stable Size at Constant Leak Rate

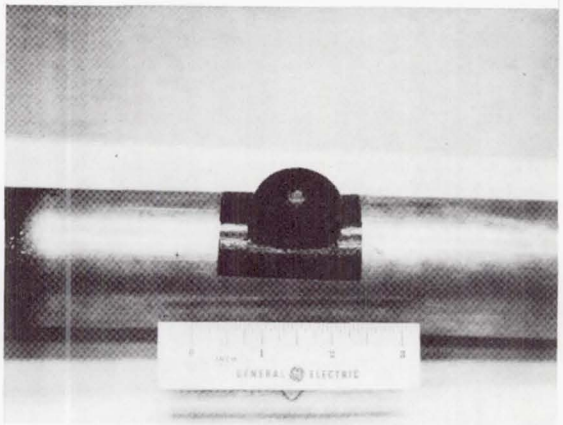

(d) One Hour after Venting System to Atmosphere

Fig. 1 - Inflation of EPR rubber by leak in 2-inch tubing

ual read-out (Figs. 1 and 2).

Over the past few months, a wide range of plastic and elastic materials has been examined and the mechanical and other properties were tabulated for their representative materials currently available in thin-film forms. The most promising materials were subsequently tested at different temperatures, down to -100° F, to determine the mechanical behavior. Later, they were tested as encapsulating membranes. It was found that leakage rates of 10^{-2} cc/sec could be detectable with this type of tape, which provided a permanent indication of leakage due to its plastic flow behavior. This type of tape can be used in hazardous locations and in complex systems where continuous visual inspection cannot readily be carried out by other means such as the soap-bubble method.

Thermal Conductivity of 0.5% Hydrogen Detector - This type of device operates on a large difference in the thermal conductivity be-

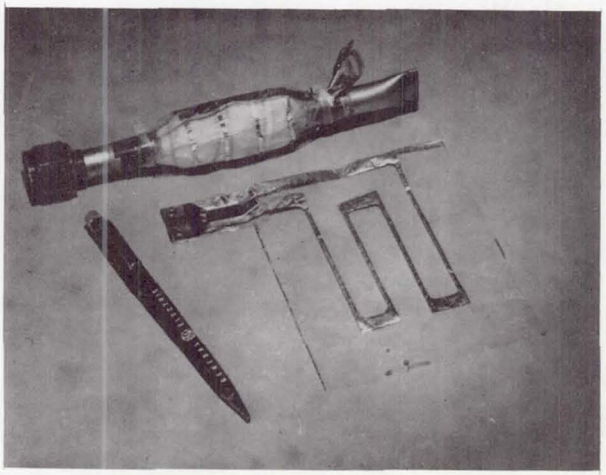

Fig. 2 - Printed circuit leak detector shown separately and as applied to 1/2-inch tube union

tween hydrogen and air and provides an electrical output proportional to the concentration of hydrogen in the air. It should be remembered that hydrogen and helium possess the highest thermal conductivity of all gases. This is why no positive identification can be differentiated.

This type of detector utilizes an electrical servo-type compensation and is reasonably sensitive. Work during recent months has reduced the size of the complete electronics (Fig. 3). No attempt has been made to miniaturize the sensing head until specific applications can be determined. This device can detect small concentrations of hydrogen below 0.5% of hydrogen by volume in air.

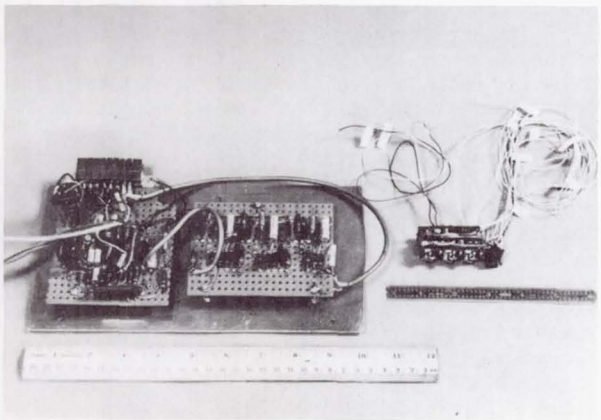

Fig. 3 - Thermalconductivity 0.5 percent H_2 detector

Compact Thermal Conductivity 1.5% Hydrogen Detector - Again, this device employs a balanced bridge circuit which is compensated for temperature fluctuations as well as humidity. The design of this detector was also altered a number of times in order to incorporate all improvements which evolved as work progressed. Figs. 4 and 5 show the essential details of this type of detector, which has been assembled in a miniature fluorescent light starter. The assembled detector is approximately 3/4 inch in diameter, 1/2 inch long, and weighs 1 ounce.

The heart of this detector is a brass cell block containing all the necessary components encapsulated in an epoxy. Tests show that this design performs very satisfactorily. In fact, it even surpassed original expectations by detecting less than 0.25% of hydrogen by volume in air.

Data was obtained during the final tests as follows: The detector was adjusted for a balanced bridge with 0 output at 25°C with an input of 28 volts dc. The full output for 1.5% hydrogen in nitrogen was 15 millivolts. For the same mixture of hydrogen with air, the output was increased 17 millivolts.

A dc vacuum-tube voltmeter was used throughout the testing program for all the output measurements. At -80°C, the detector performed with only a slightly larger error than over the 0° to 50°C range, provided the unit was operating during the time that the temperature was decreased to this value. Exposure to -195°C for a period of 1 1/2 hours did not appear to have any damaging effects on the detector. Upon return to room ambient temperature, the detector's performance was not altered from previous test data. The detector's output for a number of cases with different molecular weights is shown in Fig. 6. All cases tested appear to follow a curve showing a definite relationship between molecular weight and detector output. Some stability tests for humidity were also conducted and when the mois-

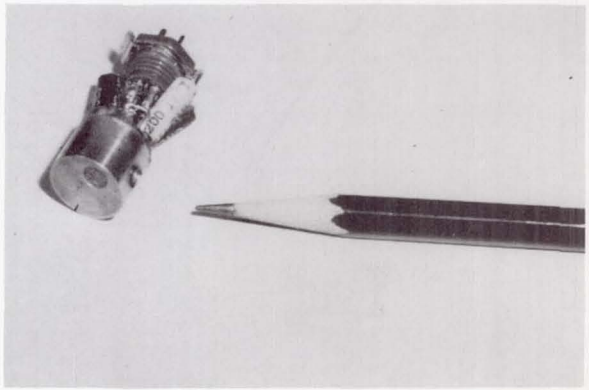

Fig. 4 - Compact type H_2 in air detector - out of case

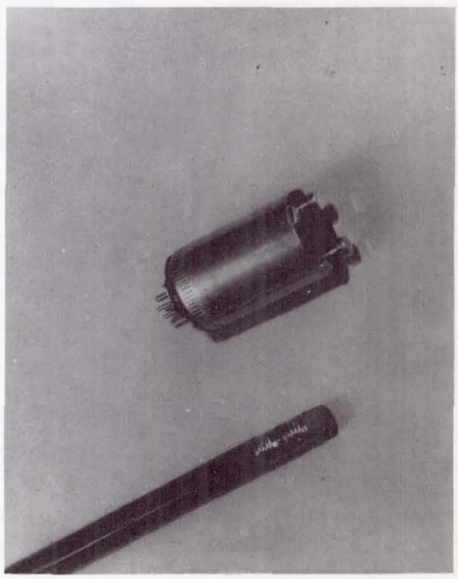

Fig. 5 - Compact type H_2 in air detector - in case

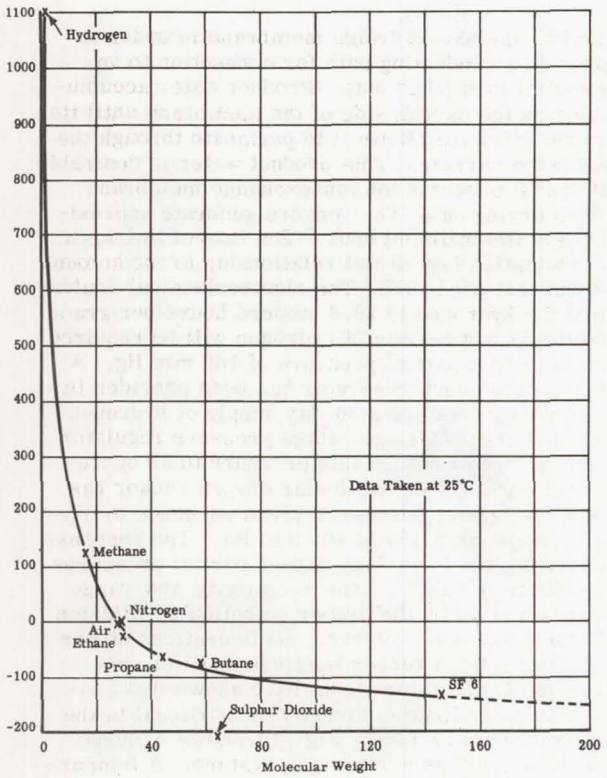

Fig. 6 - Detector sensitivity to various gases

ture content was increased from 0 to 100% relative humidity, the detector output increased only approximately 0.3%. The detector operated satisfactorily when being rotated 360° and held its readings in all possible positions.

Additional research is now being conducted for further development of Permselective membranes which are capable of passing specific gases, or restricting others, thereby increasing the specificity of this detector to any desired gas analysis.

Halogen Type of Hydrogen Detector - This type of detector operates by aspirating a sample of air between electrodes of a diode-type sensitive element. Usually, the positive electrode is a heated platinum cylinder which contains platinum on a cylindrical coil and a negative electrode is a relatively cool cylindrical metallic surface which surrounds the positive member. Using correct operating temperatures of the positive electrode (900°C) with appropriate field excitation (300 vdc), small positive ion current flow is detectable when air flow is approximately 1 cubic ft/hour. However, when the air flow is contaminated with a slight trace of hydrogen vapor, a substantial increase of ion current is obtained. This type of halogen detector is commercially available and is manufactured by the General Electric Company. To adapt this device to hydrogen detection, different types of coils were used on which many different types of electrodes were wound. With the air flowing at the rate mentioned, which is accomplished by a small blower, it was possible to detect the small amount of hydrogen or other types of inflammable gases. This leak detector appears to be suited only to certain sensing tasks, and is most efficient in small enclosures which surround potential leaks. To obtain sensitivity, especially with hydrogen, much lower operating temperature levels must be maintained. The reduction in the operating temperature also reduces the sensitivity, making this detector impractical for large-scale hydrogen detection.

Palladium Wire Hydrogen Detector - This detector works on the principle of absorption of hydrogen by palladium which causes the resistivity of palladium to change. There were many tests conducted on this device during the initial development which produced some optimistic results. The bulk of the tests conducted was concerned with different types of geometrics of the wire filament sensing element and the alloy composition of palladium. Further experiments consisted of combining palladium and silver into an alloy which produced maximum sensitivity to hydrogen. The sensitivity could be controlled by increasing or decreasing the specific wire diameters.

A life test was conducted on the final configuration of this detector (Fig. 7). The test revealed that after the prolonged exposure to hydrogen, the sensing element became saturated to a point where no fixed reading could be taken. Finally, the detector became completely insensitive to hydrogen, until the filament was baked out at an elevated temperature. The work on this project has been suspended since the reliability of this detector is questionable. However, the combination of thermal conductivity principle and palladium reaction to hydrogen might still produce an effective sensor.

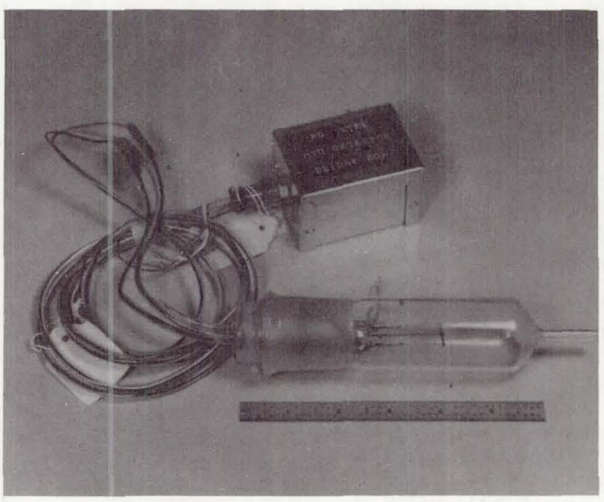

Fig. 7 - Palladium change-in-resistivity H_2 detector

FUEL CELL AS A SPECIFIC H_2 OR O_2 DETECTOR

For the past several years, the General Electric Company has been involved in the development of oxygen partial pressure sensors employing a novel concept which is proprietary to the General Electric Company. (See U.S. Patent 3,149,921, assigned to the General Electric Company.) The concept uses an ion-exchange membrane as a key element. Hydrogen (in a closed circuit) is supplied to one side of the membrane; the opposite side is exposed to the gas mixture whose oxygen partial pressure is to be measured. Specially constructed catalytic current collector-electrodes are bonded to each face of the ion-exchange membrane. The result is, in effect, a miniaturized fuel cell whose output is proportional to the oxygen partial pressure.

In addition to the General Electric Company funded effort, two development contracts have been funded by NASA. Under contract to NASA-JPL, a program was conducted to determine the adaptability of this type of oxygen sensor to the special requirements of measuring the atmospheric oxygen level on the planet Mars. The program included material studies, response to minimum oxygen concentrations, effect of interfering gases, and establishment of operating temperature limits. Based on these results, a laboratory model was fabricated which provided a voltage output of 0.52 volt at an oxygen partial pressure of 10 mm Hg. Response was deliberately nonlinear, providing maximum sensitivity, half of the voltage response, in the zero to one mm Hg oxygen partial pressure region, a desirable performance characteristic for this application.

Under contract to NASA-MSC, a laboratory prototype oxygen partial sensor development program for monitoring the oxygen content in a manned space vehicle atmosphere was recently completed. When used as an oxygen sensor, the cell is starved of oxygen by the use of a diffusion barrier on the oxygen side of the ion-exchange membrane (Fig. 8). This diffusion barrier is selected to limit the amount of oxygen available at the ion-exchange membrane and thus permit operation over a wide range of oxygen partial pressures. Metallic current collectors are pressed against the ion-exchange membrane in order to provide a conducting path for connection to an external load (read out). Product water accumulates on the oxygen side of the membrane until its vapor pressure allows it to permeate through the diffusion barrier. This product water is desirable in that it prevents the ion-exchange membrane from drying out. The sensors generate approximately two milliamperes. The rate of hydrogen consumption is a direct relationship to the amount of current produced. The electrochemical equivalent for hydrogen is 26.6 ampere hours per gram, so that 0.014 cc/min of hydrogen will be required at an oxygen partial pressure of 160 mm Hg. A three-cubic-inch reservoir has been provided in this design to store a 30-day supply of hydrogen at 2000 psig. A single-stage pressure regulator is provided to reduce this pressure to an operational level. This particular oxygen sensor has been designed to provide a given response to oxygen levels from 160 to 400 mm Hg. The response of the sensor to various oxygen partial pressures is shown in Fig. 9. The sensitivity and range can be varied by the proper selection of diffusion barrier and load. Present configurations utilize one-mil silicon rubber barriers and 100-ohm loads. Temperature tests have shown that sensor output voltage is directly proportional to the ambient temperature. Fig. 10 shows a curve of output voltage versus temperature. A temperature compensating network utilizing thermistors is applied to the output signal to supply the necessary correction. After stabilization, the sensor will run continuously for a long time period with only a slight signal change. A trimming potentiometer is provided so that the sensor can be calibrated while exposed to reference oxygen concentrations. Humidity testing at relative humidities of 90 to 95 percent has no appreciable effect on sensor outputs over a 24-hour period.

Design Features -

1. Weight - 1 pound.
2. Volume - 14 cubic inches.

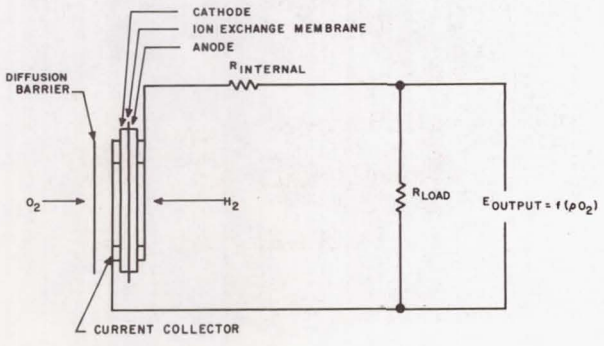

Fig. 8 - Fuel cell type pO_2 sensor schematic

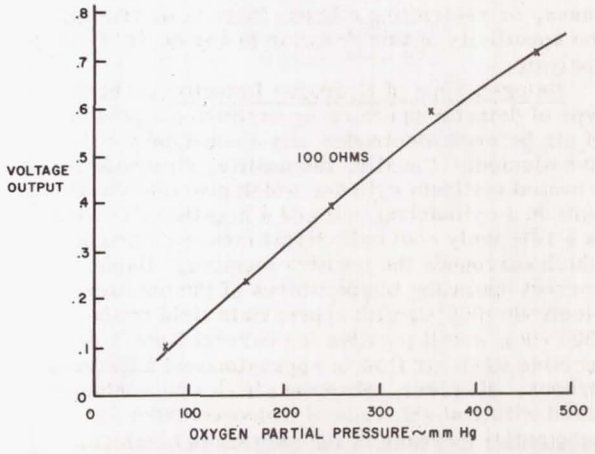

Fig. 9 - Oxygen sensor performance curve

3. Life - Sensor is designed to operate continuously for 30 days with no venting of the hydrogen supply.

4. Leakage - Hydrogen leakage will not exceed 1 x 10^{-6} cc/sec.

5. Range - Range of sensor currently under development is 160-400 mm Hg partial pressure of oxygen.

6. Electrical Output - Output voltages from 0.2 to 0.8 volt at 2 milliamps are generated by the fuel cell depending on the partial pressure of oxygen. A small connector serves as the electrical interface with a readout instrument.

7. Temperature - The sensor is intended to operate over a range of 35 to 110° F with a thermistor temperature compensation network.

8. Accuracy - Linearity of the sensor is intended to be within ±2% of actual oxygen partial pressure.

9. Time Response - The response of the sensor is 5 seconds or less to reach a 63% value of a step change of 400 to 160 mm Hg partial pressure of oxygen.

10. Humidity - The sensor operates in humidities varying from 0 to 100% relative humidity for temperatures of 35 to 110° F.

Early in the development of the ion-exchange membrane, i.e., fuel cell, approach to oxygen partial pressure sensing, it was evident that by reversing the sensor action, the presence of hydrogen in an unknown gas mixture could be determined. Sensor action would be reversed by supplying oxygen, in a closed circuit, to one side of the ion-exchange membrane and exposing the opposite side to the atmosphere to be tested. The resulting output current should then be a function of the pH_2 in the unknown gas mixture.

Recently, in order to test this hypothesis, a lab development model pO_2 sensor element (similar to those developed for the NASA-MSC program) was operated in a reverse mode. With oxygen supplied to one side of the ion-exchange membrane, hydrogen directed at the opposite side caused an immediate current flow; the output voltage was almost the normal open-circuit value experienced in the opposite operating mode. Of even greater significance was the next experiment conducted. A synthetic mixture of air and hydrogen (at 1% concentration) was directed at the sensor. Again, the response was almost immediate (a few seconds), the 1% hydrogen concentration being easily detected. Subsequent tests indicated that 0.1% hydrogen concentration and probably lower could be readily detected. The question arose that perhaps any highly combustible (oxidizable) gas in the unknown gas mixture would also cause an output current to be generated. Pure propane gas was directed at the sensor, but no current output was detected.

In summary, this General Electric Company concept appears capable of providing a very small, lightweight, hydrogen partial pressure sensor which generates its own output signal, provides a high-level output signal for direct meter readout without an amplifier, is insensitive to the presence of other gases, and is adaptable to sensing pH_2 over a wide range, from less than a mm Hg full scale to many psi (Fig. 11).

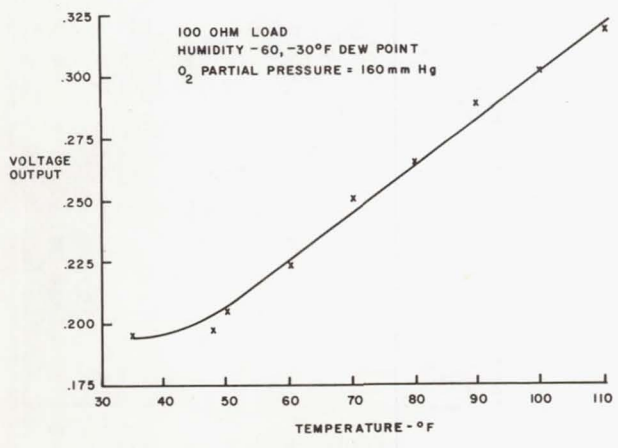

Fig. 10 - Oxygen sensor - effect of temperature on output

CONCLUSIONS AND RECOMMENDATIONS

The necessity for saving time while maintaining an excellent record in systems performance means that no portion of launch vehicle operation can be neglected. One area that is receiving more attention from day to day is that of leak detection. Not only is detection of hydrogen and oxygen fuels which are new to the missile industry required, but detection of pressurization gases, hydraulic fluids, etc., continues to be necessary.

Fig. 11 - Fuel cell as H_2 detector

Many methods and many instruments are available for the detection and location of leaks. No one instrument or method is ideal for any particular application in the space industry.

The most common liquid or gaseous fuels which are presently used on typical missile launching sites are hydrogen, RP-1, hydrazine, and unsymmetrical dimethylhydrazine. The common oxidants are liquid oxygen and fuming nitric acid.

An additional leak detection problem is encountered by use of large quantities of dry nitrogen and helium; and the only solution to this problem lies in the key word, which is "THE SPECIFICITY."

Therefore, an urgent need exists for new, sophisticated sensors that can "specifically" detect and quantitatively measure each of these gases in any environment, before they reach hazardous proportions.

The General Electric Company fuel cell is an ideal sensor for detection of hydrogen or oxygen only. No signal shall be generated or deteriorated by any other gas; no other method can compare in the sensitivity, accuracy, or response.

The only other efficient device for specific measurements of leaks is the mass spectrometer, which can be designed to any degree of sophistication, depending on the applications and the initial capital investment.

It appears that further research is in order to enhance the state of the art in the leak detection area. The ideal system is yet to come; and, in the author's opinion, it should consist of hybrid type transducers. A combination of the laboratory mass spectrometer in conjunction with a gas chromatograph, a fuel cell, or a thermoconductivity bridge, etc., will provide the flexible and reliable instrumentation that can assure a success and not a disaster.

Page Intentionally Left Blank

AN EFFICIENT PROCEDURE FOR THREADED-CONNECTOR SELECTION

By

J. W. Adam
Battelle Memorial Institute
505 King Avenue
Columbus, Ohio 43201

ABSTRACT

The purpose of this paper is to suggest a more reasonable procedure for the selection of threaded connectors and to provide a basis for reducing the number and cost of qualification tests required. Included in the paper is a discussion of how the various connector characteristics such as deflection rates, seal seating loads, and torque-axial-load relationships can be determined and how they can be taken into account to predict leakage under various operating conditions. How these predictions can be used to establish the most critical areas for experimental investigation is also shown.

THE SELECTION OF THREADED CONNECTORS for use in high-performance missile fluid systems is one of the major problems of the aerospace industry. Generally, a number of candidate connectors are tentatively selected on the basis of past experience and manufacturer's performance ratings. The final connector selection depends upon which of these connectors performs best during a series of tests conducted by the eventual user. Over the years this procedure has not clearly demonstrated the capabilities of the various available connectors, and generally a new series of tests is required for each new missile system. The resulting test duplication is expensive and time consuming.

In an attempt to formulate a more reasonable procedure for the selection of threaded connectors, the Air Force asked Battelle to determine whether the procedure developed by Battelle for the design of the AFRPL connector (1)* could be utilized to predict the performance of various commercial connectors. As a first step in this determination, an analysis procedure was developed for predicting the performance capability of threaded connectors. The primary criterion chosen to evaluate performance was the rate of helium leakage caused by operating structural loads and thermal gradients. Although other factors such as configuration, manufacturing and assembly techniques, weight, size, and cost enter into the final selection of a connector, these factors were disregarded except where they were critical to performance. During the development of the analysis procedure, four commercial connectors were analyzed and tests of the connectors substantiated, for the most part, the performance predictions.

The analysis procedure consists of a series of experimental and computational steps. In many cases either computational or experimental methods can be used to determine connector characteristics. Because the computational methods sometimes require interpretation and approximation, experimental methods are often preferable. The procedure is based principally on the preload diagram analysis described at the 1964 Leak-Tight Separable-Fluid-Connector Conference (2). Performance at three conditions is considered:

1. Initial assembly
2. Minimum seal load
3. Maximum nut load.

Sealing effectiveness of the connector is considered at the initial-assembly and minimum-seal-load conditions. Structural integrity of the connector is considered at the maximum-nut-load condition.

To determine the performance of a connector at these three conditions, ten factors must be determined:

1. The initial axial load resulting from the assembly torque
2. The axial-seal seating load that is required to "seat" the seal
3. The initial seal contact stress generated by the initial axial load
4. The structural loads resulting from the system pressure and bending moment
5. The residual seal load or the axial load at which the sealing contact stress begins to decrease
6. The deflection rate of the compression members
7. The deflection rate of the tension members
8. The relative change in deflection of the tension and compression members due to a cold thermal gradient
9. The relative change in deflection of the tension and compression members due to a hot thermal gradient
10. The maximum allowable nut load that can be applied before the nut yields.

*Numbers in parentheses designate References at end of paper.

The interrelationship of these ten factors and their effect on the three performance conditions is determined by means of a preload analysis.

INITIAL SEALING EFFECTIVENESS

Initial sealing effectiveness is determined by three factors:

- The initial axial load
- The axial-seal seating load
- The initial seal contact stress.

During the past 3 years, programs have been conducted at the Illinois Institute of Technology Research Institute (IITRI) (3) and the General Electric Advanced Technology Laboratories (ATL) (4) to determine the conditions required to create a low-leakage seal with different combinations of metals. While much remains to be learned about the sealing action of metallic surfaces, both programs have shown that the leakage of gases can be estimated for certain known conditions on the basis of the contact stress generated at the seal interface. Generally, both of these programs have shown that surface finish is a primary factor only if the sealing contact stress is less than about 1-1/2 times the yield strength of the softer material. If the ratio of stresses is greater than 2 to 2-1/2, the surface finish of the sealing surfaces becomes a secondary factor and the initial sealing effectiveness can be approximated by a procedure in which it is assumed that the sealing-surface roughness is no greater than 32 rms.

INITIAL AXIAL LOAD - Assembly torques and lubrication procedures are recommended by most connector manufacturers. Exact axial loads resulting from the assembly torques are difficult to to determine theoretically because the friction factors are generally unknown. A more accurate method is to determine the minimum and maximum initial axial loads experimentally by means of the arrangement shown in Figure 1.

The flanges are welded to adapter plates that are bolted to the tensile machine platens. When the parts are lubricated properly and the recommended torques are applied to the connector, the loads are read directly on the tensile machine. A seal is not installed during this test, and care must be taken that most of the threads are engaged and that the connector flanges do not touch.

The efficiency of the assembly torque varies with connector configuration, material, method of manufacture, type of lubricant, and the number of assemblies. Sufficient tests must be conducted to determine predictable axial loads for the recommended minimum and maximum torques. The axial loads obtained on the initial assembly are the ones that should be used for the analysis, although additional assemblies are of interest

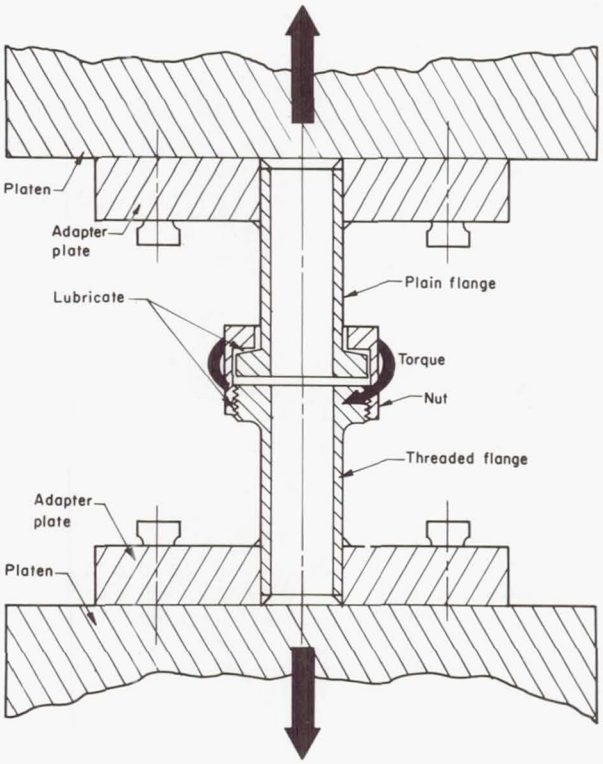

Fig. 1 - Experimental arrangement for measuring axial load as a function of torque

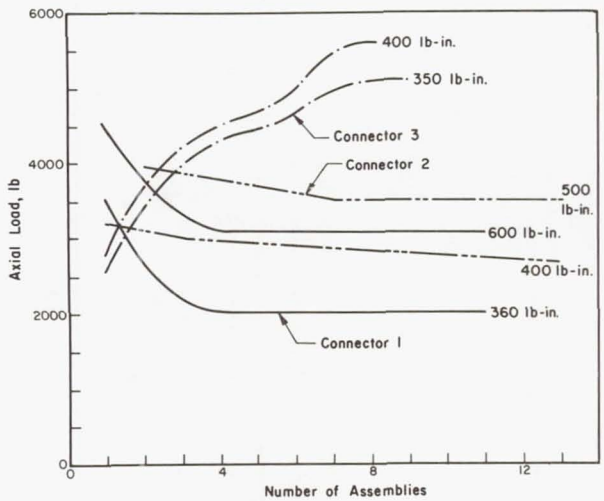

Fig. 2 - Axial load vs. number of assemblies for three typical connectors

to determine the effect of repeated assembly. The effect of the number of assemblies on the axial load is shown in Figure 2 for three different connectors.

AXIAL-SEAL SEATING LOAD - Depending on the configuration of the connector, all or part of the initial axial load is used to seat the seal. If the axial compression is transmitted entirely through the sealing surface, all of the compressive load contributes to the seal-seating load. In many connector designs, however, only part of the compressive load is used to seat the seal. After the flanges contact, the remainder of the compressive load is transmitted through the flanges, or, as in the case of the AFRPL connector, through the cylindrical tang of the seal. For each design being analyzed, it is necessary to determine what portion of the initial axial preload contributes to seating the seal.

Figure 3 shows a typical arrangement for determining this value experimentally. The plain flange is inserted into an adapter that simulates the action of the nut. The threaded stub-end flange is supported by an adapter that applies axial loads through the threads. Since only part of the compressive load is transmitted through the seal, and since the spring rate of the seal is usually much different from the spring rate of the flanges, the maximum compressive load transmitted through the seal is shown by the change in slope of the compression-load deflection curve. Because the load needed to bring the flanges of the connector into contact may vary with the dimensions of the seal and the seal cavities, it is necessary to assemble at least two connectors and to select tolerances that will give the highest and lowest seal-seating loads.

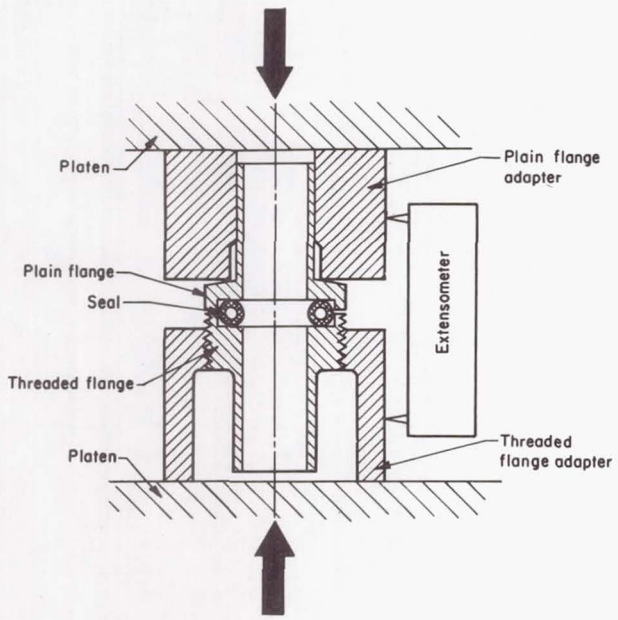

Fig. 3 - Experimental arrangement for determination of seal-seating load and compression-deflection rate

Figure 4 shows a typical seal-seating-load curve obtained for one of the connectors analyzed at Battelle. The maximum axial seal-seating load is taken as the maximum load prior to the sudden change in slope.

INITIAL SEAL-CONTACT STRESS - The initial seal-contact stress is obtained by dividing the maximum load normal to the sealing surface by the area of the sealing surface. Many seal configurations are used in threaded connectors, and the seal configuration determines the method by which the axial load is applied normal to the sealing interface. Because of the many seal types, no one analysis method can be proposed. In general, the magnitude of the load normal to the sealing surface can be determined by means of a force analysis. The normal seal-seating load may be equal to or greater than the axial seal-seating load. In the AFRPL connector, for example, the normal seal-seating load is about twice the axial load.

The possibility of accurately estimating the sealing area varies widely with connector types. In many cases it may be necessary to assemble and disassemble several connectors and to measure the width of the seal imprint. In some cases the sealing width can best be determined through examination of a microsection of an assembled connector. When the normal seal load and the sealing area have been determined, the initial seal-contact stress can be calculated.

SEALING EFFECTIVENESS - An approximation of initial sealing effectiveness disregarding opera-

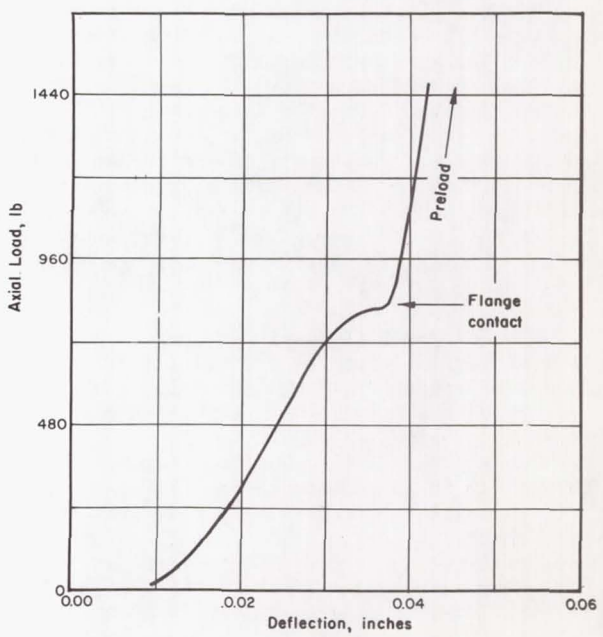

Fig. 4 - Typical seal-seating-load curve

tional loads is helpful in determining whether a connector can potentially seal adequately under operational conditions. If the initial contact stress is of the order of 2 to 2-1/2 times the yield strength of the softer seal material, this leakage will probably be on the order of about 1×10^{-7} atm cc/sec of helium or less. In only one type of configuration, i.e., a pressure-energized-type seal, is there a possibility that the initial leakage will decrease on application of the structural loads and pressure end load. Even for the pressure-energized seal, however, the initial seal contact stress must be sufficiently great to insure low leakage at all operating pressures.

SEALING EFFECTIVENESS AT MINIMUM SEAL LOAD

The minimum seal load, and hence the minimum contact stress on the sealing surface, will occur when the structural loads and the cold thermal gradient are applied to a connector assembled at the minimum preload. Because a threaded connector is an indeterminate structure, the reduction in seal load caused by these external loads is best determined by means of a preload diagram. In order to construct the preload diagram and determine the sealing effectiveness at the minimum seal load, five factors must be determined:

- Structural loads
- Residual seal load
- Deflection rate of the compression members
- Deflection rate of the tension members
- Cold-thermal-gradient deflections.

STRUCTURAL LOADS - The structural loads which the connector must withstand consist of the pressure end load and the bending moment. The pressure end load is based on the maximum seal diameter and the operating pressure. The bending moment is based on the diameter, wall thickness, and the material properties of the tubing, and can be included by calculating an equivalent axial load that will cause the same stress in the tube as the bending-moment load. The details for calculating the structural loads are given in Reference 1.

RESIDUAL SEAL LOAD - For a series-type seal, the seal load is equal to the initial axial load and any reduction in axial load will result in a corresponding reduction in the contact stress at the seal interface.

For a parallel-type seal, as long as the flanges remain in contact there will be no change in the seal-contact stress. Upon separation of the flanges, however, the seal can be considered a series-type seal and a further load reduction will cause a reduction in the contact stress at the seal interface. The load at which the flanges separate may not be the same as the load at which the flanges contacted during assembly. This separation load is defined as the residual seal load and it is important in determining the effect of the operational conditions on the connector.

Figure 5 is a typical load-deflection curve for a connector that demonstrates a residual seal load. The residual seal load is determined at the same time as the initial seal-seating load by loading and unloading the compression members several times and noting the load at which the slope of the load-deflection curve changes. If there is a residual load, it will be apparent on all loading and unloading cycles after the first loading cycle. Depending upon the configuration and dimensional characteristics of the connector, the separation load or the residual load can range from zero to the same value as the seal-seating load. Results should be averaged for at least two or three loading cycles.

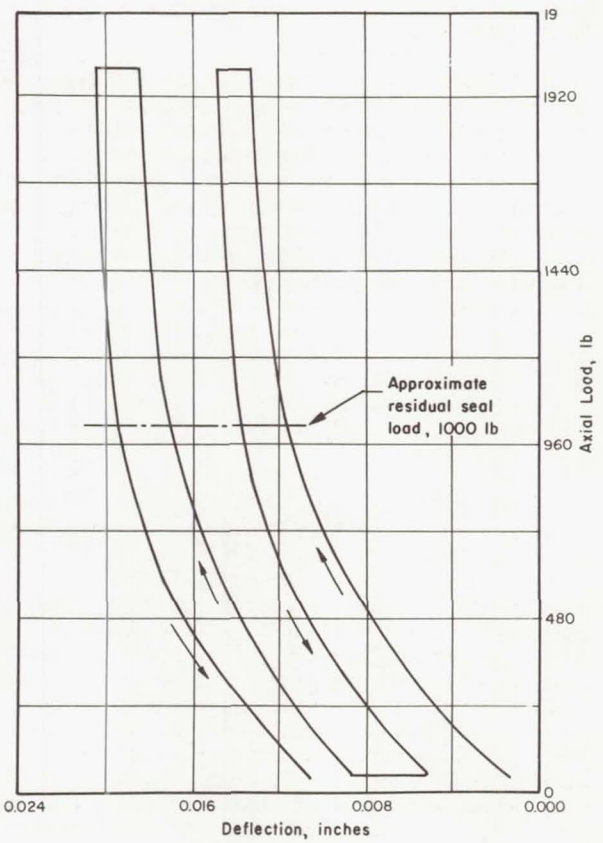

Fig. 5 - Typical compression member load-deflection curve for connector, demonstrating residual seal load

DEFLECTION RATE OF THE COMPRESSION MEMBERS - The deflection rate of the compression members is determined with the arrangement shown in Figure

3. An extensometer should be used for greater accuracy and to eliminate the need to consider the deflections of the tensile machine crosshead, which may be of the same order of magnitude as the deflection of the compression members. Even so, the compression deflection rate of the test fixture, the deflection rates due to bending of the flanges, and the deflection rates due to thread bending and shear must be calculated and subtracted from the deflection rate measured experimentally.

If a residual seal load exists, the deflection-rate curve of the compression members will have two slopes as shown in Figure 5: one for loads above the residual seal load and one for loads below the residual seal load. The average slope in in./lb for several load cycles is taken as the deflection rate of the compression members. The true deflection rates for the compression members are the experimental values minus such values as the calculated deflection rates of the test fixture and the bending deflection rates of the flanges.

DEFLECTION RATE OF THE TENSILE MEMBERS - The deflection rate of the nut is determined experimentally with the arrangement shown in Figure 6. Again, the deformations and deflections occurring in the test fixture and in the adapter flange must be calculated and subtracted from the total measured deflection. The deflection rates of the plain and threaded flanges due to bending (calculated in determination of the deflection rate of the compression members) must be added to the deflection rate of the nut to determine the total tensile deflection rate.

A typical load-deflection curve is shown in Figure 7. Again, an average of several load cycles should be taken as the deflection rate of the tensile members.

COLD THERMAL-GRADIENT DEFLECTIONS - The maximum cold thermal gradient must be determined for the connector being analyzed so that the effect on the sealing load can be predicted. Usually an accurate calculation of the maximum thermal gradient is quite difficult and unwarranted. For stainless-steel connectors used in tubing systems less than one inch in diameter, the maximum thermal gradient that will occur can be roughly estimated as one-half of the difference between the fluid temperature and the initial temperature of the connector. If this estimate, which will probably be greater than the actual thermal gradient, indicates a serious problem when the minimum seal-load condition is considered, the validity of the estimate should be checked by measuring the thermal gradients experimentally with thermocouples.

The cold thermal gradient in the connector will cause a net contraction of the compression members in relation to the tension members. This net contraction can be calculated by

$$\delta = \frac{\alpha L \Delta T}{1 + \frac{DRCM}{DRTM}},$$

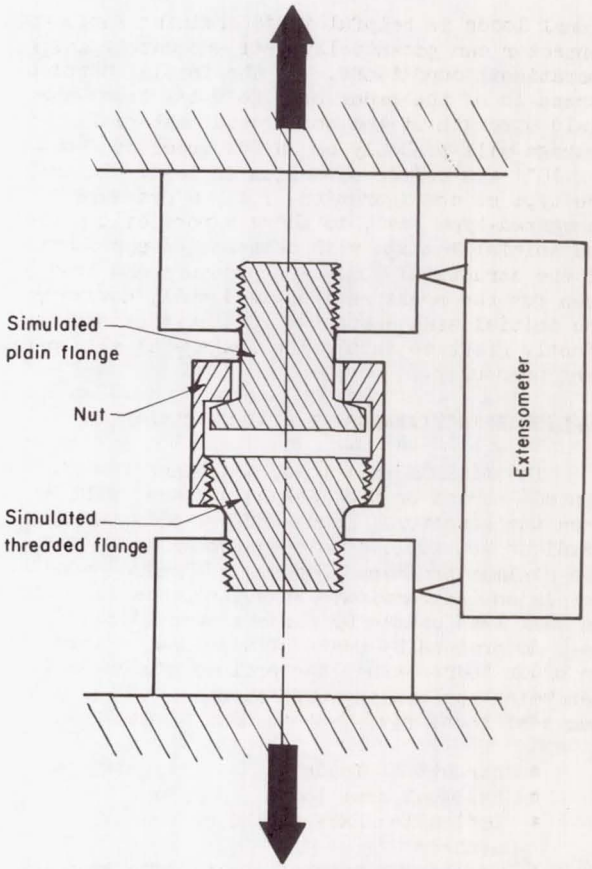

Fig. 6 - Experimental arrangement for determination of deflection rate of nut

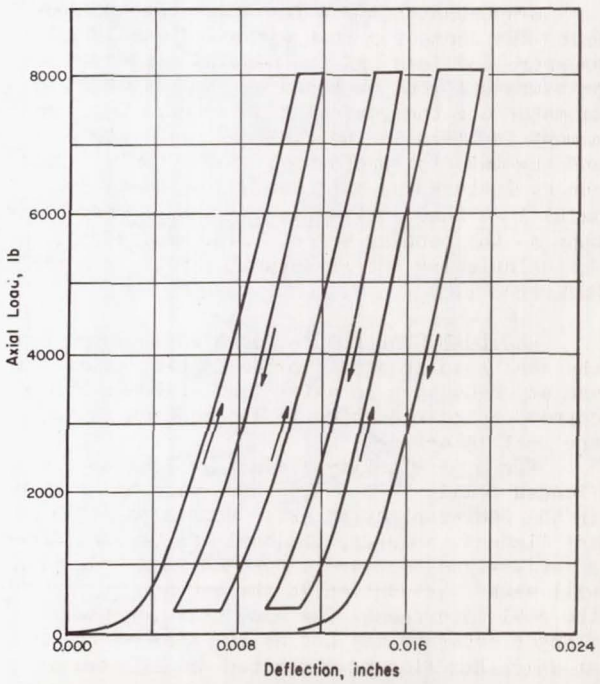

Fig. 7 - Typical load-deflection curve for tensile member deflection-rate determination

where

δ = net deflection, in.
ΔT = maximum average temperature difference, degrees F
α = coefficient of thermal expansion, in/in/degrees F
L = effective axial length of compression members, in.
DRCM = deflection rate of the compression members, in/lb
DRTM = deflection rate of the tensile members, in/lb.

SEALING EFFECTIVENESS - A preload diagram is constructed to determine the minimum seal load as shown in Figure 8, using the minimum preload provided by the minimum torque and the deflection rates of the tensile and compression members. The maximum structural load is drawn vertically between DRTM and DRCM. Point A establishes the minimum axial seal load under these operational conditions. If this minimum axial seal load is larger than the residual seal load, the flanges will remain in contact and the application of the structural load should not have a noticeable effect on the leakage rate for a parallel seal. If, however, the minimum axial seal load is less than the residual seal load, the flanges will separate and the leakage rate may increase. For a series seal, the application of any structural load will cause a reduction in the axial seal load.

The increase in leakage rate due to a decrease in the seal load depends on the ratio of the maximum prior contact stress to the contact stress at the reduced load. Although there are more exact methods for determining the increase in leakage rate (3), as a rule of thumb it can be estimated that a 60 percent reduction in contact stress will result in a 100 percent leakage increase.

In making the comparison of initial and final contact stress, the operating conditions of the system must be taken into account. If the connector is subjected to the cold thermal gradient immediately after initial assembly, the maximum contact stress for a series seal is taken as the initial seal-contact stress. If the connector is subjected to a hot thermal gradient before a cold thermal gradient occurs, the maximum contact stress for a series seal is taken as the maximum stress that occurs during the hot thermal gradient condition. For a parallel-type seal, of course, the maximum contact stress is limited by the contact of the flanges.

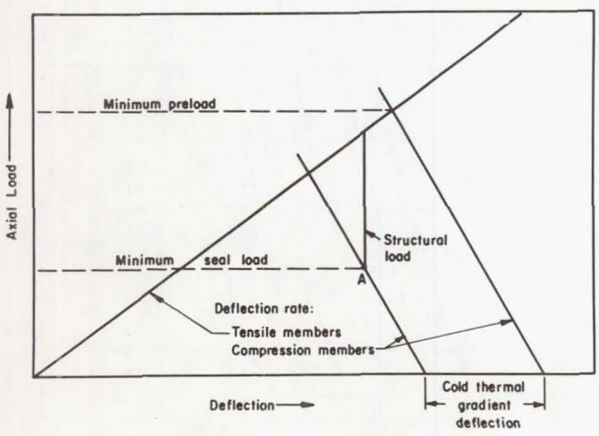

Fig. 8 - Preload diagram construction to determine minimum seal load

STRUCTURAL INTEGRITY AT THE MAXIMUM NUT LOAD

The maximum possible load on the nut will occur when the structural loads and the hot thermal gradient are applied to a connector assembled at the maximum preload. Usually, the introduction of a hot fluid into a connector will cause the load on the seal (or the load on the compression members if the connector is a parallel-type configuration) to increase because of the relative expansion of the compression members with respect to the tensile members. Therefore, leakage does not usually occur during the first hot cycle. However, if the increased load on the nut caused by expansion of the compression members causes yielding of the nut, subsequent cooling of the connector will result in partial reduction of the initial preload. Therefore it is vital to determine whether the nut will yield.

The structural integrity of the nut is affected by:

- Hot thermal gradient
- Structural loads
- Deflection rate of compression members
- Deflection rate of tensile members
- Maximum allowable nut load.

The hot thermal gradient can be estimated in the same manner as the cold thermal gradient discussed previously. Methods of determining the structural loads and deflection rates were also discussed previously.

MAXIMUM ALLOWABLE NUT LOAD - The maximum allowable nut load is determined using the test fixture shown in Figure 9. The simulated plain and threaded flanges duplicate the loads applied by the flanges of the connector to the nut. The compressometer is utilized because the nut must be loaded to failure to determine the apparent yield point. The test is performed at the maximum temperature at which the connector must operate. Because only the axial load is of interest, no correction need be made for deformations and deflections of the test fixture. The apparent yield point is taken as the point at which the load-deflection curve deviates from a straight line, as shown in Figure 10. Usable values can also be obtained if the test is made at room temperature and the values obtained corrected for temperature on the basis of published material properties.

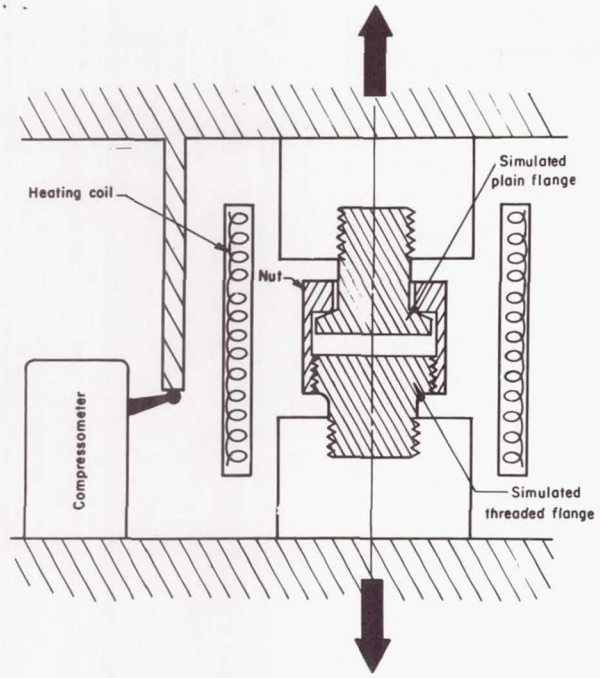

Fig. 9 - Experimental arrangement for determination of maximum allowable nut load

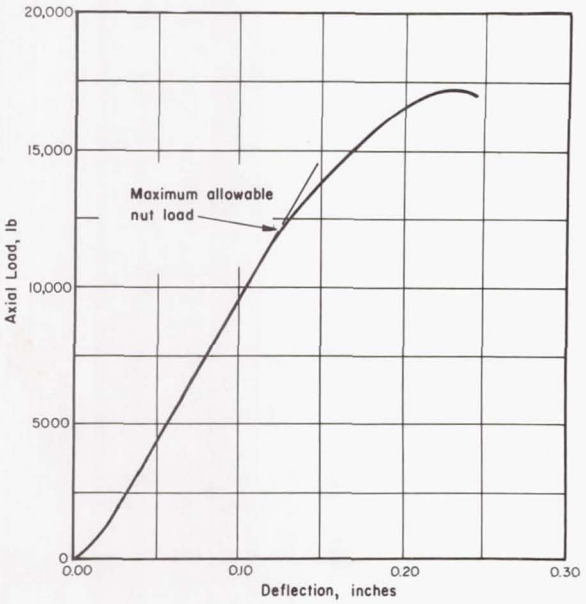

Fig. 10 - Typical load-deflection curve for determination of maximum allowable nut load

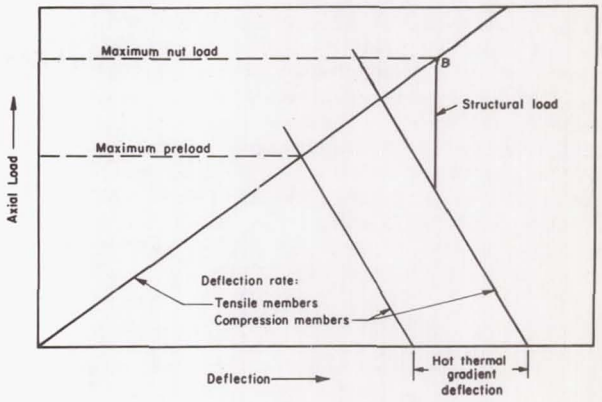

Fig. 11 - Preload diagram construction to determine maximum nut load

STRUCTURAL INTEGRITY - A preload diagram is constructed as shown in Figure 11 to determine the maximum operational load that will be applied to the nut. The maximum nut load is designated Point B in Figure 11. If this load is less than the maximum allowable nut load determined from the tensile test, the nut will not yield. The difference between the two loads is an indication of the safety factor built into the connector structure. A large difference may mean the connector is overdesigned and hence heavier than necessary.

If, however, the maximum operational load is found to be greater than the maximum allowable load, nut yielding will occur. The actual change in seal load as a result of nut yielding is difficult to predict. However, for a separable connector which must seal gases at low leakage rates, any yielding of the nut is an unacceptable situation.

CONCLUSIONS

In the procedure discussed, several approximations are made to formulate a reasonably simple method of estimating the performance of a connector. The usefulness of this procedure lies in the fact that the application of the procedure to several connectors will give not only quantitative values of important connector characteristics, but also increased understanding of the action of the connectors.

Although some experimental evaluation must still be conducted after the analysis has been completed, savings arise because of the possibility of eliminating some connectors from further evaluation and because the experimental work can be concentrated in the areas where failure is most likely to occur. For example, if the analysis shows that a connector may not withstand the estimated thermal gradient, the

qualification tests of the connector can be designed to extensively test the capability of the connector at the thermal-gradient condition.

As a logical extension of this type of procedure, the fitting manufacturers could supply test results of physical characteristics of their connectors such as deflection rates, maximum nut load, and seal-seating loads. A backlog of test data could also be accumulated so that a manufacturer could show how his connector could be modified to meet a set of system requirements.

REFERENCES

1. "Development of Mechanical Fittings - Phases I and II", RTD-TDR-63-1115, December, 1963, Contract No. AF 04(611)-8176.

2. J. W. Adam, "Elastic Displacements in the Design of Threaded Tube Connectors", presented at Conference on Design of Leak-Tight Separable Fluid Connectors, Marshall Space Flight Center, Huntsville, Alabama, March 24-25, 1964.

3. Contract No. AF 04(611)-8020.

4. Contract No. NAS 8-4012.

CYCLIC STRAIN INDUCED CREEP - A SEPARABLE CONNECTOR DESIGN PROBLEM

By

R. L. George
F. O. Rathbun, Jr.
L. F. Coffin, Jr.
Advanced Technology Laboratories
General Electric Company
Schenectady, N. Y.

ABSTRACT

Cyclic-strain-induced creep can occur in ductile metals (potential gasket materials) when exposed to cyclic stresses such as may result from thermal effects or vibration-induced forces in a connector. Sufficient stress relaxation may result, especially when compounded by acoustic vibrational effects, to allow leakage.

The resulting loss of sealing stress, particularly during the first several cycles of loading, justifies further consideration of this phenomenon in the design of separable connectors.

ONE OF THE BASIC PRINCIPLES of separable metal seal connector technology is that a sufficient stress must be imposed at the interface between mated seal components to plastically deform the weaker metal in order to insure leakage levels below 10^{-6} atm cc/sec while containing internal pressures of 2,000 psi or above. (1)* In some cases, where surface finish on the stronger metal in contact cannot be controlled or insured, the normally applied stress required may be as high as 2.75 times the yield strength of the weaker material. (1)

In order to insure the necessary intimacy of contact, various forms of contraint are used; the geometry of the components in the sealing area are often used to promote triaxial stress distributions while bringing the material into plastic flow. Knife edges, shear O-rings, thin gaskets, recesses, and many other shapes are used to provide these constraints on the soft material so as to promote the necessary contact stress. The friction existing between the metals in contact also serves to contrain the softer material. As in a compression test of a metal, as the specimen (gasket) becomes shorter, the friction forces on the loaded ends tends to retard plastic flow and to cause an increase in measured yield strength. This results in high contact pressure in the seal area of a separable connector, the magnitude of which is at least that of the flow stress of the weaker material, but can be much greater than this because of the constraints introduced by geometry and friction.

Another feature of separable connector technology is that, during the operational life of the connector, a large amount of the initial contact stress must be maintained on the interface between mated components to insure that leakage does not develop. The amount of stress which must be maintained is a function of design and surface finish. However, approximately 65% of the originally imposed stress must be maintained even for those seals most insensitive to stress removal. (1)

In the substructure of the connector, in both tension members and compression members, a light weight design will allow high stresses, quite close to the yield strength of the structural material. Under the imposition of assembly torque followed by internal pressure it is possible for the stress to diminish across the seal by plastic flow of material. This phenomenon can usually be restricted in its leak producing effect by proper design procedures.

Experience has shown, however, that separable fluid connectors do tend to develop leaks at various times during their operational life. Certainly, while not all well designed connectors develop leaks, many connectors require retorquing after initial leak checking. During severe environmental testing, leakage often develops.

The question arises whether some additional phenomenon can occur in the connector components which has not been considered in the design. Each connector structural and seal component has been designed using elastic stress analysis (or static plastic stress analysis at most) under the assumption of constant physical and mechanical properties such as Young's mod-

*Numbers in parentheses designate References at end of paper.

ulus, yield strength, and Poisson's ratio. At most, temperature dependency of these properties has been allowed. Are these assumptions and these design concepts always adequate? What phenomena occur which may have a deleterious effect on the connector performance?

Pure creep of metals at elevated temperatures can cause relaxation of sealing stresses. But, if the duration of time through which the connector must operate at elevated temperatures is known, seal relaxation during the time can be avoided by design considerations. (21) In many connector applications, contact pressure relaxation from pure creep is not a problem because of the short required life of the hardware.

Creep of metals, however, is not only induced by high temperature and the passage of time. Creep effects resulting from cyclic mechanical loading have been observed in many well controlled laboratory experiments. Two distinct phenomena have been noted, that of material flow by a lowered yield strength and that of flow by decreased friction, depending on time and number of cycles. The phenomenon does not require elevated temperature, but has been observed at room temperature and below. In recent years, a great deal of investigative effort has been expended in promoting understanding this phenomenon of cyclic-strain-induced creep. The goal of this paper is to review the literature describing this phenomenon, to view the phenomenon in the light of loadings which take place in a separable connector, and to assess the importance of cyclic-strain-induced creep in connector design.

REVIEW OF WORK IN CYCLIC-STRAIN-INDUCED CREEP

During the course of an experimental investigation on the effects of cyclic plastic strain on metals, Coffin (2) observed that when aluminum and copper were subjected to cyclic plastic strain they exhibited a lack of stability. The dial gage anvils used to measure diameter changes in a specimen undergoing cyclic plastic tension tests produced measurable indentations. These indentations were not pronounced in 347 stainless steel, nickel, titanium, SAE 1018 steel, and aluminum alloys. This lack of resistance of the metal to small steady loads in the presence of cyclic plastic strain has been designated as cyclic-strain-induced creep. Although this effect can occur over a broad range of temperatures, our discussions will be limited to low temperatures where thermal or pure creep is a negligible factor.

Load and strain cycling (3), the two common methods of loading test specimens, are depicted in Figure 1 by showing the load-deflection curve for the first several cycles. In load cycling the load applied fluctuates between two fixed load limits. This method of testing closely simulates the loadings induced by mechanical vibration. The thermal expansion is equivalent to strain cycling where the specimen is exposed to a given displacement. The magnitude of the cyclic component in relation to a mean component is expressed by the ratio:

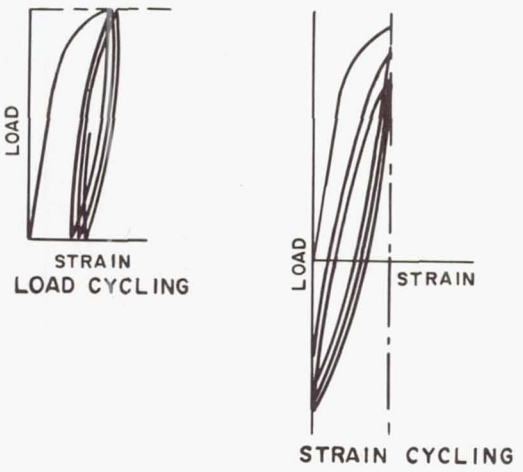

Fig. 1 - Methods of Loading in a Cyclic Test

$$R = \frac{\text{minimum stress or strain}}{\text{maximum stress or strain}}$$

Most of the data collected to date has been with R=-1, complete stress or strain reversal with no mean component, and R = 0 where the mean stress is 1/2 the maximum stress.

Benham (4) conducted a series of axial push-pull load and strain cycling tests on commercially pure copper with both R = 0 and R =-1. In load cycling he noticed the mean strain varied rapidly during the first several cycles and tended toward a steady rate which was maintained until near failure. The three regions of mean strain are analogous to those of the more familiar thermal creep curve of primary, secondary, and tertiary creep as shown in Benhams's data, Figure 2. These three regions are caused by the strain hardening of annealed metals or softening of hard metals. The primary region is a function of the strain hardening of the material while the secondary region exhibits a constant rate of creep dependent on the magnitude of the cyclic and mean stress components. Failure of the material begins in the tertiary region with the propagation of cracks. Benham also has shown that with R = 0, mean stress equal to 1/2 maximum stress, there was no significant dif-

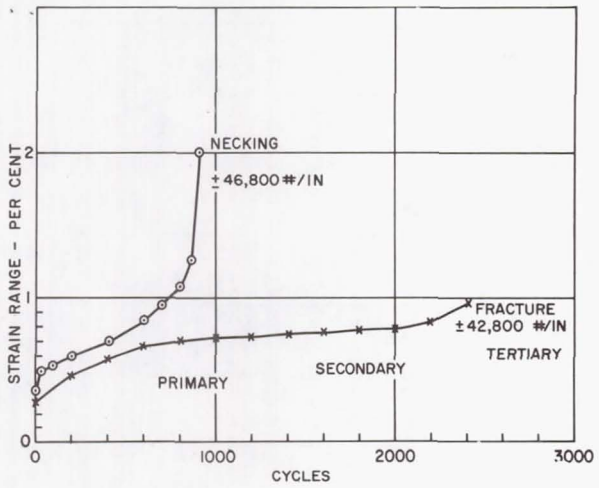

Fig. 2 - Variation in Strain Range with Cycles for Reversed-Load Cycling of Cold worked Copper, From Reference 4

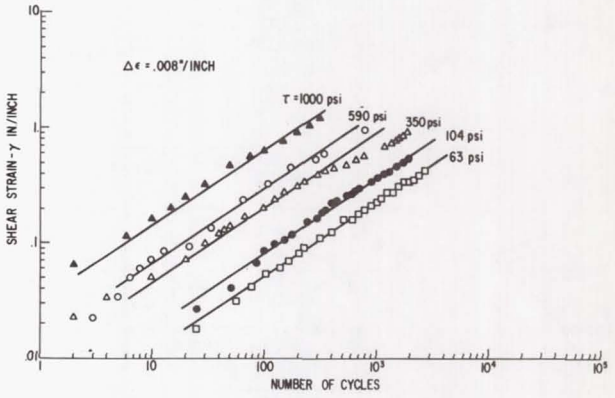

Fig. 4 - Torsional Strain Produced by Steady Torsion & Cyclic Longitudinal Strain-Annealed 1100 Aluminum, From Reference 12

ference in observed phenomena from that of creep only. This same phenomenon was also observed by Morrow and Halford (5) when subjecting lead to torsional reversals.

Feltner and Sinclair (6) investigated the effect of percent of tensile unloading in pure aluminum, copper, and cadmium. Tests were conducted by cycling between the same maximum tensile stress and different values of minimum stress. Therefore, as the percent of unloading decreased the mean stress increased. With a plastic maximum stress and 100% unloading, R= 0, the curves of strain as a function of cycles had the same characteristics as Benham's results. Highest creep rates were observed when the cyclic stress is large and the mean stress small. The effect of percent unloading on the minimum cyclic creep rate of copper at 25° C with a maximum plastic stress is shown from Feltner and Sinclair's data in Figure 3. This curve is representative of results obtained for cadmium and aluminum.

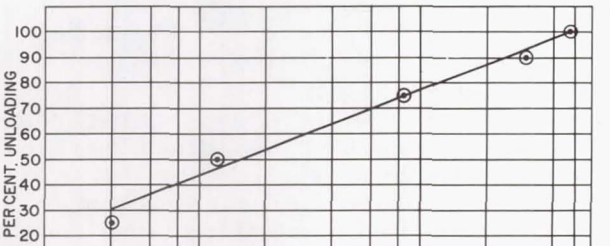

Fig. 3 - Effect of Per Cent Unloading on the Minimum Cycle Creep Rate of Copper at 25°C, From Reference 6

The phenomenon of cyclic-strain-induced creep also occurs when the cyclic loading is normal to a steady applied load. Coffin (2, 7) observed an angular deformation produced by a small torque applied to a tensile specimen undergoing axial plastic strain cycling. The biaxial loading used to study cyclic-strain-induced creep is also expected to be similar to that which exists in a connector sealing material when exposed to a thermal or vibrating environment. Coffin's results are shown in Figure 4 for 2S aluminum undergoing a diametral strain of ± 0.4%. Even for a small torsional loading of 104 psi, a shear strain of 0.07 in/in was noted after 100 cycles while a stress of 593 psi resulted in a shear strain of 0.07 in/in after only 10 cycles.

Benham (8) subjected mild steel in the normalized and cold worked condition to torsional cyclic plastic strain combined with a steady axial force. Curves showing the relationship between accumulated axial tensile strain and the cycles during a test are shown in Figure 5. The steady axial tension for all tests was 19,400 psi while the torsional strain ranged for ± 0.008 to ± 0.043 in/in. Higher torsional strains resulted in a higher strain rate for a given cycle while the cyclic strain rate for all cases decreased as the test proceeded, owing to early strain hardening. Similar curves were obtained in bending tests varying from ± 0.03 to 1.5% strain with a constant axial force. The greater the axial load

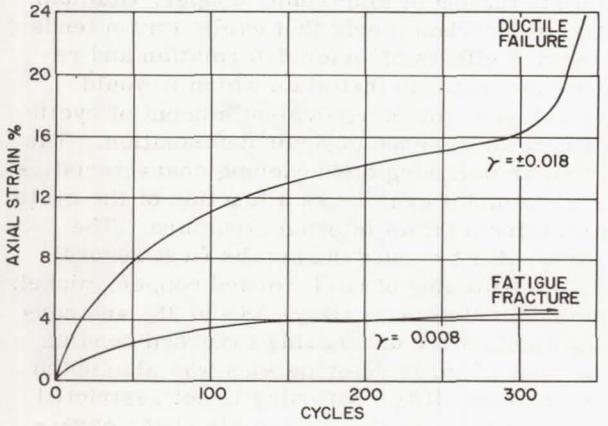

Fig. 5 - Axial Creep During Torsional Strain Cycling for Normalized Material, From Reference 8

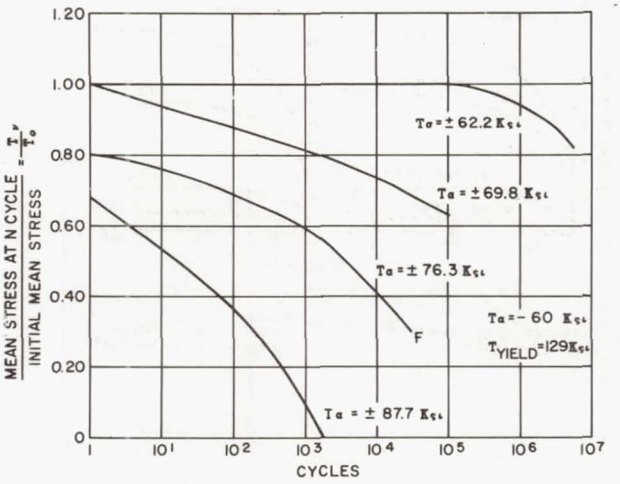

Fig. 6 - Relaxation of Mean Stress due to Tensile Cyclic Loading - SAE 4340, From Reference 11

applied, the shorter was the life. In both types of loading, if the cyclic strains remained in the elastic range, fatigue failures occurred, while if the cyclic strain was in the plastic range, ductile failures resulted.

Moyar and Sinclair (9) obtained the same characteristic curves using OFHC copper. In the investigations of Coffin, Benham, and Moyar the material was subjected to steady loads well below the yield stress. In an investigation of annealed 1100 Aluminum, Coffin (12) reported shifting of hysteresis loops produced by cyclic and mean uniaxial stresses. In summarizing his results, he finds that the cyclic-strain-induced creeps which results is a function of both the mean stress and the plastic modulus of the hysteresis loops (stress range divided by plastic strain range). He also observed that for a particular combination of cyclic and mean stresses, mostof the deformation occurred on the first cycle.

Maria Ronay (10) has recently concluded from a mathematical study that torsionally applied cyclic plastic strain will produce an axial elongation of the specimen with no axially applied force. The axial extension is considered not as a genuine creep phenomenon but a phenomenon of second order incremental plasticity. Any applied axial force amplified the second order strain accumulation. Whatever the mechanism causing these gross deformations, if the phenomenon is present in connectors used in space vehicles and boosters, the magnitude of these deformations can be expected to cause stress relaxation at the sealing interface.

REVIEW OF WORK ON RELAXATION FROM VIBRATIONS

Morrow and Sinclair (11) in an effort to obtain an empirical expression to describe the phenomenon of cycle-dependent relaxation conducted a series of experiments using SAE 4340 steel with mean stresses ranging from zero to 80% of the yield stress and a wide range of cyclic stress. Figure 6 is a representative sample of data where annealed 4340 steel initially carried a compressive stress of 60, 000 psi, 1/2 the yield strength. A specimen with a small cyclic stress, where the stress was always below the elastic limit, exhibited no significant change in the mean stress in the first million cycles. Only for cases in which the amplitude of stresses were in the plastic range did a sufficient deformation occur and stress relaxation result.

Langenecker (13) has observed that acoustic energy can produce failures in materials while lightly loaded. Sound energy as radiated to all parts of a booster is absorbed by lattice imperfections whereas thermal energy is absorbed homogeneously in the material crystals. Therefore, it is agrued less acoustic energy is required to produce a significant reduction of the yield stress of the material. Figure 7 shows a comparison of the effect of ultrasonic vibration and temperature on the stress-strain curve of aluminum. (14) An energy of 15 watts/cm^2 produces the same decrease in aluminum strength as a temperature of 200°C.

Ultrasonic vibration has been shown (14) to improve the common initial working operations such as drawing, extrusion and rolling, mainly on some materials with low yield strength and creep resistance (zinc, lead, aluminum). There is

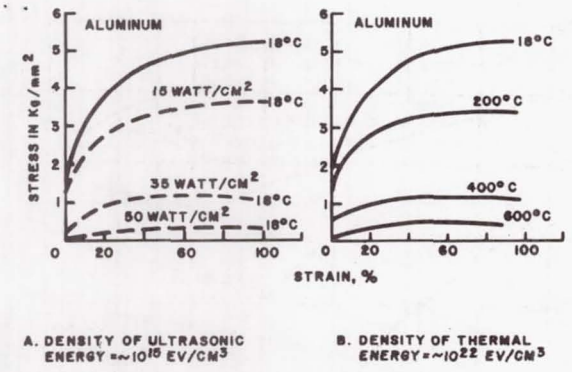

Fig. 7 - Effect of Ultrasonic Vibration and Temperature on the Stress-Strain Curve of Aluminum, From Reference 14

presently no agreement as to the cause of improved fabricability, but both lowering of the yield stress and a reduction of friction are suggested. A reduction of constraining forces from friction permits materials to flow more readily.

REVIEW OF WORK RELATED TO STRAIN SOFTENING AND HARDENING

When strain cycling aluminum, Coffin and Tavernelli (15) noticed that the stress range changed rapidly during the first several cycles tending toward a constant value shown in Figure 8 for 1100 Aluminum. Stress range of cold worked aluminum decreased, indicating softening while it increased for annealed aluminum indicative of hardening. Coffin (15) also observed

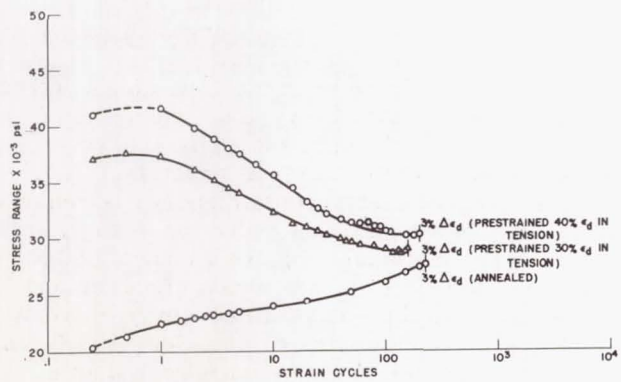

Fig. 8 - Stress Range vs Strain Cycles For Varying degrees of Cold Work: Material: 2S - Aluminum, From Reference 15

from his testing of aluminum, copper, titanium, nickel and carbon steels that cyclic strain tends to remove effects of prior deformation and restores the metal to that state which it would have achieved for an equivalent amount of cyclic strain in the absence of prior deformation. The particular softening or hardening characteristics that each metal exhibits is a function of the cyclic strain effects on its internal structure. The greatest effect occurs during the first several cycles. Softening of cold worked copper, nickel, aluminum, aluminum alloys 2S and 3S, and non-aging steels after undergoing reversed bending or torsion of large deformations was also noted by Polakowski (16). Softening is not restricted to low alloy materials. It has also been observed in 347 stainless steel. (17)

Wood (18) observed the same softening phenomenon when subjecting copper, nickel, and aluminum to alternating torsion tests with complete reversals into the plastic strain region. He postulated that the softening of preliminary cold working is the result of relaxation of internal stresses which would cause a stress relaxation at the surface of the material.

The results of investigations of Benham, Coffin and Wood confirm Polakowski's (19) observed creep of asdrawn copper, nickel, and titanium after cycling into the plastic region.

CYCLIC FORCES IMPOSED ON A CONNECTOR

Recognizing the phenomenon and its causes, we now ask ourselves whether such loadings can exist in a connector. The possible stress loadings to which a seal may be exposed from the time of its initial compression to the end of its operational life are:1) high clamping force to insure sealing (1), 2) fluctuations of the loading due to thermal expansion and contraction of the gasket and clamping structure due both to transients and possible differences in thermal expansion characteristics), 3) variations in load due to pressure excursions, and 4) vibration induced load fluctuations. These forces are shown in Figure 9 as applied to a rectangular cross-section gasket which is representative of any material placed between or embedded in the flanges to form a seal. Other configurations will experience similar stresses but usually of less analytically tractable nature. Superposition of ultrasonic vibrations from the booster may further reduce the strength of materials in the connector. (Also shown in Figure 9)

With a high clamping force the gasket material, constrained by friction between the flange and gasket, is stressed into the plastic range resulting in a complex distribution of stresses. (1) Thermal expansions and contractions are expect-

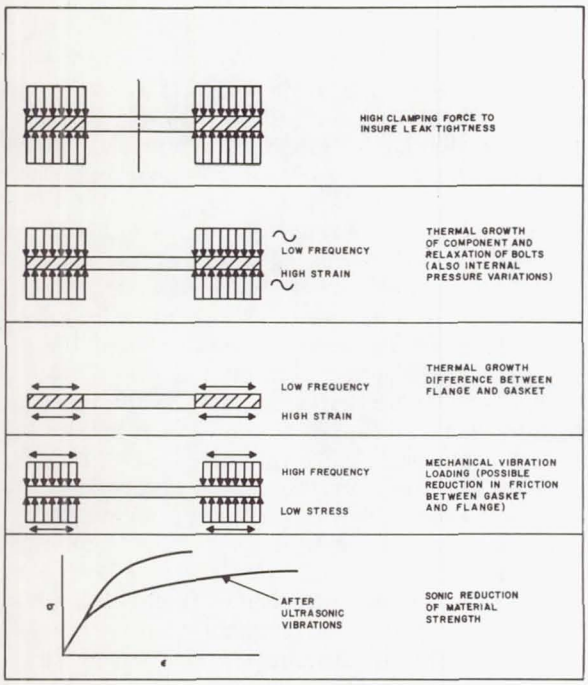

Fig. 9 - Loadings on Connector Gasket

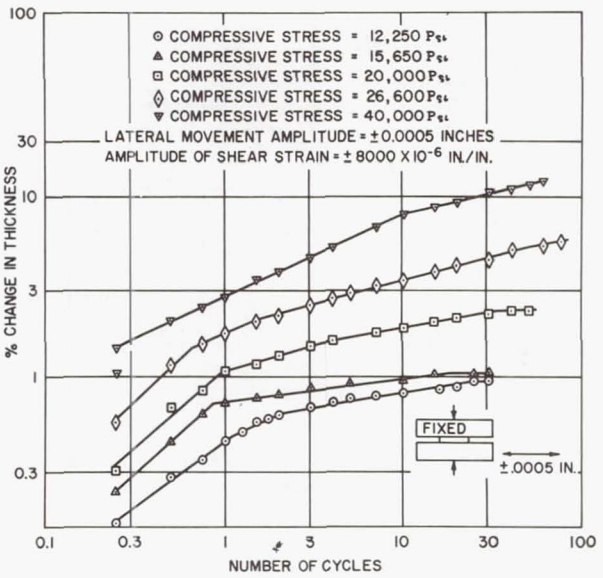

Fig. 10 - Variation in Thickness of Copper Strips under Constant Normal Stress and Cyclic Lateral Displacement, From Reference 20

ed to impose low frequency high strain variations both in the direction of the clamping force from thermal expansion of the fittings and normal to the clamping force due to differences in the possible thermal expansion characteristic of the flanges and/or gasket material. Pressure excursions also are generally expected to be of higher frequency but lower stress amplitude. Vibrations resulting from dynamic machinery induce fluctuating forces of high frequency and low magnitude. This vibration tends to reduce the frictional forces at the sealing interface between the flange and gasket. The relief of the constraint forces on the plastically stressed gasket permits plastic flow to commence. Mechanical vibration stresses induced in the gasket are multi-directional because of the random nature of the vibration forces.

RELATIONSHIP OF CYCLIC-STRAIN-INDUCED CREEP TO CONNECTOR DESIGN

The work of Coffin, Benham, and Moyar and Sinclair on cyclic-strain-induced creep was performed with cyclic plastic strains and small steadily applied loads well within the material elastic limit. In a connector, however, the steadily applied load is the clamping force which is above the yield strength of the seal material. The cyclic plastic strain may result from a difference in thermal expansion of aluminum and stainless steel flanges. For example, at a one inch radius the difference in relative displacement of two such flanges is 0.0006 inches for every 100°F change. A thin gasket will therefore be subjected to a plastic mean stress from the contact pressure and low frequency plastic shearing strain. Under Contract NAS 8-11523 (20) an investigation was conducted to discern whether cyclic-strain-induced creep occurred with a mean stress above the yield stress and to observe if the relative displacement was accommodated by slippage at the interface or deformation of the gasket material. Rectangular cross-section OFHC copper strips were subjected to a range of constant compressive stresses from 1.4 to 5 times the 0.2% offset yield stress combined with a cyclic plastic shear strain of ± 0.008 in/in. With the 1/16 inch thick copper strips, this strain corresponded to a flange relative motion of 0.0005 inches. No slippage of the copper strips on the steel anvils was noted in the reported tests. Results of these tests are shown in Figure 10, the details of which are described in the appendix. The three regions of strain rate deformation designated by Moyar and Sinclair (9) as 1) initial deformation occurring in the first cycle and analyzed using plasticity theory, 2) transient strain, and 3) steady state can be observed. After 1/4 cycle the deformation shown is that caused by initial compression

of the gasket. The greatest creep rate occurs during the first cycle ranging from 0. 5% per cycle for a compressive stress below three times the 0. 2% yield stress to 0. 08% per cycle for a compressive stress equal to five times yield stress. Thus, for a copper gasket initially stressed to twice the 0. 2% yield stress, the initial compression will be a 0. 24% change in thickness, and, after one cycle with a shear strain 0. 008 in./ in, ,the thickness would have decreased 0. 72% of original thickness or 0. 48% of the initial clamped thickness.

Materials subjected to cyclic plastic strain and a steady mean stress exhibit creep with the same characteristics as thermal creep. This phenomenon is most pronounced in low yield strength and low creep resistance materials such as pure copper and aluminum, both in the annealed and cold worked state. These mechanical properties are most desirable in a gasket material for insuring sealing at the lowest clamping forces and are also characteristic of materials most sensitive to cyclic-strain-induced creep. These same materials have also shown the greatest reduction in strength when exposed to ultrasonic vibrations.

A connector is also subjected to low amplitude high frequency cyclic loads from mechanical vibrations, pressure fluctuations, and thermal transients. Stress relaxation has been noted in steady elastic stressed components if the cyclic stress approaches the magnitude of the yield stress. The minimum creep rates occurring in the secondary region of the creep curves for pure copper and aluminum decrease with decreasing magnitude of cyclic stresses. (6) Of greater interest to the connector designer is the amount of flow deformation and number of elapsed cycles in the primary region of the creep curves for decreasing cyclic amplitude. Data of this nature aid in selection of connector configuration and material selection. Further investigations are required to obtain such data and to establish if the significant factor in stress relaxation is the reduction of material strength or if friction forces at sealing interfaces are decreasing, permitting plastic flow.

The existence of decrease in strength characteristics in a connector is detrimental in two respects. First, consider as before a flat gasket with a large clamping force producing plastic deformation. As a material is strained further into the plastic range, the force required to produce a unit of strain becomes less. A decrease in the material's strength will produce a larger change in deformation for loads in the plastic range. Therefore, ultrasonic vibration reduction of material strength will produce a stress relaxation at the seal surface due to plastic flow of the gasket. Secondly, the reduction of yield strength produces greater susceptibility of the thermal and vibrating strains to occur in the plastic range and cause cyclic-strain-induced creep.

SUMMARY

The forces exerted on a connector are 1) clamping force causing plastic deformation at the seal, 2) thermal growth causing low cycle large amplitude strains, 3) pressure excursions causing low or high cycle small strains and 4) vibrations causing high frequency low amplitude strain. Investigations have shown that if the cyclic component of strains caused by such loading enters the plastic region, cyclic-strain-induced creep will occur, causing a relaxation of clamping force and stress at the sealing interface. The same phenomenon has also been noticed in materials subjected to biaxial stress of cyclic plastic strain and a steady force ranging from zero to forces causing plastic deformation. Forces of this magnitude and method of application are possible from the thermal growth in the connector and thermal growth differentials between the gasket and flange.

In all of the investigations dealing with cyclic creep, the soft ductile metals exhibited the greatest deformation regardless of prior cold working. These metals are most extensively used for gasket materials.

A reduction of clamping stress at the sealing interface may also occur by the reduction of material strength due to absorption of sufficient acoustic energy. Such a reduction of material strength also increases the probability of the existence of cyclic-strain-induced creep since the cyclic strain component must enter the materials plastic region.

Because of the large deformations resulting from cyclic-strain-induced creep and the cyclic loads and strains expected in boosters, the effect of this phenomenon should be included in the design computations of a connector. Further investigation into cyclic-strain-induced creep for high plastic mean stresses and small cyclic stresses is required to determine the range of applicability of this phenomenon in the design of connectors.

APPENDIX - PROCEDURE AND APPARATUS TO INVESTIGATE CYCLIC CREEP IN A COPPER GASKET

To establish whether lateral translation of a gasket subjected to high normal forces will

cause gasket relaxation, a series of tests have been conducted using the test apparatus shown in Figures 11 and 12. Four copper strips, 1/16 x 1/8 x 1-1/2 inches long were loaded normally between three rigid anvils. To the center anvil is affixed a hydraulic press which allows it to move 0.0005 inch. Figure 11 shows the assembled test apparatus, the three anvils, and the hydraulic jack in the compression testing machine. Four 0.0001 inch dial indicators are used to measure the translation of the center anvil and the change in gap between the outer anvils. Figure 12 shows the test apparatus with the top anvil removed. The dark portion on the anvils is tool makers' bluing used to detect slippage of the copper strips on the anvils.

Five tests were conducted with compressive loads producing 12,250, 15,650, 20,000, 25,600, and 40,000 psi stresses in four copper strips. A new set of four copper strips 1/16 x 1/8 x 1-1/2 inch long with the load applied normal to the 1/8 x 1-1/2 inch face was used for each test. A lateral movement of 0.0005 inch from each side of a central equilibrium position was imparted to the center anvil by a hydraulic jack. The testing fixture was designed primarily to determine trends in change of the copper strip thickness, such as when do changes in thickness cease to exist. The parameters measured in each test were the change of gap between top and bottom anvil which is twice the change of thickness of a copper strip, the lateral movement of center anvil with respect to top and bottom anvil, the lateral force required to move the center anvil, the magnitude of the compressive load, and the initial and final thickness of each copper strip.

The lateral force applied to the center anvil was measured with a pressure gage in the hydraulic line of the jack. Pressure gages were calibrated using the compression machine as a load cell by inserting the ram between the bed and head of the machine, applying a load, and recording the pressure gage reading. A deviation of 100 pounds when 3500 pounds is applied was observed which corresponds to a 2.8% error. The reading error of one-half a deviation or 50 pounds must also be applied. At applied loads of 1500 pounds, the reading error corresponds to an error of 3.33%. The 1/16 dimension of the copper strips were measured at the center and both ends before and after the test with an electronic micrometer to determine if any high spots were present before testing and/or after testing.

The lateral force required in each of the tests is given in Table 1. Values given are the maximum and minimum loads required to displace the center anvil 0.0005 inch. Two trends were evident during the tests. First, as the number of cycles increased, the forces required to move the center anvil increased leveling off in the steady state region as measured within the accuracy of the test fixture. Secondly, a larger

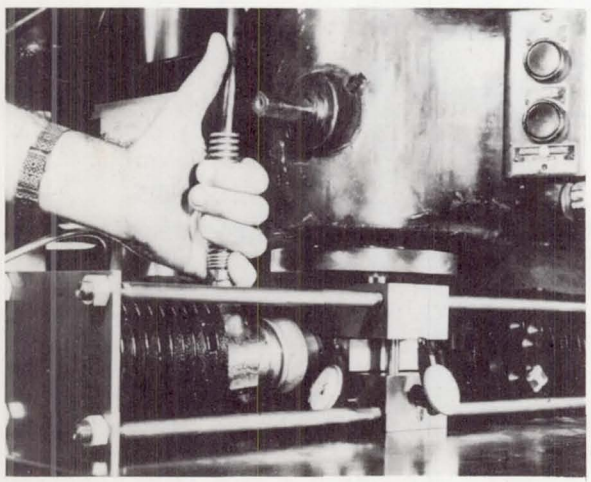

Fig. 11 - Gasket Compression - Translation Test Apparatus Showing Three Anvils, Compression Testing Machine, and Lateral Displacement Press

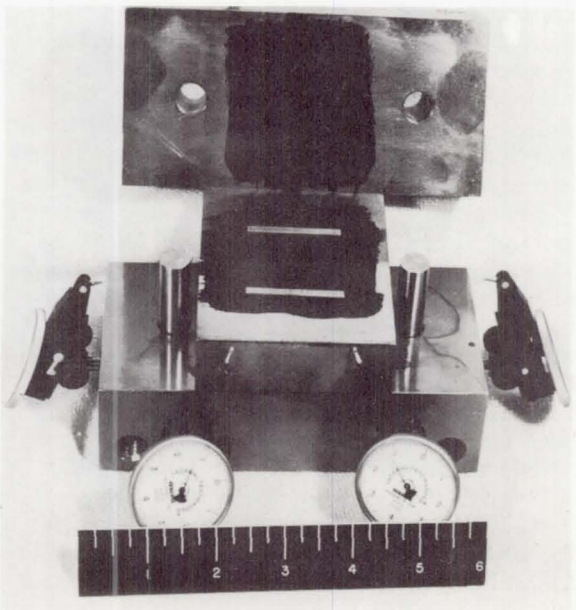

Fig. 12 - Components of Gasket Compression - Translation Test Apparatus: three anvils, dial gages, copper strips

Table 1 - Lateral Force Required to Impose a Shear Strain of 0.0008 in/in. in 4 Copper Strips

Normal Stress	Minimum - Maximum Load	
12,250	1100	1650
15,650	1300	1800
20,000	1725	2400
26,000	2100	3150
40,000	2700	5100

force was required to move the center anvil away from the center equilibrium position than to move the block toward the center equilibrium position. The difference was as much as 200 to 300 pounds.

REFERENCES

1. Rathbun, F.O. Jr., Ed. "Design Criteria for Zero Leakage Connectors for Launch Vehicles", Vol. 3, Sealing Action at the Seal Interface, G.E. TIS Report No. 63GL43, 1963.

2. Coffin, L.F. Jr., "The Stability of Metals Under Cyclic Plastic Strain", Trans. ASME J. Basic Eng. pp. 671-682, September, 1960.

3. Benham, P.P., "Fatigue of Metals Caused by a Relatively Few Cycles of High Load or Strain Amplitude", Metallurgical Reviews, V. 3, 203, (1958).

4. Benham, P.P., "Axial Load and Strain Cycling Fatigue of Copper at Low Endurance", J. Inst. Met., 89, 328 (1961).

5. Morrow, J.D. and Halford, G.R., "Creep Under Repeated Stress Reversals", Proc. International Conf. Creep, Inst. Mech. Eng. p. 43 (1963).

6. Feltner, C.E. and Sinclair, G.M., "Cyclic Stress Induced Creep of Close-Packed Metals", Proceedings of the International Conference on Creep, Inst. Mech. Eng., pp. 3-9 (1963).

7. Coffin, L.F. Jr. "Low Cycle Fatigue: A Review", App. Mat. Res., Vol. 1, No. 3, pp. 129-141, (1962).

8. Benham, P.P., "Some Observations of Cyclic-Strain-Induced Creep in Mild Steel and Room Temperatures", Int. J. Mech. Sci., V. 7, 81-86, (1965).

9. Moyar, G.J. and Sinclair, G.M., "Cyclic Strain Accumulation Under Complex Multiaxial Loading" Proceedings of the International Conference on Creep, Inst. Mech. Eng., pp. 2-47, (1963).

10. Ronay, M., "On Second Order Strain Accumulation in Torsion Fatigue", Columbia Univer. Tech., Report No. 16, February, 1965.

11. Morrow, J.D. and Sinclair, G.M., "Cycle-Dependent Stress Relaxation", Symposium on Basic Mechanisms of Fatigue, ASTM Special Technical Publication, No. 237, 1959.

12. Coffin, L.F., Jr., "The Influence of Mean Stress on the Mechanical Hysteresis Loop Shift of Aluminum 1100", Trans. ASME J. Basic Eng., Paper No. 63-WA-109 (1963).

13. Langenecker, B. "Effects of Sonic and Ultrasonic Radiation on Safety Factors of Rockets and Missiles", AAIA Journal, V. 1, No. 1, pp. 80-83, (1963).

14. Rosenfield, A.R., "The Application of Ultrasonic Energy in the Deformation of Metals", Defense Metals Information Center Report 187, August 16, 1963.

15. Coffin, L.F., Jr., and Tavernelli, J.F., "The Cyclic Straining and Fatigue of Metals", Trans. AIME, V. 215, 794-807 (1959).

16. Polakowski, H.N., "Restoration of Ductility of Cold-Worked Aluminum, Copper, and Low Carbon Steel by Mechanical Treatment", Proc. Am. Soc. for Testing Materials, V. 52, p. 1086, (1952).

17. Coffin, L.F. Jr., Jun, and Read, J.H., "A Study of the Strain Cycling and Fatigue Behavior of a Cold-Worked Metal".

18. Wood, W.A., "Softening of Cold-Worked Metal by Alternating Strain", J. Inst. Met., V. 86, p. 225, (1957-58).

19. Polakowski, N.H. and Palchoudhuri, A., "Softening of Certain Cold-Worked Metals Under Action of Fatigue Loads", Proc. Am. Soc. after Testing Materials, V. 54, p. 701 (1954).

20. Unpublished January 10, 1964, Progress Report on NASA Contract NAS 8-11523, Advanced Technology Laboratories, General Electric Company.

21. Cassidy, L. M. Rodabaugh, E. C. Roach, D. B., and Trainer, T. M., "Relaxation Design of Separable Tube Connectors", July 22, 1964, Battelle Memorial Institute Final Report to Advanced Technology Laboratories, General Electric Company, NASA Contract NASA 8-11523.

THE DEVELOPMENT OF A NEW CRYOGENIC GASKET FOR LIQUID OXYGEN SERVICE

By

James E. Curry
Materials Division
George C. Marshall Space Flight Center
National Aeronautics and Space Administration

and

William G. Scheck
Narmco Research & Development Division
Whittaker Corporation

ABSTRACT

A research and development program was conducted to develop a plastic gasket material compatible with liquid oxygen that would be superior to the gaskets presently being used for Saturn space vehicle applications. A laminated gasket composite of Teflon and glass was developed. This gasket composite was tested at 75°F, -320°F, and -423°F. The conclusion was that 500 psi of helium gas pressure could be contained by this gasket. The major advantage of this gasket composite is that it is flexible and requires no retorquing of the bolts due to cold flow as exhibited by various other materials.

THE USE OF CYROGENIC FLUIDS in today's rockets and missiles has resulted in the need for expanding knowledge of cryogenic engineering. One of the most acute problems encountered has been gasketing of the cryogenic fuel lines. One of the main problems associated with cryogenic gasketing is that materials become harder with decreasing temperatures. However, for a flanged joint to maintain a seal, the gasket must retain some flexibility or compressibility. The increasing moduli, caused by decreasing temperature, results in decreasing compressibilities. In addition, the shrinkage of most gasket materials, when going cryogenic, is greater than that of the bolt material, causing a dropoff in bolt load and consequently a decrease in flange pressure. This increases the possibilities of a leak developing.

Any seal developed primarily for cryogenic applications should be inherently compatible with liquid oxygen (LOX) so that applications within LOX systems do not require types of seals different from those used throughout the other portions of any cryogenic system. Under a research program conducted at Narmco (1)*, the dual requirements of cryogenic applications and LOX compatibility reduced the selection of plastic gasket materials to one: fluorocarbon polymers. The material that has been used most often in this program is the DuPont Company's Teflon. However, this material undergoes creep (deflection with time under a load), which is undesirable for a gasket. Attempts have been made to reduce this cold flow by adding powdered fillers to the resin.

Tests on a wide variety of filled Teflon, however, indicated conventional fillers do not reduce the cold flow to the ultimate degree required for Saturn space vehicle applications. Some cryogenic gasket suppliers add short, chopped filaments to the material. For the most part, these filaments tend to flow with the resin and only moderately restrict the creep; however, if longer, interconnected fibers were used, they would not flow with the resin. This system of reinforcement describes a glass fabric; consequently, a gasket design utilizing a fluorocarbon glass fabric laminate was conceived. The effectiveness of this design in reducing cold flow has been demonstrated by stress-relaxation tests. These tests, performed at ambient temperature, measured the reduction in compressive load with time for the solid fluorocarbon resin and for a glass reinforced laminate (see Fig. 1). These data indicate that the reinforced laminate exhibited less relaxation. In addition, the small amount of relaxation it did exhibit occurred within the first 20 minutes, while the solid resin specimen was still exhibiting relaxation when the test was terminated (after 2 hours).

*Numbers in parentheses designate References at end of paper.

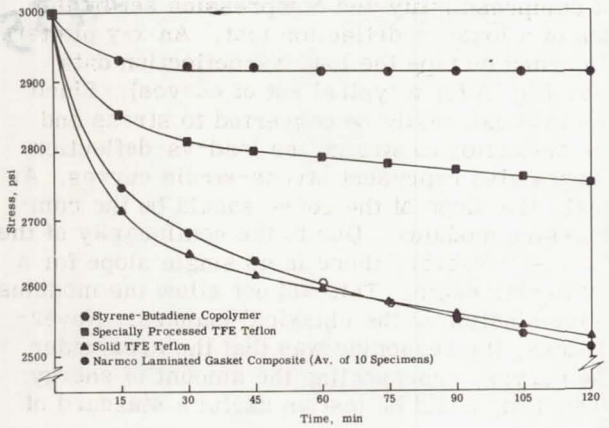

Fig. 1 - Stress relaxations at ambient temperatures

Two other materials are shown in Fig. 1: the special unfilled Teflon sample was obtained from a fabricator who processes the material under proprietary conditions intended to minimize cold flow, and the other product was an asbestos-reinforced styrene-butadiene rubber (SBR) which is now used for most Saturn liquid oxygen applications. These materials were also tested for cold-flow properties. The SBR-asbestos material is rendered safe for this use by an elaborate processing treatment which involves impregnation with a fluorocarbon oil. The specially processed Teflon indicated improved properties over the standard solid Teflon, but still showed a continuous decrease in load. The SBR-asbestos material showed the greatest decrease in load and had a steeper slope than any of the materials when the test was terminated after 2 hours. The results of these tests clearly show that the laminate construction is superior for the gasket application because it induces a lower amount of bolt-load dropoff than do the solid resins. The materials as shown in Fig. 1 were considered the most promising from previous work conducted (1).

PROCESSING TECHNOLOGY

There are two types of Teflon resins: polytetrafluoroethylene (TFE), and fluorinated ethylene-propylene copolymer (FEP). Besides the difference in appearance (TFE is opaque, while FEP is transparent), many of the properties of these materials are dissimilar. One of the most important criteria for gasket application is the modulus of elasticity, since good compressibility is quite desirable. (These are inversely related; i.e., the higher the modulus, the lower the compressibility.) The FEP resin possesses a higher modulus than TFE, making it less desirable from a compressibility standpoint. The compressive moduli of both greatly increases with decreasing temperatures.

Another important difference between TFE and FEP greatly affects the fabrication of laminates. The FEP is a true thermoplastic and melts. As FEP melts, it wets the glass fiber to form a relatively strong bond, whereas the TFE forms only a mechanical interlock. Previous work (2) showed that optimum lamination conditions with FEP have been experimentally determined to be 525°F and 100 psi, for 15 minutes. The TFE, however, does not melt: at 621°F, it undergoes transition into a gel state, but will never melt regardless of temperature or pressure. Therefore, the lamination technique that has been developed involves a relatively high lamination pressure, which serves to push the fibrous layers into the soft resin. The optimum lamination values for TFE have been found to be 800°F and 500 psi for 30 minutes. The mechanical bond thus obtained is quite strong, although not as good as that obtainable with the FEP laminates. Besides the superior compressibility characteristics of TFE resin, TFE glass laminates are also more compressible than the FEP laminates because the former does not completely wet the glass fabric under these optimum lamination conditions. Therefore, more of the mechanical compressibility of the glass fabric is retained. One of the major advantages of the glass reinforced laminate design is that the mechanical compressibility of the glass fabric is relatively unaffected by temperature; consequently, these laminates have performed very well at the cryogenic condition.

At the conclusion of the first 2 years of work conducted (2), the materials chosen for further process refinement and testing were as follows:

1. 401 Crowfoot Glass Cloth (reinforcement)
2. 0.005-in. TFE (lamination)
3. 0.005-in. FEP (encapsulation)

A typical cross section of a normal 1/8-in. thick gasket contains five layers of TFE sheet and six layers of glass cloth alternately laid up with the outside layers being glass cloth (see Fig. 2).

When a gasket is cut from a glass reinforced TFE laminate, the inner and outer circumference surfaces have exposed glass fibers. Since the resin has not melted, it has not completely wet the glass. This would allow the contained gas or liquid to soak through the gasket radially. To prevent this type of leakage, encapsulation of the inner gasket edge was desired. The ease

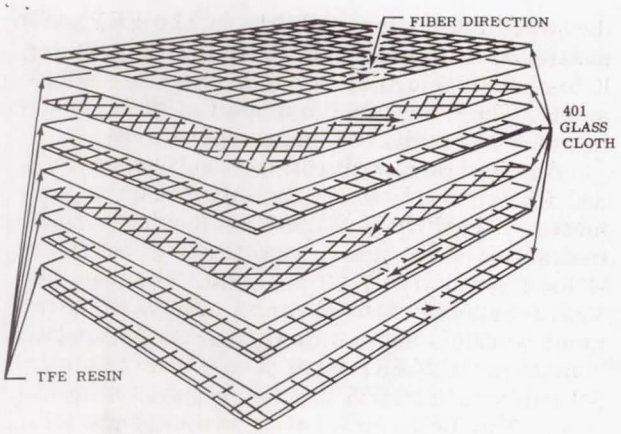

Fig. 2 - Laminate layup

of fabrication of FEP indicated that is was the preferable material for encapsulation. Moisture and contamination still had access to the gasket, however, through the outside gasket edge. Tests confirmed the hypothesis that moisture would reduce the compressibility at cryogenic conditions. Therefore, encapsulation of both inner and outer edges was adopted.

TEST RESULTS

The developed gasket composite was extensively evaluated and compared to the specially processed SBR-asbestos material on the basis of compressibility and compression set by the use of a load-vs-deflection test. An x-y plotter recorded on tape the load-vs-deflection data (see Fig. 3 for a typical set of curves). Since the load can easily be converted to stress and the deflection to strain, the load-vs-deflection curves also represent stress-strain curves. As such, the slope of the curve should be the compressive modulus. Due to the nonlinearity of the curves, however, there is no single slope for a particular cycle. This did not allow the modulus determination in the classical manner. Nevertheless, the reasoning was that the area under the curves, representing the amount of energy absorbed, could be just as useful a standard of comparison.

Therefore, these areas were measured and energy absorption figures calculated for the first, second, and tenth cycles to determine the effects of short- and long-time cycling. Candidate materials showing higher energy absorption values with minimum decrease with cycling were judged superior in compressibility.

Load-vs-deflection tests were conducted at room temperature, -320°F, and -423°F to provide data that could be utilized in the development of a reliable material and fabricating process. Small (2 sq in.) gaskets were fabricated from the SBR-asbestos reinforced material supplied by the Contracting Agency. Laminates were fabricated with TFE resins from two different suppliers by applying 500-psi pressure at 800°F. Each one of the gaskets, regardless of the origin of the resin, was encapsulated with

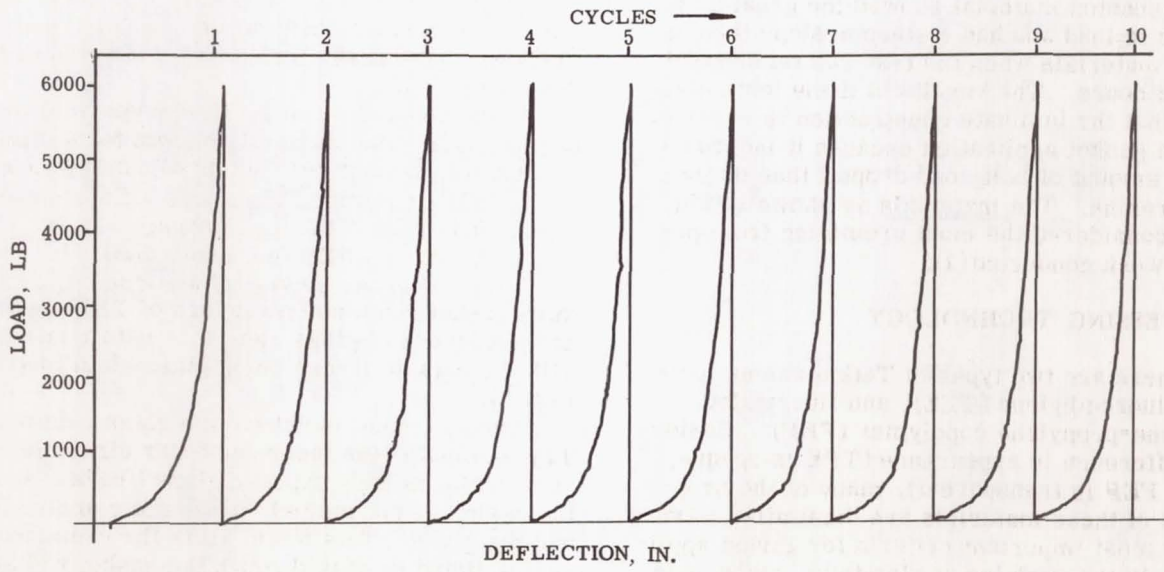

Fig. 3 - Typical set of energy absorption curves

DuPont's FEP resin at 525°F and 100-psi pressure applied.

Two gaskets from each laminate of each material were tested at room temperature and at -320°F; a fifth gasket from the TFE laminate was tested at -423°F. The data obtained have been reproduced in the form of frequency charts (see Figs. 4 through 6). These charts show the distribution or spread of the test data obtained for each material at each test temperature. The average values obtained for each group of data are given in Table 1.

The average values obtained for the energy absorption at 75°F and -320°F of both suppliers' TFE resins suggest that these two materials are very similar; however, when the distribution of data for both materials is considered, DuPont's TFE resin appears to indicate a higher degree of consistency. This is illustrated by Figs. 5 and 6, which show that the gasket made from the other resin had a spread from -40% to +30% on the tenth energy absorption cycle at room temperature, compared to ±30% on the tenth energy absorption cycle compared to -30% to +40% for Allied Chemical's G-80 material (polytetrafluoroethylene). On this basis, DuPont's TFE material was selected for further evaluation at 75°F, -320°F, and -423°F.

The fluorocarbon oil impregnated SBR-asbestos material now used for most Saturn liquid oxygen applications was tested only at 75°F and -320°F. Therefore, comparisons between this product and TFE materials could be made

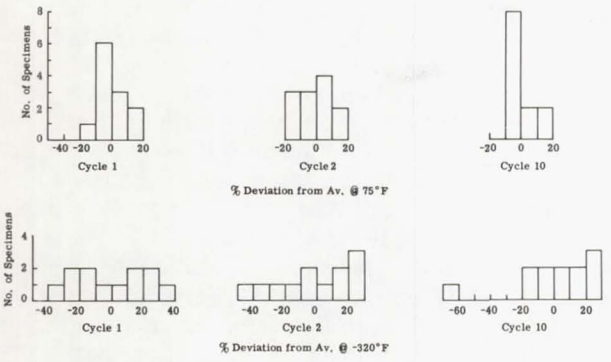

Fig. 4 - Frequency distribution of energy absorption data obtained for styrene-butadiene copolymer material tested at 75°F and -320°F

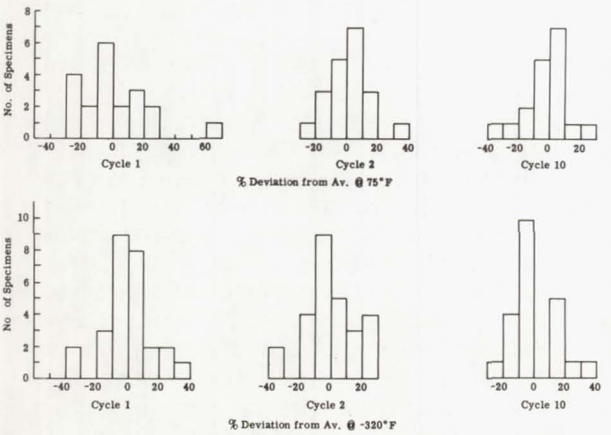

Fig. 5 - Frequency distribution of energy absorption data obtained Narmco laminated gasket composite using Halon's G-80 TFE material tested at 75°F and -320°F

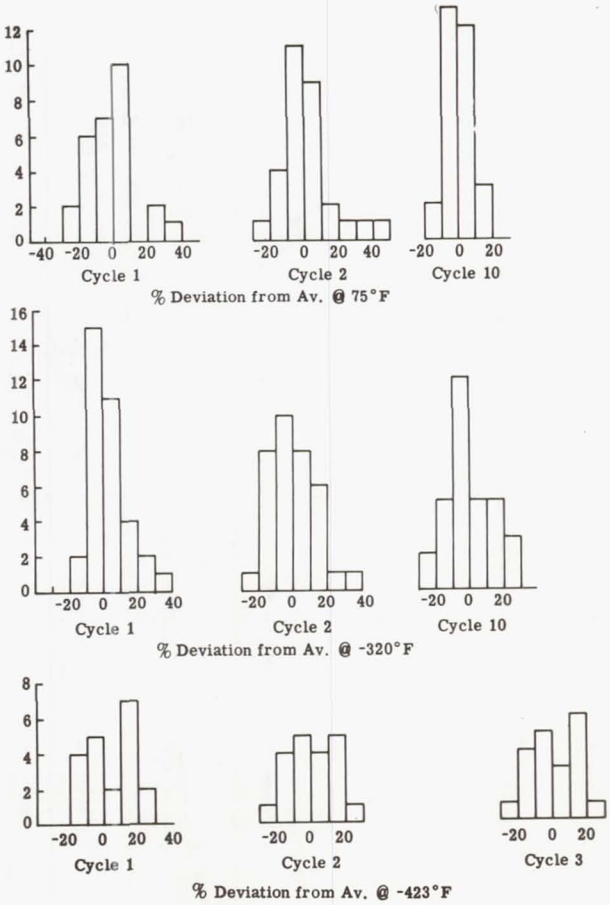

Fig 6 - Frequency distribution of energy absorption data obtained for Narmco developed gasket composite with DuPont TFE material tested at 75°F, -320°F, and -423°F

Table 1 - Average Values of Energy Absorption for Energy Absorption for Laminated Gasket Composite using Halon G-80 Resin, Teflon TFE and Resin, and Styrene-Butadiene Rubber/Asbestos Reinforced Gaskets

Type of Material	Test Temp, °F	Cycle No.	Av. Value, X
Narmco laminated gasket composite with Halon G-80 resin	75	1	84.6
		2	51.4
		10	38.5
	-320	1	30.0
		2	29.5
		10	36.1
Narmco laminated gasket composite with DuPont TFE resin	75	1	89.4
		2	53.9
		10	36.1
	-320	1	33.7
		2	31.9
		10	30.1
	-423	1	32.5
		2	30.9
		10	26.9
SBR-asbestos, reinforced	75	1	87.2
		2	58.8
		10	48.6
	-320	1	9.9
		2	9.8
		10	11.4

only at these temperatures. At room temperature, the spread of data obtained for the existing product was slightly less than that for TFE laminates. At -320°F, however, the TFE laminate was considerably more consistent in energy absorption properties than the SBR-asbestos reinforced material, as shown in Figs. 4 and 6. The average values given in Table 1 indicates that the SBR-asbestos reinforced material has a slightly higher value at room temperature, but a 300% lower value at -320°F than the TFE material. This would indicate that SBR-asbestos reinforced material had become very hard and brittle when tested at -320°F. On the basis of the data obtained, the TFE Teflon laminated gasket appears considerably superior to the SBR-asbestos material for use in cryogenic gaskets.

The TFE gasket was tested at 75°F, -320°F, and -423°F for its energy absorption properties. As shown in Table 1, the energy absorption of the TFE gasket at -320°F and -423°F is nearly the same. In fact, when the frequency distribution given in Fig. 6 is examined, the energy absorption at -423°F is slightly more consistent than the energy absorption values obtained at -320°F. The data obtained during the course of the referenced program indicate that the TFE gasket meets the requirements of the secondary program objective; i.e., that the compression-vs-deflection properties of separate TFE laminates be reproducible within the batch-to-batch percent deviation of the compressive properties of the product now used.

One of the major requirements of any gasket is that it be leakproof. Completely leakproof connections are not always required, however. A pipeline transmitting a heavy oil and a line containing helium have vastly different sealing requirements. Therefore, the material to be contained must be specified before leakage requirements have any significance. While some experimental work has been done with mass spectrometer measurements and helium gas (3), the testing performed in this program dealt only with gross leakage. However, testing with gaseous helium at the cryogenic condition was considered more severe than actual application (containment of the cryogenic liquid). Leakage tests were performed at both ambient and cryogenic conditions.

The flange pressure loading on a gasket can be obtained in the following manner: the torque applied to the bolts can be used to find the load in the bolts by the rather involved equations given in most textbooks (e.g., Reference 4) or handbooks (Reference 5), or by using the approximate formula that torque is equal to two-tenths of the product of the bolt diameter and bolt load (6). The total bolt load divided by the gasket flange area yields an apparent flange pressure. If all threads were frictionless or ideally lubricated this would be the actual flange pressure. In practice a favorable amount of torque is lost in friction and the apparent flange pressure value is higher than the actual value. There are ways of estimating the actual flange pressure from the value calculated from bolt torques.

The thickness of a gasket must be enough to allow plastic flow of the outer surfaces into the irregularities of the flanges. (Normal stress without plastic flow alone is not sufficient to effect a seal.) The thickness must also be enough to retain the seal after the relative displacement of the flange faces caused by different thermal contractions of the joint elements during large temperature changes. On the other hand, the gasket should be as thin as possible to reduce the bolting (8, 9). For this particular program, the gasket thickness was specified (1/16 in.) and therefore could not be considered a variable.

The leak-sealing ability of the Narmco-developed gasket composite was measured initially at 75°F, -320°F, and -423°F by inserting

a small 2-sq in. test specimen between flanges and increasing the load to 2000 psi. The gasket was then internally pressurized to 600 psi with gaseous helium and the pressure source disconnected and, if any leak developed after 5 minutes, it was measured and recorded. The leak-sealing ability of the gaskets was measured at cryogenic temperatures in the same fashion, except that after loading the gasket to 2000 psi at room temperature, the gasket and fixture were cooled to -320°F with liquid nitrogen or -423°F with liquid hydrogen. In each of these tests, a drop of 2 psi in internal pressure was considered to be a leak. Because the pressurized volume of the entire test assembly was only 0.4 cu in., the actual gaseous leakage was quite small.

The test results, as listed in Table 2, show that 16 of the 18 gaskets tested retained 600-psi internal pressure. The other two gaskets retained internal pressures of 552 and 596 psi respectively. At -320°F, 10 out of 18 gaskets retained the maximum internal pressure of 600 psi and the remaining 8 gaskets all held pressures in excess of 500 psi. At -423°F, 6 gaskets retained the maximum internal pressure of 600 psi, and the remaining 12 gaskets all held helium gas pressures in excess of 450 psi.

Table 2 – Test Results for 2-Sq In. Narmco Laminates Gasket Composite Tested without Bolts

Specimen No.	RT Flange Pressure, psi	-320°F Flange Pressure, psi	-423°F Flange Pressure, psi	Max.* Internal Pressure @ 75°F, psi	Max.* Internal He Pressure @ -320°F, psi	Max.* Internal He Pressure @ -423°F, psi
1	2000	2000	2000	600	600	515
2				600	600	528
3				600	600	580
4				552	589	560
5				596	576	578
6				600	562	480
7					600	600
8					600	600
9					600	600
10					600	595
11					582	472
12					600	600
13					600	600
14					600	600
15					523	465
16					544	460
17					600	584
18					521	485

* Pressure held for 5 min after reaching steady state at test temp.

Leak tests were conducted with helium gas at room temperature and -320°F at internal pressures as high as 500 psi on 4- and 8-in. diameter gaskets in order to determine experimentally the required flange pressures. These gaskets were first tested at room temperature and -320°F in unbolted flanges. A constant external load was applied to flanges at room temperature by a Universal testing machine and then the load was allowed to fall off as the temperature was decreased to -320°F. Experimental

Table 3 – Narmco Laminates Gasket of 4-In. Inside Diameter Tested without Bolts

Specimen No.	RT Flange Pressure, psi	-320°F Flange Pressure, psi	Max.* Internal He Pressure @ 75°F, psi	Max.* Internal He Pressure @ -320°F, psi
1	1787	858	200	295
2		875		325
3		920		148
4		900		245
5		920		270
6		875		350
7		903		270
8		894		345
9		1778		395
10		1778		423
11		1769		470
12		1769		300

* Pressure held for 5 min after reaching steady state at test temp.

Table 4 – Namrco Laminated Gaskets of 8-In. Diameter Tested without Bolts

Specimen No.	RT Flange Pressure, psi	-320°F Flange Pressure, psi	Max.* Internal He Pressure @ 75°F, psi	Max.* Internal He Pressure @ -320°F, psi
1	970	970	200	150
2				155
3				170
4				195
5				195
6				150
7				165
8				130
9				130
10				150

* Pressure held for a period of 5 min after reaching steady state at test temp.

results obtained for the three different sizes of gaskets are listed in Tables 3 and 4.

The 4-in. diameter gaskets were tested to an internal pressure of 200 psi at room temperature with an indicated flange load of 1787 psi. All 12 of the gaskets tested retained the 200-psi helium gas pressure for 5 minutes. The test fixture was cooled to -320°F, where the apparent flange load decreased to 858 to 920 psi due to the thermal contraction of the metal flanges. The test results obtained (see Table 3) show that seven of the eight gaskets tested maintained an internal pressure in excess of the 200-psi goal specified.

When the flange load was increased to approximately 1775 psi, the minimum internal pressure held for 5 minutes at -320°F was increased to 300 psi. The test results indicated that a flange load of approximately 2000 psi at -320°F would be required to contain an internal pressure of 500 psi at -320°F.

The testing of the 8-in. diameter gasket was limited by the capacity of the testing machine. Therefore, a room temperature flange load of only 970 psi could be applied and the internal pressure retained was the maximum pressure (200 psi). At -320°F, the retained internal pressure varied from 130 to 195 psi. The somewhat lower values of the internal pressure at -320°F were due to the low initial flange load. The tests conducted on the 8-in. diameter gaskets substantiated the idea that the newly developed gaskets would hold helium gas pressure at -320°F with an initial flange load applied at room temperature.

Since knowing the torque on the bolts at cryogenic temperatures as well as the indicated flange pressure on the gasket is of great importance, a testing procedure was conceived using strain gage bolts. Test fixtures were designed and measuring instrumentation was fabricated. Pairs of flanges for each of the three sizes were fabricated. A cryostat capable of holding the largest test flanges was built. Fig. 7 depicts the experimental setup.

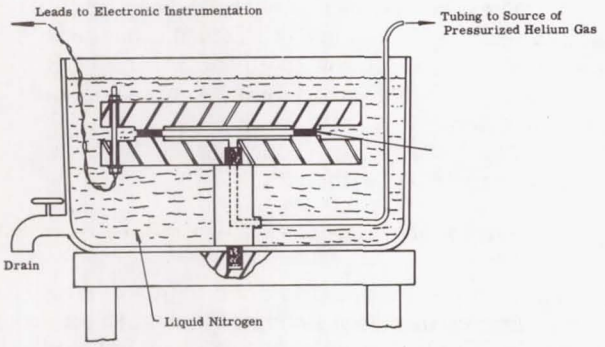

Fig. 7 - Experimental setup for large diameter gaskets

The readout from the strain gages was used to determine the load in the cap screw. These cap screws, checked for repeatability at both room temperature and liquid nitrogen temperatures, proved to be quite reliable. They were also used to evaluate the accuracy of a torque wrench. The individual operator techniques were determined to be extremely critical. However, the same operator could attain acceptable accuracy and repeatability. The decision, then, was that all of the large number of bolts required (24 for the largest gasket size) did not have to be the expensive load-indicating type but rather that 8 of these, distributed among conventional bolts, would suffice. The technique employed in the bolting-down operation involved securing the load-indicating bolts until the bolt load desired was obtained. The torque value associated with this load was then noted, these torques averaged from all of the load-indicating bolts, and then this average torque applied to the other (non-indicating) bolts. This operation was performed in stages (i.e., a desired bolt load could not be arrived at directly but was approached in increments) and slight retorquing was required, as a change in the loading in any bolt changed the loading somewhat in all bolts.

The test procedure for the 4-, 8-, and 12-in. diameter gaskets was as follows:

1. The fixture itself was leak-tested. This was accomplished by inserting a plug in the bottom flange at the gas inlet location and then pressurizing the system. The pressure was shut off at 500 psi. Maintaining this pressure for a length of time indicated that the system was leakproof.

2. The plug was removed and a gasket installed. The top flange was put in place. Cap screws, nuts, and washers were then assembled in place, and the torque wrench used to obtain the desired bolt loading. The helium gas was then again introduced to check the room temperature leak-sealing ability. The specimen must contain 500 psi for the test to proceed. The gas was then relieved.

3. Liquid nitrogen was added to the cryostat until the entire test fixture became submerged.

4. The helium gas was then increased to 500 psi. After pressure was obtained, the system was sealed off. Any dropoff in pressure (detected by a pressure gage) indicated a leak. The pressure was then relieved and the "leak point" again approached, only in smaller increments. In this manner, the maximum pressure contained at a bolt load level was determined within 2 psi.

The 4- and 8-in. diameter gaskets were leak-tested at room temperature and -320°F utilizing a predetermined room temperature flange load. The 4-in. gaskets were tested with seal flanges which were bolted together with 10 bolts. Six of the bolts were calibrated, at both 75°F and -320°F, so that the apparent flange load could be determined at both testing temperatures. A room temperature flange load of approximately 3000 psi was applied and a helium gas leak check was conducted at internal pressures of 500 psi for 5 minutes. None of the gaskets leaked at room temperature (see Table 5). The entire test fixture was cooled to -320°F by immersion in liquid nitrogen, where the flange load decreased to approximately 2100 psi because of

Table 5 – Narmco Laminated Gaskets of 4-In. Inside Diameter Tested with Bolts

Specimen No.	RT Flange Pressure, psi	-320°F Flange Pressure, psi	Max.* Internal He Pressure @ 75°F, psi	Max.* Internal He Pressure @ -320°F, psi
13	2950	2150	500	500
14		2140		500
15		2290		500
16		2150		493
17		2190		500
18		2240		500
19		2150		500
20	2980	2170		487
21	2980	1930		447
22	2930	2240		495

* Pressure held for a period of 5 min after reaching steady state at test temp.

the contraction of the steel flanges. Eight of the ten gaskets tested retained 495-500 psi internal helium pressure for 5 minutes at -320°F.

The same procedure was used when the 8-in. gaskets were tested, with the exception that the steel flanges in this case were drawn together with 18 bolts. A room temperature flange load of approximately 3000 psi was applied, which decreased to approximately 2100 psi at -320°F due to the contraction of the steel flanges. None of the 10 gaskets tested leaked at room temperature at an internal pressure of 500 psi, and 9 out of 10 retained approximately the same 500-psi internal pressure at -320°F (see Table 6). The tenth gasket retained 461 psi for 5 minutes at -320°F. The 12-in. gaskets were tested in the same manner, with the exception that the steel flanges in this case were drawn together with 24 bolts. A room temperature flange load of approximately 3000 to 4000 psi was applied which decreased to approximately 2500 psi at -320°F due to the contraction of the steel flanges. None of the five gaskets tested leaked at room temperature and the internal helium gas pressure held at -320°F varied as the flange load varied (see Table 7). The higher the initial room temperature flange load, the higher the internal helium gas pressure held at -320°F.

Table 6 – Narmco Laminated Gaskets of 8-In. Diameter Tested with Bolts

Specimen No.	RT Flange Pressure, psi	-320°F Flange Pressure, psi	Max.* Internal He Pressure @ 75°F, psi	Max.* Internal He Pressure @ -320°F, psi
11	2939	2210	500	500
12	2882	2130		500
13	2900	2009		500
14	2987	2009		500
15	2996	2200		461
16	2996	2183		500
17	3004	2096		500
18	3022	2074		495
19	3035	3114		500
20	2995	2105		496

* Pressure held for a period of 5 min after reaching steady state at test temp.

Test results from previous work conducted (2) where treated SBR-asbestos gaskets were tested in the same test fixtures under the same testing procedure are shown in Tables 8 through 10. Two important points should be noted: The gasket flange pressure obtained at -320°F was obtained by retorquing the bolts at this temperature, and the internal pressure held was held for only 30 seconds. In addition, the recommendation now in effect for a torquing sequence of bolts when utilizing the styrene-butadiene copolymer gasket was not used when these tests were conducted.

The superiority of the Narmco-developed gasket composite over the gasket product now used appears quite significant. Some conclusions that can be drawn from the tests results include:

1. No retorquing of the optimum Narmco-developed gasket composite design is required.
2. The internal gas pressures held by this same gasket were normally twice the pressures held by the material now used for Saturn LOX service under identical torquing sequences and test conditions.
3. The Narmco-developed gasket is completely compatible with LOX.

ANALYTICAL STUDIES

Various gasket designs have evolved over time. For example, a group referred to as pressure energized seals has been developed. These seals have cross sections that allow an increase in internal pressure to increase the flange pressure, thereby improving the seal. Constrained gaskets (where the gasket is confined in a groove in one of the flanges) have been

Table 7 – Narmco Laminated Gaskets of 12-In. Inside Diameter Tested with Bolts

Specimen No.	RT Flange Pressure, psi	-320°F Flange Pressure, psi	Max.* Internal He Pressure @ 75°F, psi	Max.* Internal He Pressure @ -320°F psi
1	2990	2470	500	345
2	2990	2310	500	235
3	3200	2430	500	270
4	4000	2860	500	498
5	4000	2790	500	495

* Pressure held for a period of 5 min after reaching steady state at test temp.

Table 8 – Styrene-Butadiene Rubber Gaskets Reinforced with Asbestos Fiber of 4-in. Inside Diameter Tested with Bolts*

Specimen No.	Specimen Thickness, in.	Gasket** Flange Pressure @ -320°F, psi	Torque** @ -320°F in. -lb	Contained Pressure @ -320°F, psi
4-11	0.060	500	80	85
		1000	145	100
		1500	185	200
4-12		500	45	60
		1000	90	100
		1500	135	150
4-13		500	45	75
		1000	100	150
		1500	155	170
4-14		500	50	110
		1000	90	200
		1500	135	200
4-15		500	50	145
		1000	95	250
		1500	140	250
4-16		500	65	110
		1000	120	190
		1500	165	225

* Table from Reference 2.
** Pressure and torque developed at -320°F by retorquing the bolts at this temp.

Table 9 – Styrene-Butadiene Rubber Gaskets Reinforced with Asbestos Fiber 8-in. Inside Diameter Tested with Bolts*

Specimen No.	Specimen Thickness, in.	Gasket** Flange Pressure @ -320°F, psi	Torque** @ -320°F, in. -lb	Contained Pressure @ -320°F, psi
8-11	0.060	500	50	80
		1000	95	110
		1500	130	160
8-12		500	60	60
		1000	150	100
		1500	140	125
8-13		500	50	75
		1000	100	140
		1500	140	180
8-14		500	65	80
		1000	120	150
		1500	155	170
8-15		500	65	55
		1000	100	70
		1500	140	100
8-16		500	60	90
		1000	100	125
		1500	140	170

* Table from Reference 2.
** Pressure and torque developed at -320°F by retorquing the bolts at this temp.

shown to be superior to unconstrained ones (4, 9). However, the gasket materials developed for this program were specified by the customer as being flat, so other configurations were not considered.

Table 10 – Styrene-Butadiene Rubber Gaskets Reinforced with Asbestos Fiber 12-in. Inside Diameter Tested with Bolts*

Specimen No.	Specimen Thickness, in.	Gasket** Flange Pressure @ -320°F, psi	Torque** @ -320°F, in. -lb	Contained Pressure @ -320°F, psi
12-11	0.060	3000	360	50
		3500	400	70
		4000	460	120
12-12		3000	360	80
		3500	375	80
		4000	425	110
12-13		3000	340	70
		3500	380	100
		4000	450	115
12-14		3000	345	90
		3500	440	90
		4000	550	110
12-15		3000	330	80
		3500	380	105
		4000	430	110
12-16		3000	330	100
		3500	370	120
		4000	420	175

* Table from Reference 2.
** Pressure and torque developed at -320°F by retorquing the bolts at this temp.

The relation between minimum sealing stress and the internal pressure contained by the joint is linear (see Fig. 1 of Reference 10). In addition to the pressure differential across the seal and the flange stress, the following parameters have been found to affect the leakage phenomenon (4): the yield strengths and strain hardening characteristics of the gasket and flange materials and the surface finish of the mating surfaces.

The relative displacement of the flange faces when the connection is made cryogenic is due in part to the different thermal contractions of the bolts and gasket. Usually, the gasket shrinks more than the bolts, so the flange faces tend to approach each other. The usual net result of these shrinkages is a reduction in the bolt load and hence a reduction in the gasket flange pressure. If the initial loading were not high enough to allow for this, the reduction in gasket flange pressure possibly would be sufficient to allow leakage. This problem is compounded by the fact that most gasket materials harden when cooled, so that increased flange pressure should be applied to maintain a seal. If excess load is applied initially to allow for these two factors, the gasket material might become extruded and flattened to the point where the shrinkage problem could still lead to leakage. Therefore, the required bolting for a specific gasket material in a particular joint for a given environmental condition is an important factor and one that does

not allow much latitude. One of the advantages offered by the glass reinforced laminate gasket material recently developed is that although its modulus is relatively high at ambient temperature and increases with decreasing temperatures, the modulus changes less with temperature than many gasket materials. Therefore, the changing load requirements with changing temperatures are minimized.

The increase in modulus with decreasing temperature can be explained by the fact that a polymer goes through a glass transition (from a rubberlike material to a glasslike material) when it is cooled. This increasing of moduli with decreasing temperature can also be explained by treating organic gasket materials as two-phase: elastic and viscoelastic (where stress-strain relationships are time-dependent). Above the transition temperature, the elastic phase dominates; below, the viscoelestic phase, with its higher modulus is stronger. The viscoelastic phase could also explain the creep, or cold flow, phenomenon.

The engineering studies conducted under Narmco's program (1, 2) have resulted in the determination of two analytical expressions which are expected to predict the performance of a gasket-flange joint (as shown in Fig. 8) when subjected to internal helium gas pressures at cryogenic temperatures. The first equation developed (2), is shown below:

$$T_a \geq + \frac{0.2\pi(g_a - \delta_a)(b_a^2 - a_a^2)d_a}{N_{ga}} E_{gc} + \frac{0.4\pi a_a^2 d_a Pi}{N} \mu_c$$
$$- \frac{\pi(t_a - t_c)\left[2h_a(\alpha_b^* - \alpha_f^*) + \delta_a(\alpha_b^* - \alpha_g^*)d_a^3\right]}{20(2h_a + \delta_a)} E_{bc} \quad (1)$$

The following list of physical properties indicates the values determined during the program and also the nomenclature used throughout the equation.

PHYSICAL GASKET PROPERTIES

Compressive Modulus, E_{gc}: 1×10^5 psi

Poisson's Ratio, μ_c: 0.35

Coefficient of Thermal Expansion: -2.4×10^5 in./in./°F

NOMENCLATURE

A	area, in.^{2}
B	bolt force per unit circumference, lb/in.
B_b	bolt force, lb
C	defined parameter

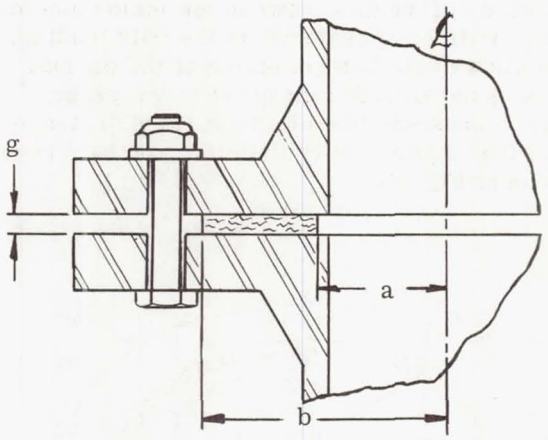

Fig. 8 - Typical joint section

E	modulus of elasticity lb/in.^{2}
F	force applied to gasket per unit circumference, lb/in.
F_g	force applied to gasket, lb
K	experimental constant
L	length, in.
N	number of bolts
T	torque on bolt, in./lb
a	gasket inside radius, in.
b	gasket outside radius, in.
c	gasket mean radius = 1/2 (a + b), in.
d	nominal bolt diameter, in.
e	gasket thickness (uncompressed), in.
h	flange thickness (assumed the same for both flanges)
p	pressure (i, inside; o, outside), psia
t	temperature, °F
α	coefficient of linear expansion, in./in./°F
δ	compressed gasket thickness, in.
Δ	increment
ϵ	strain, in./in.
σ	normal stress, lb/in.^{2}
μ	Poisson's ratio

Subscripts:

a	ambient
b	bolt
c	cryogenic
f	flange
g	gasket
t	total
1	unpressurized
2	pressurized
K_1	exponential constant
K_2	cryogenic gasket stress

The approach taken concerned the gasket only; the flange pressure was ignored and the

pressure differential between the inside and outside conditions considered as the only loading. This allowed the determination of the normal stresses developed transverse to the gasket, which represents the minimum value of flange pressure required to contain the internal pressure (see Fig. 9).

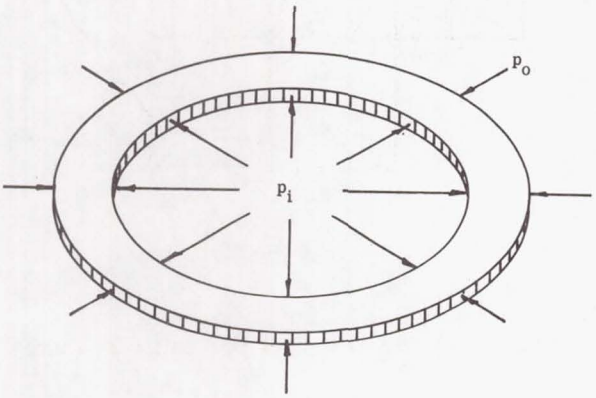

Fig. 9 - Gasket loading less flange pressure

During the course of work conducted at Narmco (2), a second expression was developed which is believed to more closely relate the room temperature sealing pressure to the internal helium gas pressure held at cryogenic temperatures. Work is presently being conducted utilizing equation (2) shown below.

$$E_{gc}\left\{\frac{4K_1(2h_a+\delta_a)\left[1+\alpha_b^*(t_a-t_c)\right]}{\pi N d_a^2 \delta_a\left[1+\alpha_g^*(t_a-t_c)\right]E_{bc}}\left[K_2 A_g - N B_{b_1} + \pi a^2 p_i\right]\right\}^{1/5}$$
$$= \frac{N}{A_g}\left\{B_{b_1} - \frac{\pi(t_a-t_c)\left[2h_a(\alpha_b^*-\alpha_f^*)+\delta_a(\alpha_b^*-\alpha_g^*)\right]E_{b_c} d_a^2}{4(2h_a+\delta_a)}\right\} - K_2 \quad (2)$$

This equation was derived assuming that the gasket is loaded in pure compression, with no rotation of flanges, no significant dimensional changes in the gasket at cryogenic temperatures, and with frictionless bolts.

APPLICATIONS

While the work conducted at Narmco was specifically directed toward the development of a LOX-compatible gasket, the newly developed laminated gasket material has already found applications outside of this program.

One such application is for a flat valve seal of a liquid hydrogen Dewar. This seal previously was solid Teflon which, after short service, fractured. The newly developed seal, with its superior strength, has not failed after 1-1/2 years of service.

A second application for the newly developed gasket composite presently under evaluation is the sealing of several windows in the liquid hydrogen tank of the Saturn-IV space vehicle. Motion pictures will be taken in space of the liquid hydrogen in its weightless condition.

A third application presently being evaluated by the Chrysler Space Division on the Saturn-IB space booster is the sealing of the LOX sump tank with the newly developed gasket material. The gasket being evaluated is of approximately 28-in. diameter, 0.125-in. thickness, and 0.500-in. width. The SBR-asbestos material presently being used has had serious liquid leaks when tested at -320°F and 80 psi. Tests to date indicate that the Narmco laminated gasket composite is capable of retaining liquid nitrogen at 80 psi with liquid or gas leaks under identical testing conditions.

A fourth application presently being evaluated by the Chrysler Space Division on the Saturn-IB space booster is the sealing of a 4-in. LOX valve. In this particular application, the newly developed gasket material is being used as a dynamic seal which has point contact loading. Test results obtained to date indicate that the seal in this particular application is far superior to that of any type of seal evaluated.

REFERENCES

1. Narmco Research & Development, "Elastomeric Gasket Materials Development for Cryogenic Temperatures: Annual Summary Report," by R. B. Gosnell, Ph.D., Contract NAS8-5053, San Diego, Calif., 15 Apr 1963

2. Narmco Research & Development, "Elastomeric Gasket Materials Development for Cryogenic Temperatures: Annual Summary Report," by F. Wilson and J. Feldmann, Contract NAS 8-5053, San Diego, Calif., 15 June 1964

3. Advanced Technology Laboratories, "Design Criteria for Zero-Leakage Connectors for Launch Vehicles," by T. P. Goodman et al., Contract NAS8-4012, Schenectady, N.Y., 15 Mar 1963

4. M. F. Spotts, "Design of Machine Elements," Prentice-Hall, Inc., Englewood Cliffs, N. J., 1958

5. L. S. Marks, "Mechanical Engineers' Handbook," McGraw-Hill, N.Y., 1956

6. K. H. Lenzen, "Strength and Clamping Force of Bolts," Product Engineering, Dec 1947

7. Armstrong Cork Company, "Techniques for Evaluating Gasket Loads in Flanged Joints," by I. G. Nolt and E. M. Smoley

8. Armstrong Cork Company, "Retaining Tension in Gasketed Joints," by E. M. Smoley and F. J. Kessler

9. Armstrong Cork Company, "Gasket Design Manual"

10. E. M. Smoley, "Design Criteria for Sealing Gasketed Joints," Machine Design, 12 Nov 1963

DESIGN AND DEVELOPMENT OF AN ELASTOMER SEAL FOR LONG TERM HAZARDOUS PROPELLANT STORAGE

By

J. P. Marcus
W. A. Day
Martin Company
Denver, Colorado

J. G. Jelinek
Parker Seal Company
Culver City, California

ABSTRACT

Containment of storable, chemically active missile propellants under long term storage conditions has normally been accomplished using stainless steel or special aluminum mechanical joints with all metal or plastic/metal gaskets. The Martin Company has found that containment of the oxidizer, Nitrogen Tetroxide using the above mentioned joint configurations has been problematical.

For approximately the last year and one-half, an intensive effort has been carried out to develop and incorporate more effective mechanical joint configurations for the Titan II ICBM. This program has resulted in the qualification of a set of elastomer seals previously considered unsuitable for the application in N_2O_4. This paper presents the details of the design and development of these seals for long term containment of N_2O_4.

The majority of the work effort covered by this report was accomplished by two Air Force contracts--AF 04(647)-576 and AF 04 (694)-472.

Containment of Modern Chemically Active Missile Propellants under long term storage conditions, such as the Titan II system as shown in Figure 1, has normally been accomplished using tankage and mechanical joints constructed of materials known to be fully compatible with the propellant in question. In the case of the Titan II oxidizer, Nitrogen Tetroxide, the mechanical joints (flanges and gaskets) have normally been all-metal configurations. Some compatible plastic gasket materials have also been employed. Based on extensive field usage and test experience, the Martin Company has found that total leak-proof containment of N_2O_4 for extended periods of time using the above mentioned joint materials has been problematical.

Fortunately, the Titan II fuel system which is filled with a mixture of Hydrazine and UDMH has not presented a leakage problem.

THE PROBLEM

Nitrogen Tetroxide is an extremely difficult fluid to contain for extended time periods. In this context, containment refers not to some allowable measurable liquid leak but to the elimination of even invisible oxidizer vapor emissions. Detection of these emissions relies on sensitive chemical vapor detectors or other high response systems.

N_2O_4, in addition to being a highly toxic fluid, exhibits three characteristics that severly tax the design of any leakproof separable connector:

1. Penetration Tendency - N_2O_4 is an excellent wetting agent. This property permits the oxidizer to migrate through minute sealing surface asperities. These seal surface flaws often defy detection even when sensitive helium mass spectrometer leak checks are employed during joint assembly.
2. Hygroscopic Property - When such seepage does occur, the N_2O_4, exhibiting a very high affinity for water, can react with ambient humidity, under the proper conditions, to form nitric acid.
3. Corrosive Effects - This nitric acid, depending upon its concentration and the configuration of the areas external to the leakage path, can cause surface corrosion and etching of missile components such as shown in Fig. 2. More alarming, however, is the damage that an all-metal gasket can experience such as shown in Fig. 3. In this case, the sealing surfaces of the flange were in a similar pitted condition thus rendering the unit useless for further N_2O_4 service.

The Titan II silo system is air conditioned to a normal temperature of approximately 65°F, therefore eliminating temperature per se as an active problem area in seal design.

THE SOLUTION

For approximately the last year and one half, an intensive effort was carried on by the Martin Company to develop a family of improved separable joint configurations for

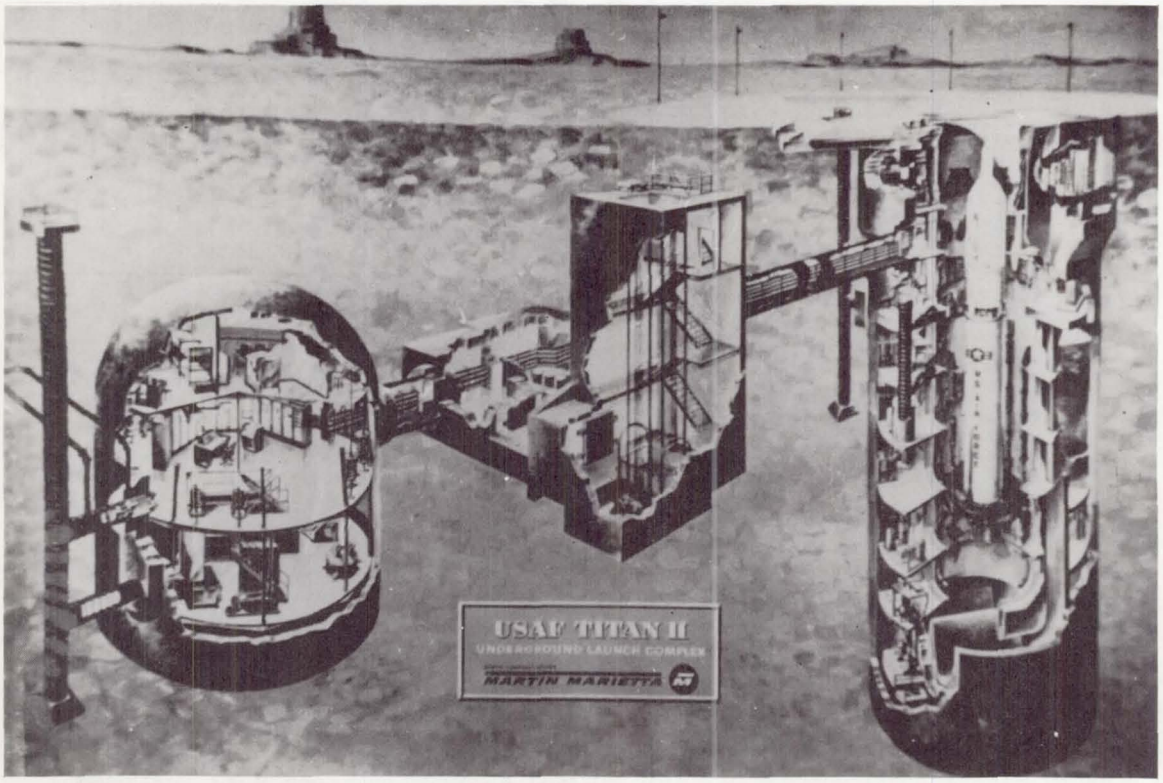

Fig. 1 - Typical Titan II installation

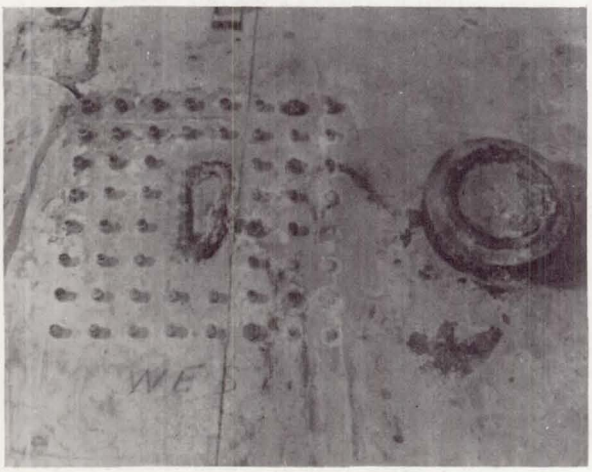

Fig. 2 - Surface corrosion of missile tank skin

Fig. 3 - Pitted sealing edge of a leaking aluminum gasket

long term storage in the Titan II ICBM. This program has culminated in the qualification of a sealing approach utilizing a material previously considered unsuitable for N_2O_4 applications...an elastomeric sealing element isolated from direct propellant attack by means of a special retainer. Since the Titan employs similar joints in both the fuel and oxidizer systems, the fuel system was also affected, primarily to minimize inventory problems. This paper presents the details of the design and application of this unique elastomeric seal called the Gask-O-Seal.

The types of separable joints investigated encompass three categories:

a. Marman Flange Joints with conical shaped interior flange seal surfaces as shown in Figure 4.

b. Zero Leak Pressure Caps with the more conventional flat faced faying surface design as shown in Figure 5.

c. And manhole cover joints as shown in Figure 6.

The following Program Objectives were established for these joints:

Table 1 - Program Objectives

a. Zero Propellant Leakage with Reliability
b. Long term storage (1 to 3 years)
c. Faying surface finish of 63 RMS
d. Elimination of joint relaxation (creep or cold flow)
e. Reduction of troublesome installation procedures
f. Retrofit existing hardware

For program direction, Table 2 was prepared to compare the vital characteristics of various seal types with the absolute seal requirements as outlined.

Reference to this table reveals that except for its incompatibility with N_2O_4, the elastomeric seal concept would satisfy each seal design criterion most effectively. For example, the compliant ability of a properly compressed elastomer to provide continuous zero leakage has long been recognized. The forgiving nature of such a resiliant seal will

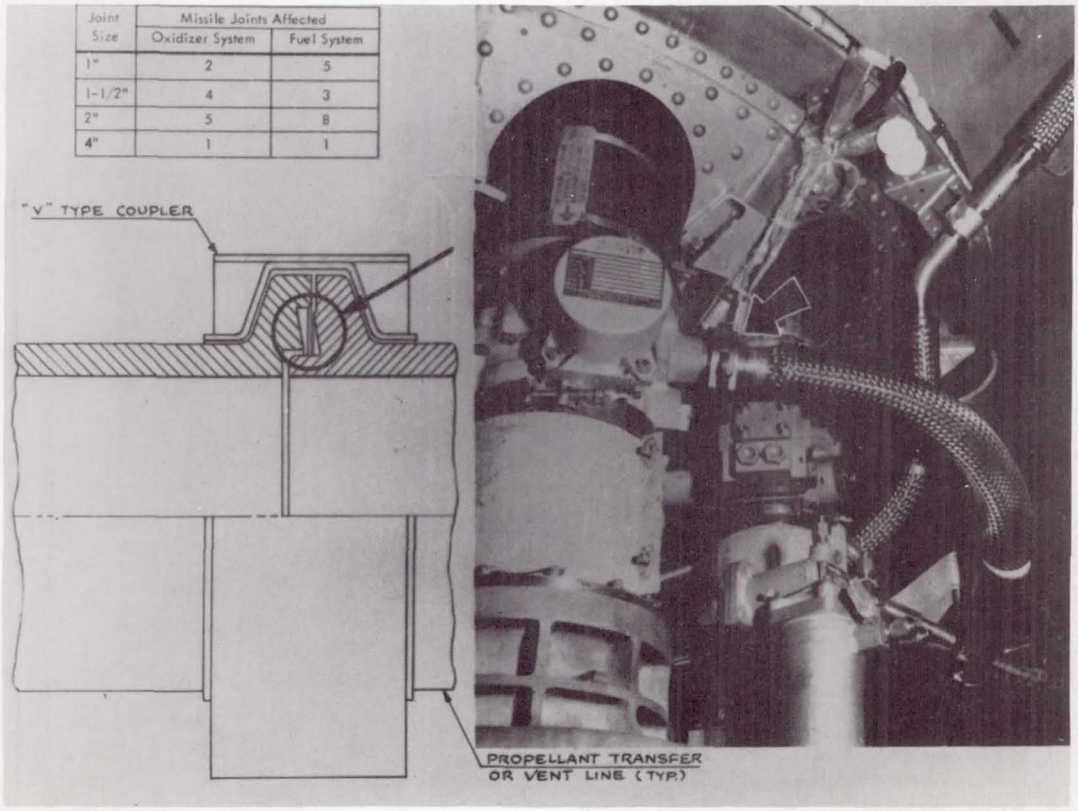

Fig. 4 - Typical Marman flange installation, Stage II engine compartment

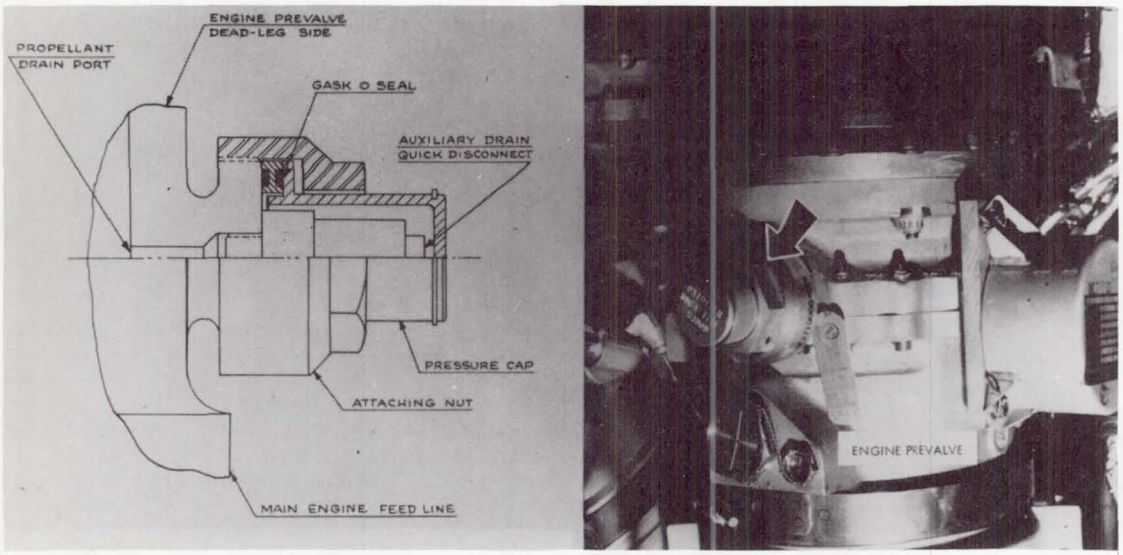

Fig. 5 - Typical pressure cap installation, Stage I engine compartment

Fig. 6 - Typical manhole cover location

Table 2 - Seal Material Characteristics			
Seal Material	Resiliance	Compression Set	Compatibility with N_2O_4
Select Metals (Al., S.S.)	Poor to Fair	Poor	Excellent
Plastics (Fluoro-carbon series)	Fair to Good	Fair	Fair to Good
Elastomers (Butyl)	Excellent	Very Good	Poor

readily tolerate surface asperities in the range of 63 RMS even under severe vibrational stresses.

The problem centered around the vulnerability of the organic elastomer. It was at this point that Martin Company and Parker Seal Company launched a joint effort to explore the proven principles of controlled confinement sealing of the Gask-O-Seal for possible implementation in the Titan program.

MATERIAL UPRATING - An investigation of elastomer materials was conducted by Parker Seal chemists to produce a formulation with maximum N_2O_4 resistance. The result of this research was a vastly improved resin cured butyl compound designated B591-8.

Samples of this new compound, and the old Parker propellant service material B496-7, were submitted to Martin Denver Materials Engineering for propellant resistance tests. Table 3 summarizes the results of physical properties measurements of "O" ring specimens which were directly immersed in both liquid and vapor phases of N_2O_4. Note that the old B496-7 compound after only one week in 90°F soak had deteriorated beyond the point of being testable, whereas the new B591-8 was still testable at the end of 29 days of immersion.

Table 4 is a similar tabulation of physical property values of "O" rings after corresponding exposures in the 50/50 Hydrazine-UDMH fuel mixture.

Practical proof of the superiority of the new B591-8 compound over its predecessor B496-7 is displayed in Figure 7. As in all previous tests, these specimens were purposely unconfined during immersion in N_2O_4 to maximize physical effects.

N_2O_4 Impact Sensitivity tests were also run by Martin on the B591-8 compound according to the procedure shown in Table 5. Twenty samples were run--none indicated a reaction.

TABLE 3

EVALUATION OF RESIN CURED BUTYL RUBBER COMPOUNDS SUITABLE FOR USE IN TITAN II PROPELLANT SYSTEMS

OXIDIZER

N_2O_4 (Nitrogen Tetroxide)

Compound	Control Values		60° F Fumes		60° F Soak		90° F Soak		Cumulative Hours Exposed to Propellant
	Tensile (PSI)	Elongation (%)	Tensile (PSI)	Elongation (%)	Tensile (PSI)	Elongation (%)	Tensile (PSI)	Elongation (%)	
B496-7	1750	292	905 (-48.5%)	655 (+124%)	604 (-65.5%)	629 (+115%)	722 (-58.7%)	609 (+109%)	22 Hours
B591-8	1758	215	1341 (-23.7%)	254 (+18.1%)	1022 (-41.8%)	268 (+24.5%)	1099 (-37.5%)	282 (+31.2%)	22 Hours
B496-7	1750	292	398 (-77.2%)	774 (+165%)	479 (-72.6%)	668 (+129%)	290 (-83.4%)	769 (+163%)	68 Hours
B591-8	1758	215	927 (-47.3%)	277 (+28.8%)	1155 (-34.3%)	318 (+47.9%)	1047 (-40.4%)	386 (+79.5%)	68 Hours
B496-7	1750	292	128 (-92.7%)	1015 (+248%)	239 (-86.3%)	701 (+140%)	Specimen Deteriorated		168 Hours
B591-8	1758	215	729 (-58.5%)	463 (+116%)	1112 (-36.8%)	349 (+62.3%)	777 (-55.8%)	462 (+115%)	168 Hours
B496-7	1750	292	Specimen Deteriorated		168 (-90.4%)	634 (+117%)	Specimen Deteriorated		334 Hours
B591-8	1758	215	204 (-88.3%)	552 (+115%)	867 (-50.6%)	373 (+74%)	297 (-83.1%)	643 (+199%)	334 Hours
B496-7	1750	292	Specimen Deteriorated		Specimen Deteriorated		Specimen Deteriorated		694 Hours
B591-8	1758	215	65 (-96.3%)	799 (+272%)	523 (-70.2%)	494 (+130%)	147 (-91.6%)	595 (+177%)	694 Hours

TABLE 4

EVALUATION OF RESIN CURED BUTYL RUBBER COMPOUNDS SUITABLE FOR USE IN TITAL II PROPELLANT SYSTEMS

FUEL

UDMH–HYDRAZINE
50:50 Mixture

Compound	Control Values		60° F Soak		90° F Soak		Cumulative Hours Exposed to Propellant
	Tensile (PSI)	Elongation (%)	Tensile (PSI)	Elongation (%)	Tensile (PSI)	Elongation (%)	
B496-7	1750	292	1683 (-3.8%)	343 (+17.5%)	1526 (-12.8%)	327 (+12%)	22 Hours
B591-8	1758	215	1539 (-12.4%)	191 (-11.2%)	1654 (-5.9%)	199 (-7.4%)	22 Hours
B496-7	-	-	1376 (-21.3%)	317 (+8.6%)	1693 (-3.2%)	389 (+33.2%)	68 Hours
B591-8	-	-	1706 (-3.0%)	205 (-4.7%)	1699 (-3.3%)	205 (-4.7%)	68 Hours
B496-7	-	-	1536 (-12.2%)	349 (+19.5%)	1508 (-13.8%)	355 (+21.6%)	168 Hours
B591-8	-	-	1420 (-19.1%)	185 (-14.0)	1666 (-5.2%)	222 (+3.3%)	168 Hours
B496-7	-	-	1636 (-6.5%)	351 (+20%)	1512 (-13.6%)	409 (+40%)	334 Hours
B591-8	-	-	1549 (-11.8%)	199 (-7.4%)	1412 (-19.7%)	215 (±0.0%)	334 Hours
B496-7	-	-	1700 (-2.8%)	380 (+30%)	1444 (-17.5%)	372 (+27%)	694 Hours
B591-8	-	-	1550 (-11.8%)	202 (-6.0%)	1309 (-25.5%)	195 (-9.3%)	694 Hours

Table 5 - N_2O_4 Impact Sensitivity of MMS D204 Butyl Rubber

Twenty (20) 1/8-inch diameter by 1/4-inch long pieces of O-ring molded to meet MMS D204 were subject to the following test:

1. Soak specimen in liquid N_2O_4 for 24 hours.
2. Place specimen in test cup and add liquid N_2O_4 to almost cover specimens.
3. Immediately drop plummet of dead weight impact machine. Weight and initial height of plummet shall be such as to produce 70 ft-lbs of impact energy when dropped.
4. Observe test for audible or visible reaction.
5. Inspect specimen remaining for signs of violent chemical reaction. None of the tests indicated a reaction.

DESIGN - In order to fully understand the Gask-O-Seal principle, one should first consider what actually makes a seal work. A good seal relies on its ability to crowd into and literally fill all the microfine asperities of the mating surfaces to be sealed. Figure 8 illustrates how the inherent resiliance of a familiar rubber "O" ring is deployed to fill the exaggerated surface irregularities. Exploring this "O" ring sealing theory further, one finds that there are at least three fundamental requisites to a reliable long term static seal as shown in Figure 9.

Close examination of the two gland cross sections in Figure 9 reveals that the compressed "O" ring exposes approximately 30 to 40% of its surface area to the media being sealed. If, however, the area of seal exposure can be significantly reduced to some minimum value, say 2%, theoretically any serious degredation of the seal element could be retarded or eliminated. This factor is the key to long term sealing of N_2O_4 with an elastomer.

The geometry of such a design is shown in Figure 10. The rubber sealing element is molded directly in place in the groove using a close tolerance mold cavity. The features of this design are summarized in Table 6.

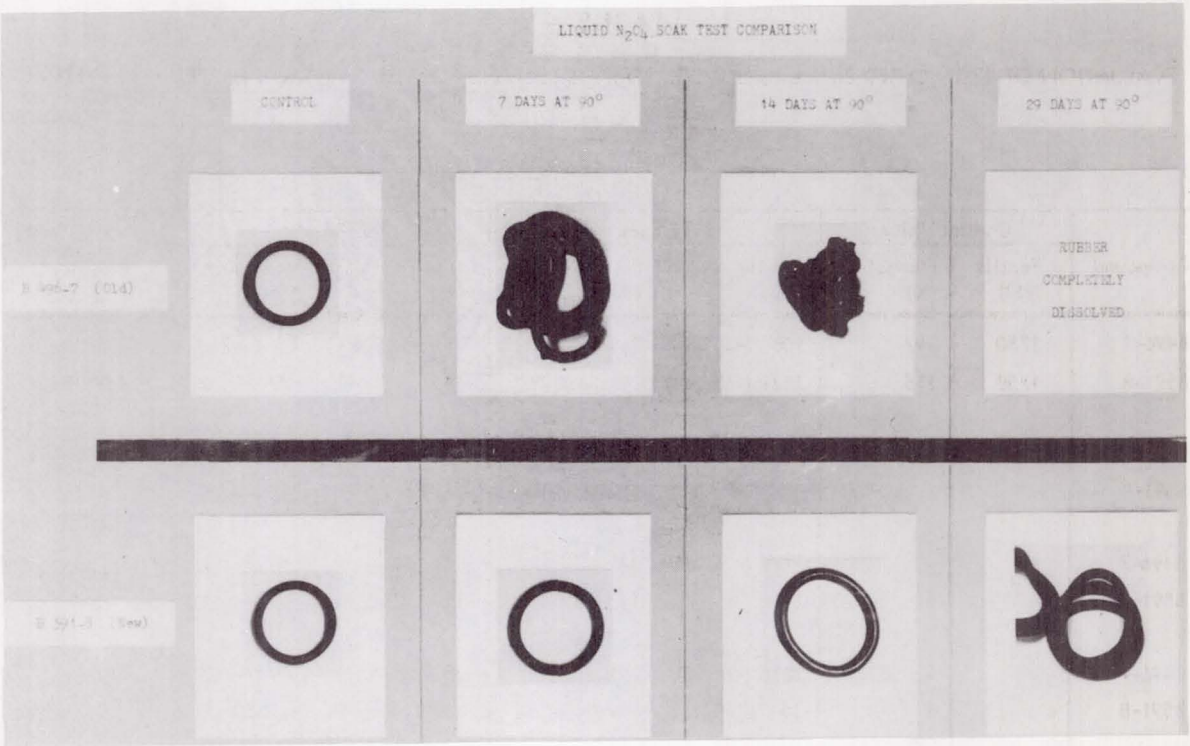

Fig. 7 - "O" rings directly immersed in N_2O_4

Table 6 - Gask-O-Seal (Mark I Style)

1. Crown Height (H) is a constant for any given configuration. The "H" value ranges from .015" to .031" depending on groove width for optimum seal performance. Seal preload force becomes essentially a constant, measuring approximately 50 lbs. per linear inch of seal.
2. Volume/Void Relationship is precisely maintained at around 92%. Notice how some clearance room remains even after complete closure.
3. Metal/Metal Contact between faying surfaces is achieved at closure.
4. Integral Elastomer/Metal Seal Design cancels the possible effect of groove tolerances and finish. The vulcanized in place element fills all irregularities.
5. Limited Area of Attack (approximately 2% as shown) inhibits elastomer decay by N_2O_4. Any minute propellant seepage between these surfaces is intercepted by the inner seal cushion which acts as a "buffer" zone. In the case of N_2O_4, this "buffer" zone absorbs some of the oxidizer, swells slightly and thus produces a tighter seal.

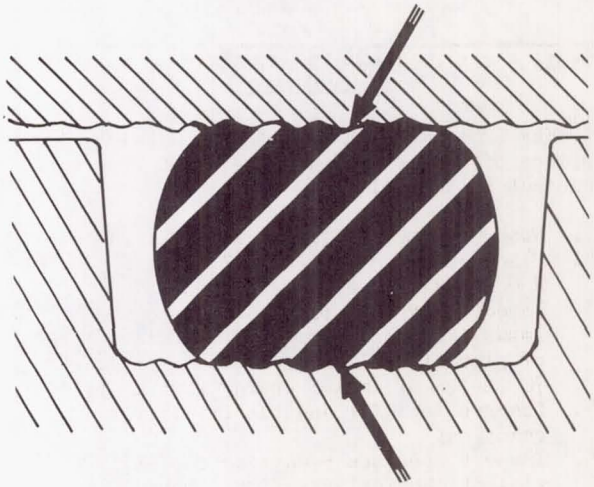

Fig. 8 - "O" ring filling groove asperities

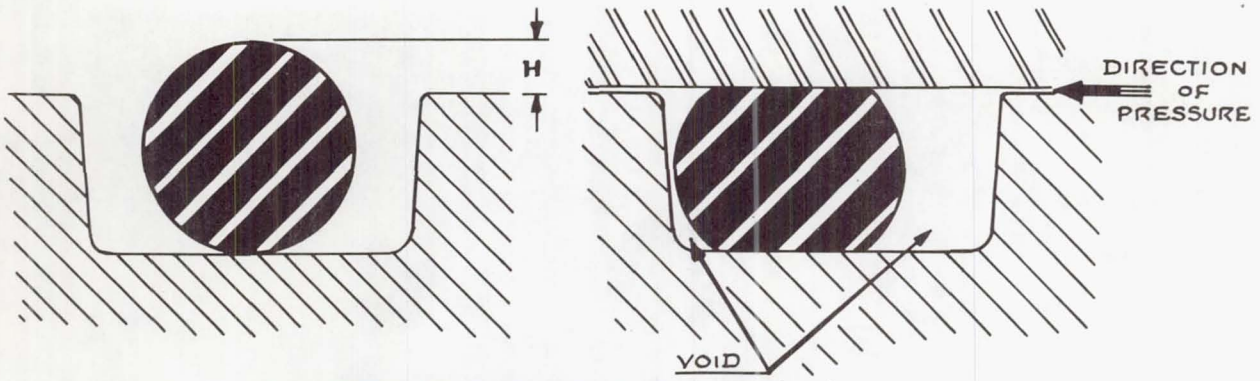

1. PREDETERMINED COMPRESSION OR SQUEEZE (H).
2. METAL TO METAL CONTACT (TO ELIMINATE JOINT RELAXATION).
3. ADEQUATE VOLUME TO VOID RATIO (V).

Fig. 9 - Elastomer seal prerequisites

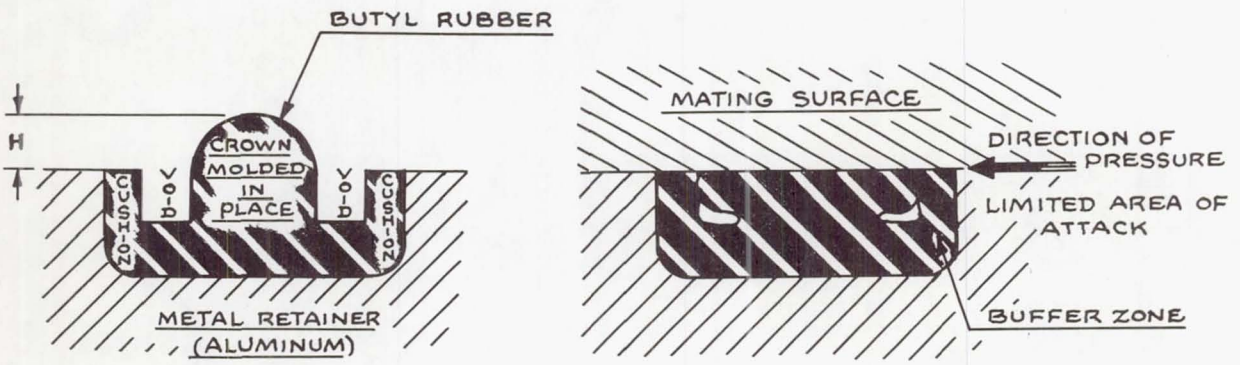

Fig. 10 - Gask-O-Seal profile

Obviously, it would be impractical in many instances to mold such a seal directly into flanges, connectors, or housings. In such cases the solution is simply to vulcanize a two sided seal in the machined grooves of a separate retainer as shown in Figure 11. For the Titan program, the retainers were constructed of 6061-T6 alloy. Small holes were drilled through the remaining web portion of metal to provide mechanical attachment of the rubber sealing element to the retainer. Coincidentally, these small holes serve as gates through which the elastomer flows during molding. The elastomer is also bonded to the metal substrate during vulcanization by using a suitable bonding system. The limited area of attack concept exists in this two sided configuration also.

Note also in Figure 11 the sectional view of the two sided Mark I Gask-O-Seal mounted in place between closed flanges. The aluminum retainer serves as a positive "stop", permitting maximum flange fastener efficiency and maintenance of flange preload without cold flow or relaxation.

The overall effectiveness of this principle may be viewed in Figure 12, a photograph taken of a 2" diameter conical Gask-O-Seal employed to seal a Marman flange joint that had been exposed to N_2O_4 for 6 months under laboratory conditions. As the photograph illustrates, the seal proper was totally functional at test termination.

Similarly, Figure 13 depicts a 2" size conical Gask-O-Seal field sample after 9 months liquid N_2O_4 exposure at 62 psia and 65°F. In both instances, the seals were molded from the new, improved B591-8 compound. The absence of any visible decay speaks for itself.

APPLICATIONS - These principles were actually utilized in each of the separable joints mentioned at the beginning of this paper.

Figure 14 describes the conical shaped Mark 1 Gask-O-Seal configuration designed for

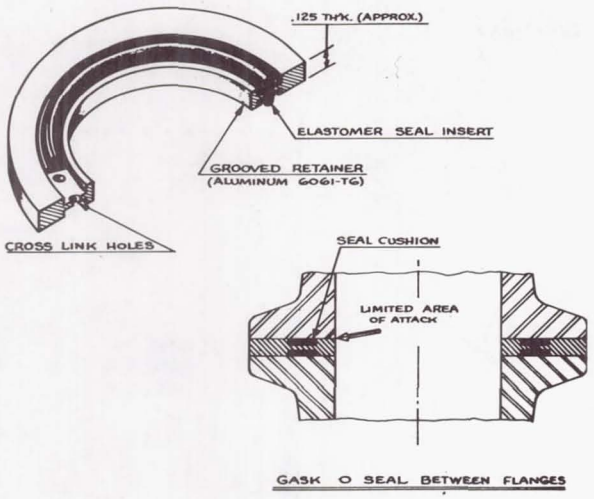

Fig. 11 - Gask-O-Seal features and installation

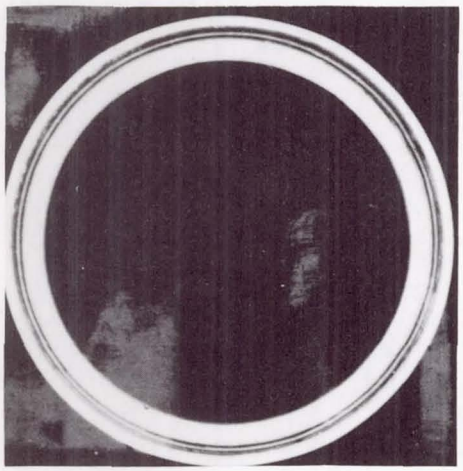

FULL SCALE

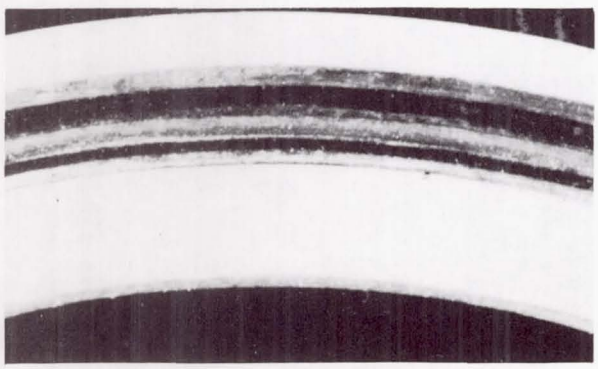

APPROX. 5X SCALE

2" SIZE CONICAL GASK O SEAL
COMPOUND B591-8

Fig. 12 - Six month N_2O_4 exposure sample

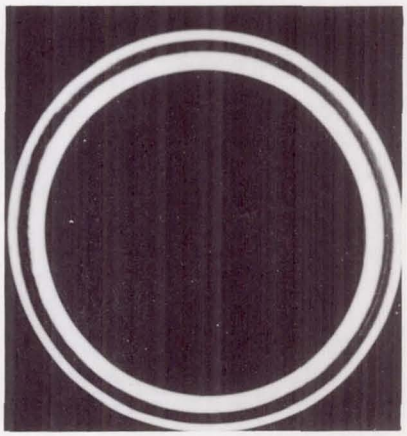

FULL SCALE

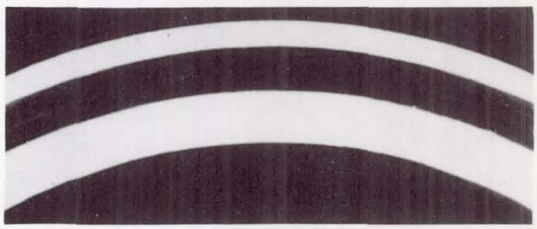

APPROX. 3X SCALE

2" SIZE CONICAL GASK O SEAL

Fig. 13 - Nine month N_2O_4 exposure sample

the quick coupler Marman flange connections. The normal line sizes are 1", 1-1/2", 2", and 4" in the propellant or "canned" areas. Twenty-nine joints use the Gask-O-Seal concept with twenty-three of these being continually exposed to propellants. Note the 10° angle on the retainer interface.

The Mark I Gask-O-Seal for the Auxiliary Drain Pressure Cap, on the other hand, is simply a flat faced seal as shown in Figure 15. The exploded photographic view of the flange components, showing the Gask-O-Seal second from the right, illustrates precisely how the seal is assembled in the flange. Two of these assemblies are used on each missile, one for oxidizer service, the other for fuel.

The Manhole Cover Gask-O-Seals represented a departure from the conventional single lip Gask-O-Seal profile discussed thus far. The typical Manhold Cover joints shown in Figure 16 reveals a "two lipped" seal design that had proven more successful during testing on larger sizes of hardware. This double crown design, designated Mark II, has its void area in the valley region centered between the two crowns. The vital cushion area still occurs ahead of the crown.

The Manhole Access Covers are located in the top domes of the four propellant tanks. Notice that the covers for the two Oxidizer tanks are circular in shape, whereas the covers for the two Fuel tanks are elliptical.

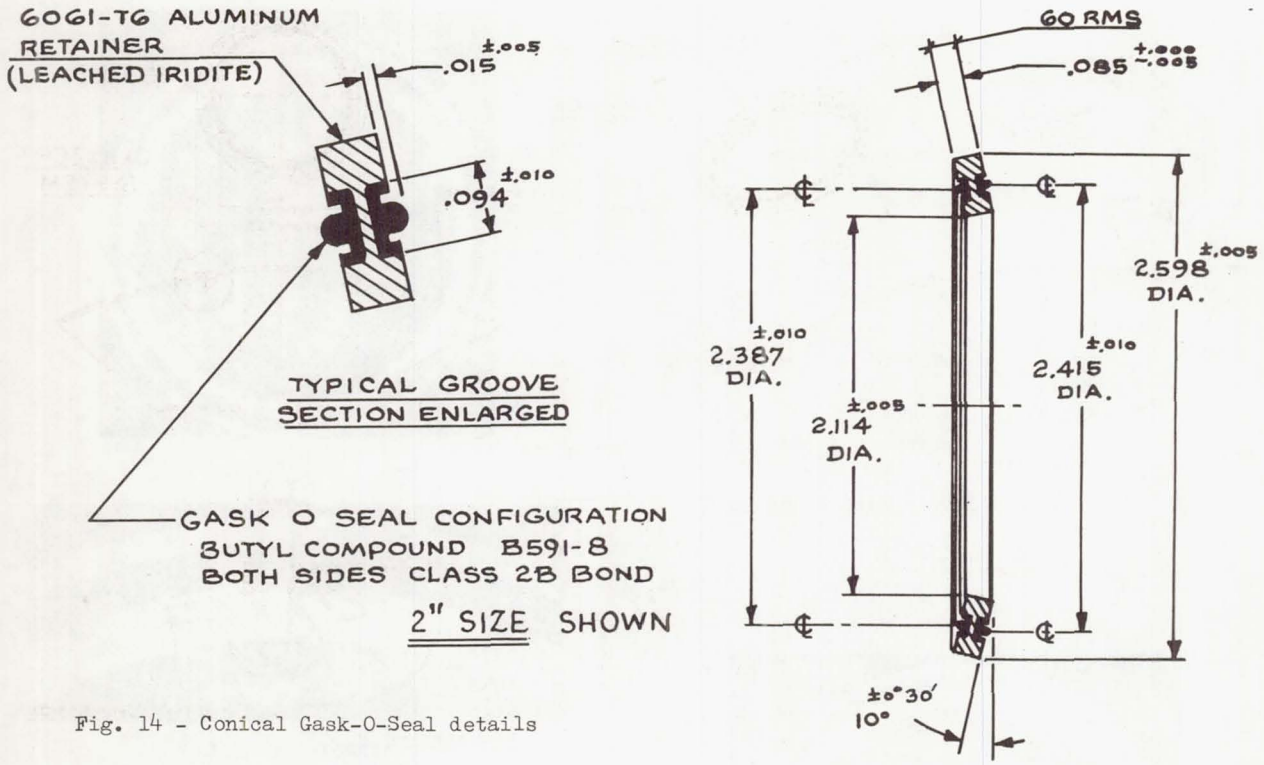

Fig. 14 - Conical Gask-O-Seal details

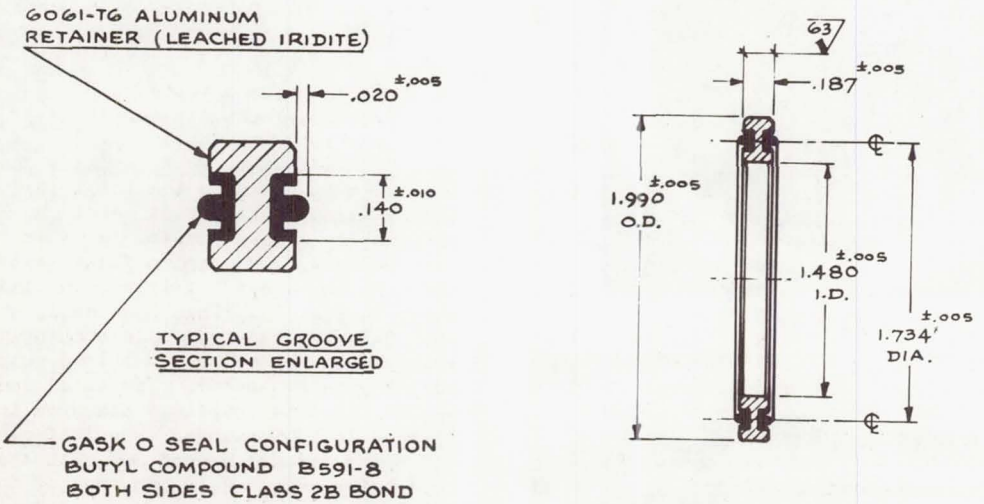

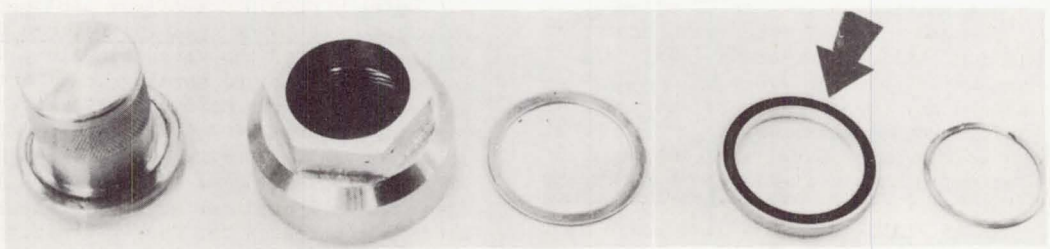

Fig. 15 - Pressure cap Gask-O-Seal details

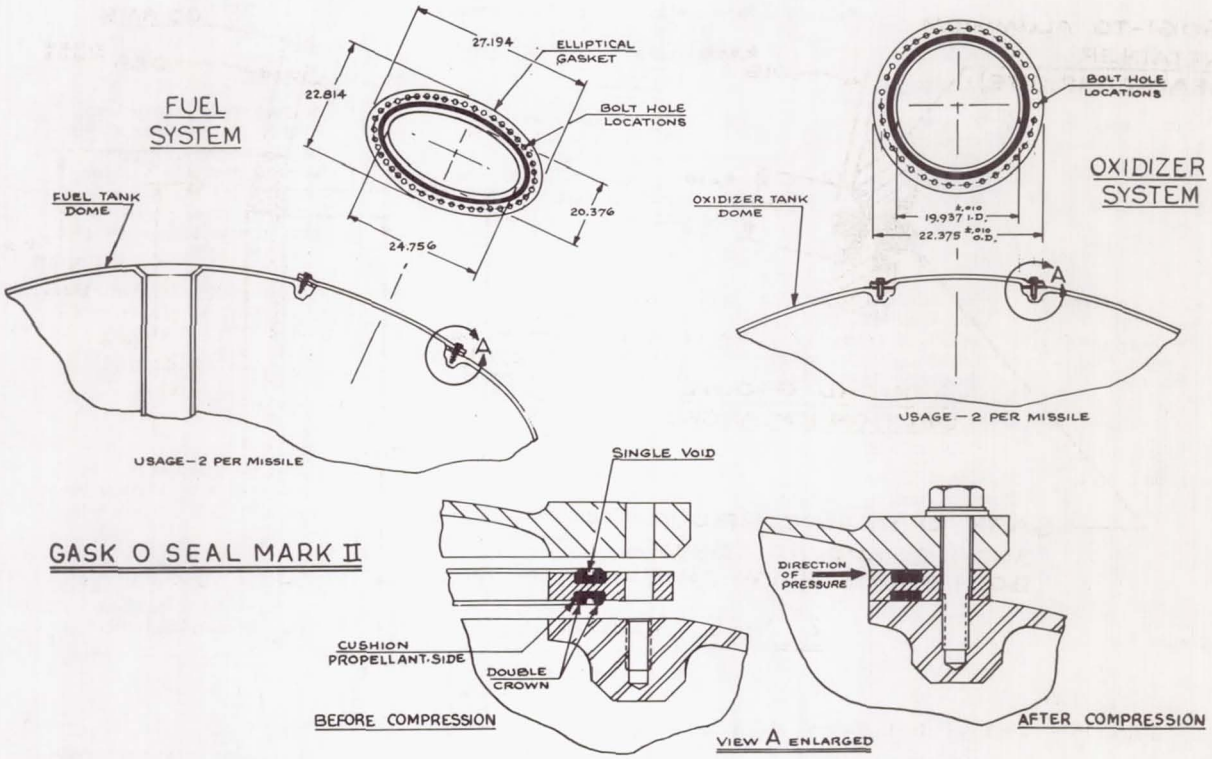

Fig. 16 - Manhole cover Gask-O-Seal details

QUALIFICATION TEST EFFORT

To qualify these new joint configurations for operational missile usage, a series of extensive evaluations were performed at Martin Denver. The location and function of the various joints on the missile combined with actual field experience strongly influenced the various test parameters and apparatus employed for these qualifications.

The helium leakage tests mentioned in the following evaluations were all accomplished using a Consolidated Electrodynamics Corporation Model 24-120A Mass Spectrometer. Both the vacuum chamber and "sniffing probe" methods of measurement were employed. The "sniffing probe" method was generally considered a qualitative indication of helium leakage. The use of the "probe" was referenced to the minimum obtainable machine sensitivity which was always less than 3.0×10^{-10} ATM cc/sec/division. Any observable mass spectrometer meter reading above the helium background count was judged as the failure criteria. Normally, systems tested to this criteria are acceptable for long term containment of propellants.

I. MARMAN FLANGE JOINTS - Five basic test categories as summarized in Table 7 were pursued for qualification of these joints:

1. "V" band clamp tests
2. External joint load and leakage
3. Functional tests
4. Propellant exposure
5. Vibration tests

"V" Band Clamp Tests - These tests were initiated to evaluate the total load and load distribution characteristics of the Marman coupling to assure compatible assembly with the Gask-O-Seal. A 2" Marman flange set was reworked to accept a triple beam load cell as shown in Fig. 17. This load cell, instrumented with B.L.H. strain gages on each beam, was designed to absorb the full load output of the coupling being tested. The total load output of the "V" band couplings measured in the range of 4000 to 5000 pounds. The load distribution variation did not exceed 20% with the highest load being measured in the area of the coupling "T" bolt. This did not affect seal performance.

External Joint Load and Leakage Tests - In some areas of the Titan missile plumbing, low order torque and bending loads are transferred through the Marman joints after system assembly. Tests were initiated using the apparatus shown in Fig. 18 to evaluate the load transfer capability of the new joint configurations as well as to establish the leakage characteristics of the Gask-O-Seals.

1", 1½", and 2" sizes were evaluated according to the following test sequence.

a. Install vacuum leakage chamber around joint.

Table 7 - Marman Flange Joint Test Summary

Test Type	Test Apparatus	Test Parameters	Sample Size	Comments
"V" band clamp tests	a) Flange load cell fixture (Ref. Fig. 17) b) Strain gages BLH Model FAB 12-12 c) Bridge circuit	a) Vary configuration of "T" bolt nut and applied assembly torques b) Vary application of lubricant to clamp friction surfaces	51	Maximum total clamp load 4000 to 5000 pounds at 45 in-lbs assembly torque with lubrication applied to "T" bolt threads and retainer face. Load variation around flange periphery less than 20%.
External load and leakage tests a) Leakage (helium) b) Torque c) Bending	a) CEC Model 24-120A mass spectrometer b) Vacuum chambers c) Joint load application apparatus (Ref. Fig. 18)	a) "Probe" and vacuum helium leak checks b) Apply torque load to joint up to leakage failure and disassemble. c) Apply bending load to joint up to leakage failure and disassemble.	34	Vacuum leakage indications consistent at approximately 1.8×10^{-7} ATM cc/sec.
Functional tests	Section of Titan II Stage II tank (Ref. Fig. 21)	a) Study assembly techniques (typ). b) "Probe" and vacuum leak check in place c) Pressure cycle 0-60 psig with GN_2 over N_2O_4	7	Joint assembly easy. No indicated N_2O_4 leakage under pressure cycle conditions.
Propellant exposure	2" flange size	a) Pressurize with N_2O_4 in system to 60 psig. b) Monitor for leakage by inclosing joint with moist polyethylene bag containing Congo Red indicator paper.	18	No signs of propellant leakage since September 1964
Vibration	a) Ling Model L-200 vibration shaker b) Standard vibration fixtures (Ref. Fig. 22)	Random vibration 2½ min/axis in 3 axes (3 samples/size) 7½ min/axis in 3 axes (1 sample/size)	4/size	Test items passed environment without leakage or structural failure.

b. Pressurize assembled joint to 60 psig with a 10%/90% helium/nitrogen gas mixture and monitor leakage as a function of time.

c. Apply torsional or bending load inputs in increasing step functions to the joint and monitor for significant change of indicated leakage rate as the failure criteria.

The applied torque and bending loads at which the joint leakage changed measurably were 160 ft-lbs and 350 ft-lbs respectively for the 2" size. After release of the applied failure load, however, the indicated leakage of Gask-O-Seal equipped joints returned to the flow value established prior to load application.

Before the torque and bending loads were applied to the joints per step c) above, the steady state vacuum chamber helium indications of the Gask-O-Seals were plotted as shown in Fig. 19. Note the consistent readings of approximately 1.8×10^{-7} ATM cc/sec for 16 samples of the 2" joint size. This quantitative leakage does not correspond to a measurable "probe" leakage for the configurations tested.

The helium indications versus time relationships are shown in Fig. 20, also for the 2" size. Note that steady state flow is achieved within 2 hours after initial pressurization and remains constant for periods of up to 20 hours. When increased pressures were applied to these joints, the indicated helium readings increase approximately as a first order function.

Functional Tests - These tests utilized an actual section of Titan II tank structure equipped with airborne propellant components as shown in Fig. 21. This allowed a comprehensive study of assembly techniques and "in-place" leakage measurement combined with pressure cycling.

After initial joint assembly, the system was pressurized to 60 psig with the 10%/90% helium/nitrogen mix and both "probe" and vacuum leak checked with the mass spectrometer. The system was then filled with N_2O_4 and pressure cycled with GN_2 from 60 psig to zero and back to 60 psig every four hours for two weeks. Each joint was enclosed in a polyethylene bag containing moist Congo red indicator paper for immediate propellant leakage determination. No leakage was observed.

Propellant Exposure Tests (Static Pressure) - These tests employed simple flanged test vessels approximately 6 inches in length. The 2" joint size was used.

After joint assembly, the standard mass spectrometer "probe" leak check was accomplished at 60 psig to the 3×10^{-10} ATM cc/sec criteria. The test vessels then were filled with N_2O_4, pressurized to 60 psig, and bagged with the leakage indicator system described in the

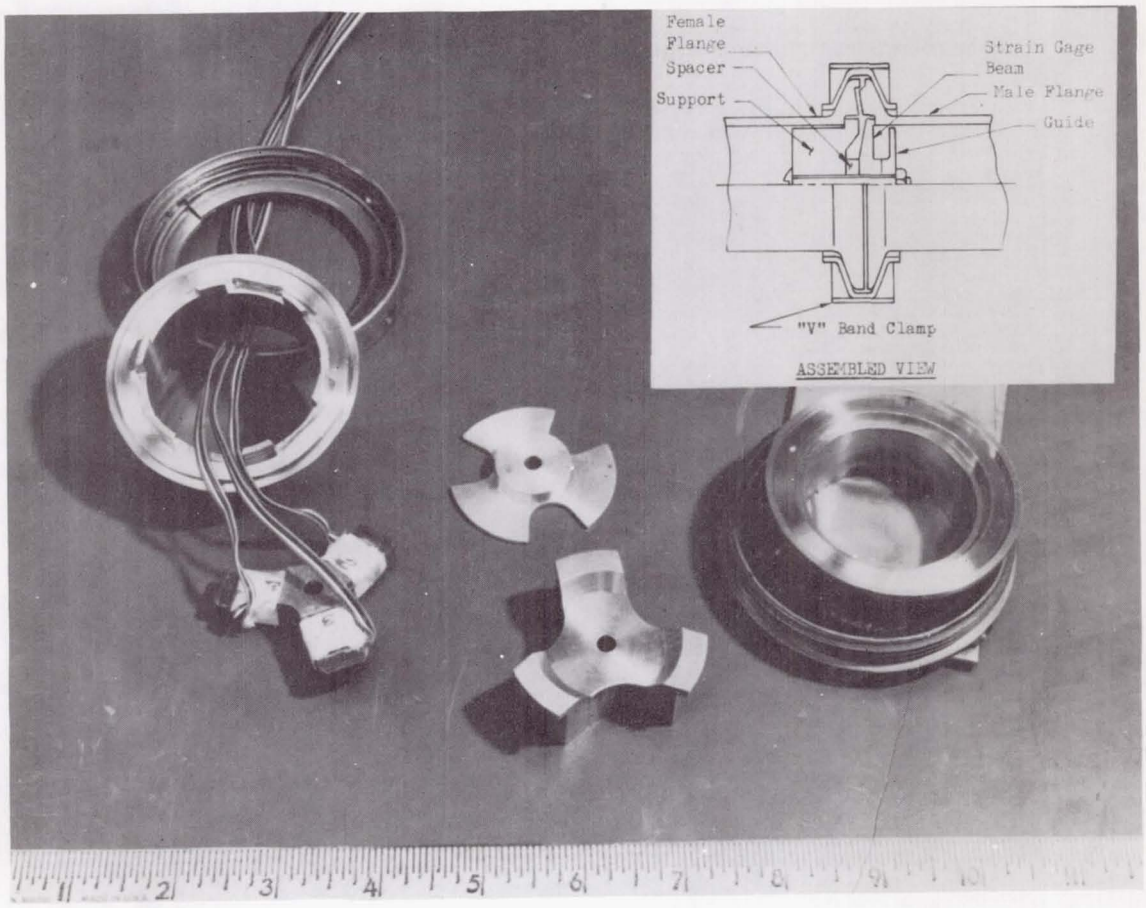

Fig. 17 - "V" band clamp load cell apparatus

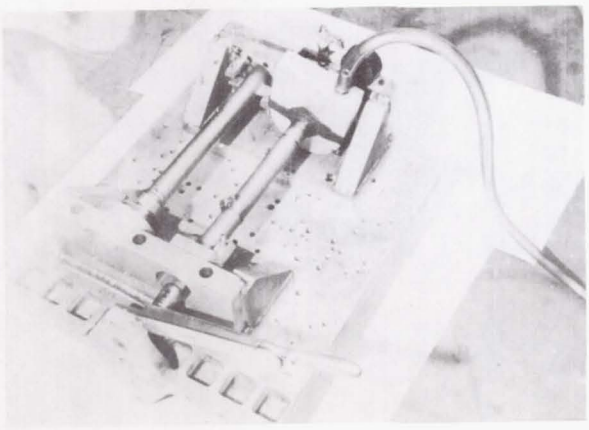

Fig. 18 - Torque and bending load fixture with vacuum chamber installed

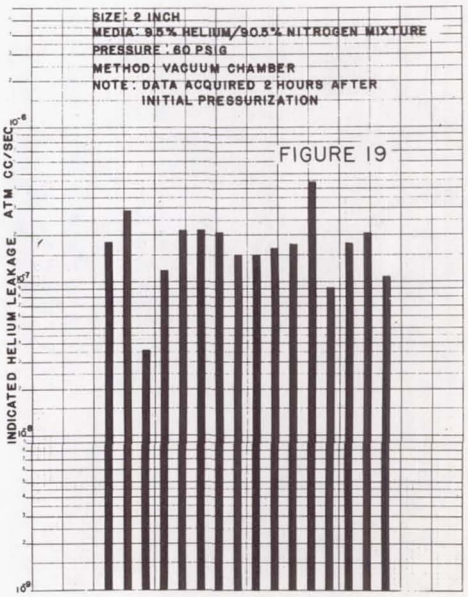

Fig. 19 - Gask-O-Seal leakage variation

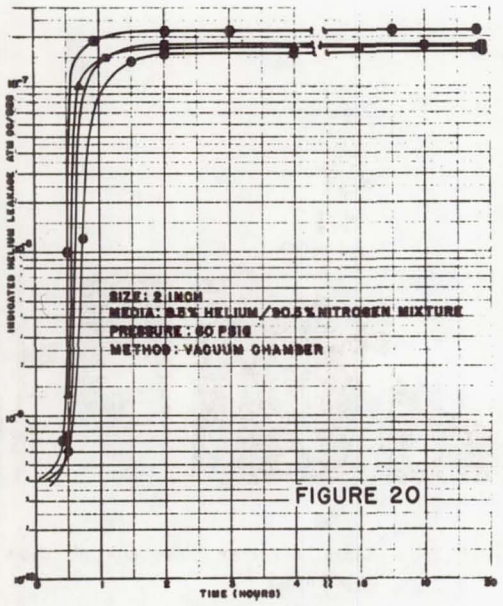

FIGURE 20

Fig. 20 - Gask-O-Seal leakage vs. time

functional tests above. These tests have continued 9 months to date. There have been no signs of leakage in 18 test samples.

Vibration Tests - Random vibration testing for each size of joint (1", 1½", 2", 4") was accomplished in each of three mutually perpendicular axes utilizing the typical apparatus shown in Fig. 22. The vibration levels utilized were based upon actual measured data obtained during the Titan II R & D program. For joint sizes employed in several missile locations, the vibration levels for each of these areas were compared by an "overlay" process. The maximum levels at all frequencies were then plotted to form a composite spectrum.

The vibration test levels employed were:

a) 1" joint size - 37.7 GRMS
b) 1½" and 2" sizes - 54.4 GRMS
c) 4" joint size - 21.7 GRMS

During vibration, the test fixtures were pressurized to flight levels with nitrogen gas. Joints and lines normally in propellant liquid were filled with water to approach simulation of propellant mass. Four joint samples per size were tested--three samples being exposed to vibration for 2½ minutes/axes and the fourth being exposed for 7½ minutes/axes for structural assurance.

II. AUXILIARY DRAIN PRESSURE CAP - The controlling environment for these items is the random vibration of Stage I engine firing.

After initial assembly, the units were "probe" leak checked at 60 psig to the 3×10^{-10} ATM cc/sec criteria. Vibration tests followed at 20.5 GRMS for 22½ minutes in each of the normal flight and auxiliary disconnect axes. Post vibration leak checks were performed to initial assembly criteria. The final phase involved N_2O_4 exposure at 60 psig. Two of these units have been periodically checked for propellant leakage since September 1964. No leakage has been detected.

III. MANHOLE COVER SEAL EVALUATION - The manhole cover zone of the propellant storage tank is functionally a component part of the tank's relatively thin membrane-type structure. This light-weight tank structure is designed to contain the pressurized propellants at high sub-yield stress levels. Such a pressurized condition, however, manifests itself in minute

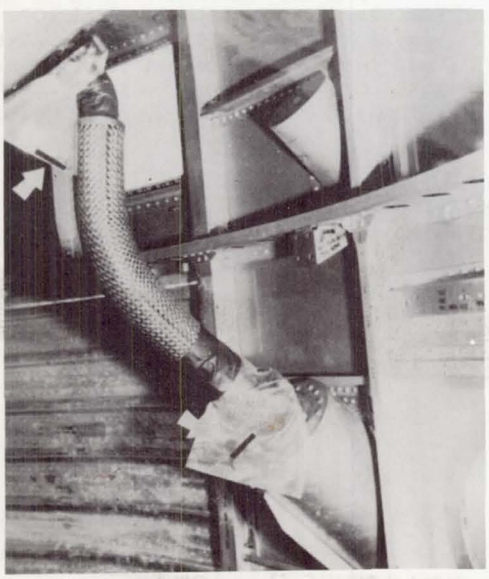

Fig. 21 - Functional test apparatus

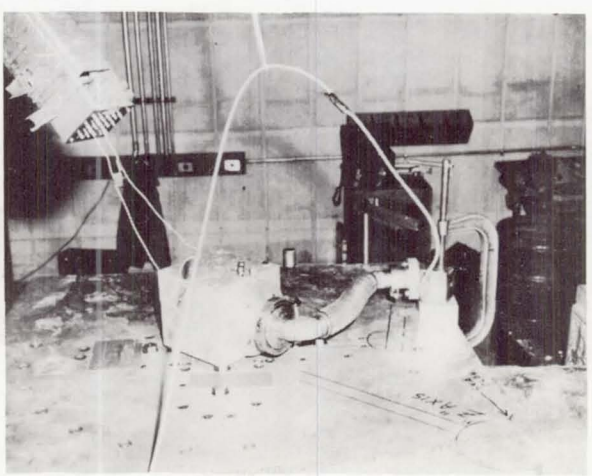

Fig. 22 - Vibration test apparatus - typical

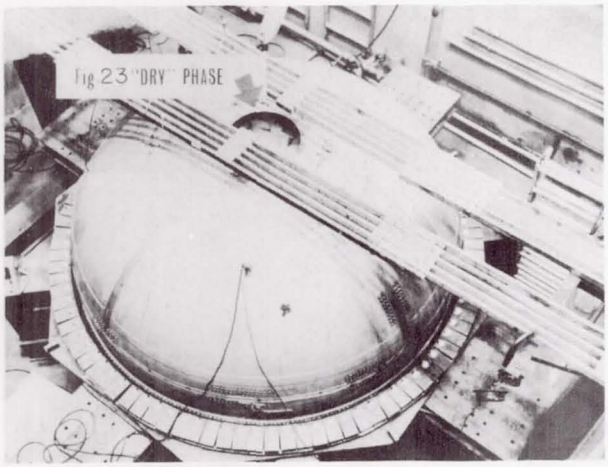

Fig. 23 - Manhole cover "dry phase" test apparatus

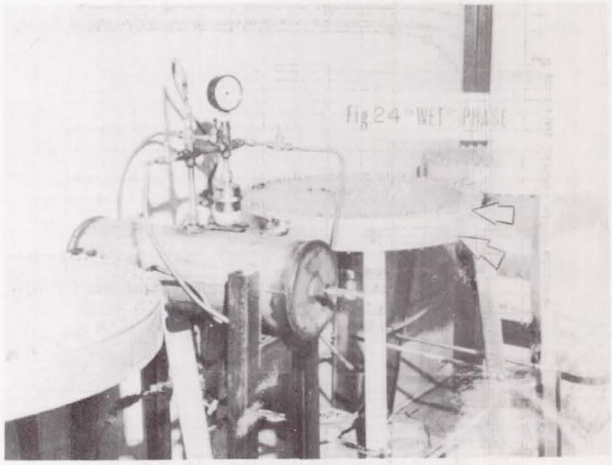

Fig. 24 - Manhole cover "wet phase" test apparatus

but measurable deflections occurring in all elements of the tank, including the manhole cover joint. Consequently, this pressure cycle function was judged to be a most severe joint environment, and was studied in addition to mere propellant exposure. Accordingly, the manhole cover test was divided into two phases:

I. "Dry" Phase - (9.5% Helium/90.5% Nitrogen Gas Mixture) - The actual missile tank dome was set up as shown in Fig. 23 to allow testing of the Gask-O-Seal joint configuration under actual pressurized conditions. A typical test sequence consisted of proof pressure checking the entire dome assembly (with Gask-O-Seal in place) at 80 psig. A minimum of 75 pressure cycles from 0 to 45 psig were then induced in the closed system.

Throughout the entire proof and cycling test spectrum, leak checks were made using the "probe" mass spectrometer technique and the 3.0×10^{-10} ATM cc/sec criteria. The configuration of the larger manhole cover hardware made vacuum chamber measurements extremely difficult and therefore this technique was not used. No "probe" leakage indications were recorded during the test sequence.

II. "Wet" Phase - N_2O_4 with GN_2 Pressurant - Special fixtures and support hardware shown in Fig. 24 were constructed for this test which involved both propellant exposure and pressure cycling.

The test vessels were partially filled with N_2O_4 and pressure cycled with GN_2 to 45 psig. The test area was maintained at 60° ±5°F to simulate silo conditions. The relative humidity was normally maintained at 80% minimum to accelerate acid formation should a leak develop. These units were pressure cycled a

Fig. 25 - Shimmed manhole cover Gask-O-Seal

minimum of once a day for durations of up to 90 days. Periodic checks were made during the test period by checking for N_2O_4 leakage. This was accomplished by wiping the periphery of all seal interface areas with moist Congo red indicator paper. These propellant tests were also made more severe by inserting .002" thick pieces of shim stock between the gasket retainer and the flange as shown in Fig. 25 in order to increase direct propellant attack on the seal element. Radial scratches were also applied adjacent to these shimmed areas using 320 grit sandpaper in order to determine gasket limitations. No indication of N_2O_4 leakage was found in any of the Mark II Gask-O-Seal test samples. The flange separation caused by the insertion of shim stock and the radial scratch marks produced no serious adverse effects as determined by post propellant helium leak checks and visual gasket inspection.

CONCLUSIONS

The successful development of the Gask-O-Seals discussed here has eliminated the leakage problems associated with the mechanical joints of the Titan II weapon system. In accomplishing this result, the following items are highlighted:

a) A semicompatible material has been employed as the seal material.

b) Degradation of the seal elements for time spans of up to 9 months has been negligible supporting the "limited area of attack" concept.

c) In over 300 oxidizer system field missile installations to date there have been no reported leaks in Gask-O-Seal equipped joints. The time duration for some of these items is up to 10 months.

REFERENCES

1. J. P. Marcus, et al., "Improvement of Fluid System Mechanical Joint Technology with Respect to Zero Leakage." Martin Company CR-64-194, Volumes I, II, III, and V, final report under Air Force Contracts AF 04(694)-472 and AF 04(647)-576, November 1964.

2. R. C. Elwell, et al., "Study of Dynamic and Static Seals for Liquid Rocket Engines" Volume 2, General Electric final report under NASA Contract No. NAS 7-102, February 1963.

SUPERFINISHED SURFACES AS A MEANS FOR SEALING

By

F. O. Rathbun, Jr.
R. S. White
Advanced Technology Laboratories
General Electric Company
Schenectady, N. Y.

ABSTRACT:

The feasibility of using superfinished surfaces on integral connector components in order to effect a separable seal which will not require a gasket, but will retain the characteristic of reusability, is discussed. The means for attaining such surface finishes, the degree of flatness required, the maximum asperity heights tolerated, and the stresses required to seal are described. The results of an experimental program in which several means of finishing, several different materials, and repetitive use of given surfaces were evaluated are outlined. The requirements for a connector in which such surfaces are used with regard to surface protection, surface cleanliness, and structural design are discussed.

EXPERIMENTAL STUDIES (1, 2, 3)* have shown that the normal stress required to effect a seal on a flat annular sealing system exceeds the yield strength of one of the mated materials. In order for the leakage to be reduced to approximately 10^{-6} atm cc/sec, depending on the surface finish of the stronger material contact, the amount of deformation required necessitates normal stresses as high as 2.75 times the yield strength of the weaker material. The actual requirement for normal stress is extremely sensitive to the original surface finish of the stronger material.

Such results dictate that, in the actual sealing interface of a separable connector, plastic deformation must occur. A likely approach under this requirement is that of using a removable gasket which can be discarded after use, and replacing it by an identical one. If the surfaces on the structural parts are mated directly, then the necessary plastic deformation during the first assembly may well cause the response of the connector during succeeding assemblies to differ from that which it was designed. The latter approach is, of course, unsatisfactory from a reliability standpoint when reusability is required. The former approach, that of using a removable gasket, is less than satisfactory due to the added complexity in the assembly procedure and the logistics involved.

A possible answer to this dilemma is, since the "sealability" is quite sensitive to surface finish, to utilize some surface on the structural components of the connector such that stresses less than the yield strengths of the materials concerned will cause near zero leakage. In that previous experimental investigations (1) had shown that surfaces having asperities as small as those resulting from diamond burnishing still require stresses above the yield strength for repetive use, it is obvious that a necessary criterion for elastic sealing is that the surfaces are even smoother than those gained from diamond burnishing techniques.

Aside from the asperity free characteristic of surfaces for elastic sealing, it is obvious that an extreme flatness requirement exists. Even though locally, a surface may be extremely free of irregularities, in order for the entire seal to mate against the opposing part, essentially all deviations from flatness must be removed about the periphery of the seal.

Adding to the actual surface quality requirements is the problem of insuring that the accumulation of damage resulting from repetitive mating and the occurrence of surface damage by improper handling or assembly techniques is sufficiently slight. A fourth problem which arises when one considers the elastic sealing phenomenon is that of the means of manufacturing available for producing such surfaces. Given that a particular set of surfaces are smooth enough and flat enough to effect a proper seal, the requirement remains that such a surface can be manufactured easily, in large quantities, and without excessive cost. Hence, four problems present themselves for solution prior to the ultimate manufacture of a separable, reusable, re-

*Numbers in parentheses designate References at end of paper.

liable, separable connector utilizing what we will call "superfinished" surfaces.

In order to determine the feasibility of using such surfaces for sealing, an experimental program, sponsored by the National Aeronautics and Space Administration has been carried out in which four finishing techniques have been used. Flat annular sealing specimens, having been surface finished by a given technique, were subjected to leakage tests under varying stresses and internal pressures. Different numbers of tests were run on each combination of specimens, depending on the relative success gained with the initial experimentation.

Altogether, 60 separate leakage tests were accomplished with eight different sets of sealing surfaces being tested. Stainless steel (347) and 2024-T4 aluminum were used as structural materials in all cases.

The goals of the program were the solutions to the four problems concerning superfinished surfaces which have been stated above.

THEORETICAL CONSIDERATIONS

Previous investigations (1, 2), have shown that the leakage through an annular sealing system results from a multitude of individual leaks of varying size and geometries. It has also been shown that as the size of the asperities is reduced and the surface becomes smoother, the leakage through such a sealing system agrees better with analytically predicted leakage using a uniform gap height analysis (even when both molecular and viscous terms have been included). Because of this, it appears that leakage through a sealing surface in which two extremely smooth surfaces are mated (superfinished surfaces), would result less from a multitude of individual flow paths and more from wide slits existing between the two mated surfaces caused from deviations from flatness which exists on the sealing surfaces.

Because of this, one can envision a simplified model of the elastic system and the stresses required to bring two such surfaces together. If a small sector of a flat annular rise is envisioned, (Figure 1), then the stress required to displace the surface downward a given amount varies inversely with the height of the rise (to a first approximation). Of course, elasticity of the sub-base and shear stress between the segment considered and adjacent segments are omitted. The deflection δ of the surface downward is given, for the assumed model, as $\delta = SH/E$, where E

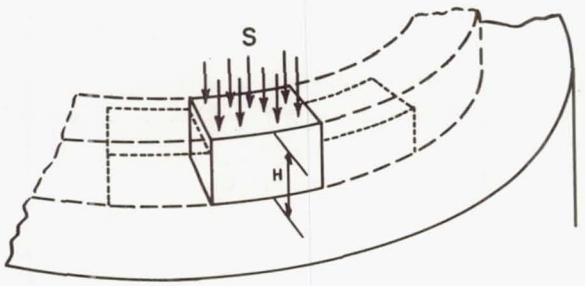

Fig. 1 - Simplified Model of Elastic Sealing Annulus

is Young's modulus of the material in question, H is the rise height, and S is the applied stress.

Assuming that the segment of rise lying immediately to the right or left of the segment in question were a measurable height higher than the one in question--thus indicating waviness of surface--then it would follow that it would be easier to promote mating between all segments of the surface around the periphery by having the rise heights higher (increasing in the governing equation).

In that very little plastic deformation at the surface is envisioned in such a system, at least the elastic sealing system lends itself to material deformation analysis whereas the sealing system which required plastic deformations defies analysis at this point in time.

EXPERIMENTAL PROGRAM

In order to assess the feasibility of incorporating elastic superfinished sealing surfaces into connectors for aerospace applications, the 60 separate experiments shown in Table 1 were accomplished.

Each set of specimens to be mated was of the shape shown in Figure 2. Such specimens fitted into a leak detection-load imposition system shown in Figure 3.

In order to gather data to evaluate the feasibility of such sealing surfaces, a specified chronological application of stress and pressure was used, and is shown in Figure 4.

In general, the stress was applied until the leakage dropped to below 10^{-6} atm cc/sec, or a predetermined allowable stress level for the materials in question was attained. The inter-

TABLE 1

SUPERFINISHED SEALING SURFACE EXPERIMENTS

Test No.	Surface Finishing Technique	Specimen Material	Height of Annulus	No. of Tests of Specimens
1	Yatabe Fine Finish Sample #1	347 Stainless Steel	0.030"	1
2	" " "	" " "	0.030"	2
3	" " "	" " "	0.030"	3
4	" " "	" " "	0.060"	4
5	" " "	" " "	0.060"	5
6	" " "	" " "	0.090"	6
7	" " "	" " "	0.090"	7
8	" " "	" " "	0.090"	8
9	" " "	" " "	0.090"	9
10	" " "	" " "	0.090"	10
11	" " "	" " "	0.090"	11
12	Yatabe Fine Finish Sample #2	" " "	0.030"	1
13	" " "	" " "	0.030"	2
14	" " "	" " "	0.030"	3
15	" " "	" " "	0.030"	4
16	" " "	" " "	0.030"	5
17	" " "	" " "	0.060"	6
18	" " "	" " "	0.060"	7
19	" " "	" " "	0.090"	8
20	" " "	" " "	0.090"	9
21	" " "	" " "	0.120"	10
22	" " "	" " "	0.120"	11
23	Jones Optical Polished Surfaces	" " "	0.030"	1
24	" " "	" " "	0.030"	2
25	" " "	" " "	0.030"	3
26	" " "	" " "	0.030"	4
27	" " "	" " "	0.030"	5
28	" " "	" " "	0.060"	6
29	" " "	" " "	0.060"	7
30	" " "	" " "	0.090"	8
31	" " "	" " "	0.090"	9
32	" " "	" " "	0.090"	10
33	" " "	" " "	0.090"	11
34	" " "	" " "	0.120"	12
35	" " "	" " "	0.120"	13
36	Jones Optical Lapped Surfaces	" " "	0.030"	1
37	Lead Lap	347 Stainless Steel	0.030"	1
38	Lead Lap	347 Stainless Steel	0.030"	2
39	Yatabe Fine Finish Sample #1	2024 Aluminum	0.030"	1
40	" " "	" "	0.030"	2
41	Jones Optical Polished Surfaces	2024 Aluminum KANIGEN Plated	0.030" "	1
42	" " "	" "	"	2
43	" " "	" "	"	3
44	" " "	" "	"	4
45	" " "	" "	"	5

TABLE 1 (CONT.)

Test No.	Surface Finishing Technique	Specimen Material	Height of Annulus	No. of Tests of Specimens
46	" " "	" "	"	6
47	" " "	" "	"	7
48	" " "	" "	"	8
49	" " "	" "	"	9
50	" " "	" "	"	10
51	Jones Optical Polished Surfaces	347 Stainless Steel (one surface silver plated)	0.090"	1
52	" " "	" " "	"	2
53	" " "	" " "	"	3
54	" " "	" " "	"	4
55	" " "	" " "	"	5
56	" " "	" " "	"	6
57	" " "	" " "	"	7
58	" " "	" " "	"	8
59	" " "	" " "	"	9
60	" " "	" " "	"	10

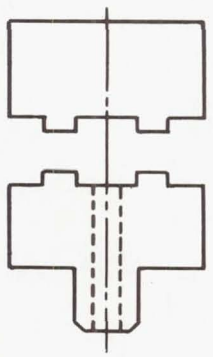

Fig. 2 - Leakage Experiment Specimens

nal pressure varied between 14.7 and approximately 2000 to 2200 psi in each case.

The data accumulated under the procedure shown was plotted for evaluation with a logarithmic leakage scale on the leakage ordinate and linear applied stress on the abscissa. A sample test result is as shown in Figure 5.

Data from the experiments were also useful in establishing the location of the transition region between molecular and viscous flow. For such evaluation, the data accumulated during Phase II of the experiment were plotted with logarithmic leakage versus logarithmic pressure. A sample plot of data taken during Phase II is shown in Figure 6.

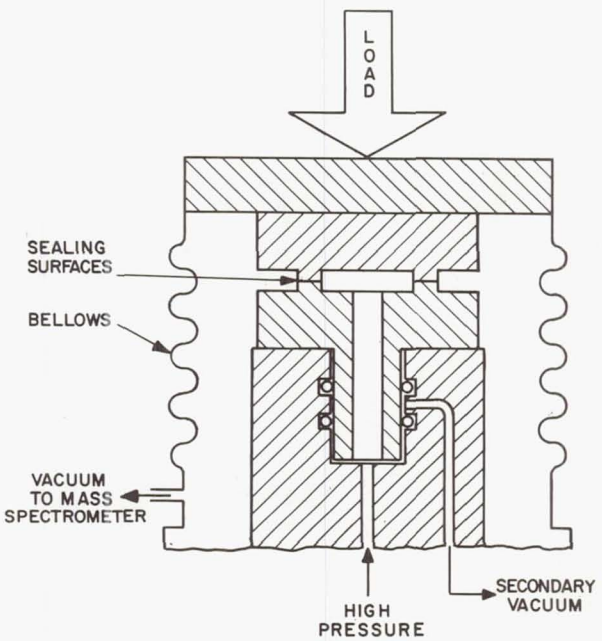

Fig. 3 - Schematic of Experimental Apparatus for Superfinish Sealing Investigations

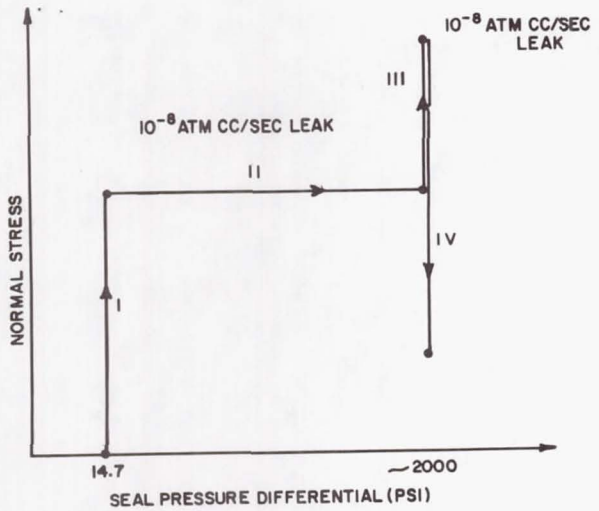

Fig. 4 - Experimental Procedure for Accumulation of Data

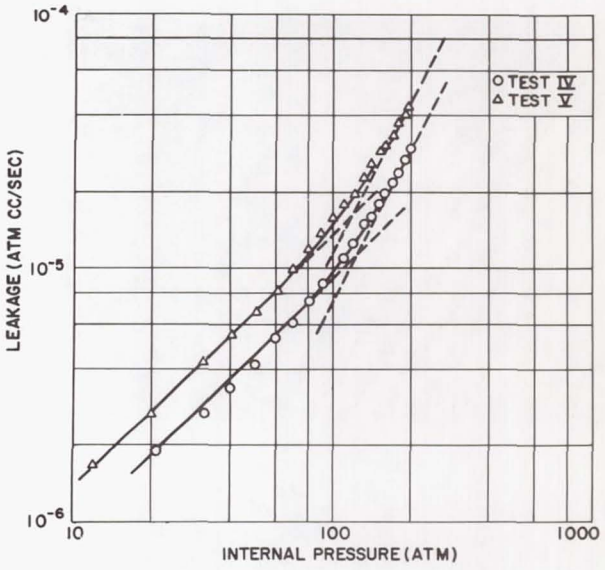

Fig. 6 - Leakage as a Function of Internal Pressure, Phase II of Experiment - Yatabe Stainless Steel

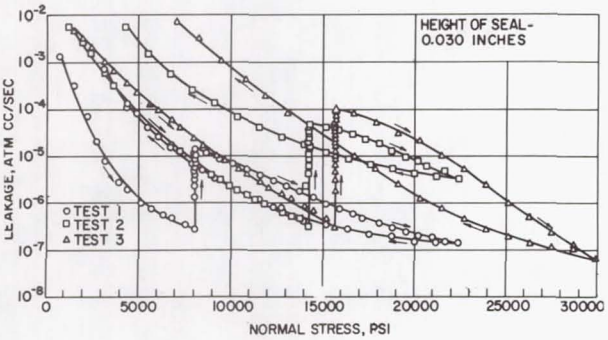

Fig. 5 - Leakage - Normal Stress Response for Yatabe 347 Stainless Steel Specimens

It is to be noted that a slope of one on such a plot denotes molecular flow and a slope of two denotes viscous laminar flow.

SURFACE FINISHING TECHNIQUES

As shown in Table 1, different combinations of material and surface finishing techniques were investigated. Within this framework, four finishing techniques were used on the two structural materials (347 stainless steel and 2024-T4 aluminum), on a KANIGEN plated aluminum surface, and on a silver plated stainless steel surface. Among the techniques which proved unsatisfactory for development of adequate surfaces were lead lapping, and lapping with a 303 aluminum oxide lapping compound backed by a cast iron plate. Surface finishing techniques which proved satisfactory were the "Monomolecule Surface Finish" produced by the Up-Hi Corporation of Tokyo, Japan, and a proprietary technique of the Jones Optical Works, Burlington, Mass., which utilizes a 0.05 micron sapphire powder on a wax backing. The latter technique was used successfully on stainless steel, and on KANIGEN plated aluminum. It was also applied to silver plated stainless steel, resulting in a surface adequate in mating experiments with superfinished stainless steel.

Each surface tested was subjected to interference photomicrography and Nomarski microscope techniques. Figures 7 and 8 show the "Monomolecule" surface finish on 347 stainless steel; Figures 9 and 10 show the surface generated by the Jones Optical technique on 347 stainless steel; Figures 11 and 12 show the Jones technique as applied to KANIGEN plated aluminum. Figure 13 shows the "Monomolecule" tech-

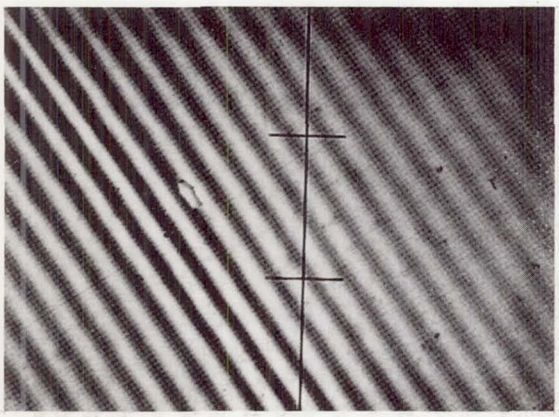

Fig. 7 - Interference Photo of Monomolecule Finish on 347 Stainless Steel - Scale: 0.00194 inches between Scale Marks; 11.8 microinches between interference lines.

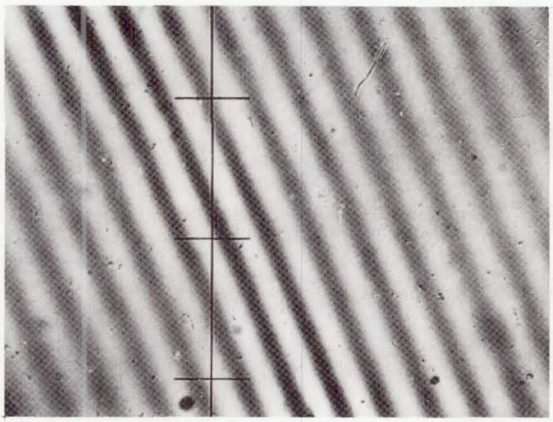

Fig. 9 - Interference Photo of New Jones Optical Co. Polished 347 Stainless Steel Specimen - 11.8 microinches between interference lines. Scale: 0.00482 inches between scribe marks.

Fig. 8 - Nomarksi Photo of Monomolecule Finish on 347 Stainless Steel - Magnification: 168.

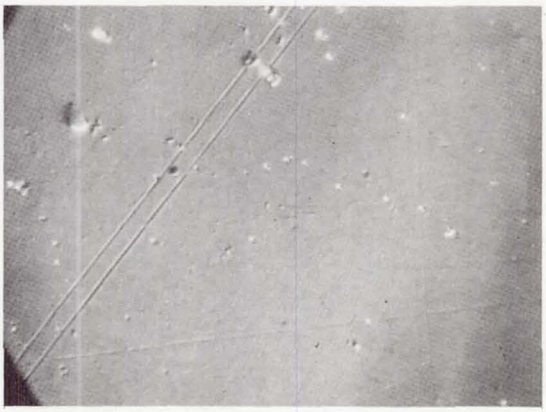

Fig. 10- Nomarksi Photo of New Jones Optical Co. Polished 347 Stainless Steel Specimen - 11.8 microinches between interference lines. Magnification: X900.

nique as applied to 2024 aluminum; it is obviously of poor quality and proved to be inadequate in the testing program.

It is to be noted that the interface photographs show low relief asperities as small as approximately one or two microinches; the Nomarski technique shows the general quality of the surface and can resolve asperities down to approximately 75 Angstroms. The Jones technique as applied to stainless steel resulted in a pebbly grained surface; the "Monomolecule" surface finish also appeared somewhat pebbly but a bit rougher.

The specifications for finishing the "Monomolecule" finish were indefinite at the time of the use of the technique. Specifications for the surfaces manufactured by the Jones Optical Works were:

(a) Flatness, within one helium lightband (11.6 microinches).

(b) Roughness, no low relief scratches deeper than one half microinch.

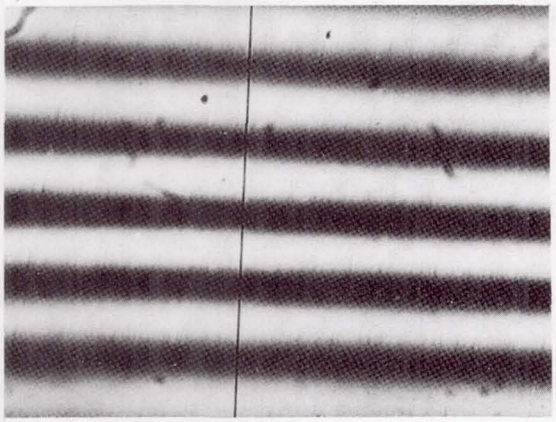

Fig. 11- Interference Photo of Jones Optical Co. Polished KANIGEN plated 2024 Aluminum Specimen - 11.8 microinches between interference lines. Scale: 0.00192 inches between scribe marks.

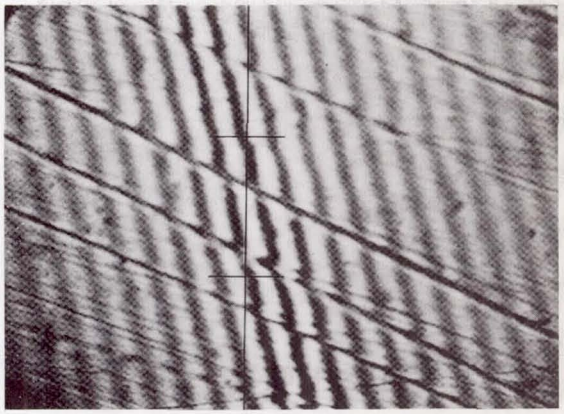

Fig. 13 - Interference Photo of Monomolecule Finish on 2024 Aluminum. Scale: 0.00194 inches between scale marks; 11.8 microinches between interference lines.

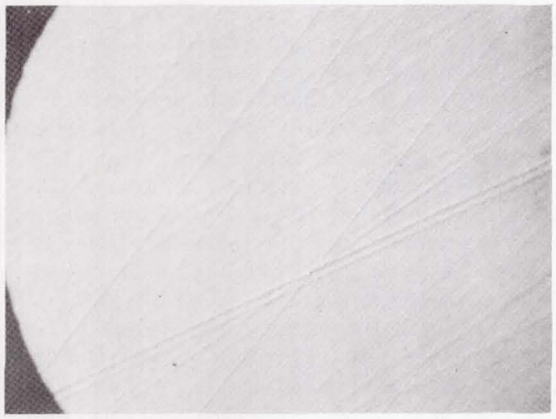

Fig. 12- High Magnification Photo of KANIGEN Plated Aluminum Specimen Superfinished by the Jones Optical Company - Magnification: X900.

LEAKAGE TESTS RESULTS

Two sets of 347 stainless steel samples with "Monomolecule" finishes were subjected to leakage tests. Eleven assemblies were made with each set. During the successive experimentation, the surface rise heights were altered by cutting back material on each side of the annular rise. In that surface damage was accumulated during the test, the effect of increasing the flexibility of the sealing system could not be assessed and the cutting back of material did not result in useful information.

For the first set of "Monomolecule" finished surfaces, of the eleven tests run, it was possible to seal to less than 10^{-6} atm cc/sec except in the second, tenth and eleventh tests. In the second test, the stress was allowed to increase only to 20,000 psi, whereas slightly less than 39,000 psi (the yield strength) could have been allowed. Review of the data showed that the slope of a leakage-stress curve was such that if the higher stress had been applied, the leakage could have been reduced. However, for tests 10 and 11, the maximum allowable stress was applied and sealing was not possible. Hence, it can be concluded that from that particular combination, nine assemblies were possible. The second set of Monomolecule surface finishes produced even more encouraging results. Only in one test of the eleven, that of assembly number 8 was 10^{-6} atm cc/sec unattainable. That test, where 36,000 psi was applied, resulted in the leakage dropping only to 10^{-5} atm cc/sec. The remaining three tests, numbers 9, 10 and 11, produced leakage rates below 10^{-6} quite easily. In general, lower stress levels were required than in the first set of specimens.

In both sets of samples, surface degradation was accumulated with the repetitive sealing. While the surfaces looked very rough locally, as shown in Figure 14, the damage remained local

Fig. 14 - Photo of Yatabe Stainless Steel Finish - After First Assembly Magnification: 510X.

and did not result in any continuous leak path being developed until the number of repetitions reached approximately 9 or 10.

Thirteen assemblies were accomplished on the stainless steel samples finished by the Jones Optical Works. Because of the high quality of surfaces noted, good results in the leak tests were expected. As before, the rise height was increased, again with indefinite results. Of the thirteen tests run, the first 9 produced leakages well below 10^{-6} atm cc/sec with stresses less than the yield strength. The tenth test resulted in leakage of 10^{-5} atm cc/sec and a very shallow leakage stress curve at a stress of 31, 000 psi. The eleventh test produced 10^{-6} atm cc/sec with a stress level of 36, 000 psi. However, tests 12 and 13 proved quite unsatisfactory with only 10^{-4} atm cc/sec being attainable in the 12th test and 10^{-5} atm cc/sec being attainable in the 13th test. Hence, the surface finishing technique is accredited with being better than the Japanese technique both from the point of view of observation and repetitive sealing.

Two other successful combinations of surfaces were tried, both involving surfaces finished by the Jones technique. Two 2024 aluminum surfaces KANIGEN plated prior to finishing resulted in ten successful assemblies; however, success in this case was accredited to leakage rates of approximately 2×10^{-6} atm cc/sec. It was noted, however, that this combination of surfaces resulted in the diminution of leakage rate down to approximately 4 or 5×10^{-6} at extremely low stress levels (approximately 20, 000 psi) and a rather shallow decrease in leakage thereafter. Also, the data was extremely reproducible from test to test.

In this case, the yield strength of the 2024 aluminum (51, 000 psi) was used and not the yield strength of the plating which is approximately 90% nickel and 10% phosphorous.

The final successful combination was that of a superfinished stainless steel specimen mated with a sealing surface plated with approximately 0. 003 in. of silver (also superfinished by the Jones technique). Herein, the superfinished sealing principle is not followed exactly. The allowable stress in the system was the yield strength of the stainless steel; hence, the silver plate yield strength was exceeded in each case. The experimental procedure in this case was modified slightly such that the same stress levels ending Phase I and Phase III were utilized in each experiment. This procedure duplicates a bit more realistically than in previous cases the stress imposition which would be applied to a sealing surface in a workable connector. The results of the stainless steel-silver test were that the system got better with the number of repetitions. The required stresses were in general lower and in no case was the system unsatisfactory.

As a result of the plastic deformation occurring on the silver surface virtually all surface degradation took place in the silver, and little change in surface characteristics were noted on the stainless steel after ten assemblies. Also, because of the plastic deformation occurring in the silver, the hysteresis slope between the curves of increasing applied stress and decreasing applied stress at high pressure was much greater. Thus, in this system the sensitivity to stress removal was less than in the previous cases, wherein purely elastic deformation had been used.

All other combinations of surface finishing and materials used proved unsatisfactory.

CONCLUSIONS

From the tests performed under the program described, it can be concluded that it is possible to seal repetitively a system made up of superfinished surfaces pressed together at stress levels of less than their yield strengths. It has been shown experimentally that for both 347 stainless steel and for KANIGEN nickel plated aluminum, satisfactory surface finishes can be obtained. It has been shown that, for the Japanese Yatabe surface finishing technique, up to seven reassemblies are possible under the framework of an allowable leakage rate of

10^6 atm cc/sec and an internal pressure of approximately 2,000 psi, and that the Jones Optical polishing technique surface was capable of obtaining nine assemblies. It has also been shown that the use of a thin soft plating on one of the superfinished surfaces produced even better results as far as the number of assemblies and the reduction in sensitivity of the seal to stress reduction is concerned.

In that sealing is adjudged to be elastic as is known from the small hysteresis loop of leakage and stress, and from post-experiment surface inspection, it is suspected, (although tests were conducted on a limited number of materials), that sealing will be effected by the elastic properties only, ie., Young's Modulus, and will not be too sensitive to yield strength itself as long as σ_y is greater than that of the materials mentioned herein. In other words, should an extremely strong material be used, with σ_y = 100,000 psi, it is expected that the stress to seal will remain appreciably less than that as long as "E" of the strong material is similar to that of 347 stainless steel.

As far as its present cost is concerned, the Yatabe surface finish can be obtained for approximately $200. The cost of a single Jones Optical surface finish is approximately $100. In that the Jones technique has proven satisfactory, and that such a surface finishing technique exists in this country, the Jones technique or its equivalent represents a better choice for future development of a prototype connector. Immediate hopes for cost reduction are such that, for a lot of ten, the Jones technique would result in a reduction of about 25% in cost. Reduction in cost beyond that for larger lots or mass production is not yet known.

The specifications for surface finish and flatness which were used as standards for the Jones Optical Works process appears to be adequate for satisfactory sealing. They are: a) flatness to within helium lightband (11.6 microinches), and b) roughness, no relief scratches deeper than one half microinch.

The remaining problem stated earlier, that of protection of the surfaces during handling and assembly, require two separate considerations. First no sliding can be allowed to exist between the mating parts. Second, in that the surfaces must be polished on high relief lands, a means of physical protection must be assured. A possibility for such protection is shown in Figure 15. In the proposed design of the connector utilizing superfinished surfaces, sheet metal rings would be attached to the connector components immediately after superfinishing and cleaning. Throughout the life of the connector, they would remain in place. Their dimensions and position in the connector would be such that no interference in connector assembly would be realized. In order to insure that no sliding exists between superfinish surfaces a tongue and groove type interlock could be used to prevent rotational sliding during the torquing operation; a shallow concentric male-female fit could be used to prevent lateral sliding.

The limitation to the concept of elastic sealing appears to be concerned with the size of a connector. In that flatness as well as surface smoothness is important, it appears that the technique would be valid only in fluid connectors having a rather small radius. Fittings up to approximately 1 inch could be considered for application of this principle. If larger diameters are considered, the problem of maintaining flatness becomes more and more acute and the radial rotation of the sealing surfaces under bolt loads becomes more and more significant.

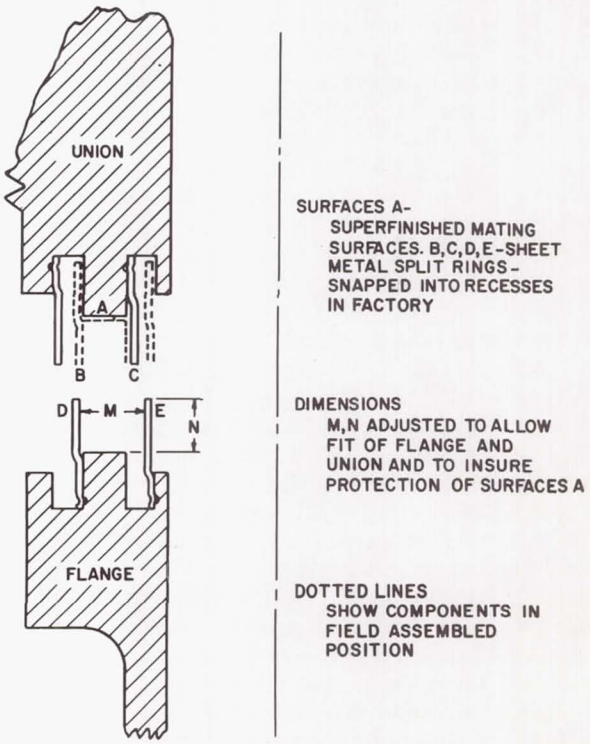

Fig. 15 - A Method of Protecting Fine Finished Connector Components.

REFERENCES

1. F. O. Rathbun, Jr., "Design Criteria for Zero Leakage Connectors for Launch Vehicles." Vol. III, Sealing Action at the Seal Interface. General Electric Company, Sch'dy, New York, N63-18159, NASA-CR-50559, (63GL43), March 15, 1963.

2. F. O. Rathbun, Jr., "Design Criteria for Zero Leakage Connectors for Launch Vehicles." Vol. III, Fundamental Seal Interface Studies and Design and Testing of Tube and Duct Separable Connectors. General Electric Company, Sch'dy, New York, N64-27305, NASA-CR-56571, (64GL97), June 1, 1964.

3. T. P. Goodman, "Design Criteria for Zero Leakage Connectors for Launch Vehicles." Vol. II, Leakage Flow. N63-18493, NASA-CR-50558, (63GL42), March 15, 1963.

AN EVALUATION OF A QUICK RELEASE FLUID COUPLING HAVING IDENTICAL MATING HALVES

By

W. T. Appleberry
Aerospace Systems Engineering
Missiles and Space Systems Division
Douglas Aircraft Company, Inc.
3000 Ocean Park Blvd.
Santa Monica, Calif.

ABSTRACT

A new quick disconnect fluid coupling features identical halves that provide male/female mating. Advantages are reduction of inventory and renewal of defective seals without installing new ones.

Two designs were evaluated: A hermaphroditic connector (coupling half converts from one sex to another), and a non-convertible coupling using a face or butt type coupling-to-coupling seal.

The hermaphroditic coupling was found superior. Advantages are (1) fewer seals used, reducing leakage, and (2) defective seals quickly replaced by simply converting both halves from one sex to another. Seals are standard O-rings and protected against contamination. The contributing factors to a low manufacturing cost are the shutoff valve and latching method.

THE NEXT BEST THING to making one part do the job of two, is to make two identical parts do the job of two which are dissimilar. At least that was the premise under which an evaluation of quick release fluid connector design was begun.

Normally, of course, the two halves of a fluid coupling consist of a male nipple and a female receptacle. The disadvantage of this coupling is that the male and female, being dissimilar, do require stocking of two different parts. Two things were to be determined: (1) can the job be done with identical halves, and (2) are such couplings economically sensible?

The mental concept of identical halves usually does not include the male/female mating principle and it was assumed that other ways must be found. Another general approach was indeed found which utilized the face seal principle. The result is a truly symmetrical coupling with no male or female features. A few companies have advertised it as being available, though not widely.

There is, however, at least one other general solution. It has been named the hermaphroditic coupling because either coupling half contains the capacity to be male or female.

As it turned out, the design evaluation consisted of a comparison between the standard, face seal, and hermaphroditic coupling.

Examining the face or butt seal design in greater detail, the two seals are placed together, then through either pushing the couplings together or twisting, the valves are opened. Latch design is usually of the bayonet variety.

On the other hand, a hermaphroditic connector could be described as containing the elements of both sexes in that each coupling half may be converted from one sex to the other.

To illustrate this principle, envision a piston in an open end cylinder (see Fig. 1). When the piston is drawn within the cylinder some distance, the assembly is female. With the piston extended past the end of the cylinder, it becomes a male fitting. Thus the two identical assemblies may be mated together as male and female.

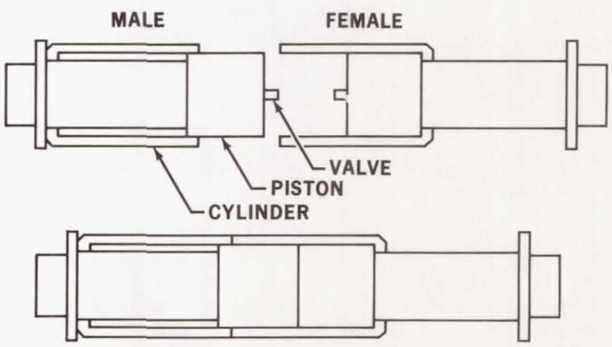

Fig. 1 - Hermaphroditic connector schematic

In a prototype design of the convertible system (see Fig. 2), the piston is the main coupling body and contains within it a standard solid poppet valve to seal the lines when the coupling is disconnected. The cylinder contains the coupling-to-coupling seals, the latching mechanism and the conversion control.

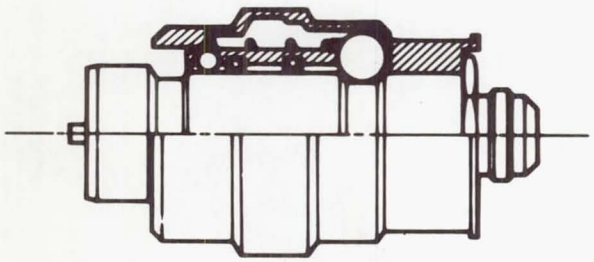

Fig. 2 - Hermaphroditic connector shown in male configuration

To convert from one sex to the other, the conversion ball located toward the aft end of the coupling is freed by moving back the outer sleeve against spring pressure. The piston may then be pushed or pulled to the male or female position (see Fig. 3).

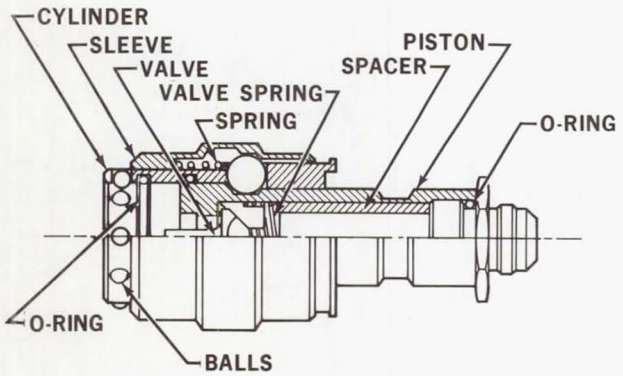

Fig. 3 - Hermaphroditic connector shown in female configuration

When going from male to female, the sleeve is held back by hooking the fingers around the rear circumference of the cylinder, then pulling the piston to the female position. While the same procedure may be used for the female to male conversion, an even simpler procedure is to grasp the sleeve in one hand and push the piston to the male position with the other. This automatically moves the sleeve back, freeing the conversion ball and allowing the piston to slide forward. The conversion ball serves the additional function of locking the coupling half together, eliminating the need for retaining rings. It should also be noted that the locking balls are prevented from scratching the polished surface of the piston because the outer sleeve cannot touch the balls while the piston passes by them.

Latching is fully automatic and is accomplished by simply pushing both coupling halves together (see Fig. 4). The male piston first moves the locking balls outward which, in turn, block the male sleeve causing it to remain stationary as the piston moves further into the female. Any scratches on the piston caused by the spring loaded locking balls begin outside the sealing area. In final position, the balls drop into the piston groove and the spring loaded male sleeve snaps over them, locking the two coupling halves together.

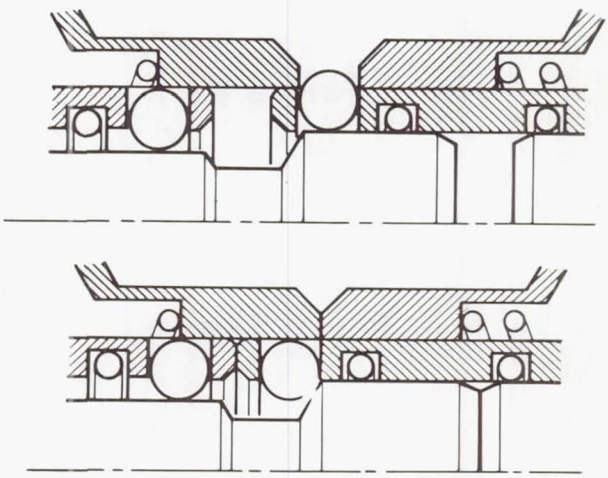

Fig. 4 - Hermaphroditic connector latching sequence

Unlatching is accomplished by pulling on the male sleeve. Like latching, it can be done with one hand if one of the coupling halves is bulkhead mounted.

When connected (see Fig. 5), sealing between the two coupling halves is provided by two internal O-rings in the female.

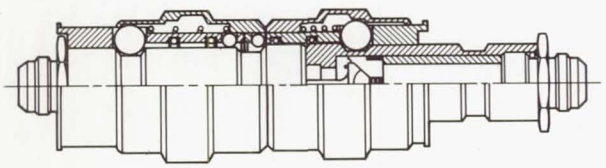

Fig. 5 - Hermaphroditic connector halves shown coupled

The first comparison to be made is between the standard coupling and both of the new couplings discussed. Reduced inventory was thought to be the primary advantage of the symmetrical class of coupling and constituted the original permise for design of such connectors. Were this indeed the only advantage, cost would become a most important consideration because the added expense of stocking two parts is but little more than for one part. Therefore, anything more than a modest increase in cost over that for a standard coupling would make the symmetrical design a sales liability.

Of course, if other advantages beyond reduced inventory could be shown, the permissible cost margin above the standard coupling would be increased. Such an advantage has been found in the hermaphroditic coupling. Should the coupling-to-coupling seal rings prove defective, permitting leakage, new rings are obtained in a matter of seconds by simply converting both halves to the opposite sex. How these spare O-rings are made available will be discussed in more detail in connection with the leakage characteristics of the different types of couplings. Compared to the advantage of reduced inventory, this feature may be of equal or possibly greater value and should serve to widen the permissible price margin above the standard unit.

The following comparison will answer the question, "how well do the three types of couplings fill their prime function of connecting two fluid lines together?" The standard coupling will be used as a reference point.

Beginning with the initial connection, both the standard and hermaphroditic coupling are joined by a single pushing motion. There is no need to orient or index the two halves before connecting. The face seal coupling, on the other hand, generally requires a bayonet type latch. Not only must the two halves be properly oriented before connecting, but after being pushed together, they must be twisted. Since the face seal type requires more attention, work, and time, the standard and hermaphroditic couplings appear more favorable in this respect.

As to weight and size, the descending order of preference would be: (1) standard, (2) face seal, (3) hermaphroditic. It may be of interest to note that one version of the hermaphroditic coupling may be attached to a standard male nipple. This interchangeability could prove advantageous both in reducing airborne weight and where more males than females are required. This latter situation arises often when several coupling halves are bulkhead mounted, but the hose is attached to only one at a time. To reduce cost, the bulkhead couplings are males and the single hose coupling is the more expensive female. The male nipples could be simply hermaphroditic couplings minus the cylinder assembly.

The foregoing leads to the possibility of two adjacent bulkhead mounted, face seal couplings causing crossed lines. Since there is no male or female, the hose could be attached to the wrong coupling. With the standard male and female mounted on the bulkhead, this could not happen, and with the hermaphrodite, the lines could only be crossed by intent.

What about leakage? Investigation showed this to be a prime factor and centered about the coupling-to-coupling seal. The standard coupling uses a single O-ring or chevron seal through which passes the male nipple. The hermaphroditic design is the same except it has two O-rings in series and, it would seem, twice the probability of leaking. However, the convertible coupling always has two spare O-rings in the male half. Should a leak develop in the coupling, it is only necessary to disconnect, convert both halves, and reconnect, thus deactivating the defective seal and bringing into use a new one. There is an enormous saving in downtime, and the life of the coupling-to-coupling seal is effectively doubled. In many applications, this will be one of the most important features of the hermaphroditic coupling. Of the inplant and commercial face seal coupling designs evaluated, all had at least two seals in series in each coupling half. While this appears similar to the hermaphroditic design, there is a difference: The O-ring in a male/female union presents two seal interfaces -- metal-to-elastomer-to-metal, and the two face seals when placed together form three interfaces -- metal-to-elastomer-to-elastomer-to-metal. Futhermore, all four seals act simultaneously in the face seal design, compared to two in the female half of the hermaphroditic. The

same two seals in the male are inactive. Counting interfaces or possible leakage paths, there are two in the standard coupling, four in the hermaphroditic, and seven in the face seal type. So as far as the static seal is concerned, the couplings should probably be rated in that order.

There are, however, other important leakage considerations in addition to the static seal. These involve principally the connect/disconnect cycle. When connecting the two coupling halves, the valves are opened before latching occurs. During this interval, tipping of one coupling half with respect to the other is possible with the face seal coupling. This opens the coupling-to-coupling seal, and, since the valves are also open, fluid is spilled. Uneven peripheral pressure on the face seal is nearly impossible to avoid. In the smaller coupling sizes, this is caused by clumsiness and, in the larger sizes, heavy flexible lines make it difficult to keep the coupling faces parallel. Inversely, if there is bending in the coupling as it is disconnected, tipping occurs before the valves can close, causing spillage or even a high pressure leak.

Tipping and the consequent spillage through open valves cannot occur in the standard and hermaphroditic couplings because of the male/female engagement.

During the mating cycle when a slip of the hand can easily occur, damage to one coupling face seal by the other coupling is possible, particularly if the connection is made under conditions of poor visibility. The face seal is exposed and, therefore, subject to damage and contamination in the course of normal handling procedures.

The standard and hermaphroditic coupling-to-coupling seals are located internally and are, therefore, protected from damage and contamination.

The importance of a narrow price margin over standard couplings has been mentioned, and a general cost comparison between the three types of couplings is in order. Maintainability will be included since it is closely related to total costs. Of the standard couplings evaluated, all had more parts of different design than found in the hermaphrodite. In other words, two convertible coupling halves contain a few more pieces than the standard male plus the female, but there are fewer different parts. Yet, because the standard coupling has only a male nipple on one side and requires but one latching system, it should be lowest in price. The standard/hermaphroditic couplings can use a conventional solid poppet valve, probably the most economical type on the market. The face seal couplings generally use either a special keyed poppet or a hollow slide valve surrounding a stationary core that is anchored to the coupling body by webs. Either of the latter valve designs are obviously more costly. The standard/hermaphroditic couplings can utilize the steel ball latching system which, because of its popularity, may be assumed to be quite economical. The nature of the face seal coupling, however, suggests a bayonet type latch which requires more elaborate manufacturing procedures.

As for maintainability, the O-rings are, of course, most easily renewed in the standard coupling, which need not be disassembled to replace the coupling-to-coupling seal. The face seal and hermaphroditic coupling must be partially disassembled to replace the aft seal. The forward seal, though, is more easily replaced on the hermaphrodite since it is a standard O-ring, whereas the face seal is of special design. This raises the question, "what has been saved by making both halves alike if a new type of seal must be added to the list of spare parts?" Space, perhaps, but not bookkeeping.

CONCLUSION

It is conceivable that overall costs could be reduced by the use of a coupling having identical mating halves. Reduced inventory is the general advantage of symmetrical couplings and where this is the only significant advantage, any additional manufacturing cost must be quite marginal. In this respect, the hermaphroditic coupling clearly was closest in price to the standard design. Moreover, the hermaphrodite possesses another prime advantage in its automatic and nearly instant renewal of the coupling-to-coupling seal. From the function aspect, the additional twisting motion required a trifle longer to latch and unlatch the face seal coupling, but on the other hand, it does not require conversion. From the human factors standpoint the need for conversion would rate the hermaphrodite downward. Yet, conversion is quite rapid, taking only about the same length of time as it does to connect the two coupling halves. Also, conversion should be a quite infrequent necessity since normally the right coupling halves will be brought together. And, of course, only one half need be converted.

The net conclusion is that the excessive cost and substandard performance of the face seal coupling leave only a choice between the standard and hermaphroditic

versions. Though the latter is heavier, function and performance levels are sufficiently close that the deciding factor will probably come in balancing the scale between increased manufacturing costs on the one hand, and the combined benefits of reduced inventory and automatic seal renewal on the other. At this early stage in the development of the hermaphroditic coupling, cost analyses to date would have it seem probable that this balance can be reached.

Page Intentionally Left Blank

TWO FLUID CONNECTOR JOINING TECHNIQUES INVOLVING LARGE METAL DEFORMATION

By

J. P. Laniewski
F. O. Rathbun, Jr.
L. G. Gitzendanner
Advanced Technology Laboratories
General Electric Company
Schenectady, N. Y.

ABSTRACT

Two separate techniques potentially useful in connector assembly, both involving large deformation of metals, are described. The first, that of cold welding or pressure welding, offers the possibility of establishing a hermetic seal which, if properly designed, is relatively insensitive to stress relaxation elsewhere in the structure. The incorporation of a cold welded seal into a prototype flanged connector suitable for 6,000 psi gas service for cryogenic temperatures is described.

The second technique, high energy rate forming (HERF), offers distinct possibilities for structural component assembly and limited potential for establishing a seal. Both magnetic forming and explosive forming, often with welding resulting in the latter case, are discussed.

THE REQUIREMENTS PLACED ON FLUID connectors for aerospace applications can be considered novel; extremely low leakage rates, minimization of system weight, and imposition of extremely harsh environments, including temperature excursions, temperature transients, and vibration, all combine to place severe demands upon the connector designer. While, very often, conventional flanged or threaded tube connector configurations can be made to fulfill these requirements if properly designed, it is not appropriate to limit consideration to those geometries only. Novel approaches to the connector design problem are indeed appropriate, if those approaches offer solutions to some connector problems which more conventional designs find more difficult to conquer.

One of the problems which separable connectors find difficult to overcome is the relaxation of stress at the seal interface during the operational life of the connector. Various seals used possess varying degrees of sensitivity to tension load reduction; hence, all separable connectors are somewhat sensitive to this phenomenon. Should a connector concept allow nearly complete insensitivity to bolt load reduction, then even though such a connector may possess the disadvantages of increased assembly complexity or disassembly difficulty, the design would possess merit.

One design for a semipermanet connector which is insensitive to bolt load reduction incorporates a cold pressure weld on flexible components which have no purpose other than sealing and which are protected structurally from the imposition of the pressure and externally applied loads.

Another technique which can be added to the list of joining (and perhaps even sealing) techniques is that of high energy rate forming of connector structural components. The two notable methods for accomplishing high energy rate forming are magnetic and explosive. Both are evaluated herein with regard to the structural joining capabilities and sealing capabilities.

While pressure welding and high energy rate forming have little in common with regard to the techniques employed for accomplishing the joining, they do have a great deal in common with regard to the amount of deformation imposed on the metals. Both require deformations well into the plastic range of the materials. Pressure welding deforms the metal in a quasi-static manner and does not rely specifically on the flexibility of the geometry. High energy rate forming deforms a connector geometry grossly, thus effecting an interlock between components. In some cases, depending on the speed of the operation, welding is effected.

To assess the potential of cold welding as a connector sealing mechanism, a prototype 2 inch flanged connector, constructed from 6061-T6 aluminum and designed for 6,000 psi service at temperature extremes of liquid helium to +100 ^{o}F was designed, fabricated, and subjected to an

environmental testing program. The results of the use of pressure welding in such an application and under such an environment is described herein. With regard to high energy rate forming, the techniques of magnetic forming (Magneform*) and explosive forming were investigated experimentally as applied to varying potential connector geometries. The results of this investigation form the second portion of this paper.

COLD WELDING OPERATION

Cold welding is the technique of causing a weld to develop across an original interface between two like metals by the imposition of forces, generally normal to those surfaces such that stresses sufficient for the breakdown of the interface occur and a metallurgical bonding is effected. While many metals can be pressure welded, the more ductile, and very often the weaker materials are more prone to the phenomenon. Very often, the stresses necessary to cause welding result in material deformations reducing the thickness of the plates to be bonded by as much as 70% to 80%. Inherently, the phenomenon of cold welding depends on material thickness, material cleanliness, and shape of the die which is used to impose the load. For connector application there exists the added parameter of sufficient flexibility such that material adjacent to the weld can flow, along with the requirement for rather exact placing of the dies opposite to one another.

While several materials might have been chosen for experimentation and incorporation into a semipermanent connector design, only that of 2S aluminum was utilized since it is inherently compatible with welding to an aluminum structure and it is one of the better materials for cold welding in a normal atmosphere. One of the requirements for the cold welding technique to be useful in a connector assembly is that it not require an inert atmosphere or a vacuum. In a preliminary study conducted prior to the application of cold welding in a connector geometry, certain parameters with regard to die shape, cleanliness, and material thickness were studied. It remained until the application of the process to an actual connector for the problem of exacting requirements of die location and flexibility of the material to be welded to arise and be solved.

With regard to cleanliness, we scratch brushed the aluminum surfaces to be welded with a stainless steel brush with a scratch brush velocity of 4200 ft/min. The question immediately arose as to how long after the scratch brush cleaning a weld could be made. It is known that immediately upon producing a new surface and subjecting it to an air environment, an aluminum oxide layer is formed. It was found that, if only normal precautions were taken, i. e., plastic bagging the specimens shortly after scratch brushing, that welding could be accomplished at least up to 30 days after the scratch brushing.

Having gained some assurance that the cleanliness requirement was such that it could be met in the normal logistics requirement, the next problem addressed was that of the shape and dimensions of the dies and the material to be cold welded. The preliminary study showed that die shape had a very important effect on the resultant weld. It was concluded that the width of the die should be approximately twice the thickness of the sheet to be welded. Also, the die closure should be provided with a stop such that between 70% and 80% decrease in thickness will result. Both rectangular profiled dies and semicircular die cross-sections were used. Only with the rectangular cross-sections (with slightly rounded corners) was success found repeatably. The thicknesses of the 2S aluminum plates used were 1/16" and 1/32". Both resulted in adequate cold welds. However, because of reasons associated with the connector configuration, the 1/32" plates, although inherently weaker structurally, were chosen for incorporation into the final connector design.

APPLICATION OF PRESSURE WELDING TO A SEMIPERMANENT CONNECTOR DESIGN CONCEPT

In that pressure welding can be practically accomplished only on thin materials having limited structural capacity, the concept as applied to fluid connectors containing high internal pressure, requires the cold weld to replace the seal only. It must not be required to withstand any structural loads. In other words, the cold weld must be backed up almost completely by structural members. While it is not necessary for the structural members to impose a high stress on the weld, it is necessary that a large degree of separation between the supporting members does not occur, thus causing the weld itself to take on a structural task. While the hermetic seal so effected offers a leak-tight connection, it also requires that it be effected at the assembly site, preferably without special tools. In that it is a weld, provision in the design must be made to disassemble and reassemble the connector, at least a limited number of times. Provision for three operations of this nature were made in the test connector.

A requirement of the tension members of the connector, in this case the bolts , was to

*Magneform - trademark, General Dynamics Corporation

have sufficient strength to impose enough load to the weld area to effect the seal. The resultant connector, if successful, would then be a "zero" leakage connector having a degree of insensitivity to the relaxation of the tension members. It would fall into the category of a semipermanent connector, not for assembly purposes, but for disassembly purposes in that a limited number of assemblies could be made and a special cutting tool of some sort would be necessary for the weld cutting.

BASIC CONNECTOR CONFIGURATION

The basic prototype connector configuration is shown in Figure 1. It must be mentioned at this point that the dimensions of the test connector shown were not optimized in that the investigation was to be a test of the concept of pressure welding only. Since a portion of the testing program called for the gross reduction in bolt load, such as might occur during the operational life of the connector, the sensitivity of the cold weld to the remainder of the structural design became somewhat limited, i. e. the seal and structural members were somewhat decoupled. In other words,

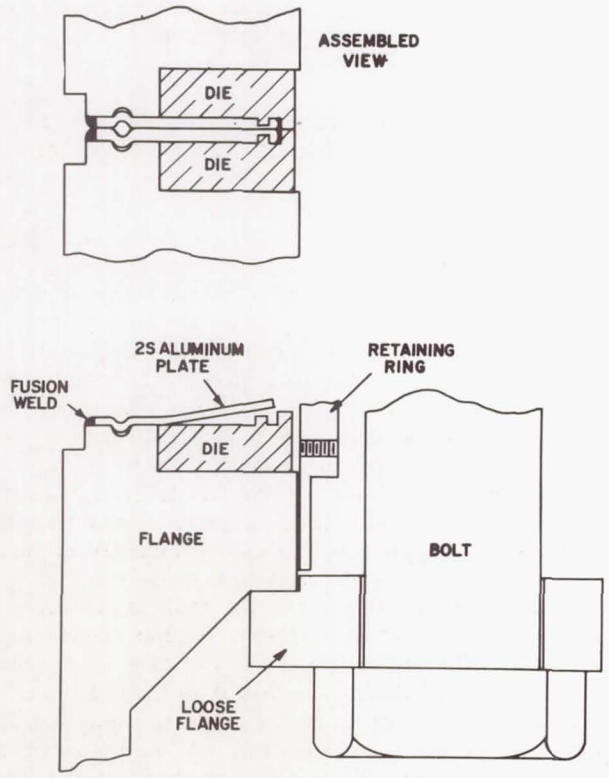

Fig. 1- Basic Cold Welded Flanged Connector Configuration

the particular design fabricated and tested was not an effort to achieve an ultimate light weight design. However, the use of the cold welding technique in a flange connector does inherently allow ultimate weight of the design to be dictated by internal pressure and external load configurations, and not the maintenance of a sealing load on a gasket.

Essentially, the design called for two round plates of 2S aluminum to be fusion welded to the main flange elements. The flanges, being made of 6061-T6 aluminum were typical structural aluminum. Two sets of split dies made of stainless steel were inserted into the flange recesses before an assembly was to take place. The inner surface of the dies have an annular projection machined on them. As the bolt forces were applied through the loose flanges, the projections were forced into the soft aluminum by virtue of the displacement of the connector flanges. The dies possessed an integral physical stop so that they could be pressed together the predetermined amount resulting in a 70% to 80% reduction in thickness of the 2S aluminum plates under the die projection. Upon completion of the tightening of the bolts, the connector then became ready for service. The dies remained in place to supply the structural backup for the 2S aluminum cold welded seal. Should the bolt loads become relaxed, then although the stresses imposed on the cold weld by the dies decrease, the amount of displacement is minimized due to the alternate load path existing in the connector design. The alternate load path is accomplished by having the split die rings stepped up near the outside edge, thus fulfilling two requirements, that of the physical stop and the alternate load path.

For prescribing the location of the dies during the assembly procedure, an aluminum ring was placed outside the connector periphery, but inside the bolt circle. Set screws through the aluminum ring hold the dies in the correct position. The ring has several viewing ports machined into it such that visual inspection of the dies during the bolt tightening operation can be made. When the dies came together, the sufficient degree of bolt tightening would have been accomplished. Figure 2 shows the two 6061-T6 flanges with 2S aluminum plates fusion welded to them. It can be noted that, in order to fit the split dies beneath the 2S aluminum plates, the plates have been tilted upward approximately 15^{o}, thus affording room for the split dies. Figure 2 also shows the die locating ring, with the viewing ports and set screws.

For disassembly of the connector, the procedure calls for removal of the loose flanges, bolts and nuts, and slight separation of the lap

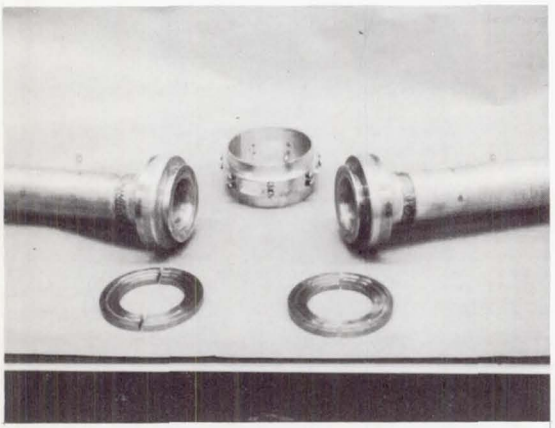

Fig. 2- Integral Connector Flanges With 2S Aluminum Plates Welded to Them, Along With Retaining Ring and Split Dies

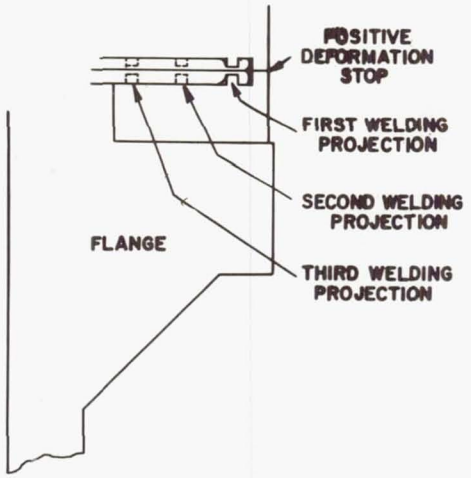

Fig. 3- Welding Die Operation

flanges by an axial force. This allows the split dies to be removed from beneath the aluminum plates. In that a weld exists between the aluminum plates at this time, the system will remain integral, although only by virtue of the weak aluminum. When the split dies are removed, a set of split cutting dies are put in their place. The cutting dies have a knife edge such that when the bolts are retightened, the 2S aluminum plates are severed just inside the initial cold weld. Now the flanges are completely separate and the connector can be completely disassembled. For the second assembly, a second set of welding dies are placed into position, these with welding projections placed closer toward the center of the connector. The assembly and disassembly procedures for the second weld are identical to the first, the only difference being the use of cutting dies with a smaller radius. The geometry for the typical duct connector is such that the flanges will support 2S aluminum plates and dies in a space envelope allowing three different sets of welding and cutting dies, thus allowing the connector to be assembled twice after initial assembly. One negative attribute to such a system is that the area over which the internal pressure acts is near the outside of the internal flanges for the first assembly and decreases with each assembly. However, the structural components of the connector must be designed for the first case, which offers the most stringent loading on the system. Figure 1 shows the welding die-aluminum plate configuration in the before and after welding condition. Figure 4 shows the actual dies used in the connector assembly. Figure 5 shows the operation of the weld cutting dies. Figure 6 shows

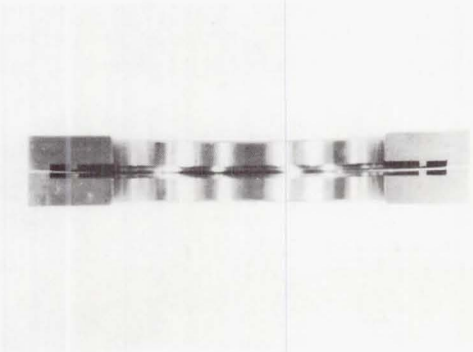

Fig. 4- Welding Dies Actually Used

a closeup of the connector as seen through an observation port in the die locating ring. In the figure, it can be noted that the space between the dies has been reduced to zero. Figure 7 shows the connector in a completely assembled condition.

PROBLEMS ASSOCIATED WITH APPLICATION OF COLD WELDING TO FLANGED CONNECTOR DESIGN

In basic studies of cold welding, previous investigators (1-9)* have treated the problem of cleanliness, die geometry, and relative dimensions between die and welding plate. In most of those investigations, the ability of the material

*Numbers in parentheses designate References at end of paper.

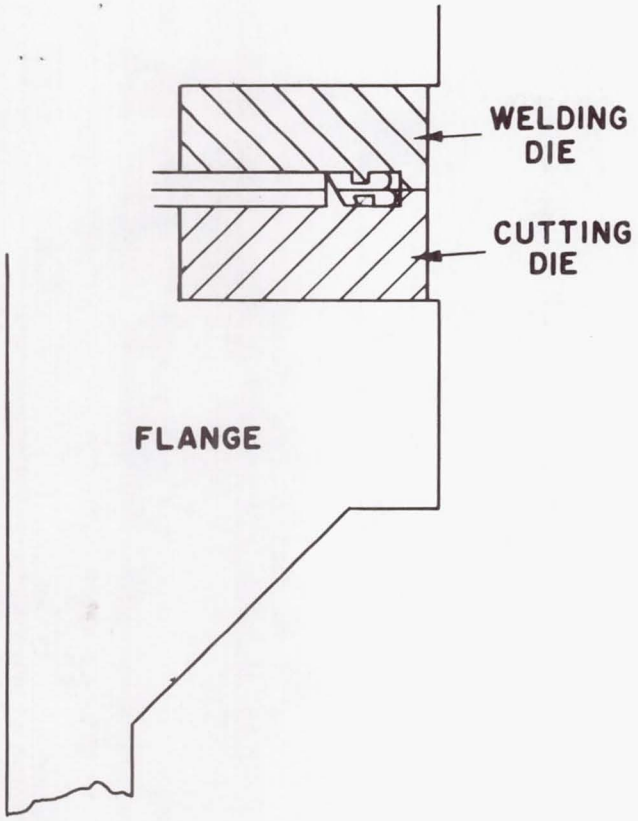

Fig. 5- Weld Cutting Die Operation

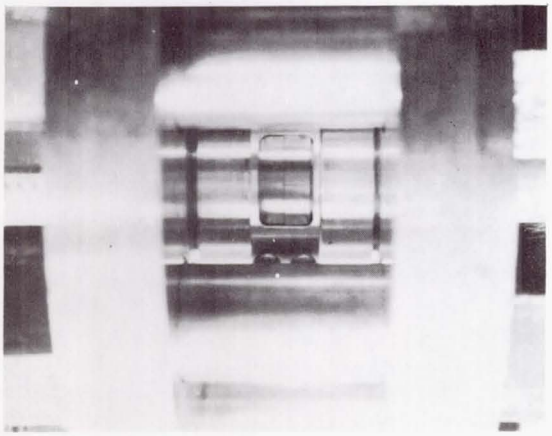

Fig. 6- Closeup of Assembled Connector - Welding Dies Can Be Seen Through Observation Holes

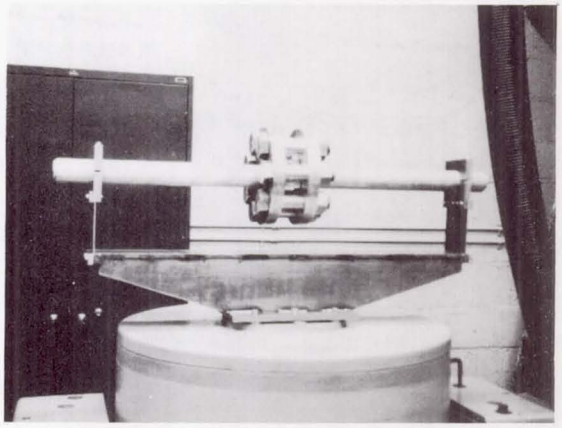

Fig. 7- View of Assembled Cold Welded Connector

to be welded to flow in a direction perpendicular to die application was assured by the nature of the experimental setup. In a fluid connector, however, the shape considered is that of an annulus. In such a shape, in that the inner radius of the annuli must be rigidly fixed to structural flanges by fusion welding, a great deal of resistance to flow inward of the welding material exists. Similarly because of the tangential tensile stresses developed in the aluminum plate outside the weld, a resistance to radial flow outward exists. Nothing needs to be done about the latter problem, but it was found during the development program that something had to be done about the former problem. The tendency to flow radially inward is so great that,in one instance, the fusion weld between the 2S aluminum plates and 6061-T6 flanges was broken locally by the force imposed upon it. The radial distance between both welds was one-half inch. Hence, some means had to be employed to introduce flexibility into the 2S plate system. The first design, shown in Figure 8, had very little flexibility. A second proposed design, shown in Figure 9, had increased flexibility; the plates could bend inward with radial flow because of the axial section of soft aluminum. However, the configuration was not possible because of the difficulty in making the fusion weld on the inside of the duct wall. The third configuration which proved to be almost completely successful, was that shown in Figure 1. The flexibility is gained with the presence of a semicircular convolution which fits into a recess on the 6061-T6 aluminum flanges. As the

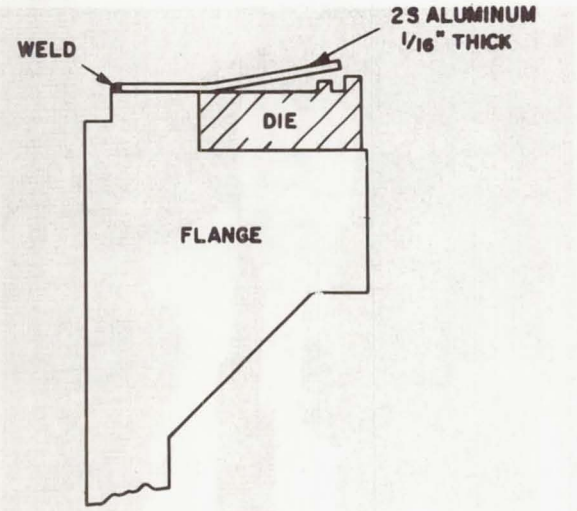

Fig. 8- Initial 2S Aluminum Plate Configuration

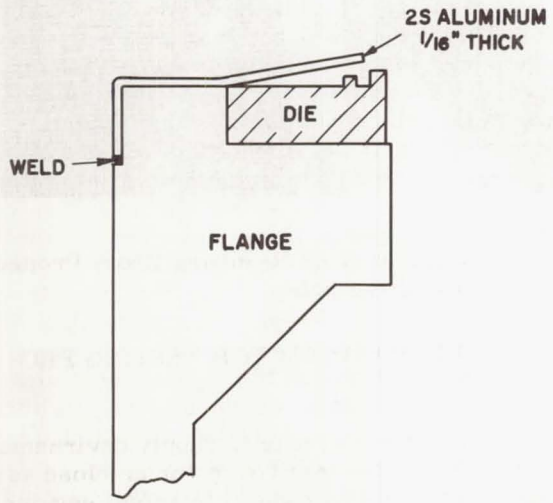

Fig. 9- Second 2S Aluminum Plate Configuration

2S aluminum tends to flow inward, bending occurs at curves in the "knee" which exists at the semi-circular depression.

The remaining problem, not obvious from initial studies on cold welding was solved by requiring die concentricity. In one instance, a weld was made with the dies not concentric, and the weld shown in Figure 10 resulted. As a reference, the reduced thickness area is 1/16", the width of the die. The irregularity of the weld junction line can be noted. If dies were concentrically located, the thicknesses of the 2S aluminum plates in the weld area should have been

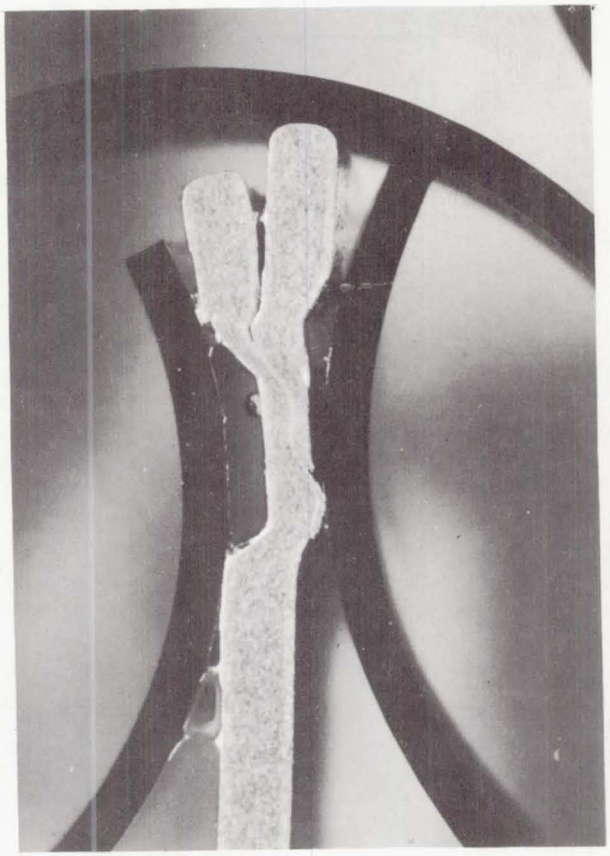

Fig. 10- Weld Resulting From Eccentric Dies

equal. Correction of this deficiency was attained by a general tightening up of die dimensions and the placing of a shim between the external surface of the dies and the die locating ring. In a finalized connector design, this problem is envisioned to be minimal, in that normal quality control would preclude eccentricities of the magnitude causing the weld shown in Figure 10. However, even with the vast eccentricity existing in the test cited above, a reasonable weld did exist, and is shown in high magnification in Figures 11 and 12. The large black globules are entrapped foreign material such as aluminum oxide or other matter.

After the design had been modified to assure die concentricity, all remaining welds made were of the type and quality shown in Figures 13, 14 and 15, which are a typical cross-section.

The torque on the seven bolts of the prototype connector necessary to seat the dies and thus cause a pressure weld was 200 foot pounds. The magnitude of this torque is not considered to be indicative of the torque required in a finalized design.

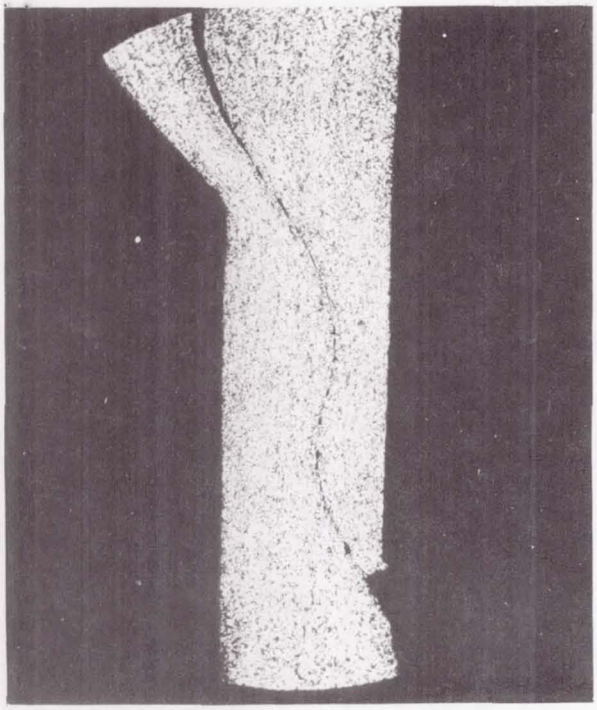

Fig. 11- Higher Magnification of Weld Shown in Figure 10

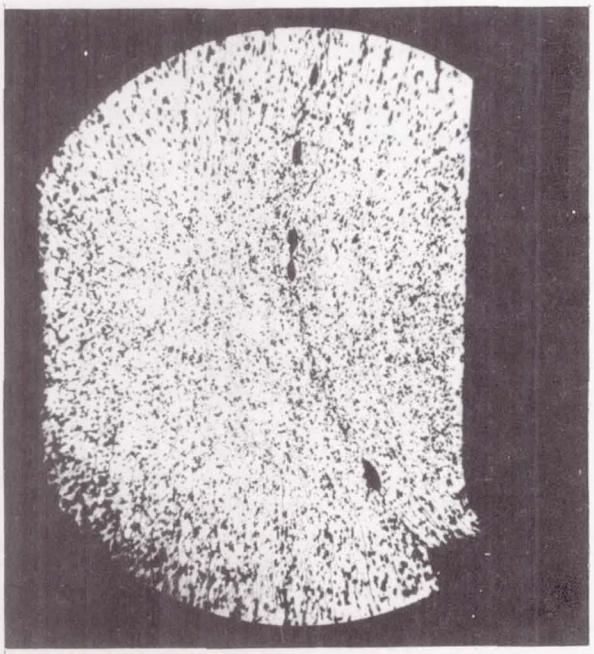

Fig. 12- Higher Magnification of Weld Shown in Figure 11

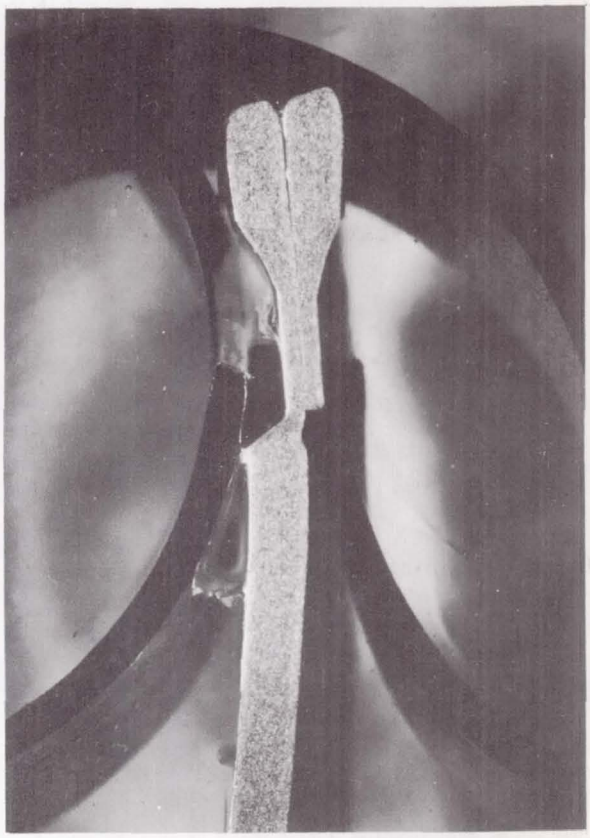

Fig. 13- Typical Weld Resulting From Proper Die Positioning

COLD WELDED CONNECTOR TESTING PROGRAM

Attempts were made to supply environmental conditions to the test connector as close as possible to those experienced in actual service. In all high pressure tests made, helium gas was used as the pressurizing medium. A helium mass spectrometer leak detector was used to record connector leakage. A bellows assembly completely enclosed the connector assembly when a leakage test was made. It provided the necessary vacuum chamber for the leak detector, as well as allowing freedom for connector movement during shock and vibration.

"Zero" leakage as defined herein means no measurable leakage within the sensitivity of the mass spectrometer ($< 1 \times 10^{-7}$ atm cc/sec).

Table 1 is a summary of the tests accomplished on the pressure welded test connector and the resulting leakage recorded. High gas pressure is achieved using a booster compressor with the capability of boosting to 30, 000 psi an inlet pressure of 2, 000 psi.

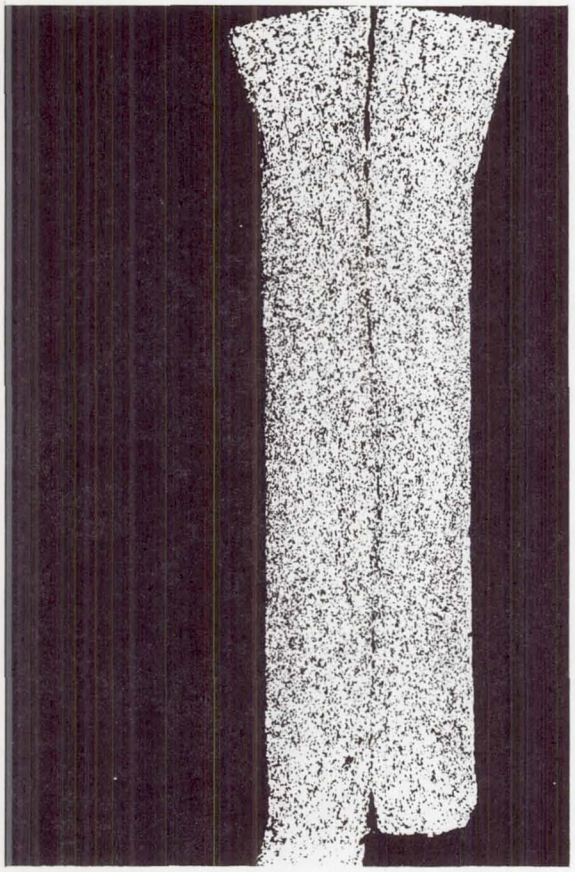

Fig. 14- Higher Magnification Photo of Weld Shown in Figure 13

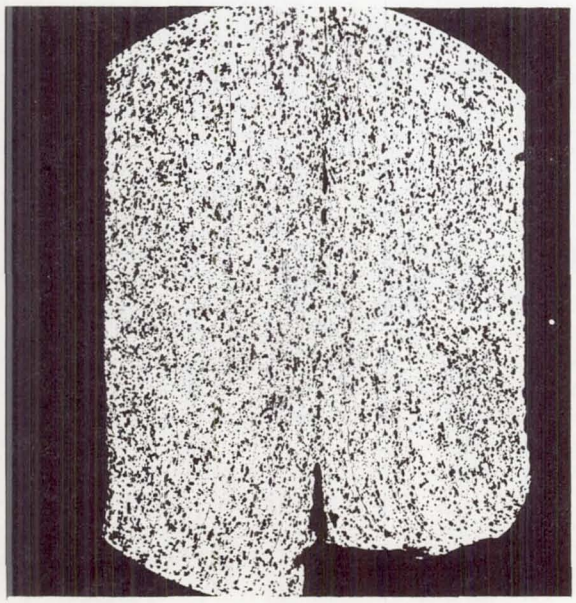

Fig. 15- Higher Magnification Photo of Weld Shown in Figure 14

Table 1- Cold Welded Connector Tests and Results

Test			Leak
Pressure (psi)	Temperature (°F)	Description	
Vacuum	Room	Initial vacuum check, tight bolts	0 ($< 10^{-7}$ atm cc/sec.)
Vacuum	Room	Second vacuum check, loose bolts	0
4600	Room	Initial pressure test	excessive
Pressure weld annulus cut from connector; second pressure weld made at smaller radius; die eccentricity corrected			
5200	Room	Second pressure test	not recorded
Duct failure, new ducts welded on to connector; fusion weld between plates and flanges repaired			
6000 (rated)	Room	Successful pressure test	0
6000	-321°F	Cryogenic test	0
200	Room	Vibration test, 200, 000 cycles, 10, 000 psi bending stress applied	0
6000	Room	Post-vibration pressure check	0
200	Room	Vibration test, 200, 000 cycles, 10, 000 psi bending stress, 1/4 original bolt torque	0
4800	Room	Post-vibration pressure check	excessive

As indicated in Table 1, an initial vacuum check showed the seal to be effective. No leakage resulted from the application of an internal vacuum to the connector. A second vacuum check with the bolts loose precluded the existence of only a vacuum seal. This check showed a complete cold weld seal.

The first application of internal pressure to the connector resulted in leakage occurring at a pressure level of 4, 600 psi. An immediate large leak occurred and of such high magnitude as to overcome the ability of the leak detector to operate at this level of leakage. Subsequent investigation showed a leak in one of the thinned out sections resulting from lack of die concentricity described earlier (Figure 10).

After the pressure test, the ducting in the immediate area of the lap flange weld was noticed to have yielded. After correction of the die concentricity problem, a second pressure test was made without the bellows attached. At a pressure of 5, 200 psi a rupture occurred in this weld section as seen in Figure 16. The rods visible at the inside of the connector were inserted for the purpose of reducing the inner volume of the connector assembly. This was necessary to conserve time, since the booster compressor output was very small. Subsequent investigation showed the fusion weld between the weld plates and the lap flanges had been ruptured by one of the aluminum rods during the sudden failure. The pressure weld, however, was intact. Rupture, evidently, started at a poorly welded area and propagated from that point.

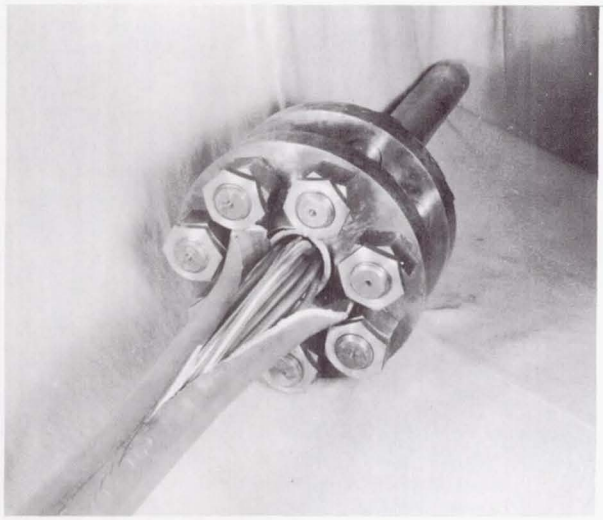

Fig. 16- Failure of Duct-Flange Weld at 4600 psi Internal Pressure

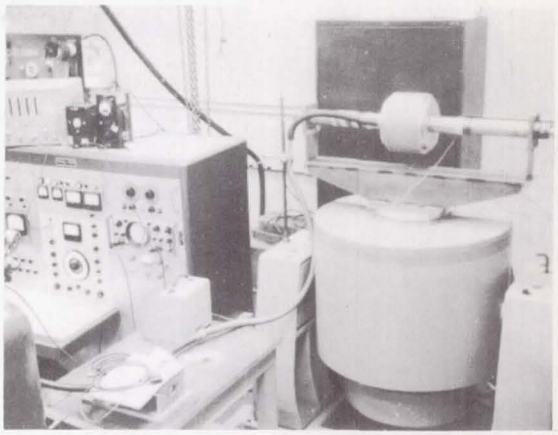

Fig. 17- Cold Welded Connector With Vacuum Bellows Mounted on Vibration Fixture

With the correction of these deficiencies the connector was reassembled and a third successful pressure test was made to a level of 6, 000 psi, the design pressure of the connector. No leakage was observed for this test. It is to be noted that the final cold weld was accomplished on 2S aluminum plates previously cold welded, with the first weld removed by the cutting die operation. The cutting technique proved completely successful, and, coupled with the attainment of a new cold weld in an already strain hardened area, proved to be two major accomplishments.

A cryogenic temperature test followed. The connector assembly was placed in an insulated tank and liquid nitrogen poured in over it. A thermocouple mounted directly on one of the welding dies gave a temperature indication, and when it stabilized at the liquid nitrogen temperature, the gas pressure was introduced until the rated 6, 000 psi was attained. No observable leakage was recorded for this test. After the connector successfully passed this portion of the test, the rods were removed from the ducting and the connector was mounted in the vibration fixture, as shown in Figure 17. The fixture, mounted directly to the shaker coil of the vibration machine, is designed to transmit amplified vibrations to the connector through the thin flexural supports. The supports are placed to simulate typical connector mounting, and, rather than impose a specific "g" level loading which could result in any stress depending on the mounting, a stress level was decided on instead. A figure of 10, 000 psi maximum bending stress was chosen to be representative of the stresses witnessed by a connector during vibration in actual service. The stress was monitored by strain gages mounted to the surface of the ducting, and arranged so that this stress level would appear at the joint between the lap flanges and the ducting.

A 200 psi internal pressure was applied to the connector and leakage was monitored during vibration . The lower pressure figure was necessitated by the safety aspect because of the physical location of the vibration machine. No measurable leakage resulted during the test of 200, 000 vibration cycles.

Application of 6, 000 psi rated pressure as a post vibration check showed the connector and seal to be sound with no leakage recorded.

In that the major goal of a cold weld as applied to a flange connector is that of insensitivity to bolt load reduction which may occur during the operational life of the connector, the bolts were then relaxed and retorqued to approximately one quarter of their original value, now being torqued to 50 foot pounds. The connector was then subjected to an identical room temperature vibration test as before. During this test no leakage was measured.

However, when a 6, 000 psi room temperature leak test was attempted with the bolts remaining in their loose condition, as the pressure reached 4, 800 psi, a leak was noted via the mass spectrometer measurement. The vacuum bellows was removed from the connector, and the location of the leak was sought. By vacuum leak test techniques, the peripheral location of the leak was determined.

In order to evaluate the extent of the leak, the cold welded plates, after being removed from the connector by the knife die cutting operation, were sectioned and photomicrographed after etching. Six cross-sections were picked in the area of the leak. A sample cross-section, very close to the suspected leak area is shown in Figure 18. Five other cross-sections of the weld were made about the remainder of the plate periphery. Essentially, each cold weld looked the same. No obvious leak passage in the weld was noted. Thus, the actual location of the leak, which was of the order of magnitude of 7×10^{-6} atm cc/sec at an external pressure of 14.7 psi (vacuum check) was not found. However, as can be noted in Figure 18, near the inside diameter of the weld (top of photo) a crack from the inside toward the outside of the weld can be noted. Two possible causes exist for the crack. Upon removal of the cold welded plates from the connector, the two lap flanges are moved apart axially, thus resulting in a bending of the aluminum plates in an area which is to be no longer used, namely the cold welded area. Cracking at that location could have resulted from this action. Also, it is to be noted that since the die had the ability to move axially slightly because of the reduced torque on the bolts, the internal pressure acting up to the weld, further compressing the aluminum plates. Thus, it is possible that internal pressure caused the crack by shear deformation fracture of the aluminum plates. The degree of seriousness of the latter phenomenon is expected to be minimal, in that the same cracking was noticed all about the periphery, and that the amount of displacement of the dies would not be expected to be as great in an optimally designed connector. Nor would the bolt load be expected to reduce itself to one quarter of its original level.

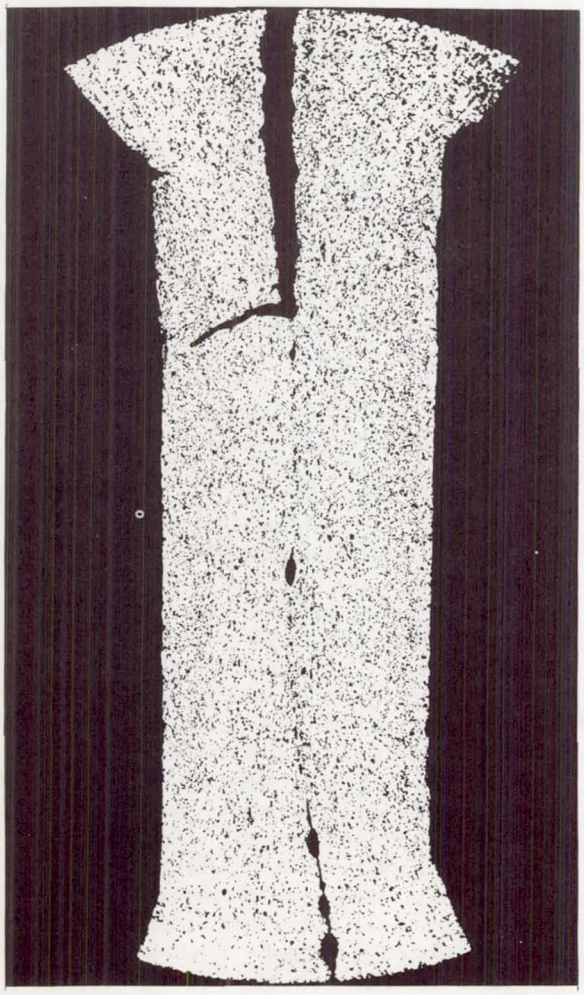

Fig. 18- Cross-section of Cold Weld in Final Leak Area

HIGH ENERGY RATE FORMING

High energy processes in existence today provide a means of plastically forming metals at very high strain rates. These processes have characteristics which are different from those of processes which form metals at slower rates, and there is reason to believe that the characteristics of high energy processes may be advantageous in making fluid connector joints. High energy processes have been used in place of mechanical swaging to join tubular pieces with excellent mechanical strength resulting. They have also been used in other applications to cold weld metals together. Thus, the possibility exists that one could form a joint which would be both mechanically sound and hermetically leak tight.

An investigation was conducted to determine the feasibility of applying and further developing high energy processes for forming fluid connectors. Factors considered included the technical feasibility, performance characteristics of the joint - its advantages and disadvantages compared to more conventional design joints - ease of using the process and special equipment required.

Following a preliminary investigation it was decided to investigate in greater depth the possibilities of two high energy processes, namely, magnetic forming and explosive forming.

Magnetic forming requires the use of an electrical apparatus, while the explosive process employs the potential energy of explosive material. Each technique possesses advantages and disadvantages. However, it was felt that each could be adapted, with some development to field application.

The magnetic method will be discussed first, with the explosive technique to follow. Since the use of each method was an attempt to obtain an intimate seal, and in some cases cold welding along with structural soundness, a variety of tests were made with each technique. The test test configurations as well as the results will be described in detail.

MAGNETIC FORMING TECHNIQUE

The magnetic forming machine used in this study was a General Dynamics Corporation product called Magneform. It is a device which applies stored electrical energy to a workpiece - in this case a tube joint - by means of a coil and field shaper combination. A charged capacitor bank is suddenly discharged through the coil which is placed around the tube. The changing magnetic field produces an induced emf in the workpiece. (10) The reaction produced by the induced magnetic field with the primary inducing field results in high forces being generated on the workpiece. In all of the magnetic forming tests made, the machine was operated at its maximum output of 6 kilojoules. The primary purpose of the shaper piece is to direct the lines of force where required.

This technique is most successful when used on workpieces made of materials with a high conductivity and low permeability. It is possible to use other materials, such as stainless steel, having poorer conductivity or higher permeability, but the process would not be as efficient and would require either a larger machine or use of a "driver". For initial work, and having limited capacity in the machine which was available, it was desirable to minimize development problems by using aluminum.

A basic tube joint design was chosen to be used in the investigation of the magnetic and explosive forming methods. Figure 19 shows this configuration. It consists of an insert, and two lengths of close fitting tube sections. The insert material was 2024-T4 aluminum and the tube, for comparison tests, was relatively soft 3003-H 14 aluminum for some samples, and the hard 6061-T6 aluminum for others.

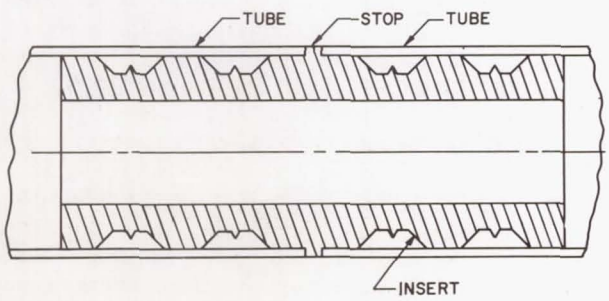

Fig. 19- Basic Configuration of Insert and Tubes for HERF Assembly Techniques

The reduced inner diameter of the insert bore, while detrimental, is not inherent in the process. It must be kept in mind that this was a feasibility program with no finalized design for this or for the other configurations to be described. Inner tube diameters would be preserved by the simple sizing up operation used for some tube installation today. This would result in essentially two bell shaped tube samples to be joined with an insert of the same inner bore diameter as the tubes. For the development work, this sizing up operation was not included.

The insert geometry (Figure 19) possesses two knife-edged sections on either side of the stop. The magnetic energy was directed into each section and the tube deformed over the knife edges. This procedure results in slip between the two materials - an ideal condition for producing a cold weld.

Two inch and three-eighths inch outside diameter tubing samples were chosen for the investigation as sizes which would be indicative of results one could expect over the range of interest. The low power limitation of the Magneform machine available ruled out testing with the two inch size, while problems associated with reducing power with the explosive process necessitated working with this size. Hence, 3/8" tube samples were used in the magnetic forming and 2" for the explosive forming.

MAGNETIC FORMING TESTS

The first magnetic forming tests resulted in excellent tube joints. One joint made in this manner was leak tight in a vacuum test before and after a 200 g's vibration test for 15 minutes' time. A second joint was pressurized with helium up to 2,000 psi internal pressure for a period of 24 hours with no resulting leakage. An axial pull test resulted in the tube's fracture rather than separation of the joint. This is indicative of a sound connector assembly.

As experience was gained in the use of the magnetic process, an inconsistency of results was realized. When the same sample configuration was retested, some were successfully leak tight and others were not. Several factors were thought to be contributing.

In the small sized (3/8") samples tested, a circumferential nonuniformity of the tube joint was observed. It was commonplace in this

size and was due to the existence of the shaper piece gap width. The gap is necessary for proper coil operation, since without the gap the shaper would be a one turn short circuit secondary winding. To overcome the nonuniformity produced by the gap in the shaper a procedure was adopted whereby two magnetic pulses were used to make each joint, with the tube rotated relative to the shaper by 180° between pulses. Some improvement in results was noticed with this method, but not enough to be of great importance.

A second effect of the magnetic swaging operation was observed following a similar observation made in the study of the explosive method. Figure 20 shows a sample made by exploding a wire charge that had been wrapped around the joint at the insert trough area. The intended high deformation was achieved and the layover of the knife edge can be observed - especially noticeable at the left knife edge. A magnified view of this zone is shown in Figure 21. The tube material was deformed enough to contact the knife edge, but with the removal of the impulse forces, it immediately sprang back due to its own elasticity. Cold welding did not occur. In that close observation of cross-sections of magnetically joined connections showed the same phenomenon, the remaining effort was devoted to attempts at solving the springback problem. Relative position between tube and insert was also observed by means of x-ray techniques.

Figures 22, 23 and 24 show three insert configurations designed to make use of material elastic properties. Each relies on its inherent springback qualities to travel with the tube while the tube is being deformed and again while it springs back thereby maintaining a seal. Leak testing for this series consisted of an initial vacuum check, followed by a pressure test if successfully leak tight.

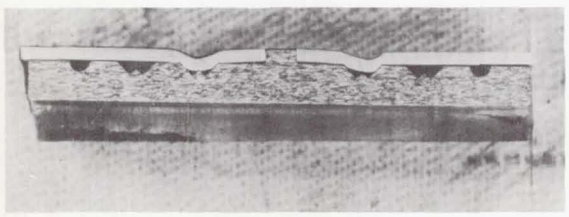

Fig. 20- Cross-section of Explosive formed Permanent Joint Design (2024-T3 Insert, 6061-T6 Tubing, both aluminum)

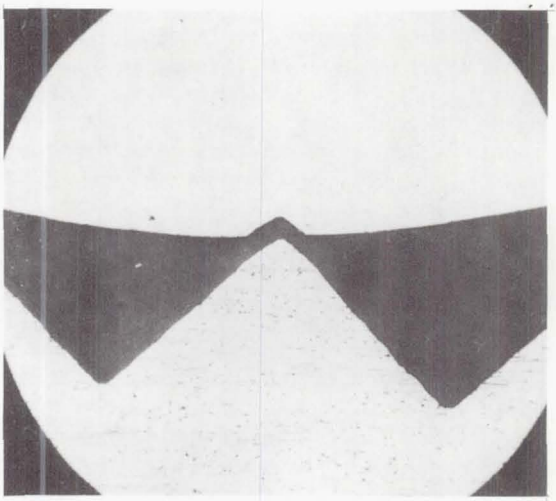

Fig. 21- Magnified Cross-section of Explosive formed Permanent Joint

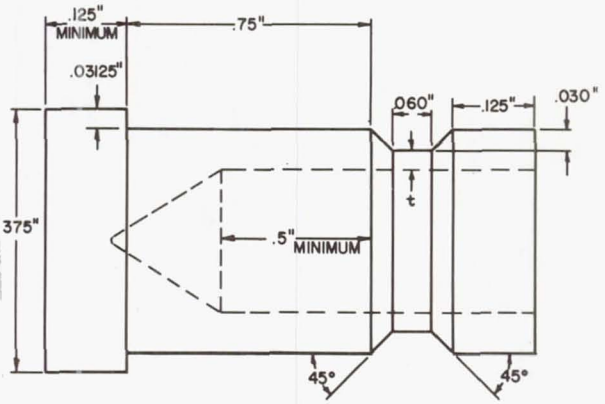

Fig. 22- Insert with Varying Wall Thickness

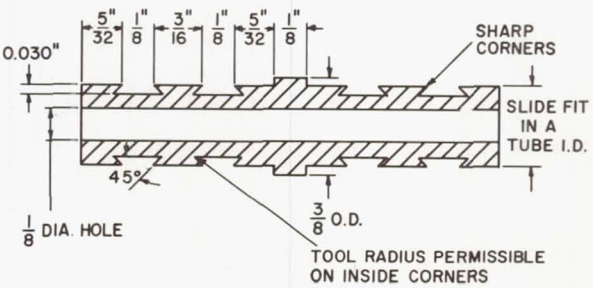

Fig. 23- Sharp Edge Cantilever Insert

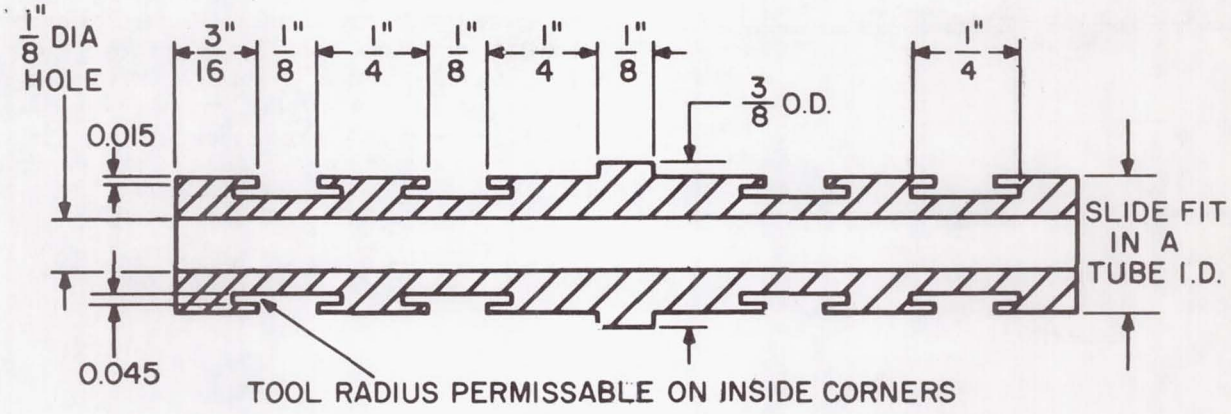

Fig. 24- Straight Cantilever Insert

The insert shown in Figure 22 was fabricated with varying wall thicknesses. Results of this series of tests showed the thinner, more elastic inserts produced more successful joints.

Figures 23 and 24 configurations employ a cantilever principle to supply springback energy. While joints made to these two configurations were successful in the vacuum test, each failed when subjected to a pressure test.

The configuration in Figure 25 is slightly different in character. It makes use of a ramp section. When the tube is positioned by being deformed into the outboard groove, the end of the tube is deformed down the ramp. If welding did not occur during this phase of the deformation, the tube's springback would cause it to wedge against the ramp and still maintain a seal. A number of joints made in this manner successfully passed the vacuum and pressure leak tests, but results were not consistent.

Magnetic forming appeared to have three difficulties, two of which were understood, the third is not understood. These problems are: 1) springback of the tube, which one may be able to cope with by appropriate design details, 2) nonuniformity of forming due to the slot in the field shaper, which trouble may again be avoidable, and 3) inconsistent results, the cause of which are not yet adequately known. We concluded, therefore, that the magnetic forming in its present form may be a very useful alternate to mechanical swaging for structural joints and for fluid connectors where sealing requirements are not too stringent, but that it would require considerably more development before it could be used in general for fluid connectors as a sealing technique. Should elastomeric gaskets be placed between tube and metal insert, sealing could probably be effected; but the value of a semipermanent connector subject to the temperature and compatibility problems associated with an elastromer would not merit its development.

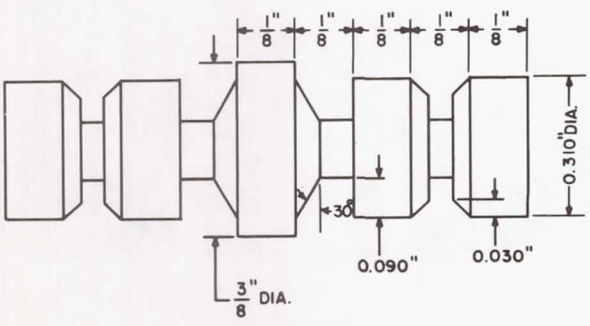

Fig. 25- Ramp Type Insert

EXPLOSIVE FORMING

Explosive forming, it was felt, had a better chance of producing a satisfactory fluid connector than did Magneform, for considerable work has been published on the formation of explosively formed welds. Initial tests with wire explosive wrapped around the tube joint in Figure 19 in a free air nature resulted in exceptionally high deformations. A difficulty arose in the use of the wire explosive and resulted in refining the technique. At the junction of the lead wire and the wrap wire was an area of high charge density which repeatedly ruptured the tube. Because of this, new configurations were designed and fixtures for containing the explosion were fabricated.

Figures 26 and 27 are representations of two configurations used. The first is a tube-to-tube joint where one tube fits closely into the other. The second is the more common flange

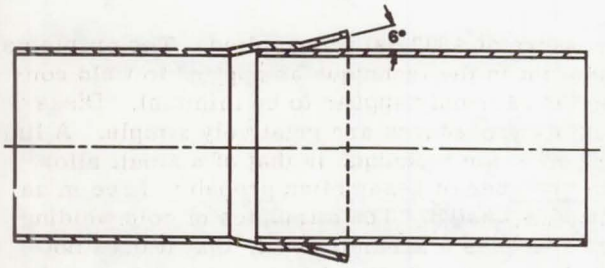

Fig. 26- Tube Configuration - Explosive Technique Test

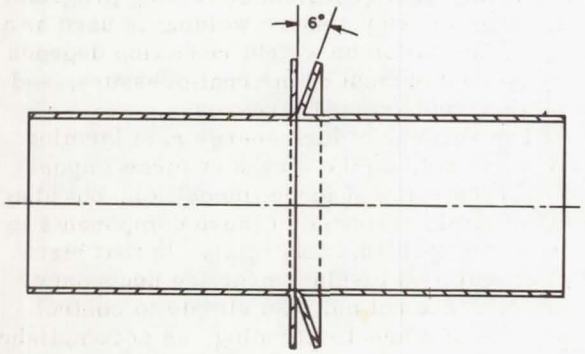

Fig. 27- Flange-Type Tube Joint Configuration

type, although it uses only the tube for its structure. The 6° angle is common to both and is a critical one. (11) It effects the relative velocities between the members to be joined, which is an important parameter in the process.

For the configurations of Figures 26 and 27 sheet explosive in the lowest density manufactured ($1g/in^2$) was used in the form of a washer. It was simply cemented to the area to be deformed and by means of a lead-in charge, detonated at the apex of the angle. In this manner, the shock wave would start at the apex and travel outward, accelerating the motion of one thickness of tube relative to the other.

The tests made with these configurations were done with the sample completely housed, and with the detonator - a blasting cap - located outside the housing. A solid steel mandrel was used to support the tube walls during the explosive tests. A later test showed that a 1/4" thick cylinder of 2024-T4 aluminum was all that was required to withstand the detonation forces. Because of this, and carrying the design one step further toward practicality, a connector similar to the one used for magnetic forming could be designed with an insert having a wall thickness of 1/4" for a 2" diameter tube size. Other sized tubing would require different insert wall thicknesses.

Excellent results were derived from tests using these two configurations. Figure 28 shows one of the successful joints prepared from the Figure 26 configuration. The highly deformed area is the point at which the lead-in charge was attached to the main charge, thus forming a high density charge condition. Figure 29 is a section

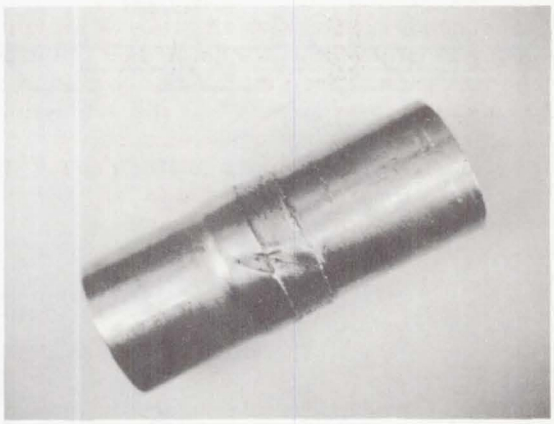

Fig. 28- Ignition Point of the Joined Explosive Sheet Ring

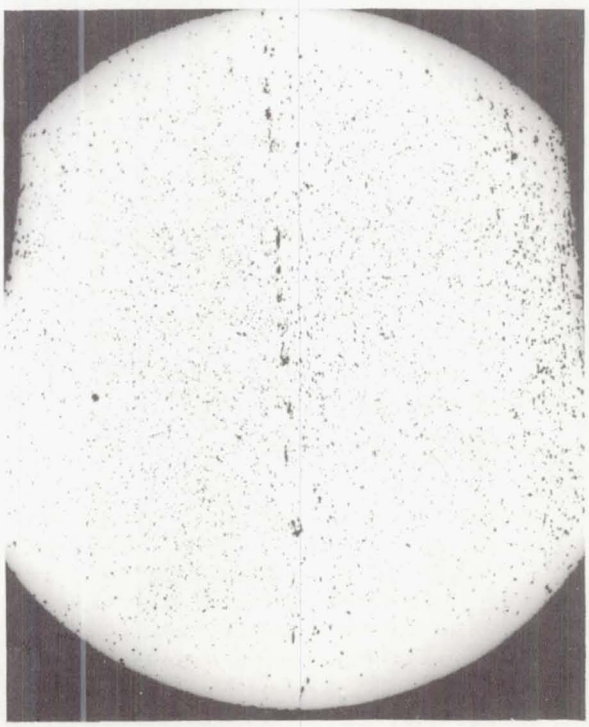

Fig. 29- Sample of Explosive Weld - Straight Sleeve Joint

taken from a typical weld area using this technique. It illustrates the existence of a weld and in the familiar "jetting" pattern (11) common to explosive welding processes. The tube joint formed in this manner did not leak when subjected to an internal vacuum test nor when a pressure was applied high enough to stress the tube walls to the material yield point.

A secondary effect which could be detrimenal in any circumferential welding made in this manner was experienced in these tests. Diametrally opposite - 180°, radially - the detonation point, an area of high deformation resulted. The deformation was high enough, in some cases, to rupture the tube wall. This results from the reinforcement effect of two shock waves, each being created separately at the point of detonation travelling about the tube's periphery in different directions and meeting 180° from their creation. No efforts were made to counteract this effect, but in cases of practical application of this technique, it would necessarily have to be done. Techniques for avoiding this phenomenon involve programmed fusing.

The degree of relative velocity of the joining materials is a very important criterion and is the one which determines whether successful welding takes place. Experience gained from using this technique showed where the impact velocity was either low (at the apex of the 6° angle) or high (at a point near the end of the weld), little or no welding took place. For a broad range between these extremes welding did occur. The investigations reported here are far from complete and are confined to 2" tube; 3/8" diameter tube joints were not tried because readily available sheet explosive was too powerful. However, sufficient success has been obtained to indicate that the process could be developed if the advantages warrant it. For joining tubes in space, for example, the process appears to have unique advantages over other permanent tube connecting means.

CONCLUSIONS

The cold welding technique, being quasi-static, is relatively easy to control and is quite easily adaptable to connector design. The state-of-the-art of cold welding has been advanced to the point where it could be tried in a particular configuration. The parameters governing successful cold welding are known. In the particular connector design fabricated and tested under all conditions not involving large reduction in compressive forces on the seal, complete success was attained. Even when the compressive forces were reduced to one quarter of the initial value, the cold weld maintained itself until an internal pressure of 4800 psi was applied. The problems inherent in the technique as applied to field connector assembly appear to be minimal. Disassembly procedures are relatively simple. A limitation to the technique is that of a small allowable number of assemblies, probably three in an ultimate design. The attributes of cold welding are that it is a hermetic seal, that it does not produce contamination inside a connector such as may occur in fusion welding, and that it has certainly been proven to be leak tight under a multitude of imposed loads. Refinement of geometry is necessary before such a connector could be committed to a qualification testing program. In all cases where pressure welding is used as a seal, the limitation on weight reduction depends solely on containment of internal pressure, and not on the required seal stresses.

The success of high energy rate forming depends not only on the means of force imposition, and the rates of force imposition, but also on the dynamic response of those components to be formed or welded. Inherently, in that high rates of material displacement are necessary, parameters are not quite so simple to control. In the case of magnetic forming, as accomplished on the Magneform machine, repeatability of imposed forces can be controlled. When utilized on tube-metal insert configurations, Magneform technique yields extremely strong structural joints. Geometries wherein an interlock is formed between tube and insert produce joints much stronger than the virgin tube. With regard to seals attained in the same manner, because of springback (inherent in dynamic forming) and because of a singularity in the force field generated by magnetic forming with a shaper coil, less than satisfactory results can be presently expected. Techniques in which a shaper coil to axially concentrate the force is used may in the future be developed to overcome the eccentricity of shape. Techniques to employ the elasticity of an insert to overcome the springback problem may also prove successful, although much more development work would be necessary. The use of elastomers as an intermediate material for sealing is possible. However, the advantages of resultant joints as established by magnetic forming over quasi-statically swaged joints presently obtainable has not been demonstrated.

Explosive welding has more inherent potential in that a hermetic seal can be effected. However, in that it is less easily controlled, added difficulties are found. Similar problems of elastic springback and lack of concentricity of resultant metal forming persist. By extremely careful programming of burning rates, the latter problem may be overcome. Structural and seal welds are certainly possible by the explosive

welding technique. In that a weld resulting from the explosive technique is also a cold weld, and not subject to fusion welding contamination, as a joining technique it must hold promise for aerospace field joint assembly application.

REFERENCES

1. "Welding by Cold Working," Welding Handbooks, Section 3, Chapter 53.

2. "Pressure Welding of Light Alloy Without Fusion," Welding Research Council, Research Report, Vol. XII, 1947, 895.

3. "Some Application of Cold Pressure-Welding", Machinery, (London) V. 93, pp. 207-217, July 23, 1958.

4. "Materials Joined by Cold Welding Process," Material & Methods, Nov. 1948, page 60.

5. "Recrystalization Welding," Welding Journal, May 1953, V. 32, pp. 209S - 222S.

6. "Pressure Welding Attracts Interest", Steel, June 8, 1953, V. 132, pp. 90-91.

7. "Putting the Squeeze on Cold Welding," Product Engineering, Feb. 1953, V. 24, pp. 176-181.

8. "The Influence of Surface Films on the Pressure Welding of Metals," British Weld Journal, January 1958, pp. 21-38.

9. "Roll Bonding of Aluminum," British Weld Journal, August 1962, pp. 469-475.

10. "High Energy Rate Forming," - an editorial reprint of articles appearing in Product Engineering, American Machinist and Metalworking Manufacturing .

11. "Explosive Working of Metals," Rinehart and Pearson, Pergamon Press (distributed in Western Hemisphere by Macmillan) 1963.

FLANGED OMEGA SEAL AND DIFFUSION BONDED CONNECTOR DESIGNS

By

L. G. Gitzendanner
F. O. Rathbun, Jr.
W. J. Harwick
Advanced Technology Laboratories
General Electric Company
Schenectady, N. Y.

ABSTRACT

Two semi-permanent flanged fluid connector designs applicable for large diameter ducting systems and designed specifically for insensitivity of sealing to reduction of bolt load, are described. The first, an omega seal connector, designed for 4700 psi service at 1440°F, incorporates a hermetic seal by the fusion welding of two segments of a thin toroidal shell about the periphery of the connector. In order to make and break the seal, special welding and weld cutting equipment is required. In that an alternate load path exists for the compressive loading across the connector and in that the toroidal omega seal has inherent flexibility, the system has the ability to withstand flange displacements and rotations. The design is similar to that used by the United States Navy on its primary loop nuclear submarine systems.

The second design, that of utilizing a diffusion bond as the hermetic seal, allows the seal to be made in the field by the application of moderate heat and bolt stress. The diffusion bonded flanged connector was designed for 6,000 psi service at temperatures ranging between -450° and +100°F.

Both designs are described, along with their inherent advantages and disadvantages. The results of the program in which a prototype of each design was manufactured and tested are described.

IN SEPARABLE FLUID connector design, one of the major problems is that of maintaining the necessary sealing stresses on the mating components throughout the life of the connector. The compressive load which effects the seal, whether it be imposed on a metal gasket, a seal having its own geometric flexibility, or a composite material seal such as a spiral wound gasket, is of such magnitude to cause plasticity in the sealing area so that the true flexibility of the seal is often not known and in all cases is quite slight. Because of this, loss in bolt load due to relaxation, the vibration environment, and the temperature extremed or transients, often causes loss of sealing. Thus, interest is aroused in fluid connectors having the attribute of being truly zero leakage connectors possessing the characteristic of being insensitive to bolt load reduction. However, with these advantages come the disadvantages of more effort being required in assembly and disassembly. But, for connections which need be opened only a small number of times, or not at all except for repair functions, such advantages outweigh the disadvantages.

When the idea of semi-permanence is open to the fluid connector designer, many new concepts become available. Explosive welding, magnetic forming, pressure welding, and many other techniques are at least possible for forming the seals, the structural junction, or, in some cases, both. Two flanged fluid connector designs having the intended capability of being insensitive to bolt load reduction during their operational lives are described herein. Other than this design goal, the designs have little in common. One design, that of the omega seal, is not new. It has been used for applications other than aerospace for some time. The second design uses a diffusion bond, which is not new to the aerospace industry, but is new in connector design. Each design has its own area of application in the aerospace field; each has its advantages; each certainly has disadvantages. In order to be made ready for utilization in any given fluid system, each would have to be developed beyond its present stage of design shown herein.

Each of the designs described in this paper has been brought to its present design state under the sponsorship of the National Aeronautics and Space Administration. Neither of the configurations nor the specific dimensions are considered optimum. By design techniques

now available, they can be improved. The purpose of the developmental program under which the connectors were constructed and tested was that of showing feasibility of the concepts and the applicability of such designs to aerospace use.

OMEGA SEAL FLANGED CONNECTOR

The term omega seal herein refers to a thin fusion welded toroidal shell joining two flanges about their periphery. Where the toroidal shell encompasses 360°, the term omega is somewhat descriptive of its cross-sectional geometry. The term, however, may refer to a 90° arc of thin shell, a 180° arc of thin shell, or any other enclosed angle which is appropriate for its use. The significant aspect of the design is that the thin shell possesses geometric flexibility between points of attachment to the flanges, and it is circular in cross-section such that it provides the optimum pressure containment configuration. Typical geometries are shown in Figure 1. In that the

Fig. 1 - Typical omega seal configurations

omega seal provides the pressure containment, its location must, of course, be inside the bolt circle which somewhat complicates the overall shape of the connector. Inherently, the configuration calls for one seal fusion weld, which may be made between the two segments of toroidal shell or, in some cases between one segment of toroidal shell and a thick flange segment although the latter technique is not deemed as satisfactory generally. The omega seal's thin components may be made separately and welded to the thicker structural segments of the connector or they may be machined from the original forgings from which the flanges are machined. The choice of manufacturing technique depends on the material from which the connector is made. Most important are the material's grain size and weldability. In that a final fusion weld must be made in the field, in general an inert atmosphere must be present both inside and external to the omega seal to avoid oxidation which could contaminate the fluid system and to insure a sound weld.

The field fusion weld also requires a welding machine which assures uniformity of weld about the periphery in a reliable manner. When separation is required a weld cutting machine must be used such that the weld may be cut in a way which does not allow chips or grinding debris to contaminate the system.

The attributes of such a connector, if completely developed along with its associated welding machine and weld cutting equipment are: it is a hermetic seal, it retains its seal even when the bolt loads are reduced, and in certain diameter-pressure combinations, it provides for a lighter overall connector.

In order to evaluate such a design for aerospace applications, a particular configuration was established for a particular specification; such a configuration was built, and subjected to a test program. No sophisticated welding machine or weld cutting machine was developed, conventional equipment in a laboratory being used in their place. While all of the remarks thus far deal with the omega seal configuration in general, the remainder of the paper dealing with the omega concept has to do specifically with the design which has been constructed and tested.

APPLICATION OF DESIGN TO A POTENTIAL AEROSPACE USE-OMEGA SEAL

The omega seal configuration chosen for the particular environment specified was that as shown in Figure 2. The connector was

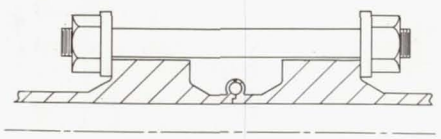

Fig. 2 - Omega seal connector schematic

designed for 4700 psi service at 1440°F maximum temperature. The required proof pressure for the connector was one and a half times the operational pressure, 7050 psi. The burst pressure required was 2 1/2 times the rated pressure, 11,750 psi. Because of the high temperature extreme, the material used was of a high nickel alloy type. The lap flanges were made from Hastalloy C; the nuts and bolts were constructed from Rene' 41. The loose

flanges, utilized in the design mainly as bolt containment rings, were constructed from 347 stainless steel.

For test purposes, since Hastalloy C ducting was not obtainable, stainless steel tubing was welded to the lap flanges as a substitute. The nominal inside diameter of the duct was two inches. The two inch size is quite small in comparison with the general application of the omega concept to pressure containment. However, it was not the size but the environment of aerospace application with regard to vibration and temperature which were considered to be the factors under which the design had to be evaluated.

The original dimensions of the omega seal and flanges are shown in Figure 3. Since the flanges were used as a means of initial evaluation of the omega seal, their dimensions were not optimized with regard to weight and it was possible in later activities described herein to reduce the weight considerably. The initial thickness of the flanges was intentional in order to decrease the rotation between the flanges thus minimizing the stresses of the "rigidly" fixed ends of the omega seal.

The omega seal in this case was constructed integrally with half on each flange. Welding of the omega seal was done in a laboratory type bench setup as shown in Figure 4. The lap flanges were held between the rotating chuck and live center tail stock. The setup possessed the capability of rotating the joint to be welded at a very slow rate of speed. The two halves of the omega seal were made a radial fit such that the positioning of one flange with respect to the other posed no problem. Once the flanges were assembled in the test setup as shown, they ran concentrically with respect to one another. Surrounding the lap flange assembly can be seen a plastic bag. For the welding operation this was filled with argon gas. Along with this, the gas atmosphere provided by the tungsten inert gas welding head provided the ideal situation for successfully welding the two omega halves together.

The weld was made using the TIG process and employing a filler metal which was Hastalloy W made in the shape of a flat washer. Prior to putting the two halves of the omega seal together, the washer was placed into position, the omega seal lips having been machined back far enough to allow clearance for this added ring. This technique allows the filler material to be melted and thereby fill the gap between the two halves of the omega seal. The filler ring was of such a size as to make up the deficiency of the removed omega seal and resulted in the weld area being slightly thicker than the nominal 1/16" thickness of the omega wall. Figures 5 and 6 show the two half sections of the flanges and omega seals prior to being welded. Two small feed through holes can be observed starting from the inside diameter and proceeding into the omega section. The holes were necessary to allow any entrapped gas to escape during the welding process. Without these holes, gas pressure building up in the seal during the welding operation conceivably could result in a poor-

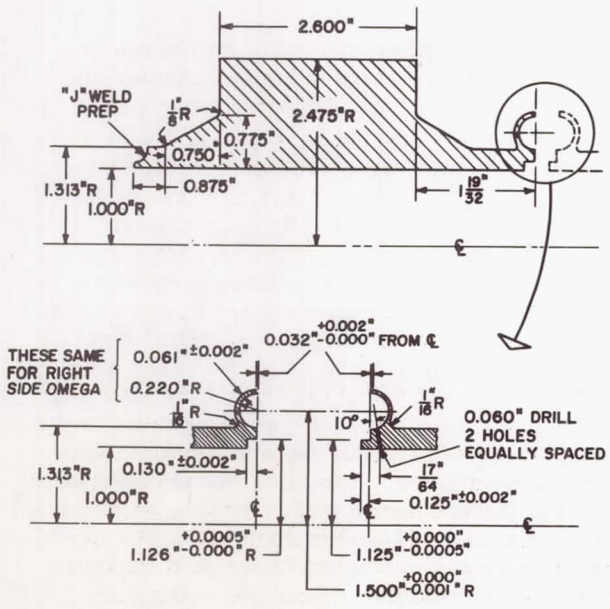

Fig. 3 - Dimensions of original omega seal and flange

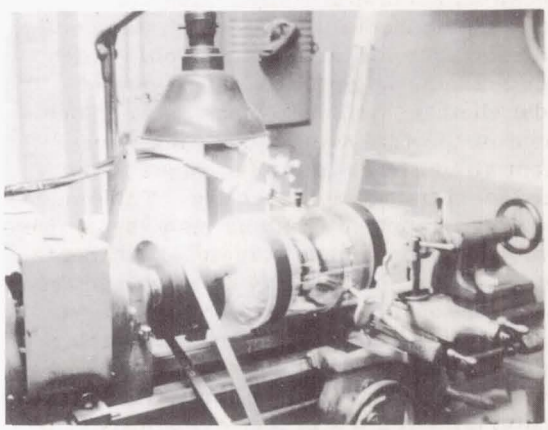

Fig. 4 - Laboratory weld set-up

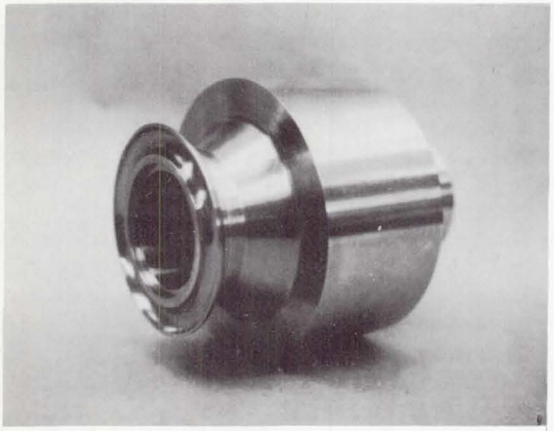

Fig. 5 - First half of omega flange

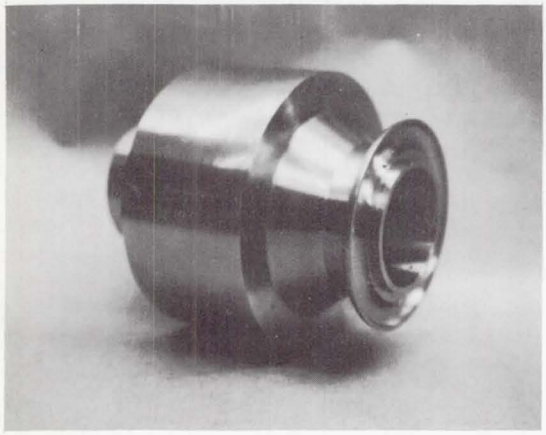

Fig. 6 - Second half of omega flange

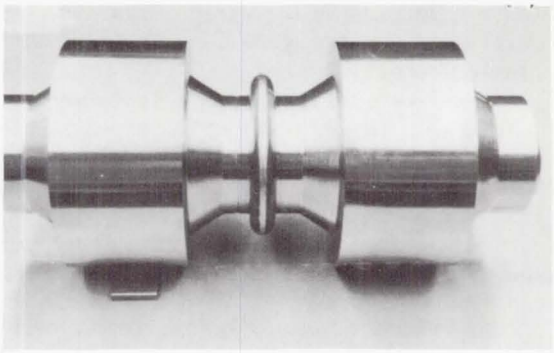

Fig. 7 - Omega connector after welding

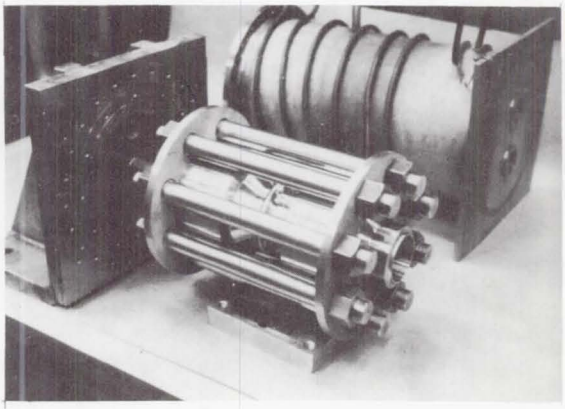

Fig. 8 - Bolted omega connector and high temperature vacuum chamber

ly welded joint. Figure 7 shows the completed omega seal welded together. One problem associated with fusion field welding is that of inspection. For the connector described herein, the weld was x-rayed in an effort to determine its integrity.

Figure 8 shows the omega seal in its assembled condition complete with bolts, nuts and loose flanges. Adjacent to the connector is shown the oven in which the connector was placed for pressure leak testing at high temperature.

Although the connector was designed and fabricated for use at 1440° F, the actual high temperature leak test of the connector was accomplished at 700° F since facilities adequate for such a test were available and the increase in temperature, in the case of a welded hermetic seal, was thought to affect only the material properties and not the configuration itself. The high temperature oven enclosure shown in Figure 8 also provides a vacuum chamber about the connector such that helium mass spectrometer leak tests can be conducted. For the vibration and shock testing, sections of stainless steel ducting were welded to the connector such that the tangential bending stresses imparted to the connector by such environments duplicated more realistically those found in an aerospace application. During the vibration testing, a stainless steel bellows welded over the connector provided the vacuum enclosure for the helium mass spectrometer leak tests.

After determining that the omega seal had been successfully welded, the connector was subjected to the testing program shown in Table 1.

Table 1 - Omega Seal Connector Tests and Results

Test			Leak
Pressure (psi)	Temperature (°F)	Description	
4700	Room	Check-out test	0(<10^{-7} atm cc/sec.)
4700	+700°F	High temperature test	0
200	Room	Vibration test, 200, 000 cycles, max. fiber stress of 5, 000 psi	0
7050	Room	Proof pressure (1 1/2 times rated)	0
1500	Room	Post-modification check-out	0
200	Room	Vibration test, 200, 000 cycles, max. fiber stress of 10, 000 psi	0
1500	Room	Post-vibration pressure test	0
7050	Room	Proof pressure with thin flanges	0
0	Room	Shock	Leakage not monitored
4700	Room	Post-shock pressure test	0
4700	Room	Loose bolts test Bolts 1/2 original torque	0
4700	+700°F	High temperature, loose bolt- bolts 1/2 original torque	0
11750	Room	Burst test (2 1/2 times rated pressure)	Leakage not monitored

TESTING PROGRAM - OMEGA SEAL CONNECTOR

The initial test made was a checkout of the connector at rated pressure. This was accomplished at room temperature utilizing helium gas as the pressurizing atmosphere. No leakage was observed when the rated pressure of 4700 psi was attained. Following this test, the connector was raised to 700° F and subjected to the same internal pressure. Again no leakage was observed. At this time, the connector was removed from its oven enclosure and sections of stainless steel heavy wall tubing were welded to it in preparation for the vibration and shock tests.

The vibration was made at room tempera - ture with an applied pressure of 200 psi. The reduced pressure was necessitated because of safety requirements in the location of the vibration machine. With the vacuum enclosure in position, leakage was actually monitored during vibration. The connector assembly was vibrated at its resonant frequency, which was 86 cycles per second for 200, 000 cycles with the maximum applied fiber stress of 5, 000 psi at the junction of the tube and lap flanges. The stress level was monitored by strain gages mounted to the two outer walls. Again, the test was successful with no leakage being measured. Following this test, a room temperature proof pressure test was made. With 7050 psi applied to the connector, no leakage was noted.

Having passed the tests thus far, the connector was modified in an effort to reduce the overall weight. The lap flanges were machined down to a thickness of 1.5 inches as opposed to the original length of 2.6 inches. This resulted in a weight reduction of 40%. The flanges after modification are shown in Figure 9.

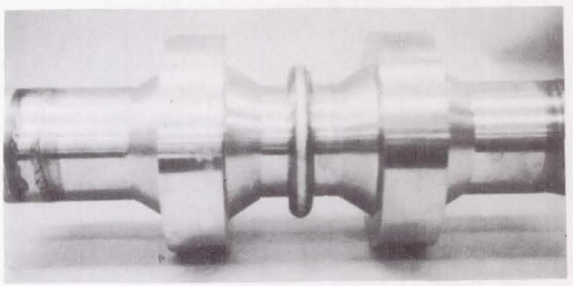

Fig. 9 - Omega seal flange after modification

Some question arose as to the loading on the omega seal weld during the machining operation. Thus, after reassembly of the loose flanges and bolts, a 1500 psi internal pressure test was made to determine whether the welded joint was still intact. As indicated by zero leakage, the weld was still sound and a second vibration test was run. The same parameters were used as in the initial vibration test with the exception that the bending stress was increased to 10, 000 psi. The same number of cycles, 200, 000, were achieved in this test, raising the accumulation of cycles to 400, 000. Figure 10 shows the connector

Fig. 10 - Omega connector in vibration machine

mounted in the vibration fixture. Following the vibration test, a second room temperature, 1500 psi internal pressure test was made to determine whether any deleterious effects were produced due to the vibration. Again, no leakage resulted. At this point, a second proof pressure test was made at 7050 psi resulting in no measured leakage.

The connector was then shock tested in a Navy medium weight shock test machine. Figure 11 shows the omega connector in preparation for the shock test. The same fixture was used for the support in this test as in the vibration test. Acceleration of the shock table and the connector were both recorded during the test. Strain gage readings were also taken in order to determine the stress level caused by the shock. Prior to shocking the omega seal connector, a dummy connector with a similar resonant frequency was subjected to various shock levels in order to determine an appropriate shock level for the actual connector. The shock test was conducted at room temperature with no internal pressure or leakage measurement. During the test, a fiber stress at the junction of the tube and the lap flanges of 39,000 psi was recorded. Approximately 55 g's were applied to the connector during the test. To evaluate whether damage was done to the connector as a result of the shock test, a room temperature, 4700 psi pressure leak test was made on the connector immediately thereafter, resulting in no measurable leakage.

In that the original goal design was that of a connector which would be insensitive to bolt load loss, a next step in testing was that of loosening the bolts holding the two lap flanges together and then proceeding with further testing. The bolts were loosened to approximately one half of their initial torque, now being torqued to 28 ft-lbs. A subsequent 4700 psi room temperature pressure leak test showed no measurable leakage. Again, the connector was subjected to a 700°F pressure leak test with no resultant leakage. The final test in the program was a burst pressure test, conducted at room temperature with an internal pressure of 11,750 psi. During this test, leakage was not measured. However, maintenance of the integrity of the connector during the burst pressure test indicates the maintenance of the zero leakage capability.

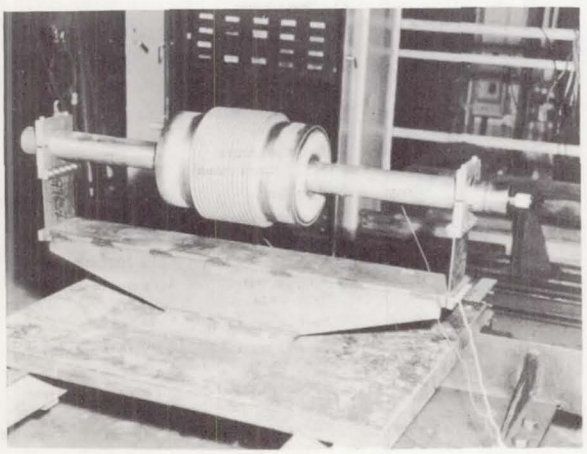

Fig. 11 - Omega connector on shock stand

DIFFUSION BONDED CONNECTOR

Field diffusion bonding offers the possibility of attainment of a hermetic seal by subjecting previously prepared surfaces to a pressure and a temperature low enough such that no structural material properties will vary. Also, for some combinations of materials to be bonded, the process can take place in an atmospheric environment. Should a diffusion bonding process under those limitations be effective, then one could use such a technique in a flanged connector, imposing the necessary stresses for the bonding process by the bolt loads already needed for the containment of pressure, thus gaining a hermetic seal which has the potential of being insensitive to relaxation of the bolt loads. The resultant tensile stresses of the sealed materials are, of course, less than those of the structural materials, but because of the overall connector design, the seal will normally not be subjected to tensile stresses, but merely to reduced compressive stresses down to approximately a zero level.

Within the above mentioned framework for a suitable field diffusion bonding technique, the remaining parameter of interest is that of time. All other parameters being equal, the most desirable combination of materials for a diffusion bond would be that which offers the lowest required time for attaining the bond. In order to establish materials and parameters for diffusion bonds suitable for a single prototype flange connector, a preliminary study was carried out at the Battelle Memorial Institute. The resultant connector, shown schematically in Figure 12, and incorporating the results of the preliminary study, used as the bonding materials copper foil (0.008 inches thick) sandwiched between two gold plated sections of flange. A sealed area is placed at the innermost possible position in the connector. The

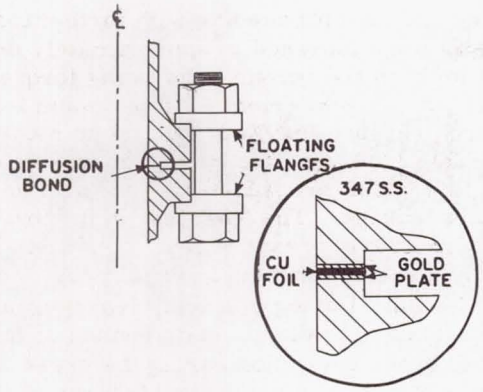

Fig. 12 - Diffusion-bonded connector schematic

parameters for the bond are the imposition of a stress level of 25, 000 psi, at a temperature of 700°F, for a duration of fifteen minutes.

The flanges of the connector, constructed from type 347 stainless steel, were designed for a service of 6, 000 psi internal pressure over a temperature range of -450°F to +100°F. Nominally, the prototype connector was 2 inches inside diameter. The dimensions of the flanges and bolts were not optimized, but merely designed such that a reasonable configuration would result for testing the diffusion bonded concept. Figure 13 shows the resultant connector assembled along with the vacuum bellows arrangement necessary for mass spectrometer leak detection. Figure 14 shows the constructed connector complete with bellows, tube extensions, and end plates. The wires protruding from the side of the end plate are the thermocouple wires used to monitor the connector internal temperature.

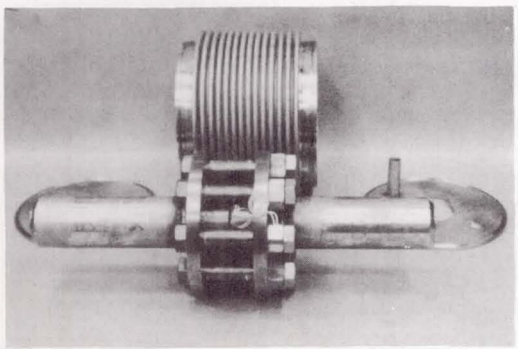

Fig. 13 - Assembled connector with bellows vacuum chamber

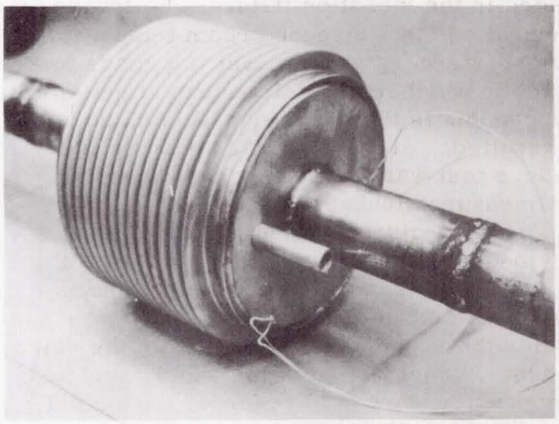

Fig. 14 - Connector with tube extensions and bellows

TESTING PROGRAM - DIFFUSION BONDED CONNECTOR

In order to evaluate the diffusion bonding process for an aerospace application, a testing program as shown in Table 2 was undertaken. The initial test of the connector was a 6, 000 psi internal pressure room temperature leak test. Using a mass spectrometer leak detector, no leakage could be detected. Next, a similar test was accomplished at liquid nitrogen (-321°F) temperature. Again, no leakage resulted. The following test, that of a vibration test, was conducted at room temperature with 200 psi

Table 2 - Diffusion Bonded Connector Tests and Results

Pressure (psi)	Test Temperature (°F)	Description	Leak
6000	Room	Check-out Test	$0 < 10^{-7}$ atm cc /sec.)
6000	-321°F	Cryogenic test	0
200	Room	Vibration test, 200, 000 cycles, max. fiber stress 10, 000 psi	0
9000	Room	Proof pressure (1 1/2 times rated)	0
0	Room	Shock test	Leakage not monitored
75	Room	Post-shock pressure test	5×10^{-4} atm cc/sec.
Vacuum	Room	Vacuum test	4×10^{-5} atm cc/sec.)
Vacuum	Room	Vacuum test, loose bolts	24 atm cc/sec.
Vacuum	Room	Post-re-bond test	0
Vacuum	Room	Post-re-bond test, loose bolts	2×10^{-2} atm cc/sec.
Vacuum	Room	Pre-vibration test, 1/2 bolt torque	7×10^{-4} atm cc/sec.
0	Room	Vibration test, 200, 000 cycles, 10, 000 psi max. fiber stress	Leakage not monitored
Vacuum	Room	Post-vibration test	1×10^{-2} atm cc/sec.
0	Room	Tensile pull test - 15, 200# max.	Not applicable

applied internal pressure, the connector being vibrated at its resonant frequency of 87 cycles per second for 200,000 cycles at a stress level of 10,000 psi maximum fiber stress in the duct at the junction between the duct and the lap flanges. As in the case of the omega seal, leakage was monitored during the test with no leakage being recorded. Subsequent to the vibration test the connector was subjected to an internal pressure of 9000 psi, which equalled one and one half times operational pressure or the proof pressure. Again, no leakage resulted.

At this time, the connector was subjected to a shock test at room temperature and no internal pressure. A dummy connector was used in the shock test facility to obtain acceleration data suitable for the actual connector shock test. The Navy medium weight shock machine was used with the connector being supported in a simple standard with the connector half way between the supporting ends. Figure 15 shows the connector on the shock test stand. The assembly was subjected to a hammer blow from below, the blow being applied to a girder arrangement on which the connector assembly and its base plate are bolted. The base plate weighs approximately 600 lbs. Two accelerometers were used to monitor the acceleration during the test, one being attached to the tube adjacent to the bellows flanges and the other being attached to the base of the fixture. When the shock test was made, the accelerometer which was attached to the tube was thrown off by the force of the shock. The strain gages showed that a 35,000 psi fiber stress existed in the duct during the shock. This figure was much higher than had been intended for such a test. The shock which the connector experienced exceeded that intended by approximately a factor of three.

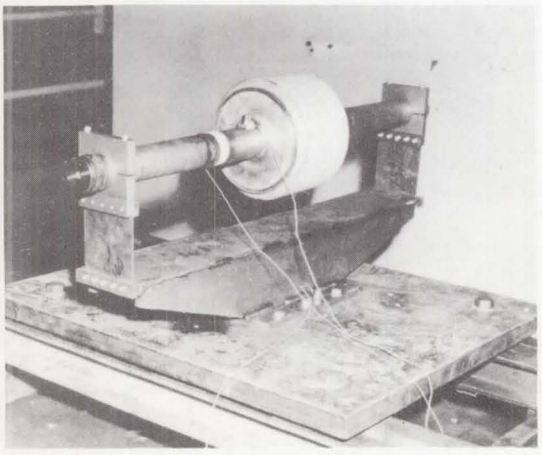

Fig. 15 - Diffusion bonded connector on shock stand

Immediately after the shock test, a leak test was made on the connector. At an internal pressure of 75 psi, a leakage rate of approximately 5×10^{-4} atm. -cc/sec was noted. As the internal pressure was increased, leakage increased to the point where the leak detector could not be used. At this time, the diffusion bond was subjected to an internal vacuum leak check wherein the point of leakage could be ascertained. During the vacuum leak check, a leakage rate of 4×10^{-5} atm cc / sec was recorded. To insure that the diffusion bond had not been completely destroyed, the bolts were removed from the connector and again an internal vacuum leak check was made and the leakage recorded. The leakage was approximately 24 atm. cc/sec. However, it was noted that the connector did not separate; the connector would hold itself together under its own weight as well as some mildly applied axial forces, thus indicating that a bond was present.

In the hopes that the leakage rate could be reduced or eliminated by reimposition of heat to the bonded area, the connector was subjected to 700°F for fifteen minutes, prior to which the bolts were retorqued to their original value, namely, 140 ft-lb., imposing 25,000 psi to the connector. Initial vacuum leak tests after this endeavor showed zero leakage. However, when the bolts were again removed, a vacuum leak check showed leakage to be approximately 2×10^{-2} atm. -cc/sec indicating that the attempted bonding cycle was unsuccessful.

Having damaged the bond beyond repair by an extremely severe shock, testing was continued in order to determine the effect of vibration and bolt load loss on the leakage rate. The bolts were tightened to one half their original full torque in preparation for a second vibration test. It was felt that the one half torque level would be indicative of the loosening of the bolts which could be achieved during actual service. Since a pressure test could not be made on the connector at this time, the criterion for evaluation of the connector performance was the vacuum leakage test. With one half full torque applied, the connector showed leakage to be approximately 7×10^{-4} atm. cc/sec.

At room temperature and with zero internal pressure the connector was then vibrated for 200,000 cycles at 10,000 psi maximum fiber stress in the tube adjacent to the lap flanges. A vacuum leak check immediately following

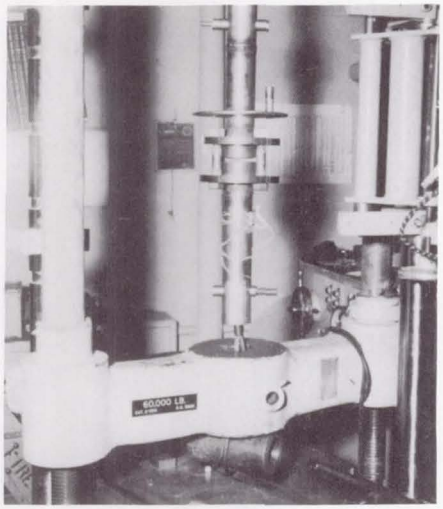

Fig. 16 - Pull-to-destruction test, diffusion bonded connector

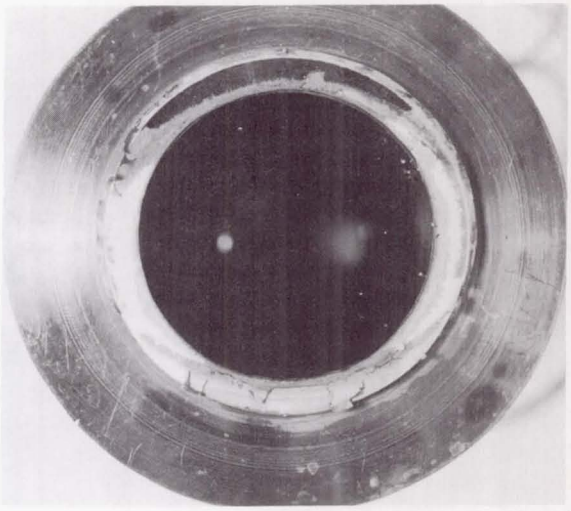

Fig. 17 - Diffusion bond after pull test failure

the vibration test showed the leakage to be approximately 10^{-2} atm. cc/sec, indicating an increase in leakage.

To determine the actual strength of the diffusion bond, the final test accomplished was that of an axial tensile pull test. Figure 16 shows the connector in the testing machine. Pins were placed normal to the center line of the connector and the axial load applied through cables wound around the pins. In this way, a true picture of the force required to pull the connector apart was realized. The bolts were completely loosened to allow the connector to pull apart approximately one half inch. The load required to separate the connector segments was 15,200 lbs. Based on the original area of the bond this resulted in a stress of approximately 9,000 psi. However, after a study was made on the true bond area, this figure was realistically increased to approximately 15,000 psi. Figure 17 shows the normal view of one of the diffusion bonded surfaces. It can be seen that the bonded area of contact was not complete at the time it was photographed. The darker areas shown were those portions of the bonded area near the top and bottom of the connector during the shock test. Hence, they received the highest bending stresses. Based on inspection of the remaining true bond area, it appears that initially, an excellent bond was made and it was leak tight. However, the excessive shock caused a segment of the bonded area to separate. However, in that the total bonded area did not separate, and that the final break in the bond due to the tensile test appears ductile, this suggests that the technique may well be adequate for the environments found in aerospace application.

CONCLUSIONS

In comparing the two connectors designed, fabricated, and tested, the omega seal connector certainly appears adequate on the basis of the tests conducted. The diffusion bonded connector, because of its failure with regard to leakage after a shock test, has not been proven to the same extent. However, because it exhibited extremely high bond strength during the pull to destruction test, and earlier success, its applicability to aerospace industry cannot be dismissed.

With regard to ease of assembly, the diffusion bonded connector is adjudged to be the simpler, requiring only externally applied heat, whereas, the omega seal requires a rather sophisticated welding machine. With regard to the disassembly, while the omega seal requires a weld cutting machine, the diffusion bonded connector would require some means of prying the actual bond apart.

Both concepts, those of omega seal and diffusion bond, need not be considered only in the geometries of flange connectors. Other configurations which utilize diffusion bonding in a shear loading geometry appear warranted for added investigation. With regard to the omega seal, in that a great deal of developmental work has already been done for Naval applications, future use of the concept to the aerospace industry could be considered.

Page Intentionally Left Blank

SWAGED TUBE AND DUCT CONNECTOR FEASIBILITY

By

K. R. Bragg
Parker Aircraft Company
5827 West Century Blvd.
Los Angeles, California

ABSTRACT

The P and VE Laboratory of NASA's Marshall Space Flight Center has funded a design and feasibility demonstration of a new concept for fluid line connectors. This semi-permanent connector depends solely upon cold forming of metal to carry structural loads and to make the helium leak-tight seal. The paper is a progress report on the first year's effort. The design objectives are stated. The connector is described The preliminary test results are reported. The extent to which the objectives are met is reviewed. And finally, the follow-on effort required to make the connector available for production is visualized.

DURING THE PAST YEAR we have had the rare satisfaction of engaging in a program which has proved successful beyond our best hopes. It is almost needless to say that all too seldom have I been able to indulge in such pleasures.

The program includes the design, development and feasibility demonstration of an entirely new concept for connecting tubes and ducts. The connector depends solely upon the cold forming of metal to carry the structural loads of the connector and to accomplish the helium "leak-tight" seal. It is intended for semi-permanent connections of fluid pressure conduits for spacecraft where the ultimate in reliability, performance and weight are warranted.

The program has been funded by the P and VE Laboratory of NASA's Marshall Space Flight Center. Mr. Herbert W. Fuhrmann, the Propulsion Engineering Branch Chief at MSFC, is the technical director for the effort. Parker Aircraft Co. is conducting the program as a subcontractor to General Electric, Advanced Technology Laboratory with supervision by Lou Gitzendanner and Forrest Rathbun.

The connector concept is the result of a specific effort to take proper account of the complete forest, or perhaps we should say complete jungle of spacecraft tube connector requirements. It is the result of the line of thinking presented in last year's symposium paper: "The Problem of Stating the Tube Connector Problem".

The basic purpose of the program is to determine the "feasibility" of the connector concept. Feasibility has two connotations. One is mechanical feasibility; what can be built and how well does it work. In order to investigate the mechanical feasibility in depth, we intentionally limited our scope in breadth. We concentrated on the 1/2 inch tube union and the 4 inch diameter duct coupling. We aimed the design at immediate operational requirements similar to those of the MC fitting. We did not attempt the ultimate in optimization, trying, rather to land on the safe side. We assembled connectors with tools which would form them in the way production tooling would form them, but which were not optimized with respect to weight, size or convenience of operation. We tested elements of connectors and complete connectors to destruction in critical modes using helium leakage of 10^{-7} cc/sec at 3,000 psi as the criteria of failure.

The other connotation of feasibility is somewhat more subtile. It relates to how important a contribution the concept can make to the overall NASA spacecraft objective. That is, how much is this concept worth in terms of investment to develop. This depends on how well it does the job that connectors have to do, and how important it is that the job be done. In order to investigate this type of feasibility we defined what we felt to be the proper objectives for an advanced connector and then analyzed our design and test results to see how well it met the objectives.

This paper is a progress report of the first years effort. The design objectives are stated. The connector is described. The preliminary test results are reported. The extent to which the objectives have been met is reviewed. And finally, the additional effort required to make the connector available for production is visualized.

DESIGN OBJECTIVES

Defining an ideal set of design objectives is a major part of any development task. This is particularly important when a serious effort is being made to advance the state of the art.

The design objectives which guided our approach are listed below in their general order of importance.

1. Provide the ultimate in reliability. This objective must be resolved into three more specific ones, all of which must be faced.

1.1 Provide the greatest probability of successful connection in service.

1.2 Provide redundant, absolute means of verification of successful connection.

1.3 Provide uniform, predictable margins of safety.

2. Provide improved performance, i.e.: helium leak-tight connections with increased ruggedness under MC fitting design conditions.

3. Provide the greatest range of applications with the least number of configurations.

4. Provide for the least tube or duct system weight.

5. Provide practical separation and reconnection.

6. Provide for minimum engagement and assembly tool space.

7. Provide for minimum vehicle cost commensurate with the desired performance.

At first glance this array of objectives may appear to be too ambitious to be taken seriously in a single step. We will show later, however, that we are coming close enough to each of them to be willing to admit that we are aiming at them.

CONNECTOR CONFIGURATION

The connector concept is adaptable to all of the typical fitting shapes: unions, tees, bulkhead, boss, etc. and to all sizes of lines from 1/4 inch to the largest diameter duct currently visualized in vehicle design. Our detail design and test work to date has been directed toward the 1/2 inch tubing union and the 4 inch duct coupling.

TUBING UNION - As a union for tubing, the connector parts consist of two identical sleeves and a collar as shown in Figure 1.

The sleeve is made of a high strength stainless material. It has a locating ledge, contacting rings and a reduced cross-section fantail as identified in the figure. The locating ledge assures locating the sleeve correctly on the tube. The contacting rings provide high stress contacts with the tube to progressively transfer shear from the tube to the sleeve. They also provide redundant seals to the tube. The progressively reducing section of the fantail minimizes the stress concentration where the tube emerges from the sleeve. The fantail in addition serves as a friction pad to provide

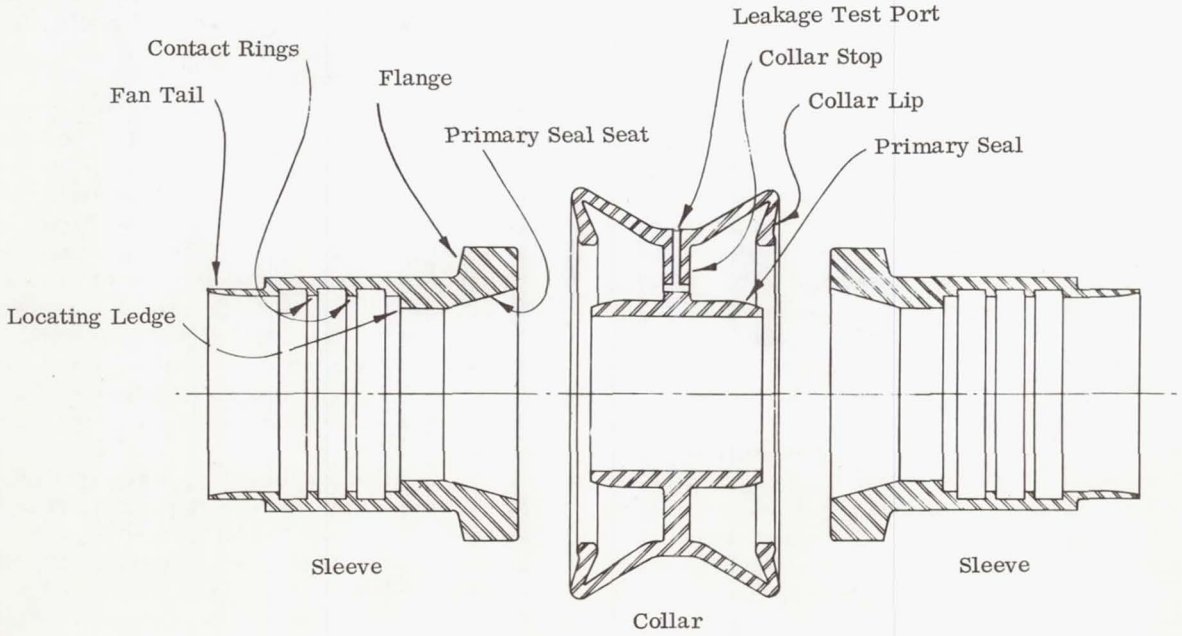

Fig. 1 - Swaged connector union, unassembled

coulomb damping in the tube system to minimize resonant vibration of the tubing spans.

The sleeve also has a primary sealing surface and a coupling flange as shown. The primary surface is a machined cone. The possibility of damaging the seal surface is minimized by its being recessed. The flange is designed to receive the collar lips and to transfer the lip engaging forces back into the collar stops.

The collar consists of an hour glass shaped cylinder with lips at each end, two integral seals and two sleeve flange stops. In section, the hour glass cylinder with its lips can be seen to resemble two back to back toggle mechanisms. It is this cross-section which leads to the name "X Connector" by which the connector is becoming known.

The seals are sized to engage the primary sealing surfaces of the sleeve with an interference fit. They also are protected by being recessed. They are gold plated to provide a caulking compound and to lubricate the seal engagement to prevent galling of the sleeve sealing surface. The holes shown are provided for the leakage check described later.

Subassembly - The sleeve is attached to the tube as a subassembly as shown in Figure 2, in a subassembly shop. This is a step generally equivalent to making up sleeve, nut and tube subassemblies for the MC fitting.

With the tube held in an assembly tool, the sleeve is slipped onto the tube end. The condition of the tube end is not particularly critical as to squareness, edge condition or radial dimensions, within standard tube tolerances. An internal roller swage tool is inserted into the tube and against the sleeve end. It expands the tube outward against the sleeve until the sleeve itself has been expanded a predetermined amount. A gage measuring the sleeve outside diameter will determine when expansion is complete.

The sleeve, incidentally, cannot be misplaced on the tube because the expander tool must develop thrust against the sleeve which must be reacted by the tube end before expansion can take place.

The expansion of the tube stretches the sleeve beyond its yield stress and imbeds the contact rings into the surface of the tube. The spring back of the sleeve grips the tube with live residual forces. By imbedding the contact rings into tube surface the sleeve is keyed to the tube. This also provides local, heavy deformation to penetrate the surface imperfections of the tube to ensure sealing.

By stretching the sleeve, as well as the tube, beyond its yield stress the radial tolerances of the tube and the sleeve are minimized as factors determining the gripping force of the sleeve onto the tube. Thus, the repeatability of results is enhanced; the possibility of an occasional weak joint resulting from combinations of tolerances or overlooked errors of dimension is eliminated.

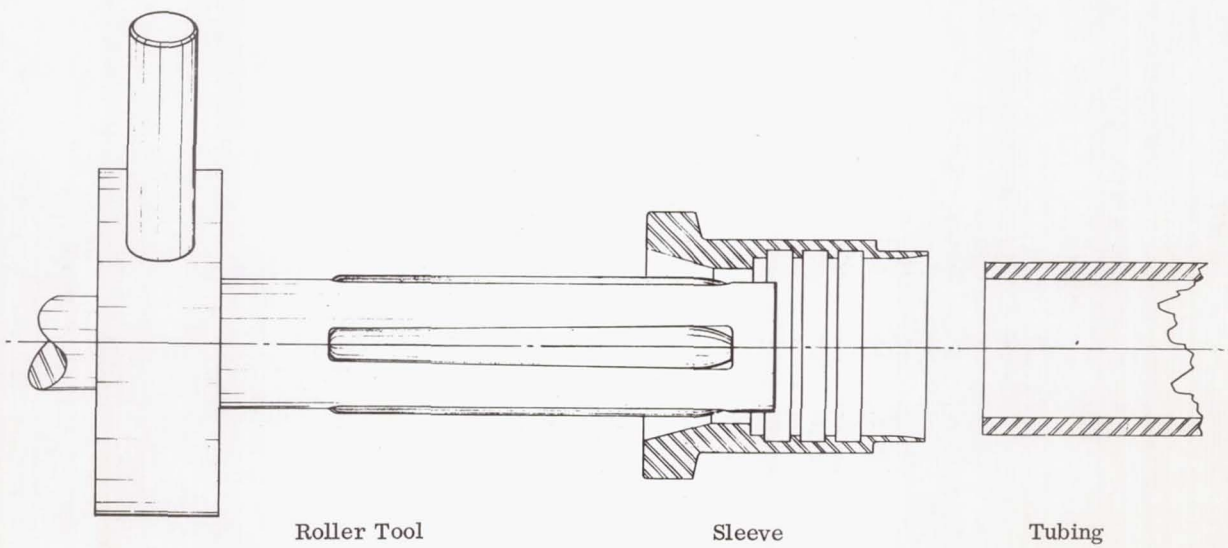

Fig. 2 - Tube - sleeve subassembly and roller swage tool

The sleeve to tube swaging machine is visualized as generally similar to a conventional, powered flaring machine. It would have interchangeable expander tools and tube jaws for each tube size.

Assembly - After the tube assemblies are installed in the vehicle, they are to be connected by a clam shell type swaging tool as shown in Figure 3, powered by a portable hydraulic pressure source.

The sleeve flanges are engaged into the collar. Then the swage tool is closed around the unformed connector. If the tool can be closed, it is proof that the parts are sufficiently engaged and aligned so that the collar can be formed properly.

The tool is then axially tightened to bring the parts into close engagement so that the collar can be formed over the sleeve flanges. Then hydraulic pressure is applied. An inter-

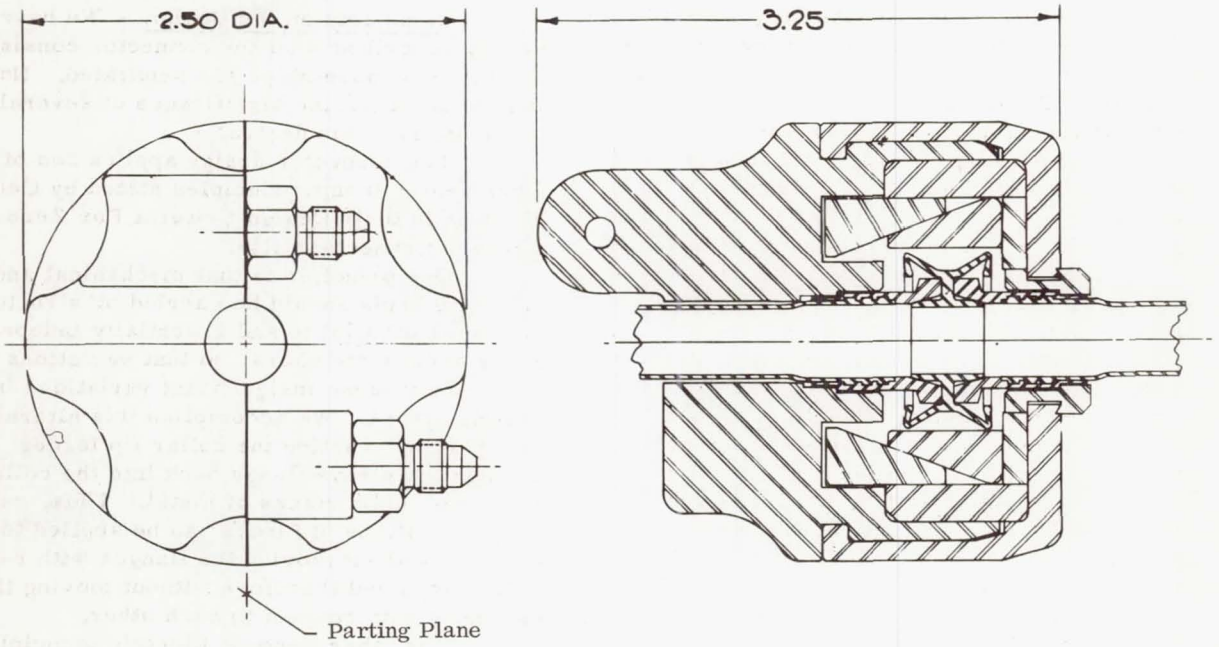

Swage Tool

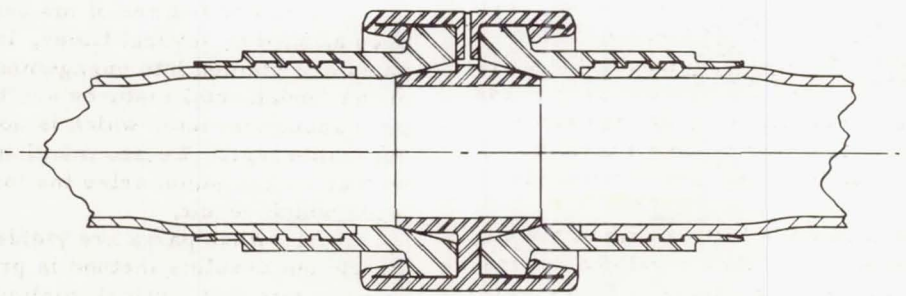

Swaged X-fitting

Fig. 3 - Collar swaging tool showing assembly of union and a completed connection

lock prevents application of hydraulic pressure before the tool has been sufficiently tightened. The hydraulic power causes a ring of radially moving pads to squeeze the hour glass shaped collar into a straight cylinder.

In this action the collar lips move in radially to engage the flanges of the two sleeves. Then the lips begin to move axially toward each other with high mechanical advantage. They finally drive the flanges into the solid stops of the collar closing an extremely high spring rate circuit of forces.

It is interesting to note that, with this so-called circular toggle action, the forming forces are radial while the resulting coupling forces are axial. Thus, since the direction of spring back of metal is inherently opposite to the direction of forming forces, the spring back of the collar is radial and does not diminish the axial coupling forces. This is the central idea upon which the X Connector concept is based.

The toggle action drives the seals into their seats with a yielding, wiping action. There is sufficient interference between the seals and their seats so that the collar seals are yielded into engagement with the sleeve sealing surfaces. This yielding tends to eliminate affects of dimensional tolerances of the seals and seats as variables in the sealing stress. During this engaging action, the gold on the surface of the seals shears into the asperities and imperfections of the sealing surfaces as a caulking compound.

Here again, both with the basic seal member and with the gold, we are yielding metal into place. The parts which have to work together are thus forced to match each other with a minimum dependence on dimensional control. The repeatability and confidence level of performance of the seal members is thereby enhanced.

During the forming of the collar, the legs of the toggle mechanism are also yielded. In addition to the obvious radial forming of the collar, the legs are yielded in length; the collar is stretched axially and the lips are compressed as the flanges are clamped rigidly against the stops in the collar. Here again we take the advantages of yielding which are mentioned above.

The stresses are high enough at the edges of the collar lips so that they develop a secondary seal with the sleeve at the flange. This creates a leakage measuring manifold between the primary and secondary seals which is tapped by the leakage port.

The production assembly tooling described above and shown in Figure 3 is taken from preliminary designs. The design is based on measured forming forces but it has not been thoroughly debugged or optimized. The picture is shown to give a general idea of the nature and size of the tools visualized.

Separation - In order to separate the connector the collar lips are cut off so that the shoulders can be withdrawn. The cut off is made with a pipe cutter type tool located and guided on the sleeve. It cuts the collar adjacent to the shoulder. The lips are then slipped back on the tube and nipped off. The tube assemblies are then ready for reassembly with a new collar.

Comments on the Design - We have briefly described what the connector consists of and how it is assembled and separated. Now we want to point out the significance of several of the features of the design.

The connector design applies two of the fundamental design principles stated by General Electric in their Design Criteria For Zero Leakage Connectors (1)*.

One principle is that mechanical and pressure loads should be carried by structural members parallel to and essentially independent of the sealing members, so that variations in these loads cause insignificant variations in the sealing stress. We accomplish this alternate load path by reacting the collar lip forces through the sleeve flange back into the collar stops with solid stacks of metal. Thus, relatively large variations of forces can be applied to the coupling without moving the flanges with respect to the stops and therefore without moving the seal members with respect to each other.

The other General Electric principle is that the sealing stress should be raised to well above the yield stress of at least one of the sealing surfaces in order to obtain a helium leak-tight metal to metal seal. This is accomplished by the fresh gold plate which is available on the collar sealing surfaces for every engagement.

Another feature of the design, which has been alluded to several times, is that the mating parts are yielded into engagement. This is one of the fundamental features available in the semi-permanent connector which is not available in the separable type. We are mentioning this again so that we can summarize the four basic advantages which result.

1. When parts are yielded into place a simple but absolute method is provided to demonstrate that critical minimum forces have in fact been developed within the connector. It is only necessary to gage particular dimensions.

---

*Numbers in parentheses designate References at end of paper.

This is a major factor in the effort to increase reliability.

2. Yielding essentially wipes out the effect of dimensional tolerances in the resulting coupling forces and in the sealing stress of the connector. This greatly increases repeatability, which is a second major factor in the effort to raise reliability.

3. Yielding the connector into the engaged condition absolutely eliminates the possibility of leakage or disengagement because of thread back off.

4. Yielding allows the use of materials at maximum efficiency - close to the maximum useable stress of materials in their work hardened condition. This minimizes connector size and weight.

5. The fifth advantage of yielding is that outstanding performance, repeatability and weight of precisely matched parts can be attained without the usual penalty of extremely tight dimensional control. This minimizes cost.

Still another feature of the design is that it tends to favor the typical weak spot of previous connector concepts, the point at which loads are transferred between the connector to the tube. The X Connector arrangement does not reduce the physical properties of the tube by heat at the typical stress concentration point. In fact, it tends to strengthen the tube at this point by increasing the section modulus and by cold working the material. In addition, it minimizes the stress concentration where the tube leaves the connector by the progressively reducing cross-section of the fantail.

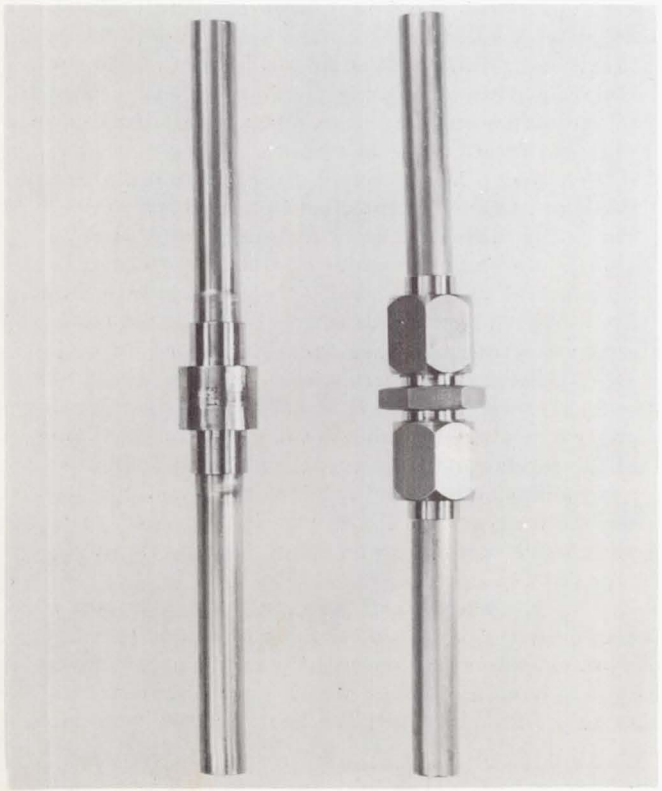

Fig. 4 - Comparison of swaged connector with 1/2" flared type connector

A final feature to mention is the leakage check manifold created between the collar and the sleeves by the primary and the secondary seals. By connecting proper tooling to this manifold, it will be possible to helium leak check every joint at its operating pressure. This provides the second independent and absolute method of inspection which is a must to reach the reliability levels required.

This manifold also makes it possible to measure leakage during flight on development vehicles, which is a specific NASA objective.

DUCT COUPLING - What has been said about the X Connector tubing union applies generally to duct couplings of any size. In addition, however, the following observations are significant.

The proportional weight advantage of this connector over a conventional bolted flange is considerably higher than its advantage over tubing connectors. This is because of the inherent inefficiency of bolted flanges with their rolling moments and intermittent tension members. With the X Connector, forces are transferred at a diameter only slightly larger than the duct and with a much higher average stress level. See Figure 5 for a comparison of a bolted flange with a swaged connection.

The forming forces required for duct couplings is proportionally much less than for tube connectors. This is because the percentage yielding required to make the engagement is less. Therefore, the assembly and separation tools are proportionally much smaller.

ASSEMBLY AND TEST RESULTS

The assembly and performance demonstrations have been gratifying to date. The work started with three separate design element investigations: the connection of sleeves to tubes, the forming of collars and the performance of sealing members. The designs were developed with a series of analytical and empirical steps. Since we are operating in the plastic range with most of the members of the connector, considerable reliance on actual forming of likely candidates and then measuring the results proved to be the most effective path. From this work we selected the connector configuration which has just been described. Complete connectors were

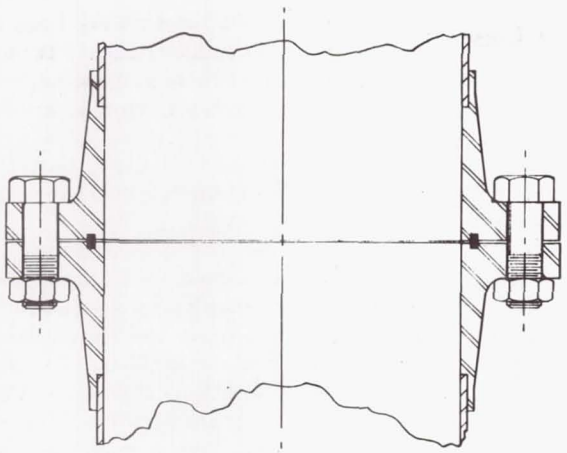

4 Inch Bolted Flange - 1500 Psi

(Interpolated/ 3 in. & 6 in.)

From "Dev. of Mech. Fittings" - RTD-TDR-63-1115

Edwards A. F. B., Calif.

Weight: 5.6 lbs. over Tubing

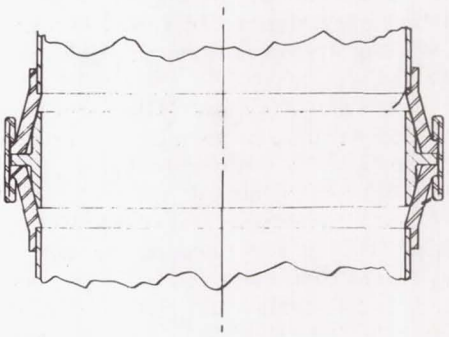

4 Inch Swaged Collar

Weight: 1.6 lbs Over Tubing

Fig. 5 - Comparison of 1500 psi 4" bolted flange with swaged connection

then built up on a one and two of a kind basis. These have been tested to show that what was learned on a separate element basis also applies to a complete connector. We are currently completing optimization changes as a result of the single piece investigations. These designs will then be built up for repetition tests to show that the results are in fact repeatable over a number of cases.

The individual investigations have included the following:

1. Connection of sleeves to tubes.

1.1 With .049 wall condition A and .028 condition B tubing.

1.2 With 10, 5 and 3 contact sleeves.

1.3 With various degrees of yielding of the sleeve.

2. Forming of collars.

2.1 With rotary dog and radial dog tools.

2.2 With various cross-section collars.

2.3 With various degrees of forming.

2.4 With 304, 305 and Inconel 718 material.

3. Performance of seals.

3.1 With 303 and Inconel 718 seals.

3.2 With and without gold plate.

3.3 With 303 and Inconel 718 sealing seats.

3.4 With various depths of engagement for up to 4 assemblies and re-assemblies.

The testing of the finally chosen individual configuration of each element can be summarized as follows:

1. Assembly of Sleeves to Tubes

1.1 Axial pull: tubing overstressed past 0.2% offset yielding (3,000 lb.) with zero leakage* between tube and sleeve.

1.2 Vibration flexure: vibrated without leakage or structural failure for 1,000,000 cycles of bending stress at stresses up to 50,000 psi (see Figure 5).

1.3 Vibration flexure with interspersed high temperature soak: 4 million total 10,000 psi bending stress cycles, with increasing temperature 75 minute heat soaks between vibration period. Achieved 1,440°F without leakage.

2. Assembly of Collars to Sleeves

2.1 Axial pull: Collar loaded to 3,625 lb. force before leakage detected past seal element. (For reference, the axial force

*"Zero leakage" is defined as less than 10^{-7} cc/sec. It was monitored up to 0 - 6,000 psi.

caused by 12,000 psi burst pressure would be less than 1,500 lb.

2.2 Vibration flexure: Vibrated without seal leakage or structural failure with increasing bending stresses through 30,000 psi (see Table I).

2.3 Heat soak: Collar and seal withstood increasing temperature 75 minute heat soaks to 1,550° F without leakage.

3. Seal Element

3.1 Axial interference: Using both Inconel 718 and 303 seals no leakage shown in engagement distances of .005" or greater.

3.2 Impulse and burst: Seal element was exposed to MIL-F-18280B impulse and burst testing. Withstood 200,000 impulses of 4,500 psi and subsequently withstood 15,000 psi prior to tubing rupture.

The testing of complete connectors is in progress at the time of this writing. By the time of the conference presentation there will be considerable additional information which will be reported at that time.

EXTENT TO WHICH OBJECTIVES HAVE BEEN MET

Now that we have described the connector and presented the test results, we want to discuss the objectives and to evaluate the extent to which this connector meets the objectives.

RELIABILITY OBJECTIVE - As with all spacecraft components, "reliability" is the first objective for connectors. It is important to realize, however, that the urgency of this objective with connectors is many times higher than

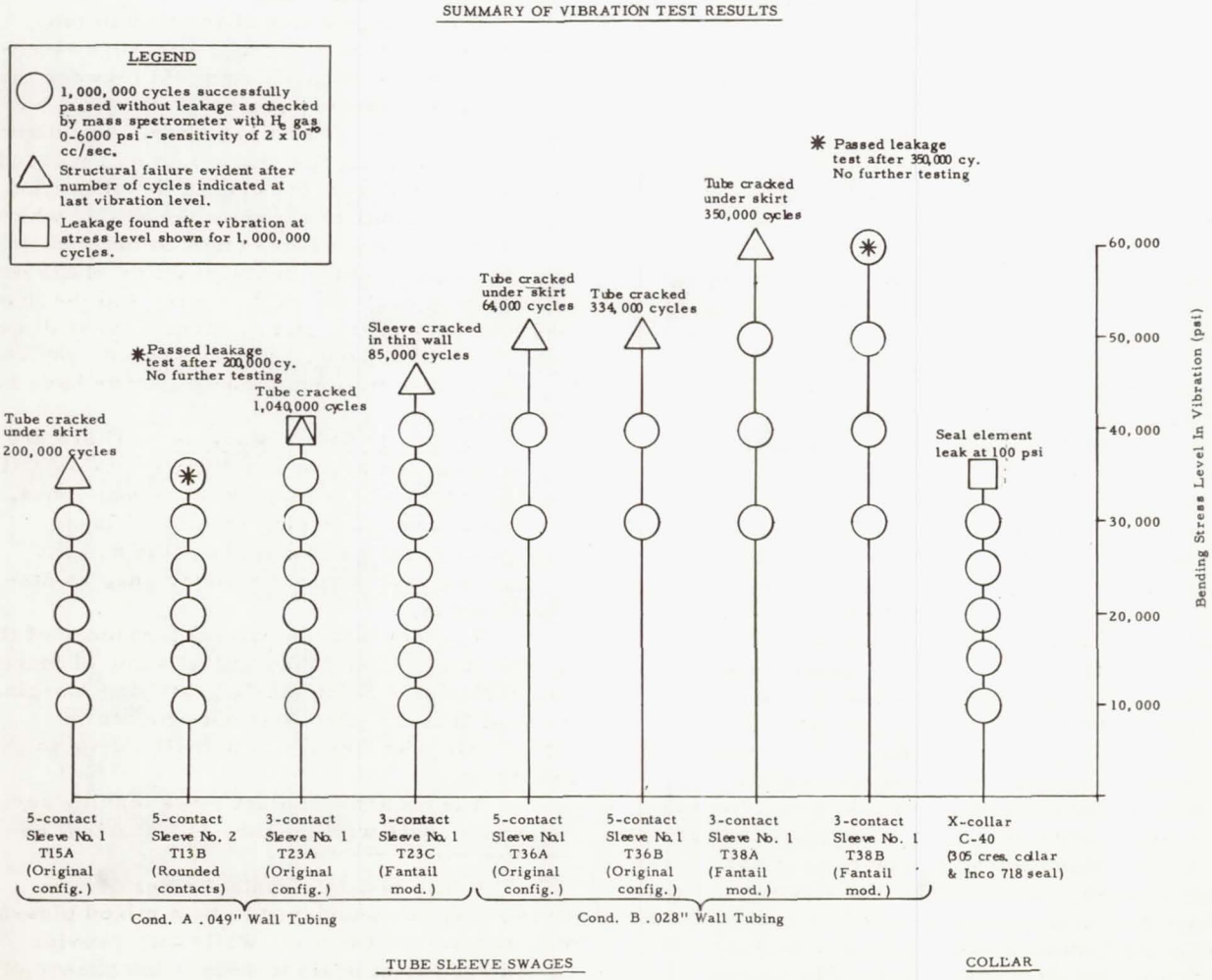

Fig. 6 - Summary of vibration test results

with individual components. Connectors must demonstrate reliability orders of magnitude higher than individual components because of the number of units involved. There are in the neighborhood of 10,000 vehicle connectors involved in a manned moon shot.

Our approach to reaching the necessary level of reliability is three pronged as outlined in our Design Objective section above. We consciously went after obtaining each of these three characteristics.

Probability of Success - In the normal course of using these connectors it must prove out that there is an extremely high probability of successful connection. Considering all the kinds of people who will assemble them and all the conditions under which they will be assembled, it must turn out that there is an extremely high probability that every connection is entirely suitable for service with no further attention.

Redundant, Absolute Inspection - Coupled with a high probability of correct assembly there must be two or more ways to check out critical aspects of the connection to assure that the connector has in fact been put together correctly. Furthermore, these inspection methods must be essentially black and white; that is, they should depend as little as possible upon the skills or judgement of the inspector.

Safety Margins - There must be margins of safety which are repeatable. This is necessary to assure some margin will invariably be available.

Answer to Probability of Success - The following features tend to fulfill the probability of success objectives. There are relatively few, relatively unskilled steps required to make the connection. To connect sleeves to tubes, the sleeve is slipped on the end of the tube; the expander is inserted; power is applied; and the expansion is continued until an O. D. dimension is reached. The process would be automatically cut off when the correct diameter is reached. To connect tube to tube, the tool is closed over the connector (which proves adequate engagement), the tool is tightened (which arms the power switch), the switch is actuated (to apply the hydraulic pressure), the tool is opened and removed from the completed connection. Chemical cleanliness is not a factor. Neither time nor temperature are involved. The primary seals are independent of tube conditions. Fresh gold caulking compound is available for every connection and reconnection. The sealing members are factory machined on production tools with systematized inspection. The sealing members are recessed to protect them from damage prior to assembly.

Answer to Redundant, Absolute Inspection - The redundant inspection consists of helium leakage tests at rated pressure plus go no-go gage measurements of critical dimensions of the formed connector. The checks of the tube to sleeve joints would be made in the subassembly shop. Leakage tests would be made by plugging the ends of the line, applying rated helium pressure and checking with a mass spectrometer sniffer.* The go no-go measurement would be on the diameter of the fantail of the sleeve. If it has yielded some minimum amount you can be certain that some minimum stress has been developed at the interface between the tube and sleeve. You know the stress is there regardless of the dimensions of the tube or sleeve, regardless of the tool adjustment, setting or wear, and regardless of how the operator went about it. This measurement can also, of course, be made in the vehicle for reverification at any time.

The leakage check of the tube to tube connection would be made by a pressure retention test of the leak check manifold between the primary and secondary seals. This would be done with helium at rated pressure. The direction of pressurizing the seal would be reversed but this is a safe test because in this direction the pressure tends to separate the seals, where as in service the pressure tends to close them. The go no-go measurements would be of the new diameters at each end of the collar and the new length of the collar. Here again, if these dimensions are within predetermined ranges, you can be certain that minimum coupling loads have been generated.

Answer to Safety Margins - There are several features aimed at fulfilling this objective. Yielding parts into place, as discussed above, is a major one. Carrying structural loads through high spring rate force paths and not through the seal is another major one, as discussed above.

The fact that the natural frequency of the tube to sleeve joint shows initial signs of increasing, indicates a particularly gratifying margin. It shows that the joint does not proceed to deteriorate with flexure; it actually tends to tighten up.

The multiple contact rings making series redundant seals with the tube is important be-

---

* The multiple contact rings of the sleeve may be considered to be a mixed blessing with respect to leakage. While they provide series redundant seals to reduce the chance of leakage, they make very small leakage rates more troublesome to detect.

cause here we are somewhat at the mercy of the tube surface condition.

The gold on the seal provides a margin in that it fills imperfections that shouldn't be there. We assembled one connector with a clearly visible longitudinal scratch on the sleeve sealing surface. The leakage at 3,000 psi helium was undetectable in the range of 10^{-10} cc/sec. Upon disassembly the imprint of the scratch was clearly visible on the gold of the seal with the unaided eye. There is also margin in the primary seal in that specification leakage is typically reached by the time the seal is engaged only 35% of its planned engagement. Continuing the engagement increases the seal stress and there by enhancing the seal capability.

The fact that the connector is stronger than the undiminished tube strength in: flexure, bending, tension and burst is reassuring. Our problem is to be careful not to be too much stronger than the tubing; it represents a waste of weight.

IMPROVED PERFORMANCE OBJECTIVE Improvement in performance of leakage over the MC fitting is considered to be mandatory. Increase in ruggedness and range of operation is desirable.

Answer - It is quite clear at this point that the objective of 10^{-7} cc/sec helium leakage at 3,000 psi can be attained with relative ease. The ruggedness objective is also well within our grasp. We can easily make the connector stronger than the virgin tube. The only question is one of optimization; how much do we want to reduce the ruggedness in return for weight reduction.

RANGE OF APPLICATION OBJECTIVE - There are important indirect reliability and cost advantages to be gained by minimizing the number of connector styles and the number of configurations within each style. Reducing the number of styles and configurations reduces the chance of failure because the wrong parts are used or because of an application error resulting from confusion. Minimizing the number of connectors also reduces training costs, development costs, tooling costs and procurement and stocking costs.

Answer - The connector has several features directed at this objective. The same approach applies to any line size. The configuration we have been working with is suitable for all fluids with which the 300 series CRES tubing is compatible and for the full temperature range of the tubing; even higher temperatures seem to present no basic problem. It can be designed for any operating pressure. Thus, the connector concept seems to have as broad an applicability as could be desired.

SYSTEM WEIGHT OBJECTIVE - In considering the weight of a connector, the weight of the whole tubing or duct system is the significant parameter since the connector may have a major affect on the system weight. It is, therefore, the objective of the connector to not only be light in itself, but also to minimize the weight of tubing and bracketry.

Answer - The overall weight savings associated with the connector itself are somewhat indefinite at this time because we have been working with only two sizes and they have not yet been optimized for weight. As an indication however: the 1/2 inch 3,000 psi current connector parts have been weighed at less than one third that of an MC fitting and a 4 inch 1,500 psi duct coupling weights onethird that of the standard NASA flange connection.

This coupling contributes to minimizing system weight as well. It allows the use of Condition B tubing without reduction of physical properties which allows reduction to tube wall thickness by 40%. It eliminates the typical weak point in tubing systems. This presumably would allow the use of wider spans between tube supports. The system vibration damping provided by the friction under the fantail should also allow wider spans. * Wider spans in general increase design latitude which is in the direction of reducing weight.

In order to save weight for upper stage vehicles it does seem probable that a lightweight version would be worthwhile. A series of connectors designed for operating at 1,000 psi would apparently be suitable for approximately 90% of spacecraft connector applications, with a system weight saving of approximately 60%.

SEPARATION AND RECONNECTION OBJECTIVE - The practicality of separation and reconnection depends upon the extent to which several requirements are met.

1. It must be practical to separate and reconnect lines without introducing contamination into the system. This requires at the very least that no chips be generated.

2. It must be practical to separate and reconnect lines without removing them from the vehicle. This means that there must be no degradation of the sleeve by the connection process.

---

* This point is still hypothetical. We have not yet reached the point of evaluating the magnitude of this effect.

3. It must be reasonably convenient to accomplish the separation.

Answer - The design is proceeding with the contamination objective in mind, but this phase has not yet been proved. We do not know the extent to which loose burrs may be generated by our roller cutting tool nor the extent to which particles can be eliminated before separating the lines. Regarding reconnection, we have definitely shown that more than four connections can be made without significant deterioration of the sleeves.

MINIMUM ASSEMBLY TOOL SPACE OBJECTIVE - It is obviously important that the space required for use of the in-place assembly and separation tools be as small as possible. It is also important that the tool be oriented with the connector so that it extends axially beyond the connector as little as possible on one side. Further, the volume envelope assigned to the tools must encompass both the assembly and separation tools.

Answer - As indicated above, final designs for tools have not been prepared. Therefore the envelopes now visualized are preliminary. The are, however, based on measured forming forces and upon reasonable stresses for the materials selected in the preliminary design.

MINIMUM COST OBJECTIVE - The question of minimum cost is so broad and important a subject that it is difficult to comment upon briefly. In general, it is our objective to obtain reasonable returns in terms of reliability or weight for the overall costs involved. We have assumed that the overall cost to the program is the matter of importance rather than the first purchase cost of connector parts.

Answer - A "reasonable" dollar value for reliability is virtually impossible to state. In view of the almost inconceivable cost of the missions which will involve these connectors, our approach was: "The best we can do is none too good regardless of dollar cost".

A "reasonable" dollar value for a pound of weight saved still has not been firmly set. It is our intention, however, to obtain one so that we can proceed with a logical and consistent attack on weight.

As mentioned above, there are a number of features of this concept which favor cost saving. The most important one we expect to be related to the simplicity of assembly and the planned high probability of success.

The cost reduction potential which stems from these features are (1) a lower experience or skill level is suitable for the swaged connector; (2) the tubing scrappage due swages should be considerably lower than that presently experienced in attempts to flare tubing to the MC standards; (3) the manhours required to roller swage a tube to a sleeve should be less than that required for the MC standard flare; (4) the inspection time for the swages should be reduced due to the simpler gaging necessary; (5) no special Tallyrond or surface finish inspections should be necessary; (6) the built-in leakage test capability of the collar should reduce inspection time of the completed connection; and (7) the high probability of success on each connection reduces the rework costs of replacing connectors or tube assemblies after installation in the vehicle.

FUTURE EFFORT VISUALIZED

The current program will be completed in early fall with tests of groups of connectors.

It already seems assured that sufficient objectives will be achieved and that the connector will be a worthwhile advancement of the state of the art.

The work that lies ahead in order to make this connector available for spacecraft use is extensive. It can be outlined as follows:

1. For Tube Connectors:

1.1 Establish a tentative specification of operating conditions, functional requirements, design objectives and test procedures.

1.2 Survey the using agencies to verify or improve the specification.

1.3 Design unions for each size standard tube.

1.4 Build and test development models of each size.

1.5 Design the connector shapes for which there is sufficient demand.

1.6 Design and built assembly tooling.

1.7 Build and assemble a representative sample of each size of connector.

1.8 Demonstrate the suitability for spacecraft use of each set of samples by complete qualification testing and documentation.

1.9 Produce limited quantities of connectors and assembly tools for controlled field use.

1.10 Release for production.

2. For Duct Connectors: The logical program for duct connectors would be similar to that for tube connectors except possibly with attention directed more toward development and verification of a criteria for the design of duct connectors rather than the qualification of standard hardware.

It seems that qualified standard connectors and assembly tooling could be available in 1967 if this feasibility program show the desirability to proceed with maximum effort.

CONCLUSION

In this paper we have explored the needs for a new generation of fluid line connectors. The capabilities of the swaged connector have been compared with these needs, and the actual test data for these connectors has been presented to show the feasibility of our design approach. Finally, we have projected our experience and planning into the future. We are proud of the achievements to date, and we are looking forward to further progress in meeting all of our basic objectives.

REFERENCES

1. F. O. Rathbun, Jr. (ed.), "Design Criteria For Zero-Leakage Connectors For Launch Vehicles, Vol. 3, Sealing Action At The Seal Interface". General Electric, Advanced Technology Laboratories, March 15, 1963.

EXOTHERMIC BRAZING - A NEW CONVENIENCE FOR PERMANENT TUBE CONNECTIONS

By

Norman E. Weare
Whittaker Corporation
Controls and Guidance Division
Chatsworth, California

ABSTRACT

Permanent tube joints offer major savings in size and weight when compared to separable connectors. Exothermic brazing offers an easy new way of making such permanent joints. With exothermic brazing the heat necessary to the making of a brazement is generated by reacting metals with metal oxides. By integrating the design of the connector, choice of exotherm and geometry of packaging, a package which reliably makes tube joints can be provided.

Tests of exothermically brazed joints show them to be equal in quality to joints made by other techniques.

BRAZED FLUID SYSTEM CONNECTIONS are nothing new. Several large aerospace companies have been brazing connections of hydraulic, pneumatic and fuel lines on experimental and production bases for five years or more.

Brazed tubing connectors offer distinct advantages over mechanical couplings in areas where they may be used. Advantages gained include: (1) greater reliability; (2) fewer leaks; (3) higher flexture strength; (4) lower weight; and (5) reduced particulate system contamination. Use of exothermic heat provides greater flexibility in use of brazed couplings and permits the use of a reliable, consistent heat source for brazing in remote locations or areas where bulky induction heating equipment cannot be taken.

Brazing is a process of joining wherein coalescence is produced by wetting the base metals with a filler metal having a liquidus greater than 800°F but lower than that of the base metal. The filler metal is distributed between the closely fitted surfaces of the joint by capillary attraction. The statement of coalescence by wetting distinguishes brazing from welding. In welding, joining is due to coalescence by fusion of the base metal and/or filler alloy.

The usual sources of heat for brazing materials of interest to the aerospace community are: (1) gas torch; (2) furnace; (3) induction; (4) electrical resistance; (5) molten salt or molten metal bath; and (6) infra-red. Each of these sources of heat can make excellent brazed joints in the corrosion resisting steels used in aerospace fluid systems. Each of them has a real drawback in use. These drawbacks range from the hazard of an open flame to the large size and lack of versatility of a brazing furnace. Until recently only induction power was seriously considered for the brazing of fluid system joints. Exothermic reaction heat is the new contender for the job of joining aerospace fluid tubing through brazing.

What is Exothermic Heat? An exothermic chemical reaction can be defined as any reaction between two or more reactants in which heat is given off due to a reduction in the free energy of the system. Nature has provided us with countless numbers of these reactions. Only the solid state metal-metal oxide reactions are suitable for use in exothermic brazing units.

Some of the better known exothermic reactions are the Goldschimdt reductions. In these systems various oxides were reduced by aluminum. One of the reactions, aluminum-iron oxide, is the basis of the thermit welding process. The products of this reaction are aluminum oxide and superheated molten iron.

Reactions similar to the above are the basis of exothermic systems used to develop the heat for brazing. Some research effort has been expended to develop systems in which both the heat for brazing and the filler metal are generated by the exothermic formulations. To date these efforts have yielded only marginal results. Only the heat generated by the reaction is utilized in the current brazing units. The heat is used to raise commercial brazing filler alloys to their flow temperature.

Several formulations are utilized to exothermically braze a variety of base metals. Most of the formulations currently in use contain four or more components and design of the exothermic system is extremely critical. In addition to providing sufficient heat for brazing, the exotherm must not react with the base metal, constituents must not diffuse into the base metal, and following the reaction the residue must be ceramic in nature and easily removed from the base metal. Some characteristics of systems now in use are given in Table 1. Values can be influenced by slight changes of composition, addition of

Table 1 - Summary of Available Data on Currently Used Exotherm System

System	Calorific Output Cal/gm	Typ. Peak Base Metal Temp. °F	Max. Ignition Temp. °F
213 B	800	2400	1150
32	600	2200	1210
126	700	2200	1050
34	650	2200	--

modifying agents or by blending methods to provide a range of properties.

The key to the gateway of success when using exothermic heat for the brazing of tube connectors lies with integrated design. Exothermic heat should not be used with existing connectors designed for brazing with other sources of heat. The best brazements have resulted from the use of brazing packages such illustrated by Figure 1, which contain the connector, the filler metal, the exotherm material, an igniter, thermal insulating material and a suitable housing. With this sort of an integrated package, the amount and placement of the exothermic material can be balanced against the size and material of the tube and connector; against the amount and flow point of the filler metal and against the lost heat which flows outward from the package.

Operation of an exothermic tube coupling unit is quite simple. Tubing is inserted into the coupling until it has butted against the center stop. At this point it must be pointed out that it is extremely important that the tubing be scrupulously cleaned of all foreign material and surface oxides prior to insertion. This can be accomplished by mechanical or chemical means. Brush type electrolytic cleaning of the tube ends has proven quite sufficient to remove surface oxides. Prior to assembly the coupling and filler alloy are cleaned chemically and careful packaging methods are used to maintain cleanliness during shipment and storage.

The brazing units are designed to be used with or without flux. When flux is used both the coupling and the tube ends are coated with the appropriate flux for use with the base metal and filler alloy. Fluxless brazing requires a flow of -70°F dew point argon through the tubing. A slight backpressure on the argon stream forces argon to flow through braze area of the coupling prior to the flow of the braze alloy.

Actuation of the exothermic package is accomplished by firing the igniter. The igniter is composed of either a primer cord or electrical resistance bridge imbedded in a pad of low ignition temperature materials. This generates sufficient heat to initiate the higher ignition point, self sustaining reaction of the exotherm rings surrounding the coupling. Heat is then generated and conducted through the coupling to bring the brazement to proper temperature to cause melting and flow of the braze alloy.

Exothermic brazing is distinguished from other forms of brazing by: (1) being a very precise form of heat; (2) having an extremely rapid heat pulse; and (3) being very easy to use. Exothermic compounds can be formulated to provide total heats for brazing which can be closely controlled. Placement of rings of exotherms can induce flow of molten filler metal either way or both ways from the groove. The peel tested brazement in Figure 2 shows filler metal flow both ways from the groove which originally contained the filler alloy rings.

The rapid heat pulse is of real value in conserv-

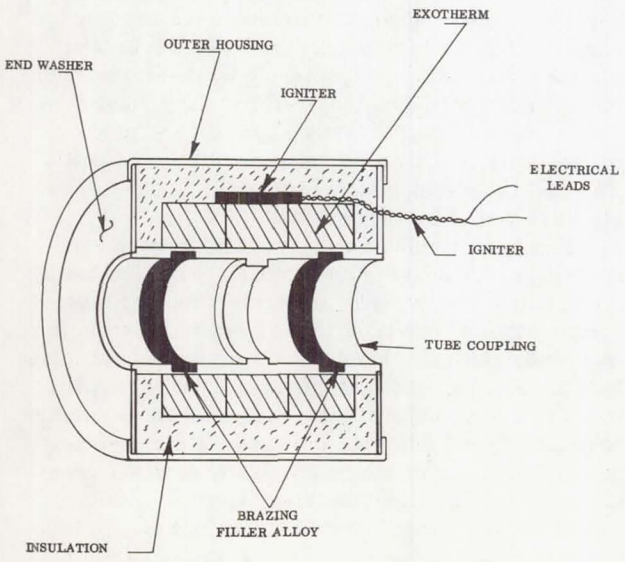

Fig. 1 - Cutaway view of pyrobraze tube coupling unit

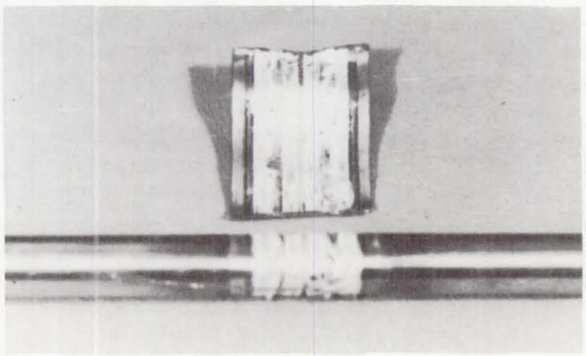

Fig. 2 - Peel tested exothermically brazed tube coupling showing flow of filler alloy

ing the initial strength of heat treated or work hardened tubing. When hardened steel tubing is joined by a thermal method such as brazing or welding, the joining process may anneal the tubing. The shorter the time and the lower the temperature, the less the annealling. A typical burning time of exotherm compositions used on tubes as large as 1" OD is about 3 seconds. Sufficient heat is generated in that time to make a satisfactorily brazed joint. While other heating methods can heat joints in times as short as this, practical limitations of power input usually extend the heating period considerably. As a result, exothermically brazed joints often are as much as 3-5 Rockwell C points harder than the same joints brazed by other methods using the same filler alloys.

As with other methods, exothermic brazing can be done with or without the use of brazing flux. Excellent joints have been made with silver based, gold based and nickel based filler metals. Satisfactory tubing materials include 302, 304, 304L, 321 and 347 austinetic stainless steels, 17-7 PH and AM 350 precipitation hardening steels, Inconel and Hastelloy. Joints have been made in tubing ranging from 3/16" OD to 2-1/2" OD and in a wide range of configurations. Filler alloys which have been used range from the lower melting silver solders to the higher melting gold based alloys.

Table 2 - Burst Test Results

Tube	Filler Metal	Pressure	Results
MIL-T-6845 1/2" OD x .035	BAg3	18,000-20,000	Tube Rupture
MIL-T-8808 1/2" OD x .020	BAg3	6000-6500	Tube Rupture
AM350 CRT 1/4" x .025	BAg8a	21,000 @ 520°F	Tube Rupture
AM350 CRT 1/2" x .025	BAg8a	13,500 @ 520°F	Tube Rupture
AM350 CRT 1-1/2" x .035	BAg8a	14,000 @ 520°F	Tube Rupture
AM350 CRT 1" x .042	BAg8a	17,050	Tube Rupture

Because brazed joints take loading in shear, they can easily be designed to develop the full strength of the tubing. Figure 3 shows how typical coupling joints remain completely leak-free when the tubes they join fail by rupture. Figure 4 shows a pressure rupture near an exothermically brazed adapter tee fitting. As can be seen from the data the brazement strength greatly exceeded the design limits. Table 2 shows typical burst test results with tube sections

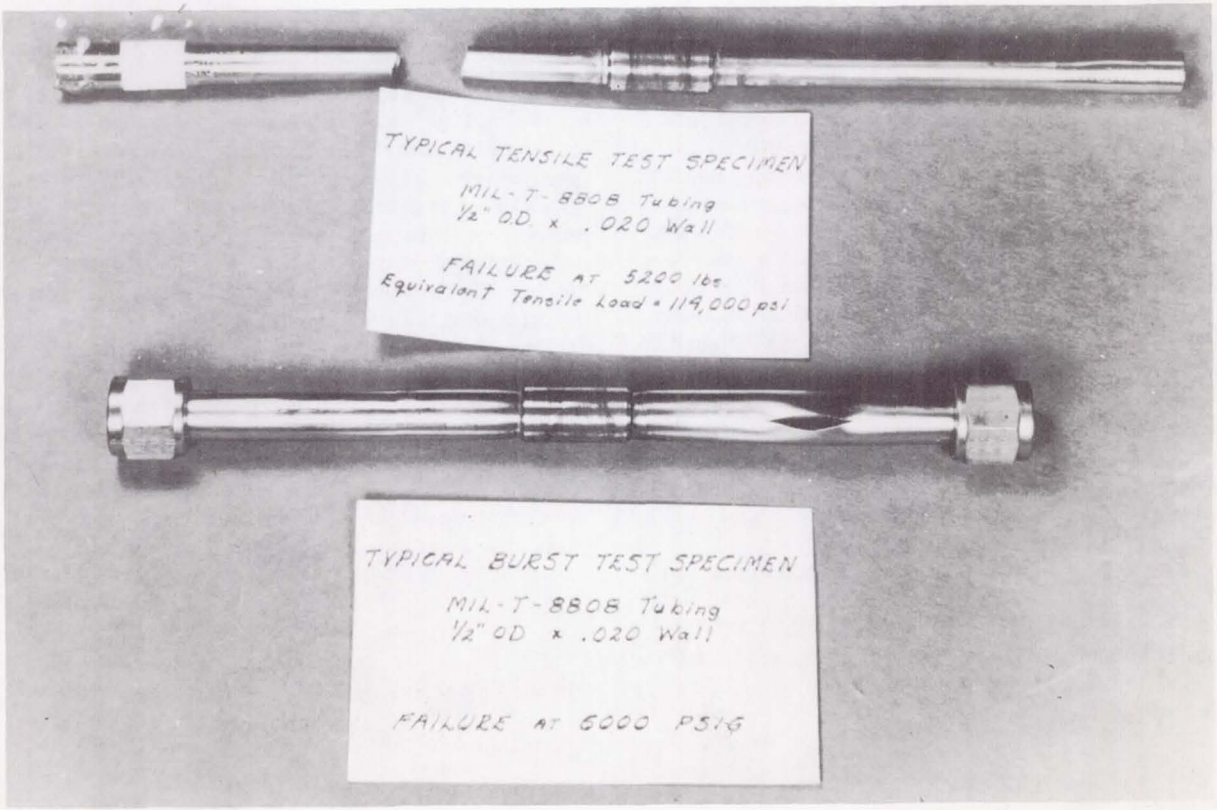

Fig. 3 - Burst test specimen - exothermically brazed coupling

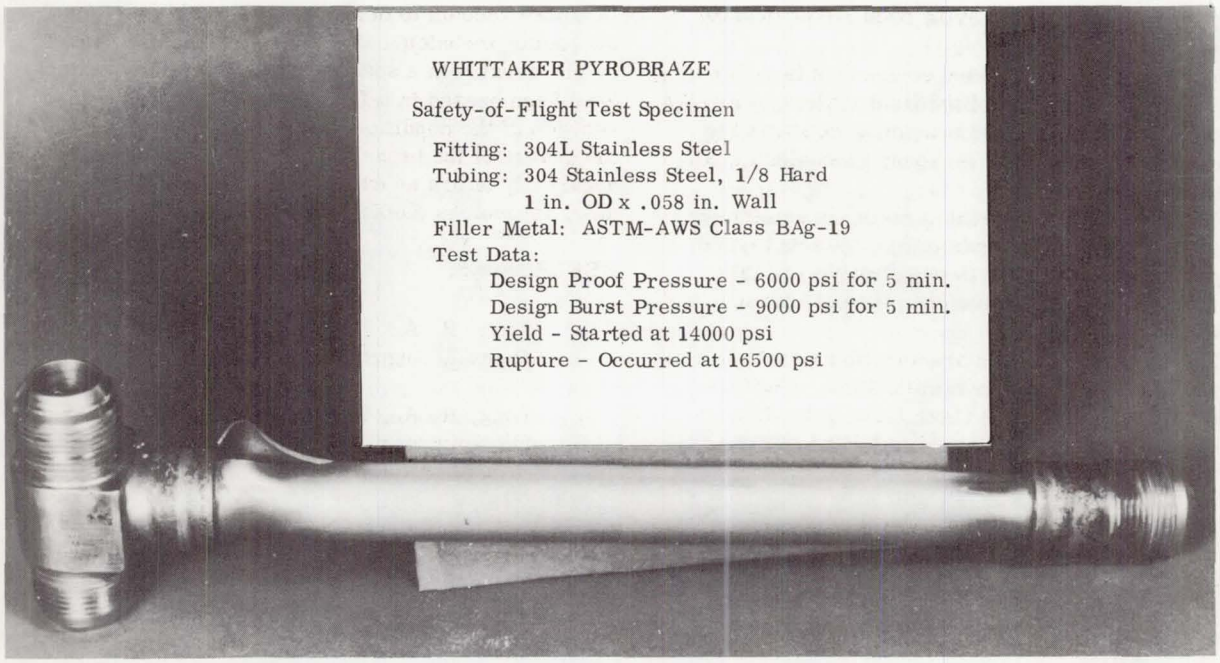

Fig. 4 - Exothermically brazed safety-of-flight test specimen

containing brazed couplings.

Under tensile testing a properly supported joint should always remain intact when the tubing has failed. Couplings are designed in such a manner that the load to cause failure of the braze in shear is greater than that to cause failure of the tubing. Under some circumstances an unsupported joint will fail in the braze under secondary tension induced by the necking down of the tubing. Typical tensile testing data are shown in Table 3. A tensile specimen is shown in Figure 3.

Perhaps the single most significant test for a tube joint is for endurance under flexure loading. The Naval Air Engineering Center found that a 1/2" exothermically brazed joint was the equivalent of a flareless joint in resistance to flexural stress. Some of the test results of various exothermically brazed joints are given in Table 4.

Most users of brazed or welded joints on aerospace vehicles use an extra low carbon alloy such as 304L or a stabilized alloy such as 321 or 347. Unstabilized austinetic stainless steels undergo a microstructural change when held in the temperature range of 800° - 1600° F. In this range the chromium and carbon in the steel form chromium carbides. These carbides precipitate out of solid solution at the boundaries between grains. Metal in which this precipitation occurs is no longer corrosion resistant. This sensitizing occurs in types 302 and 304 stainless steels during most brazing and welding operations. Exothermic heat sources provide a rapid heating cycle which presents the intergranular precipitation of chromium carbides in the 300 series stainless steels.

The measure of the degree of corrosion susceptibility as a result of brazing or welding is the Strauss Test (ASTM Method A393-55T). Strauss Tests on 1/2" OD MIL-T-6845 (Types 302 or 304) corrosion resisting steel tubing such as is normally used on aerospace hydraulic systems show little or no precipitation of

Table 3 - Tensile Test Results
(Failure occurred in Tubing)

Tubing	Failure Load	Equiv. Tensile Stress
MIL-T-6845 1/2" OD x .035	5700 lbs.	121,000 psi
MIL-T-8808 1/2" OD x .035	5200 lbs.	114,000 psi
MIL-T-8808 1/2" OD .020	2500 lbs.	109,000 psi

Table 4 - Flexure Test Data

Tubing	Filler Metal	Stress	Cycles to Failure
MIL-T-6845 1/2" OD	BAg3	27,000	10^7 No Failure
MIL-T-8808 1/2" OD x .035	BAg3	40,000	368,000
AM350 CRT 1" OD x .042	BAg8a	23,000 @ 520°F	1,250,000 No Failure
AM350 CRT 1" OD x .042	BAg8a	35,000	10^7 No Failure
304L 1/4 Hard 1" OD x .054	Premabraze 129	25,000	10^7 No Failure

chromium carbides after having been silver brazed exothermically.

Another feature of brazed connectors is the lack of internal contamination of the fluid system by foreign particles. When "fluxless" brazing is conducted no particulate contamination is found in exothermically brazed joints.

Service use of exothermic brazing is confirming laboratory data. Flight tests on two different types of supersonic vehicles are demonstrating reliable, leak-free operation of both silver and gold brazed joints.

The use of exothermic brazing offers some interesting future application possibilities. Because the exotherm mixes contain both fuels and oxidizers, at least some of them work well in a hard vacuum. Sufficient work has been done in exothermic brazing in a hard vacuum to demonstrate that this is a feasible joining technique. Joints have also been brazed by an operator in a space simulator. While no joints have been brazed in a full space environment, the addition of the condition of weightlessness should aid the quality of the brazement. Exothermic brazing apparently offers an easy, light weight, highly portable, torqueless method of tube joining in space.

REFERENCES:

1. Long, R. A. "Exothermic Brazing" Welding Journal, August 1961

2. Long, R. A., Sieuert, G, Wilson, F, "Exothermic Joining in Vacuum" ML-TDR-64-7, December 1963